Zoomorphic figures (deer and fish), Region del Cabo, Mexico. Photo: U. Méndez-Mejía

## Ancient Rock Paintings at Region del Cabo-BCS, Mexico
### *An Analytical Study*

Úrsula Méndez-Mejía, Maria Dolores Tenorio,
Melania Jiménez-Reyes, Rosa Elba Rodríguez-Tomp

# 21º ENQA | 9º CIAQA
September 15th to 18th, 2024
Hangar Convention Center

**Welcome to the 21st ENQA and 9th CIAQA to be held at Belém do Pará, one of the most prominent cities in the Brazilian Amazon**

*From September 15th to 18th, 2024*

**Venue:** Hangar Convention and Exhibition Center of the Amazon, in Belém do Pará, Brazil

ENQA is a rotating conference organized by the Analytical Chemistry Division of the Brazilian Chemical Society with over 40 years of history. It is the largest and most significant scientific conference in Analytical Chemistry in Brazil, and one of the main Chemistry events in Latin America. The 21st ENQA will be a defining moment in the conference's history, as it will be the first edition held in the Northern region of Brazil.

The 21st ENQA and 9th CIAQA will take place at Belém do Pará, Brazil, a metropolis surrounded by rivers and islands with a distinctive culture and a rich gastronomy primarily based on ingredients from the Amazon rainforest's diverse flora and fauna.

The ENQA/CIAQA 2024 has the theme **"Analytical Chemistry and its Contributions to the Development of a Sustainable Society"**. In recent years, Analytical Chemistry has been strengthening itself as a more environmentally recommendable science, encouraging actions and works that align with sustainable development. Thus, gathering knowledge that contributes to the assurance of products and environments and to the development of instrumentation and methods to address upcoming demands and challenges.



21º ENQA
9º CIAQA

# BrJAC

Brazilian Journal of Analytical Chemistry

## Aims & Scope

BrJAC is a double-blind peer-reviewed research journal, dedicated to the diffusion of significant and original knowledge in all branches of Analytical Chemistry and Bioanalytical Chemistry. It is addressed to professionals involved in science, technology, and innovation projects at universities, research centers and in industry. The **BrJAC welcomes** the submission of research papers reporting studies devoted to new and significant analytical methodologies, putting in evidence the scientific novelty, impact of the research, and demonstrated analytical or bioanalytical applicability. BrJAC **strongly discourages** those simple applications of routine analytical methodologies, or the extension of these methods to new sample matrices, unless the proposal contains substantial novelty and unpublished data, clearly demonstrating advantages over existing ones.

BrJAC is a quarterly journal that publishes original, unpublished scientific articles, reviews and technical notes. In addition, it publishes interviews, points of view, letters, sponsor reports, and features related to analytical chemistry.

For complete information on ethics and policies on conflicts of interest, copyright, reproduction of already published material and preprints, in addition to the manuscript submission and peer review system, please visit 'About us' and 'Author Guidelines' at www.brjac.com.br

## Indexing Sources

### Scopus

CiteScore$^{TM}_{2022}$ 1.0
SJR$_{2022}$ 0.165
SNIP$_{2022}$ 0.242
CiteScore$^{TM}$ Tracker$_{2023}$ 1.8
Access source details

CiteScore trend



CiteScore value — Percentile in category

### CLARIVATE ANALYTICS EMERGING SOURCES CITATION INDEX INDEXED
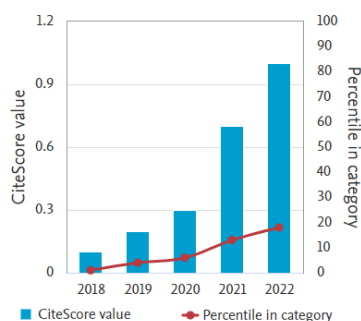
IF$_{2022}$ 0.7

### CAPES QUALIS

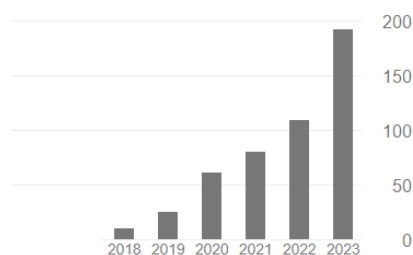**BrJAC is in the Qualis B3 stratum**
according to preliminary list
published on 2022/12/29

### Google scholar

Cited by

| | All | Since 2018 |
|---|---|---|
| Citations | 582 | 491 |
| h-index | 11 | 10 |
| i10-index | 13 | 11 |



2018 2019 2020 2021 2022 2023

## EDITORIAL ADVISORY BOARD (Continuation)

BrJAC

# CONTENTS

## CONTENTS *(Continuation)*

**BrJAC**

## EDITORIAL

# Analytical Chemistry is like the Fruit of an Apple Tree

Victor G. Mihucz 🆔 ✉

*Head of the Analytical Chemistry Department at the Institute of Chemistry, ELTE Eötvös Loránd University, Budapest, Hungary*

Analytical chemistry is deeply rooted in Europe. It started with the work of Liebig and Fresenius, among others. Then Kirchhoff, as father of spectroscopy, contributed to the development of the modern instrumental analysis techniques flourishing today. As soon as I started learning analytical chemistry at university, I fell in love with it. At that time, I could not explain why I wanted to become an analytical chemist. Having gained experience teaching and performing research in analytical chemistry, I know now that I am attracted to it because this branch of chemistry is what an apple means to an apple tree - the fruit of a myriad of results in fundamental research in chemistry, always offering solutions to real life problems. I always wanted to become an analyst and to work at the analytical chemistry department where I studied. One year ago, my life drastically changed at the institute when I was invited to apply to lead the analytical chemistry department where I have been working since 2007. I must admit that I had mixed feelings in the beginning. First of all, I was honored that my colleagues in the department fully expressed their support. At the same time, I was confused and scared. I felt that I am not the right person to lead a department with a history of almost 120 years, that I had no clear vision of what could I do for my colleagues and for the students choosing our department. However, I wanted to express my gratitude to my colleagues for their trust in me. In my application, I advocated to maintain the high-quality teaching of analytical chemistry at the department and offered to implement challenge-based learning for students choosing our department. In past years, I felt that the *raison d'être* of analytical chemistry departments as single entities would soon end. My colleagues working in other fields such as biology, geography and geology, pharmacy and medicine, all purchased instrumental analytical equipment and started performing research by themselves. Recently, analytical chemistry departments underwent important organizational and structural changes. Some of them disappeared, others incorporated into their name environmental chemistry, food chemistry, or biochemistry. Recent advances in instrumental analysis create the impression that conducting chemical analysis is an easy task that no longer requires the expertise of chemists devoted to this branch of chemistry. However, there is still a lot of work to do, especially in the field of organic analytical chemistry. Thanks to innovations in mass spectrometry and related techniques, infrared spectroscopy, miniaturization (lab-on-chips) and sensors, ultra trace analysis, green methodologies, and elemental speciation, analytical chemistry is experiencing a second Golden Era. In last year alone, I was surprised by the ever-increasing number of chemistry bachelor and major students knocking on my door asking me to provide them with analytical chemistry-related research topics. That led me to contact faculty working at the other institutes offering cooperation with the arsenal of our instruments to widen the research topic choices in our department, advocating that we should unite and complement our efforts to create synergies. Surprisingly, the response of those colleagues was very positive. In one year, I could almost double the number of research topics for diploma work in our department. This is something that makes

me happy and optimistic. I am confident that the development of analytical methods together with proper sampling and sample preparation are still important and crucial steps to produce high quality and reliable results. Moreover, participation of analytical chemists in these tasks is indispensable. The recent success of the Brazilian Journal of Analytical Chemistry achieving an impact factor of 0.7 makes me also think that analytical method development has still a bright future ahead. Long live Analytical Chemistry! Long live Brazilian Journal of Analytical Chemistry!

**Victor G. Mihucz** has been working at the Department of Analytical Chemistry of ELTE Eötvös Loránd University, Budapest, Hungary since 2007. In 2014, he habilitated in Analytical Chemistry. In 2015, he was appointed as associate professor. Currently, he is head of the Analytical Chemistry Department at the Institute of Chemistry, ELTE. He obtained the DSc degree from the Hungarian Academy of Sciences (MTA) in October 2022. He participated in about 20 national and international research, scientific cooperation, and educational projects. His main research field is elemental analysis, mainly arsenic speciation in water and food. Another research topic of Victor G. Mihucz is indoor air quality. He was the secretary of the Spectrochemical Society of the Hungarian Chemical Society (MKE) between 2015 and 2019, then its president (2019-2023). In 2019, he was elected as a member of the MKE Steering Committee. He has been secretary of the MTA Analytical Chemistry and Environmental Sciences Scientific Committee since 2018. In 2016, he received the Ernő Pungor award of MTA. In 2020 and 2022, he was awarded the Miklós Preisich award of MKE and CHARM-EU Award of ELTE, respectively.

**BrJAC**

## INTERVIEW

# Professor Patricia Smichowski, a researcher who works hard to contribute to science, kindly granted BrJAC an interview

Patricia Smichowski is a Licentiate in Chemistry (equivalent to a Master in Science) of the University of Buenos Aires. She obtained an MS in Nuclear Engineering from the Engineering School of the University of Buenos Aires in 1981 and received her Ph.D. in chemistry in 1995 from the Complutense University, Madrid, Spain. In 1982, she joined the Argentine Atomic Energy Commission (CNEA) where she is currently Head of the Analytical Developments Division. She is also Principal Researcher at the National Council of Scientific and Technical Research (CONICET). She specializes in the development and application of atomic spectrometric techniques to environmental and biological analysis. Her interests lie in the preconcentration, speciation, and determination of trace metals and metalloids in a variety of matrices by employing plasma-based techniques, atomic fluorescence spectrometry, and other coupled techniques.

She has conducted national and international projects aimed at characterizing the presence of metals, metalloids, ions, and organic compounds in airborne particulate matter, as well as elucidating their origin. She holds a patent, with other researchers, relating to the development of a sorbent for arsenic retention.

Patricia Smichowski has published 130 peer reviewed articles and 12 book chapters, given 45 invited lectures at international meetings, and has co-organized several international conferences. She is a member of the advisory board of four international analytical chemistry journals, as well as the European Virtual Institute for Speciation Analysis.

---

**How was your childhood?**

I had a happy childhood in the province of Buenos Aires, Argentina where I was born. I lived a very happy family life. My parents always supported me in my pursuits, and they were a great support throughout my life.

**What early influences encouraged you to study chemistry? Did you have any influencers, such as a teacher?**

As a child, I wanted to be an architect (today my daughter is an architect) until the age of 16, when I had an excellent chemistry teacher who made me discover the wonderful world of chemistry. At that time I thought "chemistry is very easy"; today, I don't think the same!!!

**How was the beginning of your career in chemistry?**

During my high school years, I already wanted to be a chemist. In 1980, I obtained a degree in Chemistry (equivalent to a Master in Science) from the University of Buenos Aires, Argentina. Several years later,

I obtained my Ph.D. in Chemistry at the Complutense University of Madrid under the supervision of Dr. Carmen Cámara, who was, and still is, a great friend.

**What has changed in your profile, ambitions, and performance since the time you started your career?**

Many things have changed because science, research, and life have changed during all these years. What hasn't changed for me is that, if I had to start over, I would do exactly the same. I have come a long way and I have had many satisfactions. Analytical chemistry is an exciting part of my scientific life.

**Could you comment briefly on the recent evolution of analytical chemistry, considering your contributions?**

Analytical chemistry and spectrochemical analysis have evolved and, consequently, have changed and improved significantly. These changes have gone in hand with instrumental development that has made it possible for analytical chemists to determine lower and lower concentrations, determine inorganic and organic species of the same element, combine separation and quantification techniques, and develop methods framed in the precepts of green chemistry. The advances made in the design and application of nanomaterials, biosensors, electroanalytical, sample introduction methods, chemometrics, and imaging techniques provide clear evidence of the impact of analytical chemistry in different research areas.

**What are your lines of research? You have published many scientific papers. Would you highlight any?**

I have two main lines of research: *i)* development of analytical methods that allow the preconcentration, speciation, and determination of metals and metalloids at trace and ultra-trace levels using a variety of analytical techniques and instrumental couplings; *ii)* Characterization of atmospheric particles and related matrices, identifying the presence of metals, metalloids, ions, and organic compounds, as well as the identification of their sources.

In the last 20 years, I have worked very actively in environmental analytical chemistry and I am very satisfied with the work carried out and with the contributions that I and my group have made to this discipline.

**What is your opinion about the current progress of chemistry research in Brazil? What are the recent advances and challenges in scientific research in Brazil?**

Brazil is a huge country with great potential. My first visit to Brazil was in the 90s and, since then, I have seen more and more research growing in quality and quantity. Today, we can say that there are many groups that carry out top level research and that these research groups are competitive with the most internationally recognized researchers.

**For you, what have been the most important recent achievements in analytical chemistry research? What are the landmarks? What has changed in this scenario with the COVID-19 pandemic?**

In my opinion, instrumental developments, especially in mass spectrometry, have opened new fields of research, especially in trace element analysis and -omics in biochemistry and environmental chemistry.

The COVID-19 pandemic has caused a worldwide backlog, as experimental work could not be done for a long period. On the other hand, I want to remark that diagnostic tests developed during the pandemic represented an important contribution to making appropriate clinical decisions in short periods of time.

**There are, in Brazil and in the world, several conferences on chemistry. To you, how important are these meetings to the chemistry scientific community? How do you see the development of national chemistry meetings in Brazil?**

Conferences are an important meeting point between scientists, students, and vendors. As Brazil is a very large country, conferences in Brazil attract a large number of people. This impresses me in particular

and I find it very positive. The only criticism I make, to Brazil in particular and other countries in general, is the excessive number of conferences, often with some overlapping of topics.

**What is the importance of awards for the development of science and new technologies?**

Awards are always important for seniors and for young people. They are a recognition to effort and dedication; recognition is a powerful incentive to stimulate quality work.

**For you, what is the importance of the national funding agencies for the scientific development of Brazil?**

All over the world, funding agencies play a fundamental role in making it possible to carry out quality research that will contribute over time to the continuous development of the country. Without the help of these agencies, it is impossible to carry out sustained research.

**At the moment, the situation for scientific research in Brazil is one of decreasing investment. How do you see this situation, and what would you say to young researchers?**

> *...there is a relatively small number of scientists in South America compared to other regions of the world. In this context, added to the decrease in funding, cooperation between different research groups in the region is crucial to maintain the scientific level that we have achieved with great effort.*

This is a situation that occurs in Brazil and in many other countries. To young people, I say not to be discouraged and to continue working hard to achieve their dreams. In addition, there is a relatively small number of scientists in South America compared to other regions of the world. In this context, added to the decrease in funding, cooperation between different research groups in the region is crucial to maintain the scientific level that we have achieved with great effort.

**What advice would you give to a young scientist who wants to pursue a career in chemistry?**

Young scientists bring new energies and perspectives to analytical chemistry research. I would advise them to be good students, to engage in research activities, and to have an active participation in workshops and conferences to be in contact with professors and researchers from Brazil and other parts of the world. An important point to highlight is to enjoy every step of their careers. Briefly, the most important thing is to be happy with what you are doing.

**For what would you like to be remembered?**

I would like to be remembered as an Argentine researcher who has worked hard for many years and who has made a contribution to science.

**BrJAC**

## POINT OF VIEW

# BrJAC 2023 – Growing and Building Bridges

**Joaquim de Araújo Nóbrega** (iD) ✉

*Full Professor in the Department of Chemistry at the Federal University of São Carlos (UFSCar), Sao Carlos, SP, Brazil*

*Time, flowing like a river* (Time, The Alan Parsons Project)

In 2010, in the first **BrJAC** Editorial, Kubota emphasized: "We are launching **BrJAC** – *Brazilian Journal of Analytical Chemistry* to open a discussion about the real role of the Analytical Chemistry for the development of the country and bring the improvement of the life quality. **BrJAC** is an Analytical Chemistry journal whose goal is to debate, discuss, show trends, and needs with opinion editorials and interviews with renowned investigators, besides publishing scientific papers from the academic and industry, fulfilling the idealistic purpose of a group of people to achieve actual academic industrial integration towards innovation and technical-scientific development."[1]

In this same issue I had the opportunity to write a Point of View and I stated: "The launching of Brazilian Journal of Analytical Chemistry (**BrJAC**) is a milestone with full potential to expand the flow of knowledge. The integration of academy and industry is a must and **BrJAC** will certainly play a major role in putting them in contact."[2]

After a relatively short span of time (just 13 years!), it is amazing to think about how much was accomplished. As announced since the beginning, each issue has a great combination of reviews, scientific articles, points of view, letters, sponsors' reports, releases, news, and interviews. This list of contents is part of the identity of **BrJAC** and each section plays a special role. Of course, articles are the core of any scientific journal, but to create and consolidate bridges we need to integrate academia and industry, so different forms of communication are in the **BrJAC** fingerprint.

And how could we move ahead without listening to well-known analytical chemists? Fortunately, since its beginning, **BrJAC** has opened its pages for interviews. We began in 2010 with Prof. Carol Hollingworth Collins (Institute of Chemistry, State University of Campinas)[3] and travelled all the way to Dr. Joanna Szpunar (National Research Council of France, CNRS) in the last issue.[4] I have no doubt that important landmarks of the history of analytical chemistry in Brazil were revealed in a colloquial atmosphere in these interviews.

Recently, Marco Arruda, the Editor-in-Chief, posted a letter on the journal website entitled, "From dream to reality"[5] and invited us to celebrate the indexation of **BrJAC** by Clarivate and its starting impact factor of 0.7. Certainly, the Brazilian community in analytical chemistry has a lot to celebrate and it is amazing to reach this point when we think about the challenges along the 13-year road (and please keep counting!). In his letter, Marco Arruda mentioned challenges related to logistics, economy, ethics, and scientific quality. Surely, these are critical aspects.

We live in an increasingly complex society full of opportunities and challenges. I am not thinking about political turmoil, social inequalities, and climate crisis. You know how big these challenges are. However, I would like to mention two other major challenges that we have coped with (or we are coping with) during the lifetime of **BrJAC**.

One critical moment was the years of the COVID-19 pandemic and how they affected our way of life. We are still trying to understand all that has happened and how we have changed. The economy was affected. Work routines were affected. Families and friends were affected. Institutions were affected. Once again, we have practiced important human values, such as solidarity, fraternity, and the shared goal to move ahead as a society. Once again, science has rescued us.

Another major influence when thinking about complexity and the scientific literature comes from predatory journals. The routinization of research and its diffusion are landmarks for the evolution of science, technology, and innovation. Scientific journals are important foundations for dissemination of research. Notwithstanding, nowadays we are coping with paper mills that produce fake papers just for profit. Recently, we are starting to face the dangerous combination of paper mills and artificial intelligence to produce polluted science.

Despite some clouds on the horizon, it is great to see how the **BrJAC** community was able to grow during these hard times. We have achievements to celebrate and **BrJAC** is a great one.

Recently, The Analytical Scientist asked researchers about the biggest challenge facing the analytical chemistry field.[6] I would like to highlight the comments expressed by Prof. Robert Graham Cooks: "A lack of appreciation of the intricacies of analytical science by other disciplines (especially chemists) who see it as little more than an exercise in measurement using commercial instrumentation. Like modern day pharaohs, the organic synthetic chemist commands – "measure it!" – without pausing to recognize the ingenuity that went into the slaves' work of conceiving the method, building the instrumentation, and achieving useful performance criteria. The "measure it" request at the end of that multi-year process is often a simple application, but the process that allows it is a unique combination of new scientific insights and skillful technology.".

And Richard Zare: "Simply put, gaining more respect for analytical science's importance to understanding nature.".

I do think **BrJAC** is part of the multifarious mechanism to bring better understanding and more respect to analytical sciences. Let us keep our focus and strength. As always, "time keeps flowing like a river" (Time, The Alan Parsons Project).

## REFERENCES
(1)   Kubota, L. T. Editorial. *Braz. J. Anal. Chem*. **2010**, *1* (0), p V.
(2)   Nóbrega, J. A. Point of View: Steps of Development. *Braz. J. Anal. Chem*. **2010**, *1* (0), p XXIII.
(3)   Collins, C. H. Interview: A look at Analytical Chemistry. *Braz. J. Anal. Chem*. **2010**, *1* (0), pp XV-XIX.
(4)   Szpunar, J. Interview: Joanna Szpunar, an outstanding chemical researcher in the chemistry of metal-biomolecule interactions, shares her experience as a woman scientist with BrJAC. *Braz. J. Anal. Chem*. **2023**, *10* (40), 3-9. http://dx.doi.org/10.30744/brjac.2179-3425.interview.jszpunar
(5)   Arruda, M. A. Z. Letter from the BrJAC Editor-in-Chief: From dream to reality. Available at: https://www.brjac.com.br/pdf/Letter-EiC-08-2023.pdf (accessed in September, 2023).
(6)   Features: Innovators and Trailblazers. *The Analytical Scientist* **2023**, 112, 12-24. Available at: https://theanalyticalscientist.com/issues (accessed in September, 2023).

**Joaquim de Araújo Nóbrega** holds a bachelor's degree in chemistry from the Federal University of São Carlos – UFSCar (1986), a master's degree in analytical chemistry from the Institute of Chemistry, University of São Paulo – USP in São Carlos (1989), a doctorate in science from the Institute of Chemistry, University of Campinas – Unicamp (1992) and a full professorship in analytical spectrochemistry from the Center for Nuclear Energy in Agriculture – CENA, University of São Paulo – USP (2000). He completed two post-doctoral internships (University of Massachusetts, Dr. Ramon M. Barnes - 1996 and Wake Forest University, Dr. Bradley T. Jones

- 2003). He is currently a Full Professor in the Department of Chemistry at the Federal University of São Carlos. He is or was a member of the Editorial Boards of *Analytical and Bioanalytical Chemistry* (2017 to 2019), *Brazilian Journal of Analytical Chemistry*, *Microchemical Journal* (2011 to 2023) and *Talanta* (2011 to 2018). He is a Full Member of the Academy of Sciences of the State of São Paulo (October/2015), of the Brazilian Academy of Sciences (May/2016) and a Fellow of the Royal Society of Chemistry (June/2016). He was a full member of the Chemistry Advisory Committee of the National Council for Scientific and Technological Development (CNPq) from October/2009 to September/2012 (Coordinator of the Chemistry Advisory Committee (CA-QU) from October/2011 to September/2012). He was Associate Editor and Editor of the *Journal of the Brazilian Chemical Society* (2005 - 2015). He served as Associate Editor of *Talanta* (October/2018 – July/2023). He has experience in analytical chemistry and works mainly on the following topics: sample preparation, absorption, and atomic emission spectrometry with different atomizers, ICP-OES, and ICP-MS. He has supervised 20 scientific initiation fellows, 28 masters, 32 doctors, and 13 postdoctoral fellows. Detailed information about the Group for Applied Instrumental Analysis can be found at http://www.gaia.ufscar.br. **CV**

**BrJAC**

## LETTER

# Importance of Elemental Chemical Speciation Studies in Enriched Food: Nutritional Quality, Toxicity, and Economic Improvement

Juliana Naozuka (iD) (✉)

*Universidade Federal de São Paulo, Departamento de Química, Diadema, 09972-270, SP, Brazil*

For several reasons, mainly cost and local productivity, the world population does not have access to a balanced diet that contains all the macro and micronutrients necessary to maintain physiological functions for a healthy life. Nutritional education, supplementation, and consuming enriched (or fortified) foods appear as alternatives to supply daily demands and minimize malnutrition. Adding essential elements as salts (*e.g.*, iron, calcium, and zinc) to ready-to-eat processed foods, such as milk, flour, and juices is already adopted in several countries. The choice of the compound to be added, as well as the transport vehicle (foods), must be very well evaluated since the cost, long-term consumption, and bioavailability of the added chemical species are imperative to ensure the nutritional quality of enriched food.[1]

Another alternative to produce enriched foods is cultivating an enriched medium (Figure 1), adding essential elements to soil or in nutritive solution (hydroponic procedure), irrigating leaves, or immersing seeds.[2] In this case, the chemical species used to the enrich food must be absorbed, translocated, and accumulated in the edible part.[2]
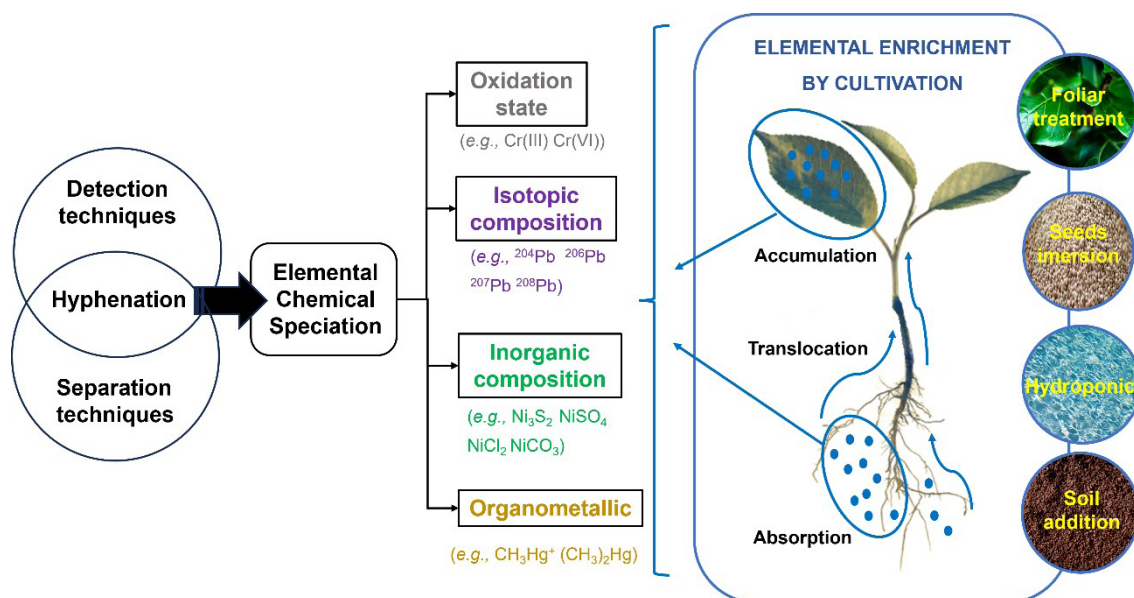


**Figure 1.** Elemental chemical speciation studies in enriched food.

Studies have shown that the iron enrichment of adzuki beans using iron nitrate or iron chloride was unsuccessful since iron inorganic species interact strongly with the antinutrients (tannins or phytates) present in the roots, forming insoluble complexes and preventing their translocation.[3] Alternatives found to overcome this obstacle were enrichment by applying iron complexes with EDTA (ethylenediaminetetra-acetic acid)[3] or iron nanoparticles, mainly encapsulated.[4] The nanoparticle application has been gaining prominence in agriculture, aiming to carry fertilizer, pesticides, and nutrients to stimulate plant growth and increase macro and micronutrient availability and absorption efficiency.[5,6]

Besides the interaction between essential elements with antinutrients, evaluating the competition between elemental species is important, because synergistic or antagonistic effects can be observed. In both cases, chemical species must interact with other components present in food or cultivation medium, altering its chemical composition when compared to food cultivated in conventional conditions. The antagonistic effect between selenium and mercury was observed in edible mushrooms, while the synergistic effect was observed with lead and selenium.[7,8] Finally, it must be evaluated if the enrichment promotes the production of non-bioavailable or toxic species.

Regardless of the food enrichment strategy, it is important to highlight the need to identify and quantify the elemental chemical species in the enriched foods by chemical speciation analysis. In the Figure 1 is shown examples of elemental chemical species; they can differ according to their oxidation states, inorganic forms, and organometallic or isotopic composition.[9] For chemical speciation studies, initial fractionation steps (*e.g.,* extraction procedures) are carried out; subsequently, chromatographic, or non-chromatographic methods can be used to identify/determine the chemical species. The hyphenation (Figure 1) between separation techniques, mainly chromatography, with high sensitivity detectors, such as inductively coupled plasma mass spectrometry (ICP-MS), is commonly applied.[9-11] Nonetheless, extremely creative procedures used in non-chromatographic chemical speciation, working only with chemical reactions and solubility differences, can also be applied to determine chemical species. Non-chromatographic strategies were applied for iron (reaction with hydroxylamine and precipitation with trichloroacetic acid and HCl) and selenium (cloud point extraction) speciation in enriched adzuki sprouts.[3]

In summary, food enrichment success is closely associated with chemical speciation studies since there are chemical species that will be absorbed in a cultivation medium, as well as the chemical species that are formed during translocation and accumulation, which must be in bioavailable forms, in order to act on the different metabolic systems of the human body, including remedying prevalences. In this scenario, it is imperative to go beyond determining the total concentration of essential elements, since quantifying their species will provide information regarding essentiality and toxicity. Finally, the formation of bioavailable chemical species will add nutritional quality and, consequently, economic benefits that are so essential for countries with specific prevalences to combat in a predominantly agricultural economy.

## REFERENCES

(1) Naozuka, J. Elemental Enrichment of Foods: Essentiality and Toxicity. *Nutri. Food Sci. Int. J.* **2018**, *4* (3), 555640. https://doi.org/10.19080/NFSIJ.2018.04.555640

(2) Oliveira, A. P.; Naozuka, J. Enriquecimento Elementar por Meio de Cultivo: Plantas e Cogumelos. *Quim. Nova* **2020**, *43* (9), 1277-1293. http://dx.doi.org/10.21577/0100-4042.20170601

(3) Oliveira, A. P.; Nomura, C. S.; Silva, S. G.; Naozuka, J. Iron and Selenium Speciation in Enriched Adzuki Bean Sprouts after Fractionation Procedures by Graphite Furnace Atomic Absorption Spectrometry. *J. Anal. Pharm. Res.* **2018**, *7* (2), 104–112. https://doi.org/10.15406/japlr.2018.07.00209

(4) Vélez, Y. S. P.; Carrillo-González, R.; González-Chávez, M. C. A. Interaction of Metal Nanoparticles–plants–microorganisms in Agriculture and Soil Remediation. *J. Nanopart. Res.* **2021**, *23* (206), 2-48. https://doi.org/10.1007/s11051-021-05269-3

(5) Arruda, S. C. C.; Silva, A. L. D.; Galazzi, R. M.; Azevedo, R. A.; Arruda, M. A. Z. Nanoparticles Applied to Plant Science: A review. *Talanta* **2015**, 131, 693-705. https://doi.org/10.1016/j.talanta.2014.08.050

(6)    Chacón-Madrid, K; Francischini, D. S.; Arruda, M. A. Z. The Role of Silver Nanoparticles Effects in the Homeostasis of Metals in Soybean Cultivation Through Qualitative and Quantitative Laser Ablation Bioimaging. *J. Trace Elem. Med. Biol.* **2023**, *79*, 127207. https://doi.org/10.1016/j.jtemb.2023.127207

(7)    Oliveira, A. P.; Naozuka, J.; Landero-Figueroa, J. A. The Protective Role of Selenium Against Uptake and Accumulation of Cadmium and Lead in White Oyster (*Pleurotus ostreatus*) and Pink Oyster (*Pleurotus djamor*) Mushrooms, *Food Addit. Contam.: Part A* **2022**, *39* (3)*,* 508-524. https://doi.org/10.1080/19440049.2022.2026494

(8)    Oliveira, A. P.; Naozuka, J.; Landero-Figueroa, J. A. Feasibility Study for Mercury Remediation by Selenium Competition in *Pleurotus* Mushrooms *J. Hazard. Mater.* **2023**, *451*, 131098. https://doi.org/10.1016/j.jhazmat.2023.131098

(9)    Templeton, D. M.; Ariese, F.; Cornelis, R.; Danielsson, L.; Muntau, H.; Van Leeuwen, H. P.; Łobiński, R. Guidelines for Terms Related to Chemical Speciation and Fractionation of Elements. Definitions, Structural Aspects, and Methodological Approaches. (IUPAC Recommendations 2000) *Pure Appl. Chem.* **2000**, *72* (8)*,* 1453–1470, 2000. https://doi.org/10.1351/pac200072081453

(10)   Garcia, J. S.; Magalhães, C. S.; Arruda, M. A. Z. Trends in Metal-binding and Metalloprotein Analysis. *Talanta* **2006**, *69* (1)*,* 1-15. https://doi.org/10.1016/j.talanta.2005.08.041

(11)   Arruda, M. A. Z.; Jesus, J. R.; Blindauer, C. A.; Stewart, A. J. Speciomics as a Concept Involving Chemical Speciation and Omics. *J. Proteomics*. **2022,** *263*, 104615. https://doi.org/10.1016/j.jprot.2022.104615

**Juliana Naozuka**, PhD, is an Associate III Professor in the Department of Chemistry at Federal University of Sao Paulo (UNIFESP). She did postgraduate studies with an emphasis on analytical chemistry and is a specialist in spectrometric techniques, such as FAAS, ICP-OES, GFAAS, LIBS, and ICP-MS. She studies chemical composition, mainly essential and trace elements, in several media (food, biological and environmental). Currently, she prioritizes studying alternatives for elemental enrichment of foods, aiming to produce functional foods. Considering this purpose, chemical speciation, bioaccessibility, total composition, and bioavailability studies are performed. CV

# REVIEW

# A Brief Assessment of the Bioanalytical Methods by using LC-MS/MS for the Quantitation of Melatonin: A Potential Biomarker for Sleep-Related Disorders

Gorav Monga[1#]* iD ✉, Sravani Yerram[2#] iD, Shailaja Koppula[3] iD, Rakesh Kumar Sindhu[1] iD, Sandeep Kumar[4]* iD ✉

[1]School of Pharmacy, Sharda University, Greater Noida, 201306, Uttar Pradesh, India
[2]Department of Regulatory Affairs, National Institute Pharmaceutical Education and Research (NIPER) Hyderabad, Telangana, 500037, India
[3]Department of Bio-analytical, Vimta Laboratory Ltd., Hyderabad, 500051, Telangana, India
[4]Department of Regulatory Affairs, National Institute Pharmaceutical Education and Research (NIPER) Hyderabad, Telangana, 500037, India

#The authors contributed equally. *Corresponding Authors.
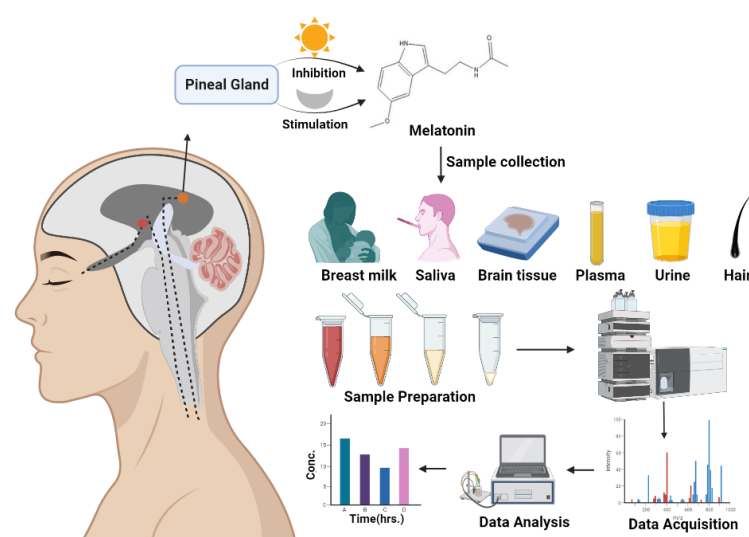
Due to its better sensitivity and selectivity, liquid chromatography with tandem mass spectrometry is the preferred choice for the quantification and identification of biomarkers, parent molecules/ metabolites in human saliva, plasma and urine etc. All such quantification methods for melatonin in biological matrices have been summarized. Melatonin is considered as a potential biomarker for circadian rhythm disturbance related disorders such as cancer, depression, insomnia, etc. Accurate quantification of melatonin is very challenging and critically depends upon the reproducibility and ruggedness of the analytical method. LC-MS/MS technique is considered as the preferred method of analysis for melatonin as compared to immunoassays. Most of bioanalytical melatonin quantification methods consist of, extraction from the biological matrix analyzing by LC-MS/MS. Our review shows that LC-MS/MS is a rugged and dependable instrument for the robust and precise quantitation of melatonin. This review compiles key elements like extraction procedure, linearity range, and chromatographic conditions.

**Keywords:** Melatonin, LC-MS/MS, bioanalysis, biological matrix/matrices, endogenous molecule

**List of Abbreviations**

| | |
|---|---|
| AA | Ammonium acetate |
| ACN | Acetonitrile |
| AF | Ammonium Formate |
| API | Atmospheric Pressure Ionization |
| CAS No. | Chemical Abstracts Service Number |
| CC | Calibration Curve |
| ESI | Electrospray Ionization |
| FA | Formic Acid |
| IPA | Isopropyl Alcohol |
| IUPAC | International Union of Pure and Applied Chemistry |
| LC | Liquid Chromatography |
| LC-MS/MS | Liquid chromatography with tandem mass spectrometry |
| LLE | Liquid–liquid extraction |
| Log P | Partition coefficient |
| mM | milli-Molar |
| MPA | Mobile Phase A |
| MPB | Mobile Phase B |
| ng mol$^{-1}$ | Nano gram per mole |
| pH | logarithm of the reciprocal of the hydrogen ion activity |
| pKa | Dissociation Constant |
| PK | Pharmacokinetic |
| pg mol$^{-1}$ | Pico gram per mole |
| PP | Protein precipitation |
| SPE | Solid-phase extraction |
| SPME | Solid phase micro extraction |
| UPLC | Ultra-Performance Liquid Chromatography |

## INTRODUCTION

Melatonin is a naturally occuring indole amine, which is chemically identified as N-acetyl-5-methoxytryptamine (Figure 1). The human body has many sources for the production of melatonin. Its physicochemical and pharmacokinetic properties are listed in Table I. In humans, the pineal gland is the major source of melatonin secretion however ocular light exposure hinders this. This secretion and inhibition process is controlled by the hypothalamic suprachiasmatic nucleus hamster clock.[1] The suprachiasmatic nucleus of the hypothalamus is the biological clock that modulates melatonin production and secretion over the full day span of 24 h.[2]

Melatonin levels are generally increased during the night hours, but these levels start dropping with the progression of the morning and decrease further throughout the day. Raised night levels of melatonin facilitate target organs to enter into an appropriate homeostatic metabolic rhythm helping the human body to protect itself from developing various diseases.[3] Therefore, subjecting the body to light at night may result in a disturbance in the production and secretion of melatonin hence disrupting the circadian rhythm. The human body has specific receptors for melatonin through which it regulates various physiological functions.[4] Apart from the pineal gland, other organs that synthesize melatonin are gastrointestinal-tract, lymphocytes, bone marrow and, skin.[5]
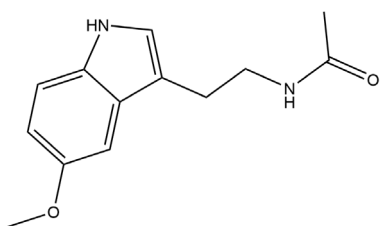
**Figure 1.** Melatonin chemical structure.

Plants have a different synthesis pathway of melatonin than animals. In plants, decarboxylation of tryptophan happens first, followed by hydroxylation resulting in the formation of serotonin. In animals, hydroxylation of tryptophan happens first followed by decarboxylation leading to serotonin formation. Serotonin is further acetylated and methylated to form melatonin.[6]

To start the production of melatonin, tryptophan serves as a starting molecule in cell species, followed by other steps like decarboxylation, methylation, hydroxylation, acetylation, etc. However, the order in which these steps take place varies from species to species. Serotonin first undergoes acetylation followed by methylation to form melatonin. The synthesis of melatonin is represented in Figure 2.
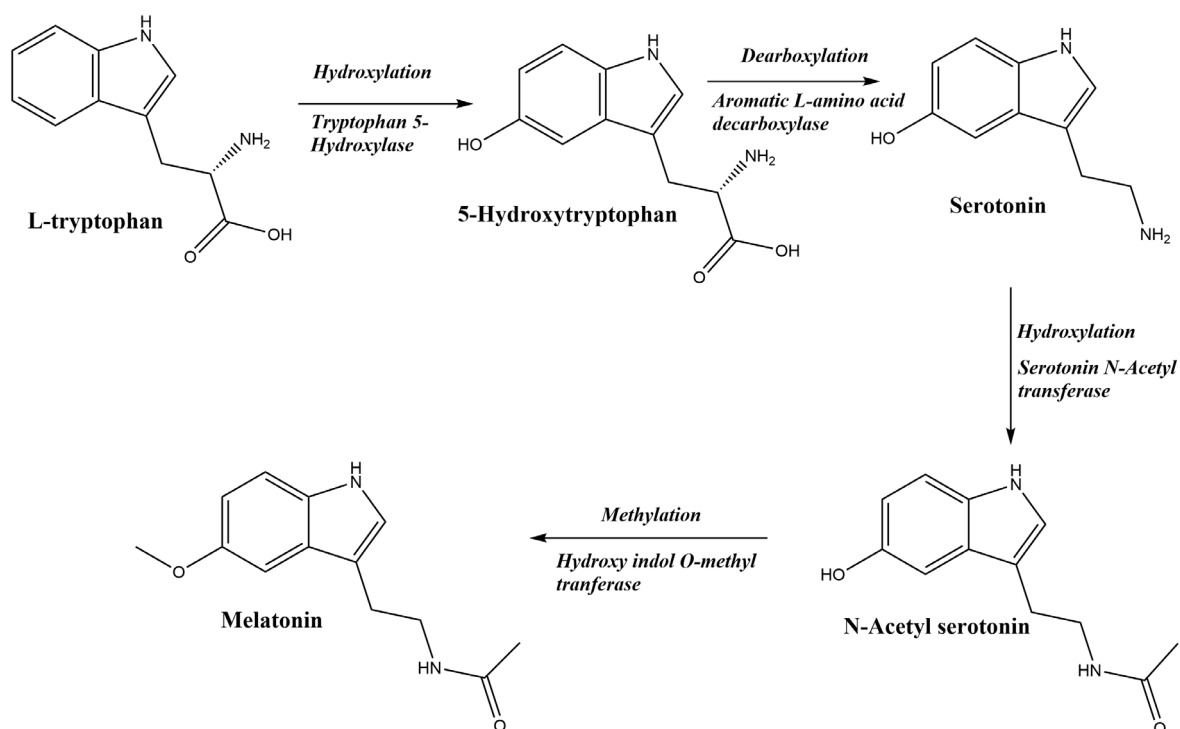


**Figure 2.** Synthesis of melatonin.

Melatonin is an endogenous hormone and potent neurotransmitter that helps regulate circadian rhythm and sleep. Modulation of the body temperature, hormone levels, sleep, and metabolism is done by the biological clock (also called as inner clock) by changing the physiology as per the different durations of the day.[7] Disturbance in this inner clock may lead to grave consequences for mental as well as bodily well-being.[8]

For example, the scientific evidence advises that sleep-wake cycles affect the hormone regulation and showing misaligned behavioural models (e.g., shift workers), so, it results by governing the risk of type 2 diabetes, obesity, cancers, and coronary diseases.[9,10]

A recent study has demonstrated that youngsters with disturbance in circadian cycles are more prone to develop drug and or alcohol abuse.[11,12] Learning issues and cognitive impairments.[13] Since the circadian rhythms regulate various hormone levels including melatonin, such hormones can be used as biological markers or pharmacodynamic markers for diseases caused by a disruption in the circadian rhythms.

Melatonin is commonly used in the treatment of sleep disorders such as insomnia and jet lag, for the reestablishment of circadian rhythms in cases of blindness and shift works. It has also found application in the prevention of developing cancer, as adjuvant therapy in cancer, and to slow down neurodegenerative diseases. Melatonin is also a highly effective antioxidant and free radical scavenger. One of the most studied actions of melatonin is its antitumor effects, which include antiangiogenic effects in several types of tumors. Additionally, melatonin plays an important role in regulating glucose metabolism and has been found to have significant anti-proliferative and apoptotic effects on various cancer cells. This hormone is also known for its pharmacological action in reducing oxidative conditions, as well as its ability to reduce inflammation and modulate immune responses (Figure 3).
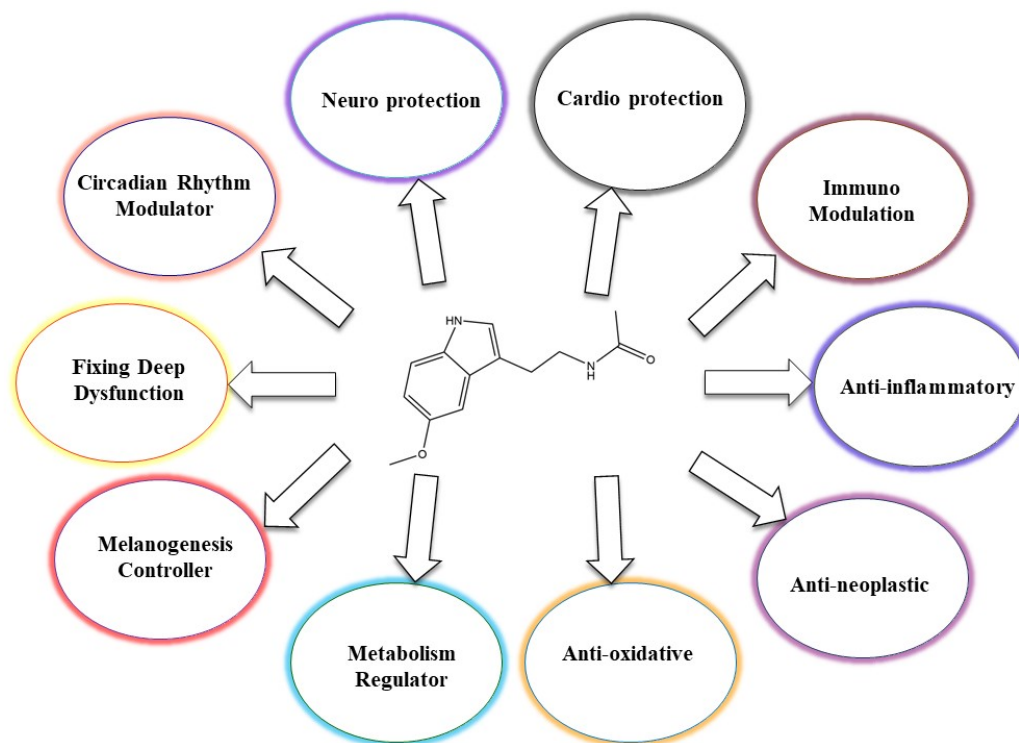


**Figure 3.** Schematic overview of other main functions of melatonin.

There are several sample types which can be used for the measurement of melatonin as well as testosterone, for example blood,[14-16] urine,[17,18] and saliva[19,20]. However, due to the pain free and ease of sampling, saliva is the most desired sample type.[21] Numerous published literature studies show that melatonin, testosterone, and cortisol all have well established correlations between hormone levels of serum versus saliva.[22-24]

The success of any treatment solely depends upon the drug's method of action, the patient's trust in the treatment (hence religiously following the regimen), and the optimum drug level in the blood. Bioanalytical methods are best suited to check the drug level in the biological matrices and also to evaluate patient adherence.

These bioanalytical methods have a noteworthy role to play in various therapeutic drug monitoring studies, toxicology or pharmacological evaluation of bioavailability, and PK (pharmacokinetic) evaluation.[25-27] Before subjecting the bioanalytical method to such usage, it has to be fully assured that the method is

fit for the intended analysis by appropriate validation experiments. Bioanalytical method validation and study sample analysis (ICH M10) provide recommendations for biological and chemical drug quantification and their application in the analysis of study samples. However, if any significant changes in method validation approach applicants can consult their respective regulatory authorities by providing proper justification. Various regulatory specific guidelines for bioanalytical method validation are published and updated from time to time by regulatory agencies like Food and Drug Administration and Therapeutic Goods Administration[25] European Medicines Agency.[28]

For various non-clinic and clinic usage, precise and accurate quantification of endogenous compounds is of utmost importance. For absolute quantification, the standard curve needs to be prepared in the same matrix as that of the unknown samples, to nullify the difference in extraction recoveries and the matrix effect. However, for endogenous compounds, it's not feasible to get a drug free matrix due to the endogenous nature of the drug.

LC-MS/MS analyses are a crucial aspect of bioanalytical research in pharmaceutical industry. However, one concern that arises in these analyses is the potential matrix effects, which can result in erroneous results. To address this concern, several approaches are used namely, surrogate matrix, surrogate analyte, background subtraction, and standard addition.

Surrogate matrix is prepared by stripping off the endogenous drug using some common adsorbent (like activated charcoal) to generate drug-free matrix which are then used to prepare calibration curve standards.[29-31] During charcoal stripping, this has to be ensured that all the charcoal particles are efficiently removed before spiking with analytes of interest. This may lead to significant false reduction of the quantified analyte concentration if not done efficiently.

The use of surrogate analyte approach in method development is easy when there is availability of stable-isotope-labeled standards. On the other hand, the surrogate matrix method requires extensive initial method development efforts; however, the benefit is that it simplifies sample analysis in the long term.[32]

The use of the standard addition method offers the advantage of utilizing the identical matrix of each study sample to construct its own calibration curve. Additionally, this method enables direct quantification of endogenous analytes, without requiring manual subtraction of background peak areas.

On the other hand, the surrogate matrix approach involves using different matrices, including artificial, stripped, and neat matrices, as substitutes for the actual matrix.[33] The measurement of melatonin in serum/plasma is further difficult due to 'Melatonin' being an endogenous substance with sub-nanogram levels in biological fluids, imposing serious challenges in developing and validating a highly sensitive bioanalytical method using. This issue has been addressed using water[34] and charcoal stripped plasma[35] as a surrogate matrix to prepare a standard curve.

Two major challenges are generally faced in melatonin quantification – basal melatonin levels (due to endogenous nature) and the desired sensitivity. The melatonin levels in the human body are very dynamic and are not same in day and night. So, blood/plasma collected for the preparation of standard and quality control samples have varying degree basal melatonin level which will give erroneous quantification and QC failure issues. The use of charcoal stripped matrix helps to get rid of this issue. Also, the correct basal value estimation for the clinical trial or patient samples (which are normally in sub nanogram levels) is very important to understand the requisite prescription dose for the patient. Hence, the sensitivity of the quantification method becomes further important.

In recent times, various bioanalytical techniques have been reported by overcoming the imposed challenges to improve the melatonin quantification using the powerful quantification instruments like LC-MS/MS. The main aim of this review article is to collate the various published LC-MS/MS based melatonin bioanalytical quantification methods in different biological matrices like serum, plasma, milk and saliva etc. Accordingly, this review has been performed by doing a literature search using web of science, Google scholar and PubMed. The keywords used are melatonin, biological matrix/matrices, LC-MS/MS, mass spectrometry, bioanalysis, validation, pharmacodynamics, pharmacokinetics. Physicochemical and pharmacokinetic properties of melatonin were given in Table I.

**Table I.** Melatonin physicochemical and pharmacokinetic properties

| Physicochemical Properties | |
|---|---|
| Chemical Composition | $C_{13}H_{16}N_2O_2$ |
| IUPAC Name | N-[2-(5-methoxy-1H-indol-3-yl)ethyl] acetamide |
| Physical Description | Solid |
| Color/Form | White-cream to yellowish crystalline powder |
| Melting Point | 117 °C |
| Solubility | >34.8 [µg mL$^{-1}$] (The mean of the results at pH 7.4) |
| LogP | 1.6 |
| PKa | 16.51 and -0.69 and is uncharged in the entire pH range |
| Mol. weight | 232.28 g mol$^{-1}$ |
| CAS No. | 73-31-4 |
| Pharmacokinetic Properties | |
| Half-life | 35 to 50 minutes |
| Majorly metabolized | Liver |
| Oral bioavailability | 3-15% |
| Major route of elimination | Urine |

**Types of Extraction Methods Used in Sample Preparation**

Sample clean-up is another way to enhance the extraction efficiency of any biological method resulting in better sensitivity and specificity. Various samples like liquid-liquid extraction, protein precipitation and solid phase extraction are the commonly employed ones for the sample cleanup prior to LC-MS analysis.[36]

*Solid-phase extraction (SPE)*

SPE is an extractive technique employing a solid bed in the form of a cartridge which acts as an extraction or separation media when liquid and/or treated matrix samples containing desired analytes are passed through it under the influence of positive or negative pressure. It is thus far the most effective and reliable extraction procedure especially for the separation of analytes of interest from the complex matrices like blood, tissues, plasma or urine. This technique not only separates the unwanted interferences from the desired analyte but a very effective way of concentrating the analyte also resulting in the enhanced method sensitivity especially required for the complex molecules like melatonin. Out of the 21 methods reported in the compilation Table II, 7 methods have employed solid phase extraction for melatonin sample clean-up.

*Liquid–liquid extraction (LLE)*

LLE is an extraction technique where the analyte gets partitioned between the two immiscible solvents based on its affinity resulting in its separation. This extraction technique is generally used in case of less complex matrices like saliva. Out of the 21 methods reported in the compilation Table II, 8 methods have employed LLE for melatonin sample clean-up. The biggest disadvantages of LLE include the use of large solvent volumes. Also, the organic solvents generally used for LLE are highly carcinogenic, resulting in a health hazard for the user.

### Protein precipitation (PP)

Protein precipitation is the desired method of extraction, especially for the discovery samples where least method developments are desired. Out of the 21 methods reported in the compilation Table II, 4 methods employed protein precipitation for melatonin sample clean-up. PP is a simple, fast and cost-effective extraction method as the precipitation is done by using commonly available laboratory reagents like acetonitrile or trifluoroacetic acid, or ammonium sulfate. PP has relatively poor sample cleanup and therefore, Due to the presence of phospholipids and oligosaccharides that are not completely removed, it is connected with high levels of ion enhancement or ion suppression. The only way to resolve high levels of ion enhancement or ion suppression is to use a deuterated IS that co-elutes with its respective analyte. As a result, protein precipitation was deemed the best method for estimating 19 analytes simultaneously in breast milk using LC-MS/MS.[37]

### Solid phase micro extraction (SPME)

SPME is a modern and highly sensitive method of sample preparation that does not require a solvent. This innovative technique operates on the principles of adsorption and absorption, followed by desorption. Out of the 21-method reported in the compilation Table II, one method has been employed SPME for melatonin sample clean-up.

Obtaining precise, sensitive, accurate and results in analysis of samples can be challenging due to the complexity of sample matrices. To mitigate sample interference effects from the environment and enhance the detection of the main analyte, prior to analysis it is crucial step to integrate suitable sample preparation method. There are some alternative and more advanced sample preparation method discovered to achieve the maximum efficiency of the main analyte of interest. Presently, there are multiple sample preparation techniques in use including, liquid-phase micro-extraction, magnetic solid-phase extraction, dispersive solid-phase extraction and stir-bar sorptive extraction and QuEChERS (quick, easy, cheap, effective, rugged, and safe), Microextraction in packed sorben, Stir-Bar sorbent extraction and Fabric phase sorptive extraction. These advanced extraction methods were used in the detection of samples of breast milk and cow milk using LC-MS/MS techniques. But no such method has been reported with respect to melatonin determination with LC-MS/MS.[38]

Till date, no such systematic review has been done for the measurement methods of melatonin in biological matrices using LC-MS/MS. Table II represents published assays covering main aspects of internal standard, sample extraction, mobile phase, CC range, and instrument used for the LC-MS/MS quantification of the melatonin in complex biological matrices.[38] The prepared pie chart indicates contribution of the use of each sample preparation techniques (Figure 4) as per the available literature.
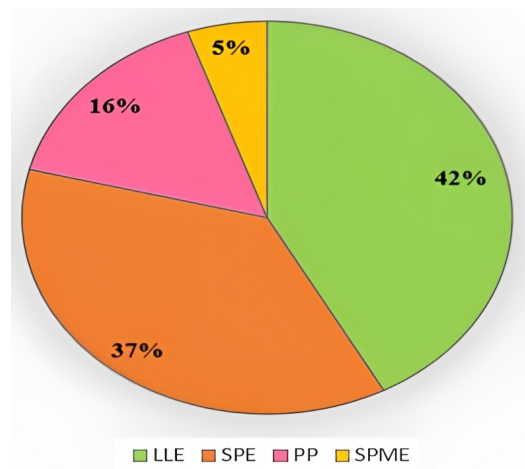


**Figure 4.** Pie chart representation of mostly used methods for sample preparation (LLE: Liquid-Liquid Extraction, SPE: Solid-phase extraction, PP: Protein precipitation, SPME: Solid phase micro extraction).

**Table II.** Compilation of the published assays for the quantitation of melatonin

| S. No | Matrix | Internal standard | Sample Extraction | Mobile Phase | Instrument | Chromatographic conditions | Calibration Curve Range | References |
|---|---|---|---|---|---|---|---|---|
| 1 | Human Plasma | Melatonin-D4 6-OH-Melatonin-D4 | PP and SPE | MPA: 7.5 mM AF in $H_2O$ pH 2.65<br><br>MPB: 0.1% FA in ACN | Acquity UPLC coupled with Xevo TQ-S with electrospray ionization source. | Column: Acquity BEH C18, 130 Å, 1.7 µm, 2.1 × 100 mm column (Waters)<br>Column temp.: 35 ºC<br>Autosampler temp.: 10 ºC<br>Injection Volume: 10 µL | Lowest concentration 2.2 nM for serotonin to 1.0 pM for 6-OH-Melatonin | 35 |
| 2 | Human Saliva | Not available | LLE | NA | shimadzu Nexera X2 UPLC coupled with Sciex QT6500 mass spectrometer | – | 0.78 to 100 pg mL$^{-1}$ | 39 |
| 3 | Breast Milk | Not used | PP | Mode: Isocratic 0.1% FA in ACN and 0.1% FA in $H_2O$ (Ratio not found) | 4000 QTRAP from Sciex | Column: Kinetex C8 column (30 × 3 mm, 2.6 µm)<br>Column temp.: 45 °C<br>Autosampler temp.: 5 °C<br>Injection Volume: 4 µL | 10 to 500 ng mL$^{-1}$ | 40 |
| 4 | Human Milk | Melatonin-D4 | PP using ACN | MPA: 2 mM AF in $H_2O$<br><br>MPB: 0.1% FA in ACN | Waters 2D UPLC equipped with TQ-XS triple quadrupole mass spectrometer | Column: ACQUITY UPLC HSS T3 column (50×2.1 mm, 1.8 µm)<br>Column temp.: 45 °C<br>Injection Volume: 30 µL | 1 to 1000 pg mL$^{-1}$ | 41 |
| 5 | Human Urine | Melatonin-D4 | SPE | MPA: 0.1% FA in $H_2O$<br><br>MPB: 0.1% FA in ACN | Agilent 1290 LC coupled to a 6500 QTrap equipped with an electro spray ionization source | Column: Kinetex® C18 column (50 × 2.1 mm, 2.6 µm) from Phenomenex<br>Injection Volume: 20 µL<br>Flow rate: 600 µL/min | Melatonin: 7.5 to 500 pg mL$^{-1}$<br>6 Hydroxy melatonin: 375 to 25000 pg mL$^{-1}$ | 37 |

**Table II.** Compilation of the published assays for the quantitation of melatonin (continuation)

| S. No | Matrix | Internal standard | Sample Extraction | Mobile Phase | Instrument | Chromatographic conditions | Calibration Curve Range | References |
|---|---|---|---|---|---|---|---|---|
| 6 | Human Salivary Samples | Melatonin-D4 Cortisol-D4 | LLE | MPA: 2 mM AA in $H_2O$<br><br>MPB: 0.1% FA in ACN | Agilent 6490 ESI source in positive mode. | Column: C18 2.1×50 mm 2.6 µm Kinetex<br>Injection Volume: 20 µL<br>Flow rate: 250 µL/min<br>Run time: 6 min | Melatonin: 2.15–430 pmolL$^{-1}$ Cortisol:0.14–27.59 nmolL$^{-1}$ | 42 |
| 7 | Rat Serum Samples | D4-Melatonin D4 -Cortisol L-Thyroxine-13C6 | LLE | MPA: 0.1% FA in $H_2O$<br><br>MPB: 0.1% FA in $CH_3OH$ | Agilent 6490 LC-MS/MS with electrospray ionization source | Column: Eclipse Plus C18 column 4.6 mm × 100 mm, 3.5 µm particle Agilent ZORBAX<br>Autosampler- 4 ºC<br>Injection Volume: 15 µL<br>Flow rate: 1 mL/min | Melatonin: 0.004-0.5 ng mL$^{-1}$ Cortisol, T3, T4 and Testosterone: 0.4-50 ng mL$^{-1}$ | 43 |
| 8 | Saliva Plasma | Cortisol-D4 Melatonin-D4 | SPE | NA | Xevo TQ-MS triple in positive ionization mode. | Column: Phenomenex® Luna Phenyl-Hexyl 2.0×100 mm, 3 µm<br>Run time: 6.5 min | In saliva Melatonin: 15–2000 pmolL$^{-1}$ Cortisol: 0.60–75 nmolL$^{-1}$. In plasma: Melatonin:15–2000 pmolL$^{-1}$ Cortisol: 40–5500 nmolL$^{-1}$ | 44 |
| 9 | Human Saliva | Melatonin-D4 | SPME | 50% $H_2O$ and 50% ACN | API 4000 from AB Sciex, in positive ion mode | Column: Inertsil ODS-3 column (50 mm × 2.1 mm, 5 µm)<br>Column temp.: 30 °C<br>Flow rate:0.2 mL/min | 0.2 – 50 pg mL$^{-1}$ | 45 |
| 10 | Dog Plasma | Desvenlafaxine | LLE with ethyl acetate | 40% of $CH_3OH$: 60% of 5 mM AA: 0.1% FA | AB Sciex | Column: C18 Luna (2.0×50 mm, 3 µm)<br>Column temp.: 35 °C<br>Autosampler: 4 °C<br>Injection volume: 10 µL<br>Flow rate: 0.20 mL/min | 0.020–10 ng mL$^{-1}$ | 46 |

(continues on the next page)

**Table II.** Compilation of the published assays for the quantitation of melatonin (continuation)

| S. No | Matrix | Internal standard | Sample Extraction | Mobile Phase | Instrument | Chromatographic conditions | Calibration Curve Range | References |
|---|---|---|---|---|---|---|---|---|
| 11 | Human Milk Samples | 7-D Melatonin | SPE | MPA: 80% of 5 mM AF in $H_2O$ and 20% $CH_3OH$<br><br>MPB: $CH_3OH$ | Agilent 6460 with ESI source | – | 1 to 150 pg mL$^{-1}$ | 47 |
| 12 | Oral Fluid Samples | Melatonin-D7 Cortisone-D7 Cortisol-D4 | Cotton swab with a rotator, Samples were extracted and purified, separated by using a Turbo Flow | MPA: Water, ACN and (mixture-1 containing 45% of ACN ,45% of IPA and 10% dimethyl ether) and mixture-2 consists of 0.1% of ammonium hydroxide in ACN)<br><br>MPB: 1.5 mM AF: 30 mM FA in $CH_3OH$and $H_2O$ | LC-MS/MS with ESI source. | Hypersil Gold column 50 mm × 2.1 mm, 3 μm | Melatonin :0.004 to 0.431 Cortisone: 5.5 to 277.4 Cortisol: 0.55 to 27.59 nmolL$^{-1}$ | 48 |
| 13 | Salivary Samples | Melatonin-D7 | To a diluted saliva sample, internal standard was added into the auto sampler vial and injected directly. | MPA: 0.1% FA in $H_2O$<br><br>MPB: 15% $CH_3OH$ in ACN with 0.1% FA | API-3200 tandem mass spectrometer Analyst software. | Column: Symmetry C8 (150×3.9 mm internal diameter; 5 μm) Injection Volume: 50 μL Flow rate: 0.8 mL/min Run time: 8 min | 3.91- 1000 pg mL$^{-1}$ | 49 |
| 14 | Sea Lamprey Brain Tissues | Melatonin-D7 | SPE | MPA: 1 mM of perfluorohexanoic acid in water<br><br>MPB: ACN | Shimadzu LC with Quattro micro mass spectrometer from waters. | – | 0.5 -100 ng mL$^{-1}$ | 27 |

(continues on the next page)

**Table II.** Compilation of the published assays for the quantitation of melatonin (continuation)

| S. No | Matrix | Internal standard | Sample Extraction | Mobile Phase | Instrument | Chromatographic conditions | Calibration Curve Range | References |
|---|---|---|---|---|---|---|---|---|
| 15 | Human Plasma | N-acetyl tryptamine | LLE with dichloromethane | MPA: 2 mM AF in $H_2O$ with 0.1% FA <br><br> MPB: ACN | API 6460 LC-MS/MS in positive electro spray ionization mode. | Column: ZORBAX Eclipse XDB C18 (4.6 mm× 150 mm, 5 µm) <br> Column temp.: 20 °C <br> Injection Volume: 10 µL <br> Flow rate: 0.5 mL/min <br> Runtime:11 min | 1–5000 pg mL$^{-1}$ | 34 |
| 16 | Human Plasma | Melatonin-D4 | LLE | MPA: 95% of 0.2% acetic acid in $H_2O$ and 5% of ACN <br><br> MPB: 5% of $H_2O$ and 95% of ACN | TSQ coupled with an Ion Max HESI source. | Waters Symmetry Shield RP18 column (2.1×100 mm, 3.5 µm) <br> Column temp.: 50 °C <br> Autosampler temp.: 5 °C <br> Injection volume: 20 µL | Melatonin: 1165–116500 pg mL$^{-1}$ <br> N-acetyl serotonin: 10.95 – 1095 pg mL$^{-1}$ | 50 |
| 17 | Human Saliva | Melatonin-D4 Cortisol-D4 Testosterone-D3 | LLE | MPA: 2 mM AA with 0.1% FA in $H_2O$ <br><br> MPB: 2 mM AA and 0.1% FA in $CH_3OH$ | Agilent 6460 operated in positive ion mode with Electrospray ion source | Column: Kinetex C18 2.1 mm × 50 mm 2.6 µm <br> Column temp.: 40 °C <br> Autosampler temp.: 8 °C <br> Flow rate: 0.5 mL/min | Melatonin: 15.0–579.4 pmolL$^{-1}$ <br> Cortisol: 0.5–90 nmolL$^{-1}$ <br> Testosterone: 15.6–622.8 pmolL$^{-1}$ | 51 |
| 18 | Human Saliva | Melatonin-D7 | SPE | MPA: 20 mM AA in 90% $H_2O$ and 10% $CH_3OH$ <br><br> MPB: 5 mM AA in 50% $H_2O$ and 50% $CH_3OH$ | Finnigan AQA mass with an electrospray ionization source | Column: silica-based octadecyl silica (ODS) column Capcell Pak C18 AQ, dp 5 µm, 2× 150 mm; Shiseido <br> Column temp.: 40 °C | 5–1000 pg mL$^{-1}$ | 52 |
| 19 | Human Saliva | 7-D-Melatonin | SPE | 40 to 95% $CH_3OH$ for 3 min and 95% $CH_3OH$ for 2 min | API 2000 with an APCI source | Waters Symmetry C8 150 mm× 3.9 mm | 3–300 pg mL$^{-1}$ | 19 |

(continues on the next page)

**Table II.** Compilation of the published assays for the quantitation of melatonin (continuation)

| S. No | Matrix | Internal standard | Sample Extraction | Mobile Phase | Instrument | Chromatographic conditions | Calibration Curve Range | References |
|-------|--------|-------------------|-------------------|--------------|------------|----------------------------|-------------------------|------------|
| 20 | Human Serum | N-acetyl tryptamine | On-Line Sample Extraction | 95% of ACN and 5% of 5 mM AF pH 4 | Triple quadrupole mass spectrometer with HP1100 variable wavelength UV detector | Oasis® HLB extraction cartridge Waters column (2.1×20 mm) Flow rate: 0.2 mL/min Run time: 9 min | 0.500 to 200 ng mL$^{-1}$ | 53 |
| 21 | Human Plasma | Melatonin-D7 | LLE | 17.5% of ACN in 25 mM FA in $H_2O$ | LC/MS system HP 1100 mass spectrometer with electrospray interface. | – | Melatonin: 4 to 80 ng mL$^{-1}$ Hydroxy melatonin 20 to 400 ng mL$^{-1}$ | 54 |
| 22 | Human Hair | d4-melatonin, d3-N-acetyl-serotonin, d4-6-hydroxymelatonin, d4-6-sulfatoxymelatonin | SPE | MeoH: 5 mM ammonium acetate (95:5% V/V) | ABI 3200 QTRAP tandem mass spectrometer-ESI positive ionization mode | Column: ODS Plastisil C18 (5 μm, 150 mm × 4.6 mm; Dikma) Column temp.: 25 °C Volume: 10 μL Flow rate: 200 μL | 0.1 pg/mg to 1.0 pg/mg | 55 |

**Method Validation Parameters**

In the literature various studies were analysed for the compilation of the bioanalytical method validation parameters depicting that the method developed and used were reliable and reproducible for intended use.

Selectivity is the ability of an analytical method to differentiate and measure the analyte, interfering substances and internal standard. Magliocco et al. depicted the method to be very selective as no interfering peaks were observed at the retention time of the compound in water and urine matrix which were collected from different volunteers in late night hours,[37] Zhao et al., reported the non-observance of interfering peaks at the RT of melatonin and used Internal standard in the tested blank matrix.[39]

Carry-over is the appearance of the analyte from previous injection in the current chromatogram. Karunanithi et al., and Fustinoni et al., reported carryover problem was not observed.[40,41]

Specificity is the capability of the developed method to differentiate the analyte from its related substances. Karunanithi et al., reported specificity by analysing 20 blank milk samples. The used blank milk batches were first treated with activated charcoal for overnight resulting in the absorption of the matrix melatonin hence making them free from melatonin The melatonin free milk samples (n =20) were analysed for specificity.[40]

Extraction Efficiency/Extraction Recovery is the amount of the analyte recovered after sample clean up processing steps of the extraction method. The percent efficiency/recovery of analyte was calculated with respect to response of the same amount of standalone standard analyte. Demeuse J. et al., reported recovery or the extraction efficiency above 70%. Monfort et al., reported the extraction recovery ranging from 87.3 to 110.8% with % CV ranging from 2.3 to 14.8%.[42,43]

The matrix effect is generally evaluated to monitor the effect of different matrix or sources. Monfort et al., reported the Matrix effects variance RSD of 11.4%.[43] Magliocco et al., reported the mean IS-normalized matrix effects between 100–109% (RSD ≤ 5%) indicating absence of any significant matrix effect.[37]

*Method Precision and Accuracy*

Weiqi Jin et al., depicted inter-day and intraday batch accuracy and precision on three validation batches. Each batch consisted of six replicates of Quality control samples in human breast milk samples at higher, mid and low levels. The intra and inter-assay precision depicted 4.1% and 6.8% RSD respectively.[44] Magliocco et al., reported the accuracy data within the acceptance criteria range for melatonin and 6-hydroxymelatonin 92.4–104.6% and 94.0–102.6%, respectively (85–115% of the theoretical value). Precision values for all QC samples of both analytes were within 15%. Good repeatability was depicted i.e., 3.4–10.4% for melatonin and 4.2–7.9% for 6-hydroxymelatonin.[37]

Reinjection reproducibility, as the name suggests is assessed by reinjecting a run at low, middle and high QCs after storage for appropriate duration and temperature conditions. The precision and accuracy of the reinjected QCs decides the validity of the processed samples. Weiqi Jin et al., reported re-injection of processed-sample after 48 h and compared with first analysis i.e., 0 h. The accuracy was depicted to be within ±12.3% deviation, and the precision was depicted to be 2.8% RSD.[44]

Dilution integrity depicts the method ruggedness in case the matrix sample needs to be diluted, if the sample volume is not sufficient or it's required to be diluted to bring within the calibration curve range Monfort et al., reported dilution integrity, to affirm the sample integrity if samples are to be diluted, at dilution factors of 10x and 100x. The accuracy was depicted to be within (85.0–113.5%) after dilution and precision was shown to be (1.4 –10.1%).[43]

Stability of the analyte in the matrix is evaluated using low and high concentration quality control samples. Aliquots of the low- and high-quality (and sometimes mid also) control samples are analysed at time zero (freshly) and after the stipulated storage requirement. The mean concentration at each quality control samples level should be within ±15% of the nominal concentration.

Monfort et al., reported short-term stability at room temperature for one day and at -20 °C for 14 days. Long term stability was evaluated by analysing lower quality control samples and high-quality control

samples after storing them at -80 °C for 30 days. Freeze-thaw stability was evaluated for 3 cycles of freezing at -80 °C and unassisted thawing at room temperature and all the results were found to be within the acceptance criteria.[43] Zhao et al., depicted the melatonin stability in dog plasma. The short-term plasma stability at room temperature was depicted to be 4 hr and long-term plasma stability at -70 °C was depicted to be for 25 days. Also, the sample were found to be acceptably stable after three freeze thaw cycles and in processed samples at 4 °C for 24.[39]

## DISCUSSION

Some distinctive procedures are covered in this section to demonstrate variations in the bioanalysis of melatonin. Firstly, quantifying melatonin in various biological matrices that is, endogenous substances with ultra-low levels make it difficult. The blank of the biological matrix is not "blank". This leads to a serious issue in the validating a method by LC-MS/MS which appeared to be difficult to removal by using the regular procedures for overcoming the same water used as calibration matrix An-Qi Wang et al. (2011)[34] and in few cases, charcoal pretreatment Duraisamy Karunanithi et al. (2013)[47] was carried out to eliminate interference.

Sebastian Hartter et al. (2001) reported a bioanalytical method for estimating melatonin and its major metabolite in plasma, including enzymatic hydrolysis and one-step liquid–liquid extraction using 17.5% ACN in FA in $H_2O$ and separation was done by using Luna C-18 column. As reported in Table II, the method was used for the plasma sample analysis from the healthy volunteers after administering a single 35 mg dose via the oral route. The $C_{max}$ for melatonin & 6-hydroxymelatonin was observed to be 19.2 ng mL$^{-1}$ & 694 ng mL$^{-1}$ respectively. With a $T_{max}$ of 1.5 hours for both analytes after melatonin intake.[54]

Shuming Yang et al. (2002) reported a fast measuring of melatonin in human serum by LC-MS/MS. N-acetyl tryptamine was used as ISTD. It applies ESI–MS–MS detection along with online preparation of the samples. Using this method, unextracted serum samples were injected directly. The technique has a wide linear range, is precise and sensitive and has excellent reproducibility with a total run time of 9 minutes per injection. This method can be used for the pharmacokinetic study of melatonin in human serum and blood.[53]

The estimation of melatonin was reported by Kare Eriksson et al. (2003) using HPLC–MS/MS. The limit of quantification and limit of detection was 3.0 pg mL$^{-1}$ and 1.05 pg mL$^{-1}$ respectively. This reported method depicted better sensitivity and increased specificity for melatonin quantification in saliva samples and the results were observed to be more reliable than immunoassay.[19]

Motoyama et al. (2004) reported a bioanalytical method for direct estimation of endogenous melatonin using Mobile Phase A (MPA) as 20 mM of AA in 90% $H_2O$ and 10% $CH_3OH$ and Mobile Phase B (MPB) as 5 mM of AA in 50% $H_2O$ and 50% $CH_3OH$ using ODS C18 column. The developed method by Motoyama et al. was the very first method to perform direct quantification of endogenous levels of melatonin is human saliva samples using the column switching technique. The method depicts a good throughput due to its smaller run time resulting from the minimal sample pretreatment. The method has been validated for 5–1000 pg mL$^{-1}$ and can be very useful for melatonin clinical trials.[52]

The first method for estimation of melatonin and cortisone in saliva in a single run was reported by Jensen MA et al. (2011) Samples were extracted using liquid-liquid extraction.[51]

Melissa D. et al. (2011) reported a method by using nano flow LC-MS/MS and electro spray LC-MS/MS for estimation of melatonin and nor melatonin in human plasma by Gradient Elution using 95% of 0.2% $CH_3COOH$ in $H_2O$ and 5% of ACN (95:5) in MPA and 5% of $H_2O$ and 95% of acetonitrile (5:95) in MPB. Waters symmetry shield RP 18 column was used for separation of human plasma by using liquid–liquid extraction. This method used nano-LC for sample injection and was validated over range of 11.65–1165 pg mL$^{-1}$ & 10.95–1095 pg mL$^{-1}$ for melatonin and N-acetyl serotonin respectively. The usage of nano-LC has resulted into enhanced sensitivity for endogenous melatonin levels up to sub-picogram levels.[50]

An-Qi Wang et al. (2011) validated bioanalytical method in plasma for melatonin by LC–MS/MS using water as a calibration matrix by using 2mM ammonium formate and 0.1% FA in $H_2O$ in MPA and ACN

in MPB and chromatographic separation was carried out on XDB C18 column manufactured by Agilent. Two complementary quality control approach were used to validate the method. The PA batches for low concentration (1 pg mL$^{-1}$ and 10 pg mL$^{-1}$) and potential matrix effect experiments were run using water as matrix whereas pooled plasma was used to perform PA batches and matrix effect at high concentration (50, 500 and 5000 pg mL$^{-1}$). The accomplished method was employed to plasma melatonin exogenous and endogenous levels quantification for dog samples.

The developed method was employed to check the PK profile of exogenous melatonin and daytime baseline level of endogenous plasma melatonin in beagle dogs after oral administration.[34]

Huiyong Wang et al. (2012) first reported an estimation of melatonin and neurotransmitters in brain tissues by LC-MS/MS. Separation was done by using a reversed-phase column with MPA as 1 mM of perfluorohexanoic acid in water and MPB as ACN. SPE Extraction method was used to extract and purify the analyte from the tissue of brain samples. Different types of solid phase extraction beds were tried during method development resulting in the extraction recoveries from 71.3 – 95.3%, however the best recovery was obtained using Bond-Elut C18 cartridges. The limit of detection for both the analytes were less than 200 pg mL$^{-1}$. The method described here is appropriate for quantifying norepinephrine, dopamine, 5-hydroxytryptamine and melatonin levels in biological samples with high accuracy, reproducibility and low inter and intra-day variation.[56]

Sohil A. Khan (2013) reported a LC-MS/MS technique for observing sleep disorders in children with melatonin concentrations in saliva. The separation was done by using a gradient mobile phase 0.1% FA in H$_2$O in MPA and 15% CH$_3$OH in ACN with 0.1% FA in MPB with C8 column. The method was found to be depicting no matrix effects and was successfully applied clinically for both children and adult samples for diagnosis purpose.[49]

First automated assay for the parallel estimation of melatonin, cortisone and cortisol in oral fluid samples was reported by Fustinoni S. et al. (2013) by LC/MS in saliva by using turbo flow system was operated by using 2 sets of mobile phases. The MPA consists of H$_2$O, ACN, mixture-1 (containing 45% of ACN, 45% of IPA and 10% DME) and mixture-2 (consists of 0.1% of NH$_4$OH in ACN). The MPB consists of 1.5 mM AF to 30 mM FA in CH$_3$OH and H$_2$O.[48]

This assay qualifies for all the checks of an ideal method like high-throughput, requirement of small specimen volumes with very minimal manual interventions. These characteristics along with the non-invasive sample collection (oral fluid) has led to its application in epidemiological studies.

Quantification of melatonin in milk was validated by using LC-MS/MS and reported by Duraisamy Karunanithi et al. (2013) in which solid phase extraction cartridges were used to purify dichloromethane before it was used to extract the samples.[47]

Earlier developed methods for melatonin quantification in milk samples using radioimmunoassay have severe selectivity concerns due to the cross reactivity from the milk components. Fluorescence detection with HPLC and GC-MS were found to be having good sensitivity but the method was time consuming due to the involvement of derivatization step.

This LC-MS/MS method was reported to be more selective and specific. Further a better LOD without the tedious derivatization can be obtained. This LC-MS method was employed for melatonin quantification of milk samples.

Huimin Zhao et al. (2015) developed a method for melatonin measurement in dog plasma, and the dog plasma samples were prepared using ethyl acetate as solvent by liquid-liquid extraction method and separation was done by using C18 column with isocratic mobile phase. The reported method has been employed to measure the melatonin in dogs. In all blank matrix samples, At the retention times of melatonin and IS, there were no endogenous compounds' peaks that could have caused any significant interference. The detected peak in plasma collected the day before administration accounted for less than 20% of the lower limit of quantification area. There was no carryover after upper limit of quantification injection.[46]

Ishizaki, et al. (2017) developed a sensitive, simple and rapid method to estimate melatonin using SPME equipped with LC-MS/MS. Chromatographic separation was done within 3 min by using an Inertsil ODS-3

column. This method was successfully applied to the analysis of saliva samples without any charcoal Peaks in pretreatment and interference. The reported method was applied to estimate the melatonin changes levels in saliva associated with lifestyle changes and light stimulation. This method can be considered as a helpful tool for the evaluation of sleep disorders and stress.[45]

M. van Faassen et al. (2017) reported a correlation between cortisol and melatonin in saliva and plasma. This is the primarily reported LC-MS/MS technique for comparison of melatonin in saliva and melatonin in plasma. The validation LC-MS/MS method for measuring cortisol and melatonin levels in healthy adults' free, total saliva and plasma. The results for saliva and plasma with respect to cortisol and melatonin were found to be satisfactory. Saliva collection through Salivette or passive drooling showed no significant difference; A substantial difference between salivary and free plasma melatonin (average, 36% higher), with salivary melatonin levels being, on, suggests that potential melatonin production in the salivary glands.[44]

Cristina Domenech-Coca, et al. (2019) reported an accurate analytical procedure for the assessment of the melatonin, testosterone, triiodothyronine, thyroxine and cortisol in serum. The samples of rat serum were extracted by using LLE and quantified by using HPLC coupled with tandem MS and separation was done by using MPA – 0.1% formic acid in Water and MPB – 0.1% formic acid in methanol. The established method has been used to examine the changes of testosterone, melatonin, thyroxine, cortisol and triiodothyronine in serum of rat by induced the light exposure.[43]

The application of this method holds high clinical significance as it enables the simultaneous assessment of hormones with dissimilar chemical structures, such as cholesterol derivatives and amino acid for the mood disorders and depressive illnesses.

Sunghwan Shin, et al. (2021) reported a method in saliva for estimation of melatonin and cortisol in single run & differentiated this method with immunoassays. SPE was used for the preparation of samples and analyzed using 2 mmol $L^{-1}$ ammonium acetate in water in MPA and acetonitrile with 0.1% formic acid in MPB and Chromatographic separation was done on XDB C-18 column. Compared with the immuno assays method, HPLC coupled with tandem MS method provides more reliable and more sensitive in the estimation of melatonin and cortisol in saliva.[42]

A newly developed high-throughput sensitive bio analytical validation method was reported by Weiqi Jin et al. (2021) which is sensitive, simple, fast and high-throughput for measuring melatonin in human milk and gives an appropriate platform to quantify human milk melatonin in large scale studies. This quantification may be very useful for the development of the infant mil formula who cannot be breastfed. This quantification method can be a reference gold standard for the human clinical research implying quantification of melatonin detection in milk samples.[41]

Estimation of 19 analytes simultaneously was validated by using HPLC coupled with tandem mass spectrometry published by Anaelle Monfort et al. (2021) and it successfully applied to samples of nursing women. This method is very useful due to its simple extraction method, allowing the measuring of multiple drugs over a 1:1000 x concentration range.[40]

Demeuse J. et al. (2021) published a sensitive procedure in saliva for the estimation of melatonin. It allows the estimation at day time with a high accuracy and selectivity. The experiments showed a recovery rate of 70% and matrix factor of over 90% for the analyte. Inter-run and intra-run accuracies ranged from 89% to 113%, and the Coefficient of Variations for both were between 1% and 7%. The limit of quantification is the lowest concentration at which it was possible to easily integrate the qualitative transition's peak was found to be 0.78 pg $mL^{-1}$.[39]

Philippe J. Eugster et al (2022) first time reported a procedure for the detection of serotonin and its main metabolites included melatonin in human plasma by using HPLC coupled with tandem MS. Samples extracted by using protein PP followed by solid phase extraction. Improved sensitivity allows the detection of serotonin and its metabolites including melatonin even at their lowest day time concentrations of 2.2 nM for serotonin to 1.0 pM for 6-OH-Mel.[35]

Minhui Zhu et al. (2022) reported a LC-MS/MS method for the accurate measurement of melatonin, glucocorticoids and its metabolites in human hair. The method was also aimed to investigate how the concentrations of these biomarkers are related to sleep state. The developed method can quantify six endogenous compounds in hair, including cortisol and cortisone, which are important stress biomarkers. While LC-MS/MS methods exist for other sample types, such as saliva, blood and urine, there is limited research on detecting melatonin in human hair. This developed LC-MS/MS method can simultaneously quantify melatonin, N-acetyl-serotonin, 6-O-melatonin, cortisol, and cortisone in human hair. The method had a convenient hair sample pretreatment procedure and high sensitivity with limit of quantification ranging from 0.1 pg/mg for melatonin to 1.0 pg/mg for cortisol and cortisone. Analysis of 65 undergraduates' hair samples revealed relationship between poor sleep quality and higher hair cortisone content. Further investigation of hair cortisone as a biomarker for long-term sleep state in a larger sample is warranted for future studies.[55]

Dermanowski et al. (2021) developed a method for the measurement of melatonin in plasma and saliva. Further a comparison under dim light for the measurement of melatonin was carried out, since it is perceived as the most precise objective bio-marker for determining the circadian phase. The LC-MS/MS validation was done as per the European medicine agency recommendations. From twenty-one volunteers between the ages of 26 and 54 plasma and saliva samples had been taken at five different times (between 8:00 PM and 12:00 AM). Melatonin concentration was measured by using LC-MS/MS. Dim light melatonin onset was defined as the time at which melatonin concentration was recorded in plasma and saliva surpassed 7 pg/mL and 20 pg/mL, respectively. The saliva/plasma melatonin concentration ratio was 2.87, and the correlation between plasma and salivary melatonin concentration was r = 0.764 (p < 0.001). Finally, the validated method of salivary melatonin determination enabled the dim light melatonin onset assessment with potential clinical implications in monitoring and diagnosing circadian rhythm disorders.[57]

Over the years the melatonin bioanalysis has evolved significantly. In the late 90s the achievable quantification limits were in ng/mL however due to significant advancements in MS technologies pg concentrations are being achieved comfortably. Earlier the quantification matrix being used was plasma or serum only even though the collection procedure for these matrices is being painful. However, with the advancement in instruments and better sensitivities, the pain-less source of matrices e.g., hair samples can also be used these days. Also, the extraction procedures have evolved significantly from protein precipitation, liquid- liquid extraction to SPE to SPME with better recoveries and least solvent wastage. In the upcoming years, bio analysts can witness the development of fully automated estimation with minimal human intervention for better reproducibility.

## CONCLUSION

Melatonin research is expected to advance significantly through the use of LC-MS/MS, a powerful analytical technique for precise and sensitive measurement of melatonin in biological samples. LC-MS/MS's capability to selectively detect and quantify melatonin in complex biological matrices, such as blood, urine, and saliva, offers the potential for more accurate measurements, even at low concentrations. This heightened sensitivity and selectivity may open up new opportunities for studying the diurnal rhythm of melatonin, investigating its physiological and pathological roles, and evaluating its therapeutic potential. This review describes various bio analytical methods developed and validated to estimate melatonin in various matrices such as serum, plasma, milk and saliva etc. The summary of review articles would help in the preparation of the latest bioanalytical methods. This review article presents various developed bioanalytical methods by using LC-MS/MS which covers key aspects of internal standard, sample extraction, mobile phase, CC range and instrument used. The application of LC-MS/MS has enabled tremendous quantitative capabilities in MRM mode with high sensitivity, selectivity and specificity. The usage of gradient programs helped in separation and quantification of drugs to prevent the matrix enhancement/suppression from the matrix compounds and to remove the analyte carry over from injection to injection. LC-MS/MS is a rugged and dependable instrument and it is extensively used for the quantification of melatonin because of its

shorter run time, sensitivity and selectivity. The review article provided a survey of various methods and its conditions to start new method development for melatonin.

**Conflicts of interest**

**Acknowledgements**

**REFERENCES**

(1) Simonneaux, V.; Ribelayga, C. Generation of the melatonin endocrine message in mammals: a review of the complex regulation of melatonin synthesis by norepinephrine, peptides, and other pineal transmitters. *Pharmacol. Rev.* **2003,** *55* (2), 325-395. https://doi.org/10.1124/pr.55.2.2

(2) Li, Y.; Li, S.; Zhou, Y.; Meng, X.; Zhang, J.-J.; Xu, D.-P.; Li, H.-B. Melatonin for the prevention and treatment of cancer. *Oncotarget* **2017,** *8* (24), 39896. https://doi.org/10.18632/oncotarget.16379

(3) Slominski, R. M.; Reiter, R. J.; Schlabritz-Loutsevitch, N.; Ostrom, R. S.; Slominski, A. T. Melatonin membrane receptors in peripheral tissues: distribution and functions. *Mol. Cell. Endocrinol.* **2012,** *351* (2), 152-166. https://doi.org/10.1016/j.mce.2012.01.004

(4) Cipolla-Neto, J.; Amaral, F. G. d. Melatonin as a hormone: new physiological and clinical insights. *Endocr. Rev.* **2018,** *39* (6), 990-1028. https://doi.org/10.1210/er.2018-00084

(5) Talib, W. H. Melatonin and cancer hallmarks. *Molecules* **2018,** *23* (3), 518. https://doi.org/10.3390/molecules23030518

(6) Zhao, D.; Yu, Y.; Shen, Y.; Liu, Q.; Zhao, Z.; Sharma, R.; Reiter, R. J. Melatonin synthesis and function: evolutionary history in animals and plants. *Front. Endocrinol.* **2019,** *10*, 249. https://doi.org/10.3389/fendo.2019.00249

(7) Van Laake, L. W.; Lüscher, T. F.; Young, M. E. The circadian clock in cardiovascular regulation and disease: Lessons from the Nobel Prize in Physiology or Medicine 2017. *Eur. Heart J.* **2018,** *39* (24), 2326-2329. https://doi.org/10.1093/eurheartj/ehx775

(8) Eckle, T. Health impact and management of a disrupted circadian rhythm and sleep in critical illnesses. *Curr. Pharm. Des.* **2015,** *21* (24), 3428. https://doi.org/10.2174/1381612821999150709123504

(9) Pan, A.; Devore, E.; Schernhammer, E. S. How shift work and a destabilized circadian system may increase risk for development of cancer and type 2 diabetes. *Circadian Med.* **2015**, 183-209. https://doi.org/10.1002/9781118467831.ch13

(10) Stevens, R. G.; Blask, D. E.; Brainard, G. C.; Hansen, J.; Lockley, S. W.; Provencio, I.; Rea, M. S.; Reinlib, L. Meeting report: the role of environmental lighting and circadian disruption in cancer and other diseases. *Environ. Health Perspect.* **2007,** *115* (9), 1357-1362. https://doi.org/10.1289/ehp.10200

(11) Taylor, D. J.; Bramoweth, A. D. Patterns and consequences of inadequate sleep in college students: substance use and motor vehicle accidents. *Journal of Adolescent Health* **2010,** *46* (6), 610-612. https://doi.org/10.1016/j.jadohealth.2009.12.010

(12) Wittmann, M.; Dinich, J.; Merrow, M.; Roenneberg, T. Social jetlag: misalignment of biological and social time. *Chronobiol. Int.* **2006,** *23* (1-2), 497-509. https://doi.org/10.1080/07420520500545979

(13) Carskadon, M. A.; Acebo, C.; Jenni, O. G. Regulation of adolescent sleep: implications for behavior. *Annals of the New York Academy of Sciences* **2004,** *1021* (1), 276-291. https://doi.org/10.1196/annals.1308.032

(14) Axelsson, J.; Akerstedt, T.; Kecklund, G.; Lindqvist, A.; Attefors, R. Hormonal changes in satisfied and dissatisfied shift workers across a shift cycle. *J. Appl. Physiol.* **2003,** *95* (5), 2099-2105. https://doi.org/10.1152/japplphysiol.00231.2003

(15) Bancroft, J.; Cawood, E. H. Androgens and the menopause; a study of 40–60-year-old women. *Clin. Endocrinol.* **1996,** *45* (5), 577-587. https://doi.org/10.1046/j.1365-2265.1996.00846.x

(16) Cain, S. W.; Rimmer, D. W.; Duffy, J. F.; Czeisler, C. A. Exercise distributed across day and night does not alter circadian period in humans. *J. Biol. Rhythms* **2007,** *22* (6), 534-541. https://doi.org/10.1177/0748730407306884

(17) Bandelow, B.; Sengos, G.; Wedekind, D.; Huether, G.; Pilz, J.; Broocks, A.; Hajak, G.; Rüther, E. Urinary excretion of cortisol, norepinephrine, testosterone, and melatonin in panic disorder. *Pharmacopsychiatry* **1997,** *30* (04), 113-117.

(18) Bartsch, C.; Bartsch, H.; Jain, A.; Laumas, K.; Wetterberg, L. Urinary melatonin levels in human breast cancer patients. *J. Neural Transm.* **1981,** *52* (4), 281-294.

(19) Eriksson, K.; Östin, A.; Levin, J.-O. Quantification of melatonin in human saliva by liquid chromatography–tandem mass spectrometry using stable isotope dilution. *J. Chromatogr. B* **2003,** *794* (1), 115-123. https://doi.org/10.1016/S1570-0232(03)00425-2

(20) Matsui, F.; Koh, E.; Yamamoto, K.; Sugimoto, K.; Sin, H.-S.; Maeda, Y.; Honma, S.; Namiki, M. Liquid chromatography-tandem mass spectrometry (LC-MS/MS) assay for simultaneous measurement of salivary testosterone and cortisol in healthy men for utilization in the diagnosis of late-onset hypogonadism in males. *Endocri. J.* **2009**, 0908270331-0908270331. https://doi.org/10.1507/endocrj.K09E-186

(21) Hansen, Å. M.; Garde, A. H.; Persson, R. Sources of biological and methodological variation in salivary cortisol and their impact on measurement among healthy adults: a review. *Scand. J. Clin. Lab. Invest.* **2008,** *68* (6), 448-458. https://doi.org/10.1080/00365510701819127

(22) Cadore, E.; Lhullier, F.; Brentano, M.; Silva, E.; Ambrosini, M.; Spinelli, R.; Silva, R.; Kruel, L. Correlations between serum and salivary hormonal concentrations in response to resistance exercise. *Journal of Sports Sciences* **2008,** *26* (10), 1067-1072. https://doi.org/10.1080/02640410801919526

(23) Granger, D. A.; Shirtcliff, E. A.; Booth, A.; Kivlighan, K. T.; Schwartz, E. B. The "trouble" with salivary testosterone. *Psychoneuroendocrinology* **2004,** *29* (10), 1229-1240. https://doi.org/10.1016/j.psyneuen.2004.02.005

(24) Mirick, D. K.; Davis, S. Melatonin as a biomarker of circadian dysregulation. *Cancer Epidemiol., Biomarkers Prev.* **2008,** *17* (12), 3306-3313. https://doi.org/10.1158/1055-9965.EPI-08-0605

(25) U.S. Food & Drug Administration (FDA), *Bioanalytical Method Validation – Guidance for Industry*. May 2018.

(26) Hill, H. M. Conference Report: Bioanalytical Procedures and Regulation: Towards Global Harmonization. *Bioanalysis* **2011,** *3* (4), 365-367. https://doi.org/10.4155/bio.10.211

(27) Huang, Y.; Shi, R.; Gee, W.; Bonderud, R. Regulated drug bioanalysis for human pharmacokinetic studies and therapeutic drug management. *Bioanalysis* **2012,** *4* (15), 1919-1931. https://doi.org/10.4155/bio.12.157

(28) European Medicines Agency. *Guideline on bioanalytical method validation*. EMEA/CHMP/EWP/192217/2009. Committee for Medicinal Products for Human Use (CHMP), 2011.

(29) Goto, T.; Myint, K. T.; Sato, K.; Wada, O.; Kakiyama, G.; Iida, T.; Hishinuma, T.; Mano, N.; Goto, J. LC/ESI-tandem mass spectrometric determination of bile acid 3-sulfates in human urine: 3β-Sulfooxy-12α-hydroxy-5β-cholanoic acid is an abundant nonamidated sulfate. *J. Chromatogr. B* **2007,** *846* (1-2), 69-77. https://doi.org/10.1016/j.jchromb.2006.08.013

(30) Steiner, C.; Von Eckardstein, A.; Rentsch, K. M. Quantification of the 15 major human bile acids and their precursor 7α-hydroxy-4-cholesten-3-one in serum by liquid chromatography–tandem mass spectrometry. *J. Chromatogr. B* **2010,** *878* (28), 2870-2880. https://doi.org/10.1016/j.jchromb.2010.08.045

(31) Zhang, D.; Rios, D. R.; Tam, V. H.; Chow, D. S.-L. Development and validation of a highly sensitive LC–MS/MS assay for the quantification of arginine vasopressin in human plasma and urine: application in preterm neonates and child. *J. Pharm. Biomed. Anal.* **2014,** *99*, 67-73. https://doi.org/10.1016/j.jpba.2014.07.001

(32)  Jones, B. R.; Schultz, G. A.; Eckstein, J. A.; Ackermann, B. L. Surrogate matrix and surrogate analyte approaches for definitive quantitation of endogenous biomolecules. *Bioanalysis* **2012,** *4* (19), 2343-2356. https://doi.org/10.4155/bio.12.200

(33)  Thakare, R.; Chhonker, Y. S.; Gautam, N.; Alamoudi, J. A.; Alnouti, Y. Quantitative analysis of endogenous compounds. *J. Pharm. Biomed. Anal.* **2016,** *128*, 426-437. https://doi.org/10.1016/j.jpba.2016.06.017

(34)  Wang, A.-Q.; Wei, B.-P.; Zhang, Y.; Wang, Y.-J.; Xu, L.; Lan, K. An ultra-high sensitive bioanalytical method for plasma melatonin by liquid chromatography–tandem mass spectrometry using water as calibration matrix. *J. Chromatogr. B* **2011,** *879* (23), 2259-2264. https://doi.org/10.1016/j.jchromb.2011.06.010

(35)  Eugster, P. J.; Dunand, M.; Grund, B.; Ivanyuk, A.; Szabo, N. F.; Bardinet, C.; Abid, K.; Buclin, T.; Grouzmann, E.; Chtioui, H. Quantification of serotonin and eight of its metabolites in plasma of healthy volunteers by mass spectrometry. *Clin. Chim. Acta* **2022,** *535*, 19-26. https://doi.org/10.1016/j.cca.2022.08.012

(36)  Hennion, M.-C. Solid-phase extraction: method development, sorbents, and coupling with liquid chromatography. *J. Chromatogr. A* **1999,** *856* (1-2), 3-54. https://doi.org/10.1016/S0021-9673(99)00832-8

(37)  Magliocco, G.; Le Bloc'h, F.; Thomas, A.; Desmeules, J.; Daali, Y. Simultaneous determination of melatonin and 6-hydroxymelatonin in human overnight urine by LC-MS/MS. *J. Chromatogr. B* **2021,** *1181*, 122938. https://doi.org/10.1016/j.jchromb.2021.122938

(38)  Alahmad, W.; Kaya, S. I.; Cetinkaya, A.; Varanusupakul, P.; Ozkan, S. A. Green chemistry methods for food analysis: Overview of sample preparation and determination. *Advances in Sample Preparation* **2023**, 100053. https://doi.org/10.1016/j.sampre.2023.100053

(39)  Demeuse, J.; Calaprice, C.; Huyghebaert, L.; Rechchad, M.; Peeters, S.; Cavalier, E.; Le Goff, C. Development and Validation of an Ultrasensitive LC-MS/MS Method for the Quantification of Melatonin in Human Saliva. *J. Am. Soc. Mass. Spectrom*. **2023**, *34* (6), 1056-1064. https://doi.org/10.1021/jasms.3c00021

(40)  Monfort, A.; Jutras, M.; Martin, B.; Boucoiran, I.; Ferreira, E.; Leclair, G. Simultaneous quantification of 19 analytes in breast milk by liquid chromatography-tandem mass spectrometry (LC-MS/MS). *J. Pharm. Biomed. Anal.* **2021,** *204*, 114236. https://doi.org/10.1016/j.jpba.2021.114236

(41)  Jin, W.; Gui, J.; Li, G.; Jiang, F.; Han, D. High-throughput quantitation of trace level melatonin in human milk by on-line enrichment liquid chromatography-tandem mass spectrometry. *Anal. Chim. Acta* **2021,** *1176*, 338764. https://doi.org/10.1016/j.aca.2021.338764

(42)  Shin, S.; Oh, H.; Park, H. R.; Joo, E. Y.; Lee, S.-Y. A sensitive and specific liquid chromatography-tandem mass spectrometry assay for simultaneous quantification of salivary melatonin and cortisol: development and comparison with immunoassays. *Annals of Laboratory Medicine* **2021,** *41* (1), 108-113. https://doi.org/10.3343/alm.2021.41.1.108

(43)  Domenech-Coca, C.; Mariné-Casadó, R.; Caimari, A.; Arola, L.; Del Bas, J. M.; Bladé, C.; Rodriguez-Naranjo, M. I. Dual liquid-liquid extraction followed by LC-MS/MS method for the simultaneous quantification of melatonin, cortisol, triiodothyronine, thyroxine and testosterone levels in serum: Applications to a photoperiod study in rats. *J. Chromatogr. B* **2019,** *1108*, 11-16. https://doi.org/10.1016/j.jchromb.2019.01.002

(44)  van Faassen, M.; Bischoff, R.; Kema, I. P. Relationship between plasma and salivary melatonin and cortisol investigated by LC-MS/MS. *Clin. Chem. Lab. Med. (CCLM)* **2017,** *55* (9), 1340-1348. https://doi.org/10.1515/cclm-2016-0817

(45)  Ishizaki, A.; Uemura, A.; Kataoka, H. A sensitive method to determine melatonin in saliva by automated online in-tube solid-phase microextraction coupled with stable isotope-dilution liquid chromatography-tandem mass spectrometry. *Anal. Methods* **2017,** *9* (21), 3134-3140. https://doi.org/10.1039/C7AY00622E

(46) Zhao, H.; Wang, Y.; Jin, Y.; Liu, S.; Xu, H.; Lu, X. Rapid and sensitive analysis of melatonin by LC-MS/MS and its application to pharmacokinetic study in dogs. *Asian J. Pharm. Sci.* **2016,** *11* (2), 273-280. https://doi.org/10.1016/j.ajps.2015.08.004

(47) Karunanithi, D.; Radhakrishna, A.; Biju, V. Quantitative determination of sialic acid in Indian milk and milk products. *Int. J. Appl. Biol. Pharm. Technol*. **2013,** *4* (1), 318-323. Identifier: https://imsear.searo.who.int/handle/123456789/164000

(48) Fustinoni, S.; Polledri, E.; Mercadante, R. High-throughput determination of cortisol, cortisone, and melatonin in oral fluid by on-line turbulent flow liquid chromatography interfaced with liquid chromatography/tandem mass spectrometry. *Rapid Commun. Mass Spectrom.* **2013,** *27* (13), 1450-1460. https://doi.org/10.1002/rcm.6601

(49) Khan, S. A.; George, R.; Charles, B. G.; Taylor, P. J.; Heussler, H. S.; Cooper, D. M.; McGuire, T. M.; Pache, D.; Norris, R. L. Monitoring salivary melatonin concentrations in children with sleep disorders using liquid chromatography–tandem mass spectrometry. *Ther. Drug Monit.* **2013,** *35* (3), 388-395. https://doi.org/10.1097/FTD.0b013e3182885cb2

(50) Carter, M. D.; Wade Calcutt, M.; Malow, B. A.; Rose, K. L.; Hachey, D. L. Quantitation of melatonin and n-acetylserotonin in human plasma by nanoflow LC-MS/MS and electrospray LC-MS/MS. *J. Mass Spectrom.* **2012,** *47* (3), 277-285. https://doi.org/10.1002/jms.2051

(51) Jensen, M. A.; Hansen, Å. M.; Abrahamsson, P.; Nørgaard, A. W. Development and evaluation of a liquid chromatography tandem mass spectrometry method for simultaneous determination of salivary melatonin, cortisol and testosterone. *J. Chromatogr. B* **2011,** *879* (25), 2527-2532. https://doi.org/10.1016/j.jchromb.2011.07.005

(52) Motoyama, A.; Kanda, T.; Namba, R. Direct determination of endogenous melatonin in human saliva by column-switching semi-microcolumn liquid chromatography/mass spectrometry with on-line analyte enrichment. *Rapid Commun. Mass Spectrom.* **2004,** *18* (12), 1250-1258. https://doi.org/10.1002/rcm.1473

(53) Yang, S.; Zheng, X.; Xu, Y.; Zhou, X. Rapid determination of serum melatonin by ESI–MS–MS with direct sample injection. *J. Pharm. Biomed. Anal.* **2002,** *30* (3), 781-790. https://doi.org/10.1016/S0731-7085(02)00387-4

(54) Härtter, S.; Morita, S.; Bodin, K.; Ursing, C.; Tybring, G.; Bertilsson, L. Determination of exogenous melatonin and its 6-hydroxy metabolite in human plasma by liquid chromatography–mass spectrometry. *Ther. Drug Monit.* **2001,** *23* (3), 282-286. https://doi.org/10.1097/00007691-200106000-00017

(55) Zhu, M.; Yuan, L.; Wu, Y.; Chu, L.; Wang, W.; Zhang, H.; Liao, W.; Peng, X.; Deng, H. Simultaneous LC-MS/MS quantification of glucocorticoids, melatonin and its metabolites in hair. *J. Chromatogr. B* **2022,** *1196*, 123217. https://doi.org/10.1016/j.jchromb.2022.123217

(56) Wang, H.; Chung-Davidson, Y.-W.; Li, K.; Scott, A. M.; Li, W. Quantification of monoamine neurotransmitters and melatonin in sea lamprey brain tissues by high performance liquid chromatography–electrospray ionization tandem mass spectrometry. *Talanta* **2012,** *89*, 383-390. https://doi.org/10.1016/j.talanta.2011.12.048

(57) Dermanowski, M. M.; Hejduk, A.; Kuczyńska, J.; Wichniak, A.; Urbańska, A.; Mierzejewski, P. Assessment of dim light melatonin onset based on plasma and saliva samples. *Chronobiol. Int.* **2022,** *39* (5), 626-635. https://doi.org/10.1080/07420528.2021.2016796

**BrJAC**

## ARTICLE

# The Determination of Ethanol Levels in Facial Freshener Using the NIR Spectroscopy and Chemometric Method

**Wahyu Eka Febriyanti** (iD)**, Nia Kristiningrum** (iD)**, Lestyo Wulandari*** (iD) ✉

*Faculty of Pharmacy, University of Jember, Jember, East Java, Indonesia, 68121*
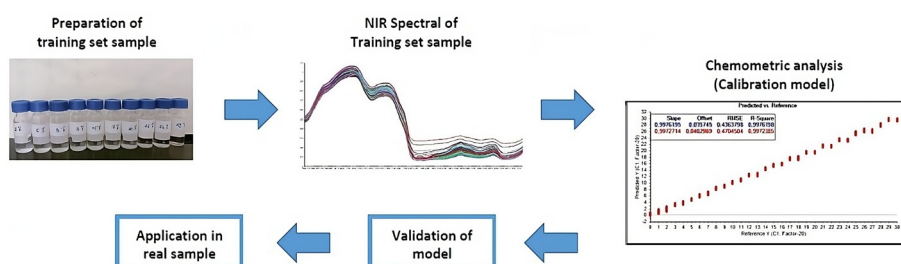
A facial freshener, also known as toner, is a cosmetic product that is commonly used to invigorate the face after a busy day. Ethanol serves as a key component in toner, serving multiple purposes such as being a solvent, preservative, and antimicrobial agent. However, it's important to note that toner formulated for normal skin types typically contain ethanol in small concentrations, adhering to a limit of not more than 10%. Therefore, this study aims to determine ethanol levels in toner using the NIR spectroscopy and chemometric techniques. The NIR spectra of the simulated samples were correlated with ethanol concentration using chemometric calibration model. The calibration models used were partial least square (PLS), principal component regression (PCR), and support vector regression (SVR). The calibration model was validated by leave one out cross validation (LOOCV) as well as the external validation, and the precision and accuracy of the method was evaluated. Among the calibration models, the PLS model exhibited the best performance, yielding an impressive $R^2$ 0.9976; with an RMSEC value of 0.4364 and RMSECV value of 0.4704. The internal validation yield $R^2$ value more than 0.99 and RMSE of less than 0,4198. Furthermore, external validation showed the $R^2$ and RMSEP value of 0.989 and 0.920 respectively. The %recovery and RSD value were 101.2% and 0.129%. Comparing ethanol measurements obtained through the NIR chemometric method with those obtained using gas chromatography as the reference method, no significant difference was observed at a 95% confidence levels, as indicated by a significance value of 0.231.

**Keywords**: NIR spectroscopy, chemometric, facial freshener, ethanol, toner

## INTRODUCTION

Cosmetics refer to substances or mixtures used externally on the human body, such as the skin, scalp hair, nails and the outer parts. They serve the purpose of cleaning, maintaining, enhancing attractiveness, and protecting the body, excluding the medicinal applications.[1] One of facial cosmetics that is commonly

used by women, especially Indonesia, is a face freshener (toner). Toner is used to cleanse the face after daily activities, refresh the pH balance of facial skin, and achieve optimal equilibrium.[2] They are typically composed of various natural ingredients. For normal skin types, toner often include moisturizing agents to restore hydration after using facial cleansers.[3] In the formulation of toner, ethanol can be used as a solvent, preservative and antimicrobial. It helps in dissolving active ingredients or substances that are insoluble in water.[4] Toner are usually recommended for individuals with normal and oily skin types.[5] The concentration of ethanol used in toner for normal skin is limited to no more than 10%, as it provides the desired therapeutic effect.[6]

According to previous studies, the determination of ethanol content was carried out using several method. In a study by Almeida et al (2021), the determination of ethanol and fragrance content in cosmetics was carried out using gas chromatography method.[7] According to the study by Pinu et al (2017), ethanol content in fermented foods and beverages were determined using the gas chromatography method.[8] Valentina et al (2010) examined the determination of ethanol content in branded foods using chemometric NIR (Near Infrared) spectroscopy method.[9] Mmaabo (2022) examined the determination of ethanol content in various types of alcoholic beverages using the gas chromatography method.[10] Rebecca's (2021) explored the determination of ethanol content in beer using gas chromatography method.[11] However, no study has reported the determination of ethanol content in cosmetic samples, especially toner, using either gas chromatography or NIR spectroscopy method. The gas chromatography method offers numerous benefits, including high sensitivity, but it has the drawback of being time-consuming and requiring the preparation of a chemical mixture. In this study, the determination of ethanol content was carried out using the NIR spectroscopy method. This method is not only applicable to cosmetic toner samples but also enables the assessment of alcohol content in beverages like beer.[12] One of the major advantages of the NIR spectroscopy is its ability to provide quick analysis results without causing pollution, as it solely relies on simple preparations without the need for chemical compounds.[13] However, the NIR spectroscopy has drawbacks, including spectra that require further interpretation due to spectrum overlap and low sensitivity. To overcome these challenges, chemometric method are employed in conjunction with the NIR spectroscopy to rapidly identify and analyze spectra.[14] In this study, toner simulation samples with ethanol concentrations ranging from 0% to 30% were used for the NIR method.

This study aims to determine ethanol content in toner using the NIR chemometric method and compare the results with gas chromatography as a reference method in order to ascertain if there is a significant difference between the NIR spectroscopy method and gas chromatography.

## MATERIALS AND METHOD
### Materials
In this study, the materials used were ethanol (Merck), n-butanol (Merck), cucumber extract, lemon extract, tween 80 (GBM), propylene glycol (Brataco), NaOH (Merck), nipagin (GBM), nipasol (GBM), lemon perfume (GBM), aquabidest (Wida). The real sampels of toner were purchased from the market in Jember, East Java, Indonesia.

### Instrumentation
The tool used were the NIR Spectroscopy (Brimrose Luminar 3070), gas chromatography (GC-FID Thermo Scientific-Trace 1300), Software The Unscrambler X 10.4 (Oslo, Norway), pH meter, and laboratory glassware.

### Sample Simulation Preparation
Sample simulation preparation involved the creation of a sample training set and a test set. The formulation ingredients, including cucumber extract, lemon extract, tween 80, propylene glycol, NaOH, nipagin, nipasol, and lemon perfume, were mixed together. Ethanol and aquabidest were then added to achieve various concentrations in the training set samples (ranging from 0% to 30% v/v) and the test set samples (ranging from 2.5% to 29.5% v/v).

### Sample Measurement Using the NIR Spectroscopy

Sample measurements were carried out using the Brimrose NIR spectroscopy instrument. Furthermore, 200 µL of each sample was placed on the sample compartment using a micropipette. Each simulation sample was scanned in the range of 850-2000 nm. The measurements were replicated three times, with 10 shooted in each replication. The NIR spectroscopy used consisted of a 3070 brimrose luminar spectrometer with a sampling area measuring 5 x 3 mm and assisted by a computer set. The NIR Spectroscopy technique was based on measuring the light reflected by a sample. The NIR spectrum was obtained by converting the energy transferred from the radiation into mechanical energy through the movement of atoms and chemical bonds within molecules. Initially, the sample was exposed to a light source at a wavelength between 780-2500 nm and the light reflected or transmitted by the sample collected on the detector which was then converted into a spectrum.

### Model Calibration and Validation

For model calibration and validation, the NIR spectras obtained were analysed by The Unscrambler X 10.4. The multivariate analysis used for calibration model were partial least square (PLS), principal component regression (PCR), and support vector regression (SVR).[15] The calibration models (PLS, PCR, and SVR) were formed by correlating the transmittance of the NIR spectra with ethanol concentration. The selected model was validated using leave one out cross validation (LOOCV) using 30 concentation samples training set and external validation using 10 concentration samples test set.[16] LOOCV was evaluated by remove one set of data in training set and the remaining data were used to form new calibration model. The precision and accuracy of the method was evaluated based on BP 2022.[17]

### Real Sample Application

The selected calibration model that has been validated was applied to determine ethanol content in the commercial sample. For each commercial sample, 200 µL was placed on the NIR spectroscopy sample compartment and scanned three times for replicability. The real samples analyzed were five samples of toner containing ethanol purchased from the market in Jember, Indonesia.

### The determination of ethanol by gas chromatography and validation method

To prepare the standard ethanol solution, ethanol was diluted in aquabidest (distilled water) to achieve a concentration range of 2-29% ethanol, with 1.0% n-butanol as the internal standard.[18] Real sample preparation involved adding 0.99 mL of the sample to 0.01 mL of n-butanol. The real samples were then subjected to gas chromatography analysis with three replicates. Subsequently, ethanol content was analyzed using the gas chromatography method with a detector temperature of 300 °C and an injector temperature of 200 °C, and the analysis was carried out by directly injecting 1 µL of sample in split mode with a split flow ratio and split ratio of 1:143. The initial temperature on the heater (oven) was set at 40 °C and held for the first 1 minute, after which it was increased by 10 °C per minute until reaching 70 °C. Subsequently, the temperature was increased at a rate of 70 °C per minute until reaching the final limit temperature of 200 °C, which took 6 minutes. The pressure in the carrier gas was maintained on the column at 60 kPa. The gas flux used for the detector was 350 mL per minute for synthetic gas and 35 mL per minute for hydrogen. Precision and accuracy were evaluated using three levels of simulated samples and replicated three times.

To compare ethanol levels in the real samples determined using the NIR chemometric and gas chromatography, a paired *t*-test was performed on the samples. The significance levels (p-value) for the test was set at 0.05 (two-tailed).

## RESULTS AND DISCUSSION

The simulation sample consists of 31 samples calibration set with a concentration range of 0%-30% v/v and 10 samples test set with a concentration range of 2.5%-29.5% v/v. The concentration range was wider than concentrations commonly used in commercial toner (1% - 10% v/v). The wider the range of calibration set sample used the better the calibration model obtained.

The spectra of ethanol, simulated samples of 0%, 10% ethanol concentrations and commercial samples are shown in Figure 1. Ethanol spectrum, simulated samples and commercial samples has the same pattern, only the transmittance intensity is different as shown in Figure 1.
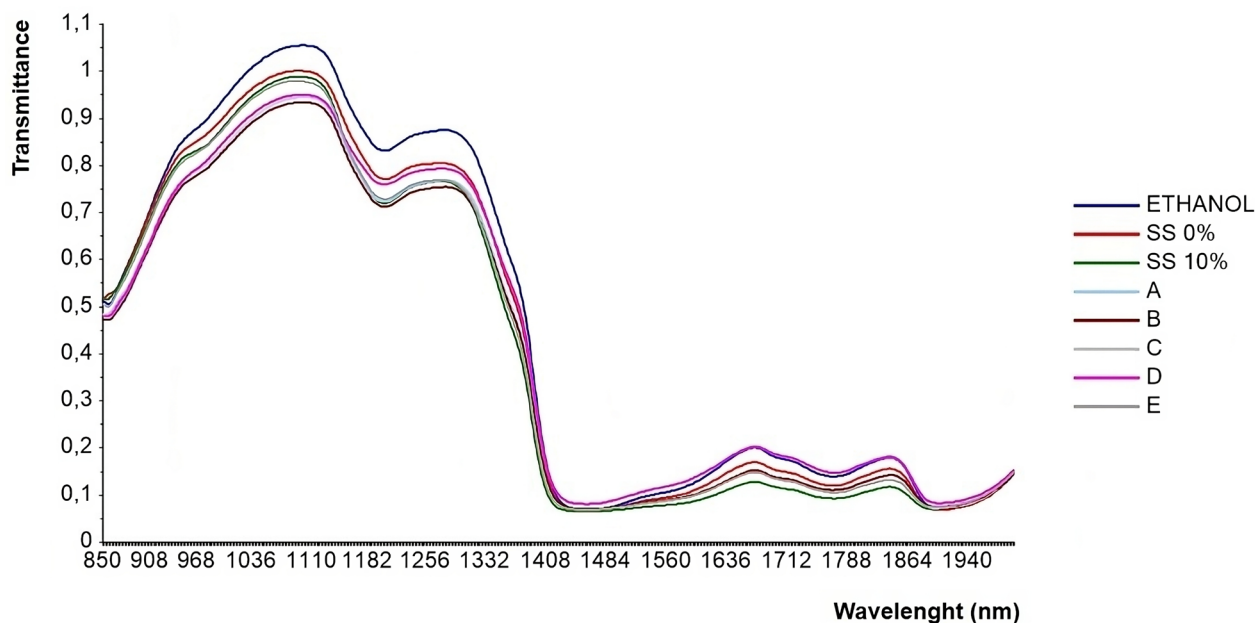


**Figure 1.** IR spectra of ethanol, simulation sample with ethanol concentration 0%, 10% (SS 0%, SS 10%) and commercial sample toner (A, B, C, D, E).

The calibration model for the NIR method was established using spectral data from a training sample set comprising 750 data points. Each concentstins in the training set samples was scanned using the NIR spectroscopy, resulting in 25 spectrum data for each concentration. In total, there were 30 concentrations, which produced 750 spectrum data used to build a calibration model. Among the calibration model tested, the best performance was achieved by the PLS using one latent variable with $R^2$ 0.9976; RMSEC 0.4364 and RMSECV 0.4704 (Table I). The $R^2$ of internal validation (LOOCV) was more than 0.99 and RMSE less than 0,4198. When evaluating the calibration models, the key figures of merit considered were $R^2$, RMSE and RMSECV.[19] A higher $R^2$ value closer to 1 indicates a better calibration model, as it signifies a stronger correlation between the NIR spectra and ethanol concentrations. A smaller RMSE and RMSECV value suggest a better model calibration, as they indicate lower average prediction errors and better predictive performance.
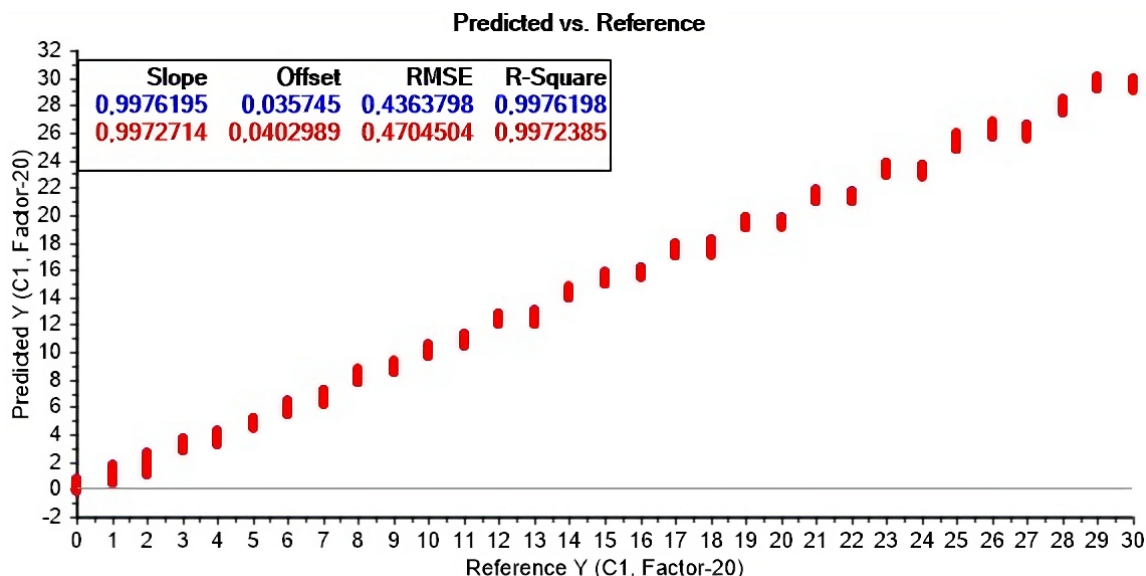
**Figure 2.** Graph of variations in the RMSECV values of the calibration samples in the PLS model.

**Table I.** The results of the formation of the calibration model

| No | Model | | RMSE | $R^2$ |
|----|-------|---|------|-------|
| 1. | PLS | Calibration | 0.4364 | 0.9976 |
|    |     | Validation | 0.4704 | 0.9972 |
| 2. | PCR | Calibration | 0.6909 | 0.9940 |
|    |     | Validation | 0.7081 | 0.9937 |
| 3. | SVR | Calibration | 0.4199 | 0.9959 |
|    |     | Validation | 0.4194 | 0.9959 |

The PLS model was selected as the optimal calibration model because it demonstrated an $R^2$ value of 0.9976, which is very close to 1. This high $R^2$ value indicates an excellent fit of the model to the data, suggesting a strong correlation between the NIR spectra and ethanol concentrations. Additionally, the PLS model exhibited a small RMSE value of 0.4364, which is below the threshold of 1.5. The RMSE value measures the average prediction error of the calibration model, and a smaller value indicates better accuracy in predicting ethanol concentrations. The selected PLS model satisfied the requirements for a good calibration model, as it had an $R^2$ value close to 1 and an RMSE value below 1.5. These criteria ensure that the model is capable of accurately predicting ethanol levels in toner samples based on the NIR spectra.[20]



**Figure 3.** External validation of the PLS model.

The comparison method has been validated with the results of the parameter assessment of each validation stage listed in Table II.

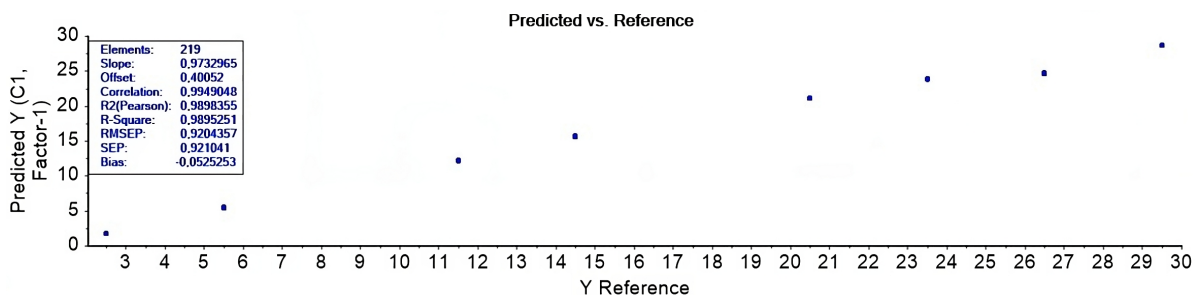**Table II.** Method validation results

| Validation Parameters | GC method | NIRS method (PLS model) |
|---|---|---|
| Linearity | | |
| Linierity range (%v/v) | 2 – 29 | 0 – 30 |
| Correlation coefficient (r) | 0.999 | - |
| Correlation coefficient ($R^2$) | - | 0.989 |
| Coefficient of variation (*Vx0*) | 2.511% | |
| RMSEP | - | 0.920 |
| LOD | 1.70 µg mL$^{-1}$ | - |
| LOQ | 5.12 µg mL$^{-1}$ | - |
| Accuracy (%recovery, n=3x3) | 101.9% | 101.2% |
| Precision (RSD, n=3x3) | 0.197% | 0.129% |

The results in Table II, show that GC method have the correlation coefficient of 0.999 and the coefficient of variation of 2.511%. This means that this method meets the requirements of linearity, the correlation coefficient (r) ≥ 0.99, and the function variation coefficient (Vx0) < 5%. The % recovery and RSD value were 101.9% and 0.197%, respectively. These results meet the accuracy and precision requirements that were % recovery within 95.0-105.0% and RSD value less than 2%.[21] For the NIR spectroscopy method, the external validation showed good results. The $R^2$ and RMSEP value using one of latent variable were 0.989 and 0.920 and the % recovery and a RSD value were 101.2% and 0.129%, respectively (Figure 3).

The commercial sample toner used were five samples with sample codes A, B, C, D and E. The results of ethanol levels in commercial samples are listed in Table III.

**Table III.** Results of the determination of ethanol content in commercial samples

| Sample code | Ethanol content (%v/v) ± SD (n=3) | |
|---|---|---|
| | NIR spectroscopy | Gas chromatography |
| A | 15.548 ± 0.032 | 15.212 ± 0.128 |
| B | 7.669 ± 0.009 | 7.481± 0.136 |
| C | 12.169 ± 0.012 | 12.131± 0.159 |
| D | 5.404 ± 0.012 | 5.468± 0.141 |
| E | 12.121 ± 0.019 | 12.114± 0.341 |

The comparison of ethanol levels in toner was conducted using the NIR-chemometric method and gas chromatography through a paired sample *t*-test. In order to proceed with the analysis, it was necessary to ensure that the data met the assumption of normal distribution (p > 0.005).[22] To assess the normality of the

variables, a Kolmogorov-Smirnov test was performed using the IBM SPSS program. The normality test results obtained from the NIR method and gas chromatography were 0.702 and 0.615 respectively, the condition for normally distributed data is significant if the value is > 0.05. These data met the requirements, meaning both method were normally distributed and suggest the paired sample *t*-test could be continued. The paired *t*-test yielded a significant value of 0.231 with a 95% confidence levels. The results of the comparison obtained are said to be meaningful if the p value (sig.) in the 2 groups is> 0.05 with a degree of confidence reaching 95%, meaning that there is no significant difference between the two method.

## CONCLUSION

In conclusion, ethanol content in toner sample was successfully determined using the NIR spectroscopy and chemometric method using PLS model with $R^2$ 0.9976; RMSEC 0.4364 and RMSECV 0.4704. The PLS calibration method exhibited favorable results with an $R^2$ value of 0.9976, RMSEC of 0.4364, and RMSECV of 0.4704. The validation tests also met the requirements, demonstrating an $R^2$ value exceeding 0.99 and an RMSE below 0.4198. External validation showed an $R^2$ and RMSEP of 0.989 and 0.920. The % recovery and RSD value were 101.2% and 0.129%, respectively. There was no significant difference between ethanol content obtained from the NIRS-chemometric method and the gas chromatography method, as confirmed by the paired sample *t*-test with a significance value of 0.231 (> 0.05). Therefore, the NIRS-chemometric method can be considered reliable, relatively fast, easy and simple method for determining ethanol content in toner.

## Conflicts of interest

There are no conflicts to declare.

## Acknowledgements

## REFERENCES

(1)   BPOM, RI – Indonesia's Drug and Food Control Agency, Regulation Number 30 of 2020 concerning Technical Requirements for Cosmetic Marking. Available at: https://notifkos.pom.go.id/upload/informasi/20220805174357.pdf  (accessed on: July 2022).

(2)   Jiang, B.; Jia, Y.; He, C. Promoting new concepts of skincare via skinomics and systems biology – From traditional skincare and efficacy-based skincare to precision skincare. *J. Cosmet. Dermatol*. **2018**, *17* (6), 968-976. https://doi.org/10.1111/jocd.12663

(3)   Zirwas, M. J. Contact dermatitis to cosmetics. *Clin. Rev. Allergy Immunol*. **2019**, *56*, 119-128. https://doi.org/10.1007/s12016-018-8717-9

(4)   Retno, A.; Materials Safety Data Sheet (MSDS), ethanol, *NCP Alcohols*, **2018**, pp 11-15. Available at: https://www.alconcp.com/products-ethanol.html (accessed on: July 2022).

(5)   Pavlou, P.; Siamidi, A.; Varvaresou, A.; Vlachou M. Skin care formulations and lipid carriers as skin moisturizing agents. *Cosmetics* **2021**, *8* (3), 89. https://doi.org/10.3390/cosmetics8030089

(6)   Shah, H.; Jain, A.; Laghate, G.; Prabhudesai, D. Pharmaceutical excipients. In: Adejare, A. (Ed.) *Remington, The Science and Practice of Pharmacy* (Twenty-third Edition), Academic Press, 2021, Chapter 32, pp 633-643. https://doi.org/10.1016/B978-0-12-820007-0.00032-5

(7)   Almeida, R.; Hartz, J.; Costa, P.; Rodrigues, A.; Vargas, R.; Cassel, E. Permeability coefficients and vapour pressure determination for fragrance materials. *Int. J. Cosmet. Sci*. **2021**, *43* (2) 225-234. https://doi.org/10.1111/ics.12686

(8)   Pinu, F. R.; Villas-Boas, S. G. Rapid quantification of major volatile metabolites in fermented food and beverages using gas chromatography-mass spectrometry. *Metabolites* **2017**, *7* (3), 37. https://doi.org/10.3390/metabo7030037

(9) Di Egidio, V.; Oliveri, P.; Woodcock, T.; Downey, G. Confirmation of brand identity in foods by near infrared transflectance spectroscopy using classification and class-modelling chemometric techniques - The example of a Belgian beer. *Food Res. Int.* **2011**, *44* (2), 544-549. https://doi.org/10.1016/j.foodres.2010.11.021

(10) Hunter, R. A. Analysis of Ethanol in Beer Using Gas Chromatography: A Side-by-Side Comparison of Calibration Methods. *J. Chem. Educ.* **2021**, *98* (4), 1404-1409. https://doi.org/10.1021/acs.jchemed.0c00962

(11) Tsenang, M.; Pheko, T.; Mokgadi, J.; Phokedi, G. N. A Validated Liquid-Liquid Extraction Method for The Quantitative Analysis of Ethanol in the Different Types of Home-Brewed Alcoholic Beverages of Botswana Using Gas Chromatography Flame Ionization Detector. *Chemistry Africa* **2023**, *6*, 417–427. https://doi.org/10.1007/s42250-022-00520-3

(12) Wójcicki, K. NIR spectroscopy coupled with chemometrics as a tool for quality analysis of beer samples. *Towaroznawcze Problemy Jakości*. (Polish J. of Commodity Sci.) **2019**, *3* (60), 27-34. https://doi.org/10.19202/j.cs.2019.03.03

(13) Psimadas, D.; Georgoulias, P.; Valotassiou, V.; Loudos, G. Molecular Nanomedicine Towards Cancer: $^{111}$In-Labeled Nanoparticles. *J. Pharm. Sci.* **2012**, *101* (7), pp 2271-2280. https://doi.org/10.1002/jps.23146

(14) Gad, H. A.; El-Ahmady, S. H.; Abou-Shoer, M. I.; Al-Azizi, M. M. Application of chemometrics in authentication of herbal medicines: A review. *Phytochem. Anal*. **2013**, *24* (1), 1-24. https://doi.org/10.1002/pca.2378

(15) Cheng, J-H.; Sun, D-W. Recent Applications of Spectroscopic and Hyperspectral Imaging Techniques with Chemometric Analysis for Rapid Inspection of Microbial Spoilage in Muscle Foods. *Compr. Rev. Food Sci. Food Saf*. **2015**, *14* (4), 478-490. https://doi.org/10.1111/1541-4337.12141

(16) Wulandari, L.; Idroes, R.; Noviandy, T. R.; Indrayanto, G. Application of chemometrics using direct spectroscopic methods as a QC tool in pharmaceutical industry and their validation. In: Al-Majed, A. A. (Ed.). *Profiles of Drug Substances, Excipients and Related Methodology*. Academic Press, Elsevier, 2022. Volume 47, Chapter Six, pp 327-379, https://doi.org/10.1016/bs.podrm.2021.10.006

(17) BP, SC. Validation of Analytical Procedures. *Br Pharmacopoeia 2*, **2022**, pp 2021-2023.

(18) Fu, C.; Liu, H.; Fu, S.; Chai, X. Rapid and simultaneous determination of acetone, butanol, and ethanol in butanol fermentation broth by full evaporation headspace gas chromatography *Cellul. Chem. Technol.* **2015**, 49 (9-10) pp 813-818.

(19) Watanabe, L. S.; Bovolenta, Y. R.; Acquaro Junior, V. R.; Barbin, D. F.; Madeira, T. B.; Nixdorf, S. L. Investigation of NIR spectra pre-processing methods combined with multivariate regression for determination of moisture in powdered industrial egg. *Acta Scientiarum. Technology* **2018**, *40* (1), e30133. https://doi.org/10.4025/actascitechnol.v40i1.30133

(20) Ziegel, E. R. Statistics and Chemometrics for Analytical Chemistry. *Technometrics* **2004**, *46* (4), 498-499. https://doi.org/10.1198/tech.2004.s248

(21) Blumberg, L. M. Theory of Gas Chromatography. In: Poole, C. F. (Ed.) *Gas Chromatography* (Second Edition). Handbooks in Separation Science. Elsevier Inc., 2021, Chapter 2, pp 19-97. https://doi.org/10.1016/b978-0-12-820675-1.00026-5

(22) Ujhelyi, Z.; Vecsernyés, M.; Fehér, P.; Kósa, D.; Arany, P.; Nemes, D.; Sinka, D.; Vasvári, G.; Fenyvesi, F.; Váradi, J.; Bácskay, I. Physico-chemical characterization of self-emulsifying drug delivery systems. *Drug Discovery Today: Technol*., **2018**, *27*, 81-86. https://doi.org/10.1016/j.ddtec.2018.06.005

**BrJAC**

# ARTICLE

# Closed-Vessel Conductively Heated Digestion of Dry Dog Food for Spectrometric Determination of Essential Nutrients

**Rayane Cristina Vieira Costa**(iD), **João Victor Biagi Santiago**(iD), **Edilene C. Ferreira**(iD), **Alex Virgilio\***(iD)(✉), **José Anchieta Gomes Neto**(iD)

*Universidade Estadual Paulista (UNESP), Instituto de Química. Rua Professor Francisco Degni 55, 14800-060, Araraquara, SP, Brazil*
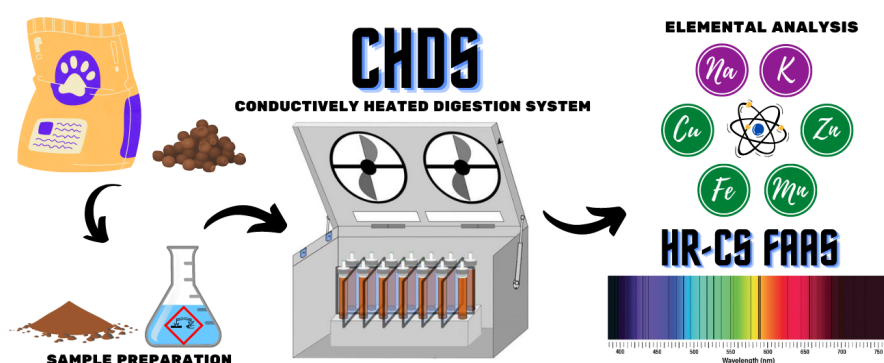
The closed-vessel conductively heated digestion system (CHDS) was evaluated to digest dry dog foods for further determination of K, Na, Cu, Fe, Mn, and Zn by high-resolution continuum source flame atomic absorption spectrometry (HR-CS FAAS). The CHDS method was optimized using a fractional factorial design with five variables ($HNO_3$ concentration, $H_2O_2$ volume, temperature, holding time, and pre-digestion time) at two levels. The accuracy of the CHDS procedure was checked by the analysis of reference materials from the National Institute of Standards and Technology (NIST SRM 1577b Bovine Liver and 2976 Mussel Tissue) and Brazilian Agricultural Research Corporation (Embrapa MR-E1002A Fish Food). Also, the digestion efficiencies were calculated from residual carbon contents (RCCs). The RCC and blank values in the CHDS digested samples were consistently low, which is suitable for determinations using ICP OES and ICP-MS techniques. For comparison, all samples were also digested by microwave-assisted digestion in closed vessels (MW-AD). Results for Na, K, Cu, Fe, Mn, and Zn determined in sample digests obtained by CHDS were not statistically different at a 95% confidence level from those observed for MW-AD. Limits of quantification (LOQ) calculated from digests in CHDS and MW-AD were comparable, and the values provided adequate limits for elemental determinations in dog foods. Data from mineral composition and moisture were employed in a clustering analysis (HCA) and the discrimination of the samples among different manufacturers and food for dogs at different life stages was possible.

**Keywords:** dog food, sample preparation, CHDS, HR-CS FAAS, pet nutrition

## INTRODUCTION

The pet industry has been experiencing substantial growth, with the global pet care market valuation around US$ 138 - 179 billion in 2020 and expected to reach US$ 240 - 270 billion by 2030.[1,2] The pet food segment stands for 70% of those values, and pet owners have been increasing their concerning about providing appropriate nutrition and healthier diets to their animals,[3] considering the quality of ingredients as the main characteristic to be taken into consideration for the food selection.[4] Considering the high demand, large-scale production of dry pet foods under controlled conditions requires manufacturers to implement good practices and strict quality control.[3] Macronutrients such as Na and K are essential in a dog's acid-base balance, regulation of osmotic pressure, and nerve impulse generation and transmission. Micronutrients are also vital in processes as the synthesis of blood components and energy metabolism (Fe); defense against oxidative damage and formation of connective tissue, blood cells, melanin, and myelin (Cu); enzyme functions, bone development and neurological function (Mn); and enzyme reactions, cell replication, protein and carbohydrate metabolism, skin function and wound healing (Zn).[5] Whereas the supplementation of essential minerals in dry pet food is crucial for health maintenance, the inorganic element analysis takes an important role in food safety and quality of both raw materials and commercial products formulated to achieve diet requirements for specific breeds and life stages.[5,6]

Most spectrometric techniques for inorganic elemental analysis rely on sample introduction systems basically fit for aqueous solutions. Thus, the solid samples must be chemically digested by dry or wet decomposition methods.[7] Wet digestions using liquid reagents in closed vessels are frequently employed in most spectroscopy methods.[8] Microwave-assisted digestion systems (MW-AD) using closed vessels are well-established, robust, and highly efficient, but the acquisition and maintenance of equipment are costly, which impairs MW-AD implementation in most small to medium-sized laboratories.[9]

The conductively heated digestion system (CHDS) is a simple and low-cost combination of closed vessels and conductively heating in digester blocks. This sample preparation technique has been applied for raw meats, milk, chocolate, coffee, biomass (sugarcane, eucalyptus, banana), vegetables, biochar, oyster shell flour, bone meal, swine manure, aiming at the elemental determinations by atomic absorption and plasma-based spectrometry.[10-13]

The elemental composition of dry dog foods obtained by chemical analysis may be a useful input to perform classifications by means of hierarchical cluster analysis (HCA), which is scarcely explored in the literature.[14] Also, the multivariate optimization and the digestion of dry dog food by CHDS have not yet been evaluated. The present work aims to evaluate the CHDS for digestion of dry dog foods (from distinct manufacturers and intended for different stages of pet development) for determination of K, Na, Cu, Fe, Mn, and Zn by HR-CS FAAS. The accuracy was assessed by analysis of bovine liver, mussel tissue and fish food reference materials. For comparative purposes, all dry dog foods were also analyzed after digestion by MW-AD.

## MATERIALS AND METHODS

### Instrumentation

All dry dog food samples and certified reference materials were digested using a conductively-heated digestion system (CHDS) composed of a 28-slot heating block, a temperature control terminal and two cooling fans built-in an acid-resisting cabinet with an acrylic safety shield. Further details on the CHDS instrumental setup can be found elsewhere.[11] A Multiwave microwave-assisted sample preparation system (Anton Paar, Graz, Austria), equipped with a 6-position rotor for 50 mL quartz vessels was used for comparison. The digestion efficiencies were evaluated by the quantification of the residual carbon content (RCC) using a TOC-L CSH/CSN (Shimadzu, Kyoto, Japan) carbon analyzer system.

The elemental determinations were performed in a contrAA® 300 high-resolution continuum source flame atomic absorption spectrometer (Analytik Jena AG, Jena, TH, Germany) equipped with a 300 W Xenon short-arc lamp XBO 301 (GLE, Berlin, BE, Germany) operating in a hot-spot mode as a continuum radiation source, a compact high-resolution double-Echelle grating monochromator (with a spectral

bandwidth < 2 pm per pixel in the far ultraviolet range) and a charge-coupled device (CCD) array detector.[15] All measurements were performed in three repetitions using an injection module (SFS 6), with a load time of 5.0 s, injection time of 10 seconds and the aspiration rate was maintained at 5.0 mL min^{-1}. The spectrometer operating conditions were automatically optimized by the ASpect CS software (Analytik Jena AG, Jena, TH, Germany), and the optimized parameters are described in Table I. Considering the fast-sequential capability of the HR-CS FAAS technique, sample throughput was estimated at 48 samples h[-1].

**Table I**. Optimized instrumental operating conditions for the determination of Cu, Fe, K, Mn, Na and Zn by HR-CS FAAS

| Analyte | Wavelength (nm) | Acetylene gas flow rate (L h^{-1}) | Air flow rate (L h^{-1}) | Air/acetylene ratio | Burner height (mm) |
|---------|-----------------|-----------------------------------|-------------------------|---------------------|--------------------|
| Cu | 324.754 | 50 | 486 | 9.7 | 6.0 |
| Fe | 248.327 | 60 | 486 | 8.1 | 6.0 |
| K | 404.414 | 80 | 486 | 6.1 | 8.0 |
| Mn | 279.482 | 80 | 486 | 6.1 | 6.0 |
| Na | 330.237 | 90 | 486 | 5.5 | 6.0 |
| Zn | 213.857 | 50 | 486 | 9.7 | 6.0 |

### Reagents, materials, analytical solutions and samples

All sample digestions and analytical solutions were prepared using ultrapure water (resistivity 18.2 MΩ cm) produced from a Master System MS2000 (Gehaka, São Paulo, Brazil), nitric acid 65% w w[-1] (Merck, Darmstadt, Germany), and hydrogen peroxide 30% w w[-1] (Merck, Darmstadt, Germany). For optimizations, 3.5 and 7.0 mol L^{-1} $HNO_3$ solutions were previously prepared by simple dilution using ultrapure water. High-purity acetylene (99.7%, Air Liquid, São Paulo, Brazil) and compressed air were used as fuel and oxidant gases, respectively. All quartz digestion tubes, glassware, and polypropylene flasks were previously decontaminated by overnight immersion in a 10% v v[-1] $HNO_3$ solution, followed by deionized water rinsing.

Multielement standard solutions were prepared by appropriate dilution of respective stock solutions containing 1,000 mg L^{-1} Cu, Fe, K, Mn, Na, or Zn (SpecSol®, QUIMLAB, São Paulo, Brazil). Analytical working solutions in the 0.03 – 0.2 mg L^{-1} Cu, 0.25 – 3.0 mg L^{-1} Fe, 5 – 200 mg L^{-1} K, 0.1 – 0.5 mg L^{-1} Mn, 10 – 50 mg L^{-1} Na and 0.3 – 1.5 mg L^{-1} Zn were daily prepared in a $HNO_3$ 5% v v[-1] medium. The certified reference materials NIST SRM 1577b Bovine Liver and NIST SRM 2976 Mussel Tissue Freeze-Dried from National Institute of Standards and Technology (Gaithersburg, MD, USA), and MR-E1002A Fish Food from *Empresa Brasileira de Pesquisa Agropecuária* (Embrapa, Brazil) were used to check the accuracy of the procedures. Dry dog foods for puppies, adults and senior animals from 3 different manufacturers were purchased in a local market of Araraquara, SP, Brazil. The samples were ground using a mortar and pestle, and dried at 75 ºC in a TE-394/2 forced air oven (Tecnal, Piracicaba, SP, Brazil) to constant weight for the determination of moisture. Then, dried samples were placed in polypropylene containers and stored in desiccators.

### Digestion procedures
#### Screening study of variables using a factorial design

The screening study of digestion conditions for the CHDS procedure was performed by means of a fractional factorial design with 5 variables (V1 = concentration of $HNO_3$, V2 = volume of $H_2O_2$, V3 = holding time, V4 = temperature, and V5 = pre-digestion time) at 2 levels (-1 = low and +1 = high). The real values for the low and high levels were 3.5 and 14.0 mol L^{-1} $HNO_3$ (V1); 0.5 and 1.0 mL of $H_2O_2$ (V2); 12 and 24

min (V3); 195 and 225 ºC (V4); and 15 and 30 min (V5), respectively. The results of these experiments were processed using the Statistica (TIBCO Software Inc. Data Science Workbench, version 14, 2020). From this design ($2^5$), the number of possible combinations would be 32, which was changed to ($2^{5-2}$) in order to reduce the number of experiments to a total of 8, corresponding to 1/4 fraction of the complete design.[16,17]

In each experiment, masses of 100 mg of dry dog food sample were accurately weighed and 2.0 mL of $HNO_3$ solution (V1) was added. The vessels were closed and kept at room temperature for the selected pre-digestion time (V5). After that, the selected volume of $H_2O_2$ (V2) was added and the vessels were sealed. The heating program was initiated using a 20 min ramp up to the chosen temperature (V4) and, after reaching a plateau, this temperature was kept for the selected holding time (V3). After cooling down for 30 min, the resulting solutions were transferred to polypropylene tubes and the final volume was made up to 25 mL with ultrapure water. RCC determinations were performed in duplicates with pH adjusted to a range of 5.5 to 6.5 with NaOH and a 100-fold dilution was made. A summary of the factorial design parameters is depicted in Table II.

**Table II.** Factorial design ($2^{5-2}$) for the CHDS digestion optimization

| Experiment | Level (real value) | | | | |
|---|---|---|---|---|---|
| | V1 $HNO_3$ (mol $L^{-1}$) | V2 $H_2O_2$ (mL) | V3 Holding time (min) | V4 Temperature (ºC) | V5 Pre-Digestion time (min) |
| 1 | -1 (3.5) | -1 (0.5) | -1 (12) | 1 (225) | 1 (30) |
| 2 | -1 (3.5) | -1 (0.5) | 1 (24) | 1 (225) | -1 (15) |
| 3 | -1 (3.5) | 1 (1.0) | -1 (12) | -1 (195) | 1 (30) |
| 4 | -1 (3.5) | 1 (1.0) | 1 (24) | -1 (195) | -1 (15) |
| 5 | 1 (14.0) | -1 (0.5) | -1 (12) | -1 (195) | -1 (15) |
| 6 | 1 (14.0) | -1 (0.5) | 1 (24) | -1 (195) | 1 (30) |
| 7 | 1 (14.0) | 1 (1.0) | -1 (12) | 1 (225) | -1 (15) |
| 8 | 1 (14.0) | 1 (1.0) | 1 (24) | 1 (225) | 1 (30) |

*Optimizations of $HNO_3$ concentration and sample mass*

After the settlement of the optimal CHDS procedure and heating program parameters, the effect of the $HNO_3$ concentration was further evaluated using the fish food CRM. In this experiment, 100 mg of sample was accurately weighed and 2.0 mL of $HNO_3$ solution (7.0 or 14.0 mol $L^{-1}$) along with 1.0 mL of $H_2O_2$ were added to the digestion vessels. The vessels were sealed and taken to the CHDS system for digestion using the following heating program: i) a 20-min ramp from room temperature to 195 ºC, ii) a 12-min plateau at 195 ºC and iii) a 30-min cooling down to 40 ºC. The resulting solutions were transferred to polypropylene tubes and the final volume was made up to 25 mL with ultrapure water.

The effect of sample mass amount in the CHDS digestions was also evaluated using the fish food CRM. In this case, sample masses of 50, 100, or 200 mg were weighed and the mixture of 2.0 mL of concentrated $HNO_3$ and 1.0 mL $H_2O_2$ was added to the quartz tubes. The samples were digested using the same heating program described in the previous experiment. The resulting solutions were transferred to polypropylene tubes and diluted to 25 mL with ultrapure water. The digested samples in both experiments (n=3) were analyzed by HR-CS FAAS for the determination of macro and micronutrients in the fish food CRM.

*Digestion of CRMs and dog food samples*

After the CHDS optimizations, 10 samples of dry dog food and 3 certified reference materials were digested (n=3). Sample masses of 200 mg were directly weighed in the CHDS quartz tubes, followed by the addition of 2.0 mL of concentrated $HNO_3$ and 1.0 mL of $H_2O_2$. The samples were processed through the same heating program described in section 2.3.2, which consisted of the following 3 steps: a 20-min ramp from room temperature to 195 ºC (step1), a 12-min plateau at 195 ºC (step 2) and a 30-min cooling down to 40 ºC (step 3). The digested samples were then diluted to 25 mL with ultrapure water.

For comparative purposes, all dog food samples were digested using a closed-vessel microwave-assisted digestion system (n=3). Sample masses of 200 mg were transferred to the microwave vessels and a mixture of 2.0 mL $HNO_3$ (concentrated), 3.0 mL water, and 1.0 mL $H_2O_2$ were added to react. The vessels were placed to digest under the following heating program: i) 100-500 W ramp lasting for 5 min, ii) 800 W plateau for 15 min, and iii) 0 W cooling down for 15 min. The final volume was made up to 25 mL with ultrapure water.

## RESULTS AND DISCUSSION
### *CHDS optimizations*

A fractional factorial design ($2^{5-2}$) with 5 variables and 2 levels was used for the optimization of several CHDS parameters as $HNO_3$ concentration, $H_2O_2$ volume, time of plateau, digestion temperature and pre-digestion time, and using the measured residual carbon content (RCC) as the target response. From these values, the organic matter decomposition efficiencies (%DE) were calculated using the following relationship: %DE = (TCC – RCC)/(TCC) * 100, where TCC is the total carbon content. In this work, the RCC contents were determined by the carbon analyzer and TCC values were obtained by considering the whole sample mass used in digestion as composed only of carbon, thus the calculated %DE may be considered as an estimated value. Results for RCC and %DE are depicted in Figure 1.
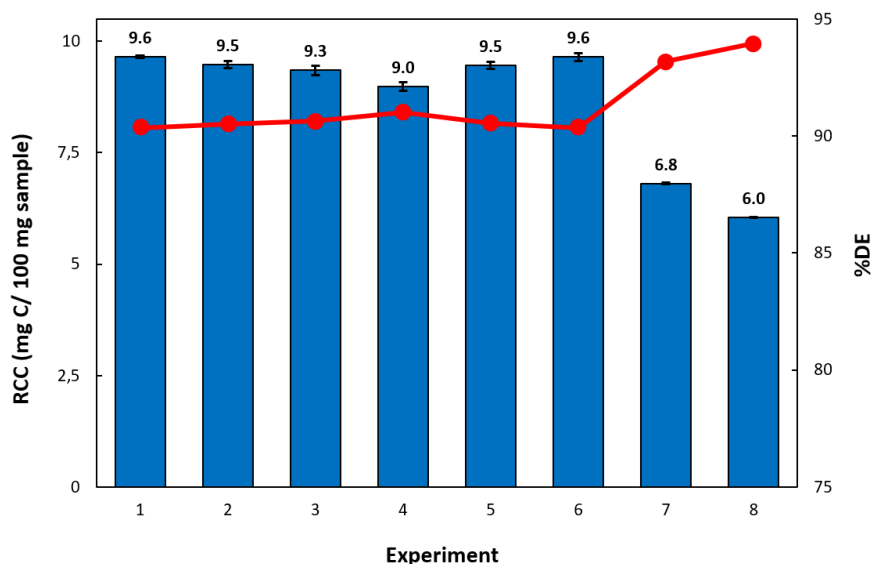


**Figure 1.** Determination of residual carbon content (RCC, bar chart) and estimated decomposition efficiency (%DE, dot chart) for the designed experiments used to optimize the CHDS digestion parameters.

For all experiments, the digested samples presented a limpid aspect and the residual carbon contents were generally lower than 9.6%. The lowest values for RCC were found in experiments 7 and 8, with carbon contents in the 6.0- 6.8 mg C per 100 mg sample range and estimated %DE higher than 93%. In common, these experiments presented high levels for the variables V1 (14 mol $L^{-1}$ $HNO_3$), V2 (1.0 mL of $H_2O_2$), and

V4 (the temperature at 225 ºC). The main differences between experiments 7 and 8 are due to the times of pre-digestion (V5) and plateau (V3), where experiment 8 presented the higher levels for these variables (30 and 24 min, respectively) and experiment 7 the lower levels (15 and 12 min, respectively). These differences may explain the slightly lower levels of RCC for condition 8, as further matrix decomposition was expected with increasing times. A closer look at the significance of the studied variables on the RCC results using a Pareto chart[17] is shown in Figure 2.
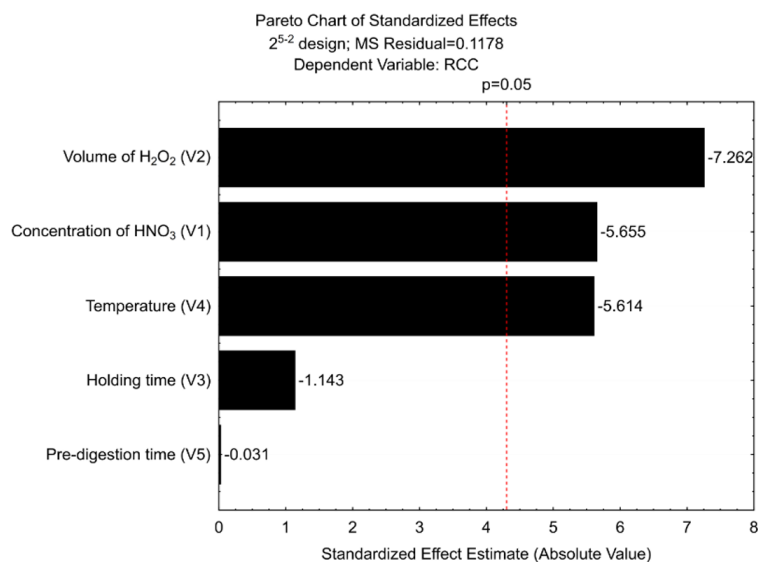


**Figure 2.** Pareto chart for the influence of variables V1-V5 in the digestion efficiency.

Figure 2 presents a standardized effect estimate for each of the variables in function of the RCC results (dependent variable). The p-value equal 0.05 with a 95% confidence interval corresponds to an effect standardized of 4.3027 (as absolute value). The minus signal of the effects indicates that variables evaluated exert an antagonistic effect under the measured RCC.

The significant variables for CHDS digestions were the volume of $H_2O_2$, concentration of $HNO_3$ and the temperature, as the times of pre-digestion and holding during the temperature plateau were not critical. These findings corroborate with the results observed for the pairs of experiments 1-2, 3-4, 5-6, and 7-8, in which the RCC contents are very close and the only difference between themselves was the levels of the time variables (V3 and V5). In this sense, the subsequent experiments were performed without a pre-digestion time and using the lower level of plateau time (12 min). Despite the significance of the digestion temperature and relatively lower values of RCC obtained for 225 ºC, the cooling down step can be performed in shorter times for 195 ºC and lower pressures were achieved, which can improve the safety of the digestion procedure and increase the sample throughput. Thus, the following CHDS experiments were conducted at 195 ºC using 1.0 mL of $H_2O_2$.

The influence of the $HNO_3$ concentration on the determinations of Cu, Fe, K, Na, Mn, and Zn by HR-CS FAAS was further investigated using a fish food CRM (MR-E1002A). Residual acidity is a critical parameter for sample introduction in spectrometric techniques, thus the digestions involved 100 mg of the material and were done using 2 concentrations of $HNO_3$, 7 and 14 mol $L^{-1}$. Although it was not evaluated in the experimental design, the concentration of 7 mol $L^{-1}$ corresponds to half of the acidity found under the previously optimized conditions. Other optimal parameters obtained using the factorial design (no pre-digestion step, 1.0 mL of $H_2O_2$, 195 ºC maximum temperature, and a 12-min plateau) were also employed in this experiment and the results are shown in Table III.

**Table III.** Results (mean ± standard deviation) for the determination of Cu, Fe, K, Na, Mn and Zn in fish food CRM by HR-CS FAAS after CHDS digestions of 100 mg of sample (n = 3) using 7 and 14 mol L$^{-1}$ HNO$_3$

| Analytes | Certified values (mg kg$^{-1}$) | Concentration of HNO$_3$ | | | |
| --- | --- | --- | --- | --- | --- |
| | | 7 mol L$^{-1}$ (mg kg$^{-1}$) | %Agreement | 14 mol L$^{-1}$ (mg kg$^{-1}$) | %Agreement |
| Cu | 10.5 ± 0.9 | 6.8 ± 0.9 | 65 | 8.4 ± 0.5 | 80 |
| Fe | 231.9 ± 20.2 | 185 ± 12 | 80 | 209 ± 5 | 89 |
| K | 5860.0 ± 310.0 | 4282 ± 130 | 73 | 4483 ± 57 | 77 |
| Mn | 19.5 ± 2.1 | 14 ± 3 | 72 | 18 ± 3 | 93 |
| Na | 2160.0 ± 190.0 | 1876 ± 158 | 87 | 1961 ± 7 | 91 |
| Zn | 129.6 ± 6.8 | 114 ± 5 | 88 | 119 ± 2 | 92 |

In general, accuracies were better when 14 mol L$^{-1}$ was used for the CRM digestion, with quantitative apparent recoveries in the 77-93% range. On the other hand, for experiments using 7 mol L$^{-1}$ HNO$_3$, apparent recoveries lower than 75% were found for Cu, K and Mn, which could be due to the greater presence of matrix as the RCC was higher than that found for 14 mol L$^{-1}$ HNO$_3$. The influence of the sample masses on the CHDS digestions of the fish food CRM (MR-E1002A) and HR-CS FAAS determinations was also investigated (Table IV).

**Table IV.** Results (mean ± standard deviation) for the determination of Cu, Fe, K, Na, Mn and Zn in fish food CRM by HR-CS FAAS after CHDS digestions (n= 3) of sample masses of 50, 100 and 200 mg using 14 mol L$^{-1}$ HNO$_3$

| Analytes | Certified values (mg kg$^{-1}$) | Sample masses | | | | | |
| --- | --- | --- | --- | --- | --- | --- | --- |
| | | 50 mg | Agreement (%) | 100 mg | Agreement (%) | 200 mg | Agreement (%) |
| Cu | 10.5 ± 0.9 | 7.6 ± 1.5 | 72 | 8.4 ± 0.5 | 80 | 8.5 ± 0.1 | 81 |
| Fe | 231.9 ± 20.2 | 208 ± 38 | 90 | 209 ± 5 | 90 | 209 ± 2 | 90 |
| K | 5860 ± 310 | 3563 ± 143 | 61 | 4483 ± 57 | 77 | 5488 ± 11 | 94 |
| Mn | 19.5 ± 2.1 | 13.6 ± 0.9 | 70 | 18 ± 3 | 92 | 20 ± 7 | 103 |
| Na | 2160.0 ± 190.0 | 1833 ± 67 | 85 | 1961 ± 7 | 91 | 2188 ± 81 | 101 |
| Zn | 129.6 ± 6.8 | 113.5 ± 0.8 | 88 | 119 ± 2 | 92 | 122.1 ± 0.7 | 94 |

In this case, the digestions of 50, 100, and 200 mg of the material were evaluated and the concentration of HNO$_3$ was 14 mol L$^{-1}$. The same optimized parameters involving 1.0 mL of H$_2$O$_2$, temperatures up to 195 ºC and a 12 min hold during the heating program were employed.  In general, average recoveries of 94, 87, and 78% were obtained for the digestion of 50, 100, and 200 mg of CRM, respectively. For 50 mg, the accuracies were systematically lower, and the apparent recoveries were situated in the 61 – 90% range. This may be explained by the use of mass amounts lower than recommended by the CRM manufacturer, which can impair the homogeneity and representativeness of samples. The best results were found using 200 mg of sample, thus this mass was employed through the next experiments.

### Analytical performance and sample analysis

The trueness and precision for the determination of Cu, Fe, K, Na, Mn, and Zn by HR-CS FAAS using the optimal procedure were checked by analyzing the CRMs of fish food (MR-E1002A), NIST SRM 1577b Bovine Liver and NIST SRM 2976 Mussel Tissue Freeze-Dried (Table V). These materials were selected because of the similarity between the matrices, as dry dog foods are mainly composed by animal protein and fat sources.

**Table V.** Results (mean ± standard deviation) for the determination of Cu, Fe, K, Na, Mn and Zn in CRMs by HR-CS FAAS after CHDS digestions (n = 3)

| Samples | | Analytes | | | | | |
|---|---|---|---|---|---|---|---|
| | | **Cu** | **Fe** | **K** | **Mn** | **Na** | **Zn** |
| MR-E1002A Fish Food | Certified value (mg kg$^{-1}$) | 10.5 ± 0.9 | 231.9 ± 20.2 | 5860 ± 310 | 19.5 ± 2.1 | 2160 ± 190 | 129.6 ± 6.8 |
| | Determined (mg kg$^{-1}$) | 8.5 ± 0.1 | 209 ± 2 | 5488 ± 11 | 20 ± 7 | 2188 ± 81 | 122.1 ± 0.7 |
| | Agreement (%) | 81 | 90 | 94 | 103 | 101 | 94 |
| NIST SRM 1577b Bovine Liver | Certified value (mg kg$^{-1}$) | 160 ± 8 | 184 ± 15 | 9940 ± 20 | 10.5 ± 1.7 | 2420 ± 60.0 | 127 ± 16 |
| | Determined (mg kg$^{-1}$) | 124 ± 1 | 149.7 ± 0.2 | 7811 ± 95 | 8.8 ± 0.1 | 2638 ± 71 | 124 ± 2 |
| | Agreement (%) | 78 | 81 | 79 | 84 | 109 | 98 |
| NIST SRM 2976 Mussel Tissue Freeze-Dried | Certified value (mg kg$^{-1}$) | 4.0 ± 0.3 | 171.0 ± 4.9 | 9700 ± 500 | 33 ± 2 | 35000 ± 1000 | 137 ± 13 |
| | Determined (mg kg$^{-1}$) | 3.8 ± 0.1 | 142.9 ± 0.3 | 7792 ± 67 | 29.3 ± 0.1 | 33131 ± 227 | 135 ± 4 |
| | Agreement (%) | 95 | 84 | 80 | 89 | 95 | 99 |

Considering all the CRMs and analytes, quantitative results were typically obtained, for Fish Food (MR - E1002A) recoveries between 81 and 103% were obtained with RSDs in the range of 0.2 at 1.2% (excluding the 35% of uncertainty observed for Mn), Bovine Liver (NIST SRM 1577b) that showed recoveries of 78 to 109% with RSDs between 0.1 and 2.7% and, Mussel Tissue Freeze-Dried (NIST SRM 2976) with recoveries in the range of 80 at 99% and RSDs from 0.3 to 3.0%. Precisions as relative standard deviations were generally better than 3.0%, and the overall average precision was around 1.6%, except for the measures of Mn in Fish Food that shown 35% of uncertainty in this determination, however in the CRM a value greater than 10% was also shown for this analyte. Considering these results, the combination of CHDS for sample digestions and HR-CS FAAS for determination provided adequate results for the analysis of animal protein matrices.

The found values for the analytes in the CRMs were checked by unpaired *t*-test against the certified values, statistical comparison shown a significant difference between these data, which can be explained considering that the standard deviation of the digested measurements was for several samples much lower than the uncertainty presented in the certificate. Only approximately 30% of values tested by unpaired *t*-test were statistically concordant with the certified, however, the found recoveries shown a great accuracy for 72% these data considering an interval from 84 to 110% of recovery.

Figure 3 summarizes the results data presented in the Table V, are plotted the found values after CHDS digestion and HR-CS FAAS determination versus the certified values for all CRMs (and analytes), in this figure it can be observed that the obtained measurements were really concordant with the certified values in these sample matrices.
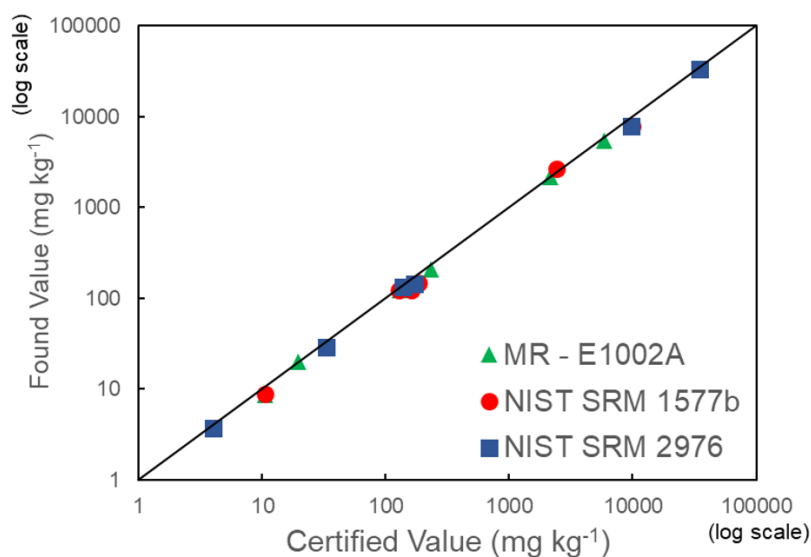
**Figure 3.** Comparison between found values obtained by FAAS after
CHDS digestion of certified materials and the certified reference values.

The developed procedure was then employed for the analysis of 10 real samples of dog food and a comparison between the well-established microwave-assisted digestion (MW-AD) and the proposed conductively heated digestion system (CHDS), both using closed vessels, was performed (Table VI). For macronutrients (Na and K), the determined concentrations were in the 3221 – 6057 mg kg$^{-1}$ range and for micronutrients (Cu, Fe, Mn, and Zn) the contents varied from 8 to 255 mg kg$^{-1}$. In general, the MW-AD and CHDS methods were comparable, and no statistical differences were found at a 95% confidence level (paired *t*-test) in all cases. Moisture is an important quality parameter which can impact shelf-life of dog foods. Determined values for moisture were in the 3.7 – 6.1%, which are lower than 12% and may be considered adequate.[21]

**Table VI.** Results for moisture and digestions by CHDS and MW-AD (n= 3) for the determination (mean ± standard deviation) of Cu, Fe, K, Na, Mn, and Zn in dry dog food samples by HR-CS FAAS and *t*-test values (*t*-critical = 4.303)

| Sample | Moisture (%) | Digestion procedure | Analytes (mg kg$^{-1}$) | | | | | |
|---|---|---|---|---|---|---|---|---|
| | | | Cu | Fe | K | Mn | Na | Zn |
| **1** | 5.4 | MW-AD | 23.4 ± 0.1 | 203 ± 2 | 5095 ± 67 | 61 ± 2 | 5693 ± 122 | 253 ± 1 |
| | | CHDS | 23.3 ± 0.1 | 235 ± 2 | 4828 ± 230 | 59.8 ± 0.4 | 5691 ± 282 | 255 ± 8 |
| | | *t*-value | 0.66 | 2.85 | 1.58 | 0.47 | 0.01 | 0.39 |
| **2** | 4.7 | MW-AD | 10.1 ± 0.1 | 174 ± 13 | 5726 ± 6 | 38.4 ± 0.6 | 4094 ± 162 | 134 ± 2 |
| | | CHDS | 10.4 ± 0.3 | 181 ± 8 | 5724 ± 48 | 38.4 ± 0.9 | 4240 ± 18 | 128 ± 7 |
| | | *t*-value | 1.75 | 0.71 | 3.63 | 0.05 | 1.21 | 3.16 |
| **3** | 3.7 | MW-AD | 29 ± 1 | 201 ± 4 | 5084 ± 179 | 30.5 ± 0.2 | 3282 ± 99 | 227 ± 2 |
| | | CHDS | 30 ± 1 | 223 ± 3 | 5038 ± 70 | 30.6 ± 0.3 | 3221 ± 94 | 229 ± 1 |
| | | *t*-value | 2.94 | 3.14 | 0.33 | 0.26 | 0.68 | 1.48 |

**Table VI.** Results for moisture and digestions by CHDS and MW-AD (n= 3) for the determination (mean ± standard deviation) of Cu, Fe, K, Na, Mn, and Zn in dry dog food samples by HR-CS FAAS and *t*-test values (*t*-critical = 4.303) (continuation)

| Sample | Moisture (%) | Digestion procedure | Analytes (mg kg⁻¹) | | | | | |
|---|---|---|---|---|---|---|---|---|
| | | | Cu | Fe | K | Mn | Na | Zn |
| 4 | 6.1 | MW-AD | 9.4 ± 0.6 | 176 ± 8 | 5951 ± 125 | 42.7 ± 0.6 | 4264 ± 62 | 140 ± 4 |
| | | CHDS | 9 ± 5 | 201 ± 1 | 5834 ± 162 | 42.7 ± 0.3 | 4141 ± 183 | 137 ± 3 |
| | | *t*-value | 0.06 | 4.25 | 2.66 | 2.39 | 1.11 | 0.83 |
| 5 | 5.3 | MW-AD | 12.6 ± 0.2 | 209 ± 5 | 5132 ± 61 | 41.5 ± 0.4 | 4988 ± 395 | 122 ± 3 |
| | | CHDS | 12.6 ± 0.2 | 194 ± 6 | 4958 ± 501 | 41.2 ± 0.3 | 5150 ± 107 | 121 ± 4 |
| | | *t*-value | 0.04 | 0.41 | 0.65 | 1.21 | 0.69 | 0.06 |
| 6 | 6.3 | MW-AD | 11.8 ± 0.7 | 198 ± 4 | 4728 ± 159 | 40.6 ± 0.3 | 4795 ± 132 | 128 ± 3 |
| | | CHDS | 12.5 ± 0.3 | 206 ± 10 | 4702 ± 56 | 41 ± 1 | 4734 ± 45 | 123 ± 6 |
| | | *t*-value | 1.21 | 2.71 | 0.26 | 1.09 | 0.76 | 2.52 |
| 7 | 6.0 | MW-AD | 9.6 ± 0.2 | 153.3 ± 0.6 | 5268 ± 157 | 55.7 ± 0.3 | 4252 ± 65 | 169 ± 3 |
| | | CHDS | 9.3 ± 0.6 | 163.5 ± 0.2 | 5281 ± 106 | 56 ± 1 | 4175 ± 245 | 175 ± 8 |
| | | *t*-value | 0.98 | 2.41 | 2.18 | 0.27 | 0.53 | 1.24 |
| 8 | 5.7 | MW-AD | 9.4 ± 0.7 | 149 ± 1 | 6057 ± 107 | 46.7 ± 0.5 | 3811 ± 39 | 119 ± 3 |
| | | CHDS | 8 ± 1 | 144 ± 6 | 5876 ± 269 | 48 ± 2 | 3919 ± 157 | 118 ± 4 |
| | | t-value | 1.45 | 1.86 | 1.11 | 1.29 | 1.16 | 0.18 |
| 9 | 5.7 | MW-AD | 11 ± 1 | 141 ± 6 | 4753 ± 84 | 47.2 ± 0.5 | 4282 ± 31 | 135 ± 5 |
| | | CHDS | 10.1 ± 0.6 | 156 ± 16 | 4660 ± 106 | 47.9 ± 0.1 | 4387 ± 113 | 138 ± 2 |
| | | *t*-value | 3.94 | 1.29 | 1.03 | 1.81 | 1.55 | 2.96 |
| 10 | 5.5 | MW-AD | 11.9 ± 0.5 | 152 ± 14 | 5416 ± 80 | 38.0 ± 0.7 | 3383 ± 85 | 140 ± 4 |
| | | CHDS | 11.6 ± 0.5 | 157 ± 10 | 5478 ± 35 | 40 ± 2 | 3489 ± 265 | 140 ± 2 |
| | | *t*-value | 0.73 | 0.47 | 1.00 | 1.44 | 0.66 | 0.39 |

The elemental concentration ranges obtained in this work were compared with data from the literature (Table VII). In general, the concentrations of macro and micronutrients in dry dog foods are in the same range as those reported in the literature described in Table VII. Limits of detection (LOD) were calculated according to the IUPAC recommendations, and the measurements were performed using the blank solutions obtained from the MW-AD and CHDS procedure. LODs for MW-AD digestions were 3.4 (Cu), 11 (Fe), 60 (K), 0.5 (Mn), 128 (Na), and 3.5 (Zn) mg kg⁻¹, while for CHDS the values were 3.1 (Cu), 10 (Fe), 56 (K), 0.7 (Mn), 96 (Na), and 3.6 (Zn) mg kg⁻¹. In both cases, the LODs were comparable and low enough to allow the determination of macro and micronutrients in dog food. Both foods intended for dogs and cats are mainly based on animal sources of protein and fat, and the levels of these macromolecules are also very similar. Thus, it is possible to infer that similar performance would be attained for CHDS digestions

of these samples. In addition, pet foods are made primarily from animal protein sources, and the CHDS system has already proven itself as a good alternative for the digestion of this raw materials.[13]

**Table VII.** Determined concentration ranges for macro and micronutrients for this work and comparison with literature values

| Analytes | Determined concentration range (mg kg$^{-1}$) | | | | | |
| | Present work | Sgorlon et al. 2022[18] | Costa et al. 2013[19] | Kelly et al. 2013[20] | Elias et al. 2012[21] | Duran et al. 2010[22] |
| --- | --- | --- | --- | --- | --- | --- |
| Cu | 8 – 30 | 7.0 – 30 | 15.5 – 34.1 | 7.7 – 18.0 | - | 3.3 – 16.6 |
| Fe | 141 – 223 | 50 – 450 | 147 - 606 | 56 - 220 | 188 – 646 | 23.9 – 71.1 |
| K | 4660 – 6057 | 4000 - 8000 | 1000 - 1300 | - | 5290 – 10500 | - |
| Mn | 30.5 – 61 | 20 – 90 | 6.5 – 149 | 16 - 70 | - | 3.3 – 24.4 |
| Na | 3221 – 5693 | 2500 - 7000 | - | - | 3180 – 7050 | |
| Zn | 118 – 255 | 90 - 550 | 106 – 419 | 79 – 330 | 44 - 633 | - |

*Estimated from data plots

### *Sample discrimination*

Concerning the dry dog food, samples 3 and 1 were from manufacturers A and B, respectively, and samples 2, 4, 5, 6, 7, 8, 9, and 10 were from manufacturer C. As for the animal life stage, samples 1, 3, 5, 6, and 7 were destined for puppies, samples 2, 4, 8, and 9 for adults and sample 10 for senior dogs. As the formulation of minerals may vary according to different manufacturers and the needs for nutrients at different dog's life stages, the determined contents of moisture, Cu, Fe, K, Na, Mn, and Zn using CHDS and HR-CS FAAS were used for the proposition of hierarchical cluster analysis (HCA), aiming for the discrimination between the samples (Figure 4). Samples discrimination may be considered an important way to check for food fraud or mislabeling, for example.[24] From the dendrogram, it is possible to check that samples may be accurately separated into three distinct groups according to their manufacturer. From the 8 samples from manufacturer C (red lines), samples 2, 4, 8, and 10 are related to adult or senior dogs and were clustered at a distance equal to 2. Moreover, samples 5, 6 and 7 are related to the puppy life stage and were also grouped at the same distance. On the other hand, sample 9 which corresponds to adult dog food was incorrectly grouped as puppy food. From the results in Table VI, it is possible to confirm that the contents found for K, Mn, Na, and Zn in sample 9 were closer to the averages of the puppy food group than the adult food group, thus explaining the incorrect clustering for this sample.
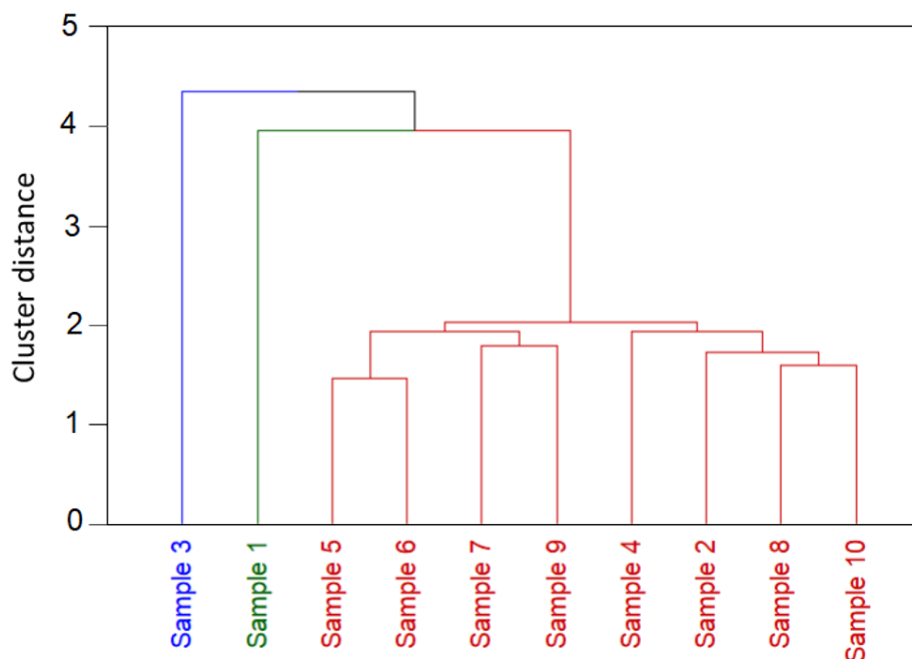
**Figure 4.** Hierarchical clustering dendrogram using mineral composition and moisture data from dog food samples from manufacturer A (blue), manufacturer B (green) and manufacturer C (red).

## CONCLUSIONS

The application of a factorial design for CHDS digestion allowed the execution of only 8 experiments to obtain the optimal conditions as 14 mol L$^{-1}$ HNO$_3$, 1.0 mL of H$_2$O$_2$, 195 ºC of maximum temperature, 12 min of holding time, and no need for a pre-digestion step for the decomposition of dog food samples. In spite of the greater efficiency of decomposition at 225 ºC, safety conditions and sample throughput were incremented when 195 ºC was used. For all tested conditions, the volume of H$_2$O$_2$, concentration of HNO$_3$ and temperature parameters were the most significant and the estimated decomposition rates were better than 90%. Furthermore, the analysis of CRMs from animal food evidenced that the use of 14 mol L$^{-1}$ HNO$_3$ for the digestion of 200 mg of sample provided the best accuracies. Under the optimal conditions, accurate determinations of Cu, Fe, K, Na, Mn, and Zn by HR-CS FAAS were achieved for three CRMs from animal protein sources. The developed CHDS procedure and a comparative MW-AD were applied to 10 real samples from dry dog food and the results showed that both were statistically equivalent at a 95% confidence level. Limits of detection calculated using the blank solutions from CHDS and MW-AD were comparable and adequate for the determination of macro and micronutrients in dog food. Although the performances proved to be equivalent in terms of efficiency, preparation time and generation of residues, CHDS may be considered simpler and less expensive than MW-AD. The hierarchical cluster analysis using the moisture and mineral composition results demonstrated similarities for samples from different manufacturers and, in most cases, for samples destined to different animal life stages for the same manufacturer. The HCA has proven to be a valuable tool for samples discrimination, with potential applications in checking for tampering and fraud in dry dog foods. The procedure combining CHDS digestion and HR-CS FAAS determination provided sensitive, accurate and precise analytical conditions, being a good alternative for dog food quality control

### Conflicts of interest

There are no conflicts of interest to declare.

**REFERENCES**
(1)    Fortune Business Insights. Pet food market size, share & COVID-19 impact analysis by animal type (dogs, cats and others), form (dry pet food, wet pet food and snacks & treats), source (animal and plant), distribution channel (supermarkets, hypermarkets, speciality pet food stores, online channels and others) and regional forecast, 2022-2029. https://www.fortunebusinessinsights.com/industry-reports/pet-food-market-100554 [Accessed 01 December 2022].
(2)    Report Linker. Global pet care industry.  https://www.reportlinker.com/p05896269/Global-Pet-Care-Industry.html [Accessed 01 December 2022].
(3)    Sanderson, S. L. Pros and cons of commercial pet foods (including grain/grain free) for dogs and cats. *Vet. Clin. North Am. Small Anim. Pract.* **2021**, *51*, 529-550. https://doi.org/10.1016/j.cvsm.2021.01.009
(4)    Schleicher, M.; Cash, S. B.; Freeman, L. M. Determinants of pet food purchasing decisions. *Can. Vet. J.* **2019**, *60* (6), 644-650.
(5)    National Research Council. *Nutrient requirements of dogs and cats.* The National Academies Press, Washington, **2006**. https://doi.org/10.17226/10668
(6)    Costa, S. S. L.; Pereira, A. C. L.; Passos, E. A.; Alves, J. P. H.; Garcia, C. A. B.; Araujo, R. G. O. Evaluation of the chemical composition of dry feeds for dogs and cats. *J. Braz. Chem. Soc.* **2018**, *29*, 2616-2625. https://doi.org/10.21577/0103-5053.20180142
(7)    Krug, F. J., Rocha, F. R. P. (Eds.) *Métodos de preparo de amostras para análise elementar*. EditSBQ, São Paulo, 2019.
(8)    Twyman, R. M. Sample Dissolution for Elemental Analysis - Wet Digestion. In: Worsfold, P.; Townshend, A.; Poole, C. (Eds.) *Encyclopedia of Analytical Science*. Elsevier, **2005**, 146-153. https://doi.org/10.1016/B0-12-369397-7/00539-2
(9)    Flores, E. M. M. (Ed.) *Microwave-assisted sample preparation for trace element determination*. Elsevier, Oxford, **2014**.
(10)  Miranda, K.; Pereira-Filho, E. R.; Gomes Neto, J. A. A new closed-vessel conductively heated digestion system: fostering plant analysis by inductively coupled plasma optical emission spectroscopy. *J. Anal. At. Spectrom.* **2014**, *29*, 825-831. https://doi.org/10.1039/C3JA50369K
(11)   Miranda, K.; Vieira, A. L.; Bechlin, M. A.; Fortunato, F. M.; Virgilio, A.; Ferreira, E. C.; Gomes Neto, J. A. Determination of Ca, Cd, Cu, Fe, K, Mg, Mn, Mo, Na, Se, and Zn in foodstuffs by atomic spectrometry after sample preparation using a low-cost closed-vessel conductively heated digestion system. *Food Anal. Methods* **2016**, *9*, 1887-1894. https://doi.org/10.1007/s12161-015-0371-8
(12)  Miranda, K.; Viera, A. L.; Gomes Neto, J. A. High-throughput sugarcane leaf analysis using a low cost closed-vessel conductively heated digestion system and inductively coupled plasma optical emission spectroscopy. *Anal. Methods* **2014**, *6*, 9503-9508. https://doi.org/10.1039/C4AY01841A
(13)  Vieira, A. L.; Miranda, K., Virgilio, A., Ferreira, E. C., Gomes Neto, J. A., 2018. Evaluation of an improved closed-vessel conductively heated digestion system for the analysis of raw meat samples by ICP techniques. *J. Anal. At. Spectrom.* **2018**, *33*, 1354-1362. https://doi.org/10.1039/c8ja00121a
(14)  Torres, E. A. F. S.; Garbelotti, M. L.; Neto, J. M. M. The application of hierarchical clusters analysis to the study of the composition of foods. *Food Chem.* **2006**, *99*, 622-629. https://doi.org/10.1016/j.foodchem.2005.08.032
(15)  Welz, B. High-resolution continuum source AAS: the better way to perform atomic absorption spectrometry. *Anal. Bioanal. Chem.* **2005**, *381*, 69 – 71. https://doi.org/10.1007/s00216-004-2891-8

(16) Beg, S.; Rahman, M., 2021. Design of experiments application for analytical method development. In: Beg, S.; Hasnain, M.S.; Rahman, M.; Almalki, W. H. (Eds.) *Handbook of Analytical Quality by Design*, Academic Press, **2021**, 191-197.

(17) Ferreira, S. L. C.; Lemos, V. A.; de Carvalho, V. S.; da Silva, E. G. P.; Queiroz, A. F. S.; Felix, C. S. A.; da Silva, D. L. F.; Dourado, G. B.; Oliveira, R. V. Multivariate Optimization Techniques in Analytical Chemistry – An Overview. *Microchem. J.* **2018**, *140*, 176–182. https://doi.org/10.1016/J.MICROC.2018.04.002

(18) Wong, K. Y.; Ng, J.; Chong, C. T.; Lam, S. S.; Chong, W. T. Pareto-hierarchical clustering framework for biodiesel transesterification. *Sustain. Energy Technol. Assess.* **2021**, *45*, 101160. https://doi.org/10.1016/j.seta.2021.101160

(19) Sgorlon, S.; Sandri, M.; Stefanon, B.; Licastro, D. Elemental composition in commercial dry extruded and moist canned dog foods. *Anim. Feed Sci. Technol.* **2022**, *287*, 115287. https://doi.org/10.1016/j.anifeedsci.2022.115287

(20) Costa, S. S. L.; Pereira, A. C. L.; Passos, E. A.; Alves, J. P. H.; Garcia, C. A. B.; Araujo, R. G. O. Multivariate optimization of an analytical method for the analysis of dog and cat foods by ICP OES. *Talanta* **2013**, *108*, 157-164. https://doi.org/10.1016/j.talanta.2013.03.002

(21) Kelly, D. G.; White, S. D.; Weir, R. D. Elemental composition of dog foods using nitric acid and simulated gastric digestions. *Food Chem. Toxicol.* **2013**, *55*, 568-577. https://doi.org/10.1016/j.fct.2013.01.057

(22) Elias, C., Fernandes, E. A. D. N.; Bacchi, M. A. Neutron activation analysis for assessing chemical composition of dry dog foods. *J. Radioanal. Nucl. Chem.* **2012**, *291*, 245–250. https://doi.org/10.1007/s10967-011-1285-6

(23) Duran, A.; Tuzen, M.; Soylak, M. Trace element concentrations of some pet foods commercially available in Turkey. *Food Chem. Toxicol.* **2010**, *48*, 2833-2837. https://doi.org/10.1016/j.fct.2010.07.014

(24) Gao, B.; Holroyd, S. E.; Moore, J. C.; Laurvick, K.; Gendel, S. M.; Xie, Z. Opportunities and challenges using non-targeted methods for food fraud detection. *J. Agric. Food Chem.* **2019**, *67*, 8425-8430. https://doi.org/10.1021/acs.jafc.9b03085

# ARTICLE

# Infrared and Electronic Spectroscopy for Assay of Dosulepin in Pharmaceuticals: *Stability Indicating Study and Quantification Approach*

**Shivarampura M. Dushyantha**[1] iD **, Chikkalingaiah Siddaraju**[2] iD **, Nagaraju Rajendraprasad\***[1] iD ✉

[1]PG Department of Chemistry, JSS College of Arts, Commerce and Science (A Research Centre Recognized by University of Mysore), Mysuru–570 025, Karnataka, India

[2]Department of Chemistry, Maharani's Science College for Women, Mysuru–570 005, Karnataka, India
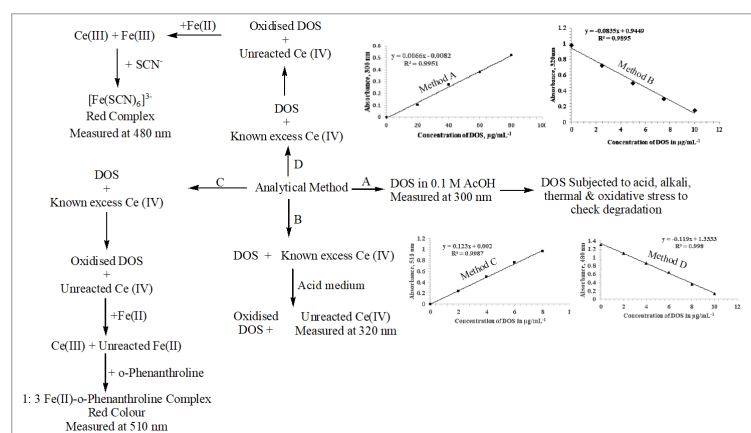
Four simple, precise, and cost-effective spectrophotometric methods were designed and validated to assess Dosulepin hydrochloride (DOS) in pure and dosage form. Two of them are direct UV (Methods A and B), and the other two are indirect visible spectrophotometric methods (Methods C and D). Method A is based on the measurement of the chromophoric activity of DOS in 0.1 M acetic acid (AcOH) at 300 nm. Method B involves the measurement of absorbance due to cerium (IV) left in excess after oxidizing DOS at 320 nm. The unreacted cerium (IV) was treated with a large excess of iron (II), which results in iron (III) and cerium (III). The surplus iron (II) forms a red colored complex with o-phenanthroline at a slightly higher pH was measured at 510 nm in Method C. In Method D the iron (III) formed in the redox reaction between unreacted cerium (IV) and iron (II) was made to form a red colour complex with thiocyanate and measured at 480 nm. The methods are applicable over good linear ranges of 1.0-80.0, 0.25-10.0, 0.5-8.0 and 0.50-10.0 μg mL$^{-1}$ with actual molar absorptivity values of $2.07 \times 10^3$, $3.11 \times 10^4$, $4.08 \times 10^4$ and $3.7 \times 10^4$ L mol$^{-1}$cm$^{-1}$ for Method A, B, C and D, respectively. The validating parameters like limit of detection (LOD), quantification (LOQ), Sandell sensitivity and others have been reported. The methods proposed were successfully applied to quantify DOS in pharmaceuticals. The Fourier Transform Infrared (FT-IR) spectra of the post degradation DOS were studied, compared with that of pure drug and reached to the possible effect of degradation to stress by stability indicating property of Method A.

**Keywords:** Dosulepin hydrochloride, cerium (IV), spectrophotometry, chromophore, pharmaceuticals

## INTRODUCTION

Dosulepin hydrochloride (DOS), also referred as dothiepin hydrochloride (Figure 1),[1] is (E)-3-(dibenzo[b,e] thiepin-11(6H)-ylidene)-N,N dimethyl propan-1-amine, hydrochloride. It is a tricyclic antidepressant that is used to treat endogenous depression and has anxiolytic qualities as well. DOS helps in relieving depression by preventing the reabsorption of serotonin and noradrenaline into the nerve cells of the brain.[2-4]
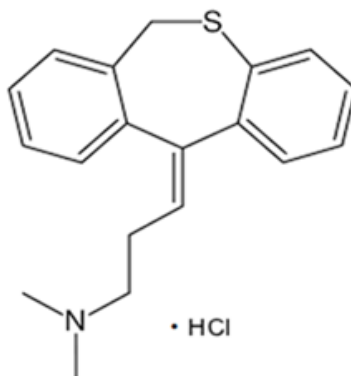


**Figure 1.** Chemical structure of DOS.

European Pharmacopoeia (EP) recognizes DOS as official one.[5] The EP describes a procedure of non-aqueous potentiometric titration of DOS in acetic acid (AcOH) and acetic anhydride medium against 0.1 M perchloric acid for quantification.

The results of the comprehensive literature review demonstrated that different methods were used to ascertain DOS quantification in pharmaceutical and biological substances. The techniques covered here include liquid chromatography,[6–10] gas chromatography,[11–13] high performance liquid chromatography,[1,2,14–20] conductometry,[21,22] potentiometry,[23,24] and capillary electrophoresis.[25]

Different authors also reported a number of spectrophotometric techniques in addition to these. Sameer et al.[3] developed two techniques for spectrophotometric estimation of DOS by measuring the drug in 0.1 M HCl at 229 nm and in methanol at 231 nm. The evaluation of the limit of detection (LOD), limit of quantification (LOQ), and other regression parameters, successful application of the method to dosage forms and recovery studies were also presented. Heba et al.[4] developed a spectrophotometric method for DOS based on the formation of a binary complex with mercurochrome that was measured at 557 nm with LOD and LOQ of 0.41 and 1.26 µg mL$^{-1}$. The method was validated statistically. Three techniques for determining DOS were developed by Wafaa[26] and quantified at 423, 498, and 625 nm with respectable sensitivity and regression parameters. Two approaches for quantifying DOS and other two species were published by Hisham et al.[27] based on the generation of mixed anhydrides with malonic and acetic acids, which may be detected in the 329-333 nm range. A method for spectrophotometric detection of DOS was established by Walash et al.[28] in which DOS was measured at 540 nm in an acetate buffer at pH 3.7. The LOD and LOQ values were found as 0.18 and 0.54 µg mL$^{-1}$, respectively. The technique was used with effectiveness in dosage formulations. Two spectrophotometric approaches have been published by Basavaiah et al.[29] based on the production of an ion pair complex of DOS with bromophenol blue (Method 1) and bromocresol green (Method 2) which were measured at 425 and 430 nm, respectively. For Methods 1 and 2, the LOD and LOQ were reported to be 0.18 and 0.53, 0.17 and 0.50 µg mL$^{-1}$, respectively. Two spectrophotometric techniques based on the production of an ion pair complex of DOS with bromocresol blue and eriochrome black-T were also reported by Umamaheswar et al.[30] The complexes formed were extracted and measured at 418 and 508 nm, respectively. The procedures were statistically evaluated. Two methods for determining DOS were developed by Sameer et al.[31] Method A was based on the formation of an ion pair complex with Alizarin red-S, its extraction into dichloromethane, and quantification at 445 nm. Method B was based on the breaking of the formed ion-pair complex and the measurement of free alizarin red-S at

570 nm. The techniques were put to use with dosage formulations and the results were statistically validated. Two techniques for quantifying DOS were reported by Elham.[32] The oxidation of DOS with alkaline $KMnO_4$ was kinetically examined in Method A for a fixed 25 minutes. The coloured manganate's wavelength was fixed at 610 nm for measurements. The absorbance at 470 nm was determined at a set time of 60 minutes for Method B, which was based on the reaction of DOS with 4-chloro-7-nitrobenzofurazan. By creating binary compounds with bromophenol blue, bromothymol blue, bromocresol purple, and bromophenol red, Sane et al.[33] devised a spectrophotometric method for quantifying DOS. In order to measure DOS, Sameer et al.[34] reported two spectrophotometric procedures. The method was based on the addition of a known excess of a bromate-bromide mixture in an acidic medium, which caused the bromination of DOS. The excess of bromine was then estimated by measuring the absorbance at 540 nm with a fixed amount of meta-cresol purple. The sensitivity and regression parameters were reported. Using the hydrochloride of dothiepin as the n-donor and 2,3-dichloro-5,6 dicyano-p-benzoquinone (DDQ) or p-chloranilic acid (p-CA) as the -acceptors, Elham et al.[35] established spectrophotometric charge-transfer complex production, which formed brightly colored complex. The colored products were spectrophotometrically detected using DDQ and p-CA at 460 and 525 nm respectively.

Despite the large number of spectrophotometric methods that have been published, no reports were found for the DOS using cerium (IV) following the direct and indirect method of estimations. The bulk of them involve the use of expensive chemicals and organic solvents for extraction, making them not environmentally friendly. Further, these techniques fell short in terms of accuracy and precision, and most of them require specialized workers, well-equipped laboratories, and strict working conditions in order to conduct analysis. Therefore, there is room for method development in terms of sensitivity and simplicity.

In light of this, an effort was made to create straightforward, precise, affordable, and cost-effective methods for measuring the DOS, and the authors believe they have achieved their goal.

## MATERIALS AND METHODS
### Instruments
A flexible benchtop Agilent Cary 630 Fourier Transform Infrared (FTIR) spectrometer (Agilent Technologies Ltd, Mumbai, India) have been utilized for measurements. It operates with the MicroLab Pharma Software in the spectral range 4,000 to 400 $cm^{-1}$ with ≤ 2 $cm^{-1}$ resolution. The thermal detector containing 1.3 mm diameter, thermoelectrically-cooled deuterated triglycine sulfate (DTGS) and potassium bromide pellet method were employed.

Shimadzu UV-Visible 1800 spectrophotometer capable of measuring the absorption in the wavelength range of 190-1100 nm with a band width of 1.0 nm was used for UV measurements in the fast scan mode. The quartz cuvette with 1 cm path length was utilized for the measurements.

### Reagents
The chemicals and reagents utilized were all of the analytical variety. Except as otherwise noted, all works were performed using distilled water (DW) of conductivity 1.34 µS $cm^{-1}$. The gift sample of pure DOS was obtained from Taj Pharma India Ltd, Hyderabad.

Acme Generics LLP, Himachal Pradesh, India's Prothiaden tablets (50 mg DOS/tablet) were bought from commercial sources. The standard glacial acetic acid (AcOH, Merck, Mumbai, India, 98% Pure) was diluted to resulting 0.1 M solvent. By diluting the necessary volume of concentrated $H_2SO_4$, a 2 M $H_2SO_4$ was created. The needed quantity of cerium (IV) sulphate (85-115% pure) (Loba Chemie Ltd, Mumbai, India) was dissolved in 0.5 M $H_2SO_4$ and heated. After cooling, the solution was standardised with sodium oxalate solution.[36] The requisite aliquots were pipetted and diluted to obtain 128 and 300 µg $mL^{-1}$ cerium (IV). In order to make 1000 µg $mL^{-1}$ of ferrous sulphate solution, 1.0 g of $FeSO_4.7H_2O$ (98% pure; from Thermo Fisher Scientific India Pvt. Ltd. Mumbai) was dissolved in 5 mL of 2 M $H_2SO_4$ and diluted to a volume of 1 L using distilled water. The required volume of this was diluted to obtain 500 µg $mL^{-1}$ with respect to iron (II). A 20% (w/v) ammonium thiocyanate ($NH_4SCN$) solution was prepared by dissolving

20 g of the chemical (S. D fine chem Ltd, Mumbai, India, 98% pure) in about 70 mL of water and made up to mark with water in a 100 mL volumetric flask. A 1000 µg mL$^{-1}$ of o-phenanthroline was prepared by dissolving 0.5 g of chemical (99.5% pure from Himedia Laboratories, Mumbai, India) in approximately 300 mL of water followed by heating and then adding water to the mark in a 500 mL volumetric flask. A 100 mL volumetric flask was filled to the proper level with water after 20.50 g of sodium acetate (NaOAc) (S.D. Fine Chem Ltd., Mumbai, 98%pure) was dissolved in approximately 80 mL of water to prepare 2.5 M NaOAc.

## Experimental procedures
### Method A
Different aliquots of the 100 µg mL$^{-1}$ DOS solution in 0.1 M AcOH, equivalent to 1.0–80 µg mL$^{-1}$, were correctly measured and carefully placed into a series of 10 mL standard flasks. The flasks were added with 0.1 M AcOH to reach 10 mL. At 300 nm, the absorbance of each solution was recorded in comparison with a reagent blank (10 mL aqueous solution contains 0.1 M AcOH).

### Method B
Into a series of 10.0 mL volumetric flasks different aliquots of 25 µg mL$^{-1}$ of DOS to get 0.25 – 10 µg mL$^{-1}$ solutions were measured and transferred carefully. One mL of 128 µg mL$^{-1}$ cerium (IV) has been added to each flask and the contents were mixed well and allowed to stand for 10 min. DW was used to further dilute the contents to the proper concentration. The absorbance of each solution was then measured at 320 nm in comparison to water.

### Method C
Various aliquots of 40 µg mL$^{-1}$ of DOS solution were introduced to a series of 10.0 mL volumetric flasks to get 0.5 – 8.0 µg mL$^{-1}$ of DOS solution followed by the addition of 1 mL of 300 µg mL$^{-1}$ of cerium (IV). Ten minutes were given for the contents to stand. To each of the flasks 1 mL of 500 µg mL$^{-1}$ of FeSO$_4$ solution was added, mixed, and allowed to stand for 5 min, followed by the addition of 1 mL of 1000 µg mL$^{-1}$ o-phenanthroline and 1 mL of 2.5 M NaOAc. Each solution was brought to the mark with DW, mixed and absorbance was measured at 510 nm against a reagent blank after the solutions had been well mixed.

### Method D
Accurately measured aliquots of the 40 µg mL$^{-1}$ DOS solution were transferred into a series of 10 mL calibrated flasks to obtain 0.5 – 10 µg mL$^{-1}$ standards. Each flask received 1 mL of the 300 µg mL$^{-1}$ cerium (IV) solution. Ten minutes were given for the contents to stand. Each flask received 1 mL of a 500 µg mL$^{-1}$ FeSO$_4$ solution, which was mixed and left to stand for 5 minutes before adding 1 mL of 20% (w/v) NH$_4$SCN solution. The flask's contents were thoroughly mixed and made up to the mark with DW. At 480 nm, the absorbance of each solution was noted after against a water blank.

The calibration curves were constructed by plotting the absorbance measured versus the concentration (µg mL$^{-1}$) of DOS. The unknown concentrations were found by calibration graph or by regression equation derived from concentration-absorbance data.

### Procedure for tablets
Weighing and lyophilizing were done on ten Prothiaden tablets. The amount of tablet powder needed for each method was 10 mg for Method A, 25 mg for Method B, and 40 mg for Methods C and D were weighed and put into individual 100 mL volumetric flasks. Each was thoroughly shaken for 20 minutes with about 70 mL of 0.1 M AcOH before being filtered using Whatman No. 1 filter paper into additional 100 mL volumetric flasks. The filtrate was diluted to the mark with DW to get 100, 250, and 400 µg mL$^{-1}$ of tablet extract respectively. A 5.0 mL of each tablet extract of 250 and 400 µg mL$^{-1}$ extracts were diluted 10 times further with the working solvent and the solute of 100, 25 and 40 µg mL$^{-1}$ DOS were put to use for the analysis using the general process already mentioned in Methods A, B, C and D above.

## RESULTS AND DISCUSSION
### *Methodology*

The chromophoric activity of DOS in 0.1 M AcOH is measured in method A. The wavelength maximum for DOS in 0.1 M AcOH medium was found at 300 nm. The absorbance at 300 nm grows linearly along with DOS concentration. As cerium (IV) is reduced to cerium (III) by the DOS in Method B, the absorbance of cerium (IV) left was measured at its maximum wavelength of 320 nm. As the DOS concentration rises, the absorbance falls. The absorption spectra of DOS in 0.1 M AcOH and cerium (IV) in 2 M $H_2SO_4$ medium are given in Figure 2.

Methods C is based on the measurement of absorbance of the red-coloured complex formed between left over iron (II) and o-phenanthroline complex at 510 nm. Method D involves the complexation of iron (III) produced with thiocyanate and the resultant iron hexathiocyanate was measured at 480 nm. Method C and D follow the indirect estimation of DOS, as the generated iron (II)-o-phenanthroline complex concentration increases linearly with the concentration of DOS, and the concentration of iron (III)-thiocyanate complex decreases linearly with the concentration of DOS.
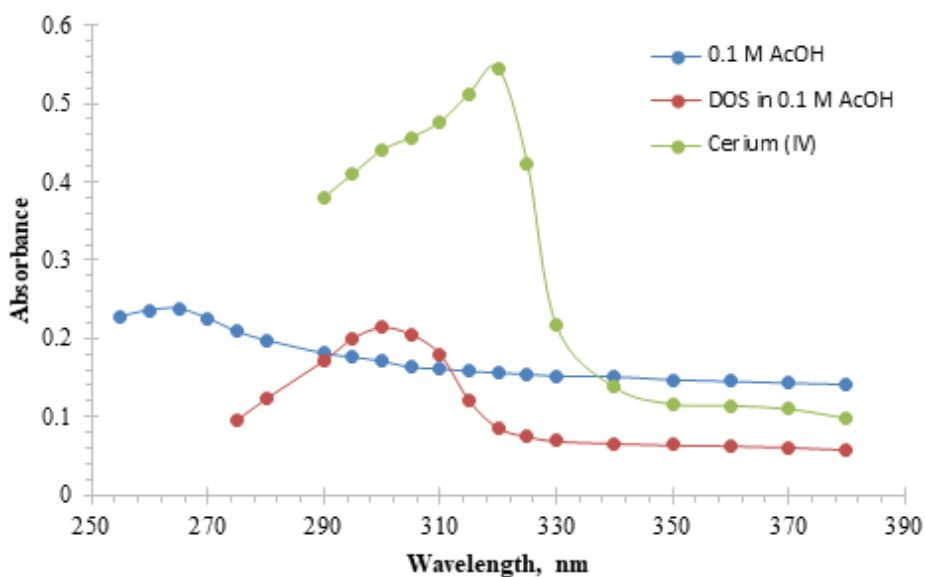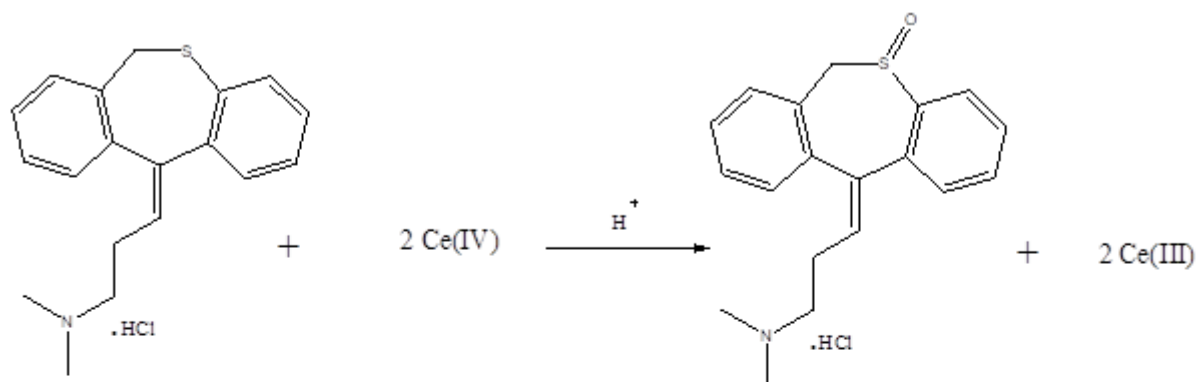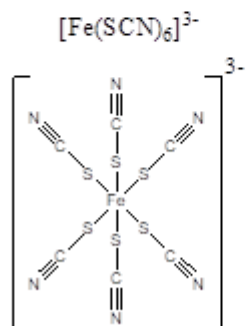


**Figure 2.** Absorption spectra of 0.1 M AcOH, DOS in 0.1 M AcOH and cerium (IV) solution.

The probable reaction schemes proposed for Methods B, C and D are presented in Scheme 1.[37,38]
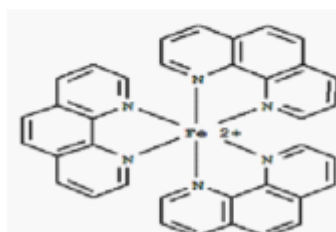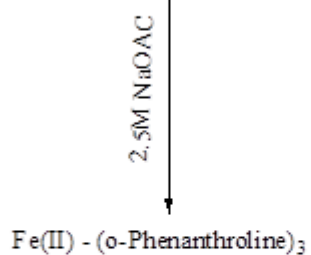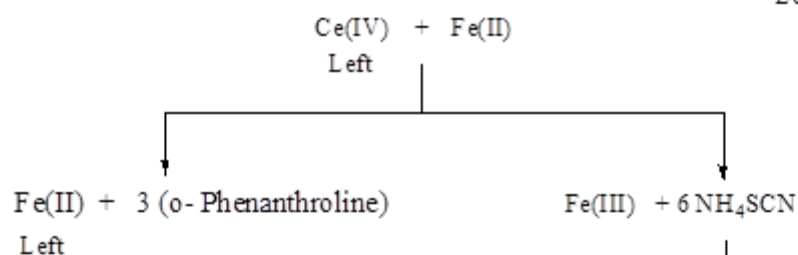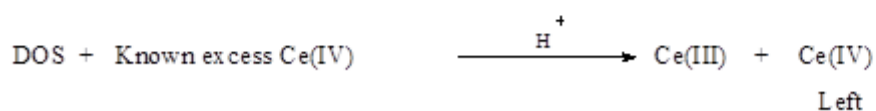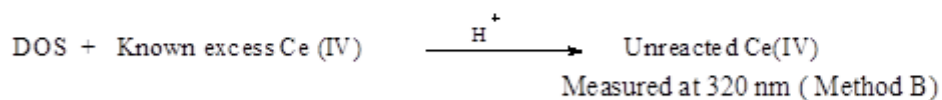


**Scheme 1.** Reaction schemes for Method B, C and D.

## Optimization of variables

By changing one variable at a time while holding the others constant, many factors, including the amount of oxidant, the choice of acid, the acid concentration, the solvent, the concentration of metal ions, and the concentration of ligands, were optimized one after the other. The optimization was based on the maximum absorbance obtained at the respective $\lambda_{max}$ in each method. The effective chromophoric behaviour of DOS was not seen when it was dissolved in solvents like $H_2O$, alcohol and methylene chloride[5] but, the chromophoric behaviour of DOS in AcOH was found to be satisfactory. So, 0.1 M AcOH was selected as a solvent in Method A, DOS showed maximum absorbance at 300 nm in 0.1 M AcOH medium. At this wavelength, the linearity was established between the absorbance and concentration of DOS in 0.1 M AcOH, made it possible to find the linear concentration range of method A. It was discovered that 2 M $H_2SO_4$ was the best acid to utilize for all techniques except Method A after experimenting with various acids of different concentrations. To fix the optimum amount of cerium (IV) to oxidize DOS in Method B, C and D, investigations were carried out using the oxidant, acid, reducing agent, viz, iron (II) and complexing agents namely o-phenanthroline and thiocyanate. Varying volumes of 1000 µg mL$^{-1}$ cerium (IV) were placed in 10 mL standard flasks, acidified with 2 M $H_2SO_4$ and added 1 mL of 500 µg mL$^{-1}$ iron (II) sulphate as reductant. After the rapid oxidation ensured to be completed, either the unreacted reductant was treated with o-phenanthroline or oxidised reductant treated with thiocyanate in Methods C and D, the contents were diluted to the mark with water and measured the absorbances at respective wavelengths of maximum. The upper limit of absorbance as either ~1 or 1.33 in Method C and D were found when the cerium (IV) present at 128 or 300 µg mL$^{-1}$. Besides, the linearity was found excellent to satisfy the Beer's law up to these levels of cerium (IV). Hence, the upper Beer's law limit for cerium (IV) was set by preliminary examinations is found as 128 µg mL$^{-1}$ for Method B and 300 µg mL$^{-1}$ for Methods C and D. To evaluate the DOS of detection range, different concentrations were reacted with 1 mL of 128 or 300 µg mL$^{-1}$ of cerium (IV). Based on the absorbance data acquired for Methods C and D, different concentrations of iron (II) were used and optimized at 500 µg mL$^{-1}$. After experimenting with various concentrations, the sodium acetate (NaOAc) was optimized, and the greatest analytical signal was found at 2.5 M NaOAc. In Method B, the absorbance measured at 320 nm with respect to cerium (IV) decreases as the concentration of DOS increases. Similarly, in Method C, $[Fe(o\text{-}phenanthroline)_3]^{+2}$ absorbance increases linearly with DOS concentration at 510 nm, while in method D, $[Fe(SCN)_6]^{3-}$ absorbance declines linearly with DOS at 480 nm.

## Study of DOS stability under various stressing media/conditions in Method-A

The stability of the DOS was ascertained by forced degradation studies of DOS solution equivalent to 60 µg mL$^{-1}$ under different stressed conditions. The solution was treated with 0.1N HCl and 0.1N NaOH starting from room temperature up to 70 ºC for seven hours to check the stress degradation by hydrolysis under acidic and basic conditions, respectively. Oxidative degradation was done by treating the solution with 3% $H_2O_2$ solution at neutral pH for seven hours. The solution was placed in hot air oven for 24 h at 105 °C to check the thermal degradation. For UV stress studies, solution was exposed to UV radiations for 24 hours.[39] The FT-IR (Figure 3) and UV (Figure 4) spectra of these stressed DOS samples were compared with that of pure DOS spectra and the results were summarised in Table I.
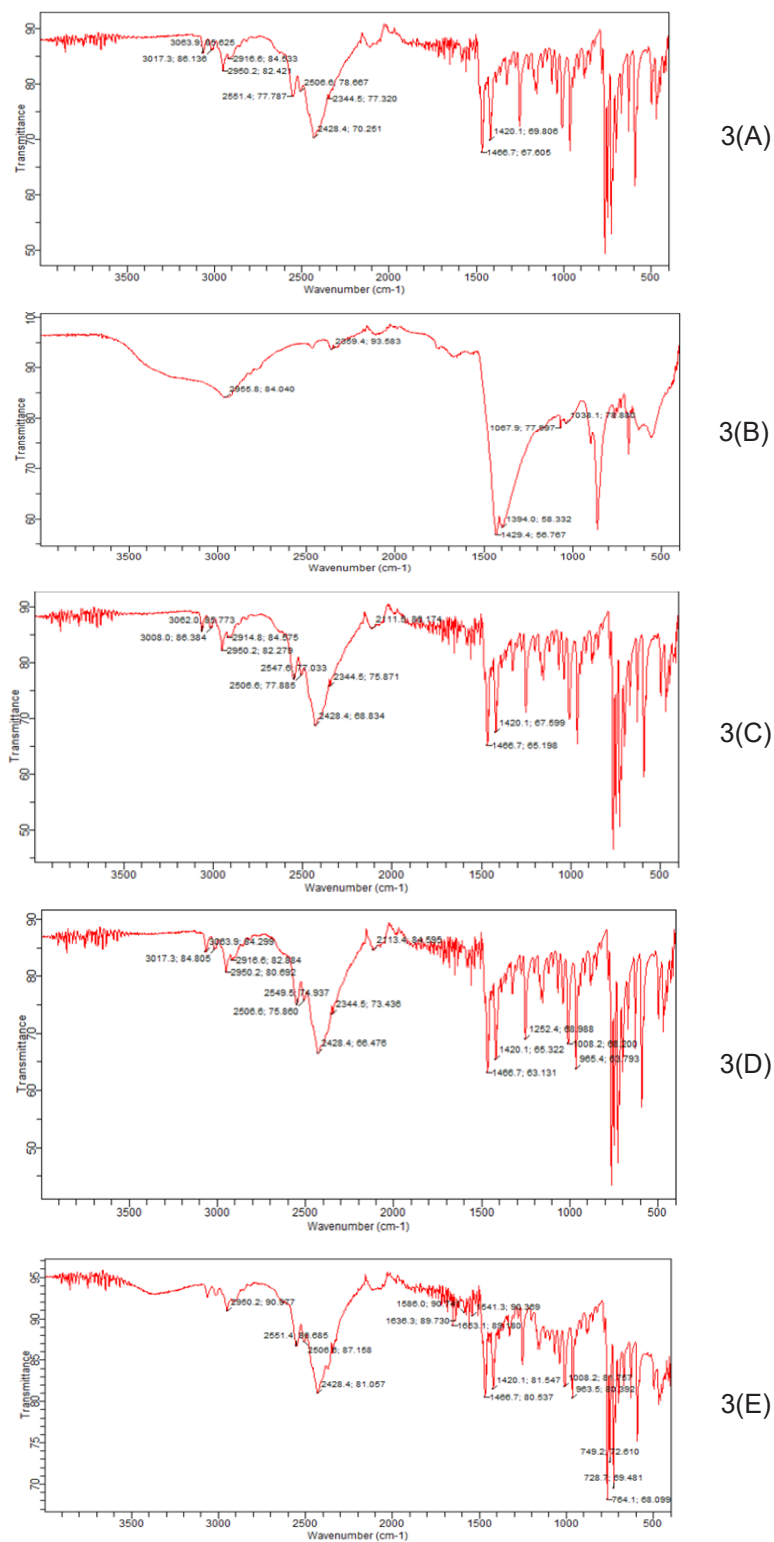
**Figure 3.** FT-IR spectra of: 3(A) – Pure DOS; 3(B) – Alkaline degraded DOS; 3(C) – Thermal stressed DOS; 3(D) – UV stressed DOS; 3(E) – Acid stressed DOS.

The FTIR spectrum of pure DOS shows asymmetric and symmetric stretching bands for methyl group in the region 2916-2950 $cm^{-1}$ and 3017-3063 $cm^{-1}$. The $CH_2$ stretching vibrations are also observed in the region 2950-3020 $cm^{-1}$. The band around 3035 $cm^{-1}$ generally represents the C-H stretching vibrations of aromatic ring and the ring C-C stretching vibrations occurs in the 1420-1625 $cm^{-1}$ region. The asymmetric and symmetric deformations are expected in the range 1420-1466 $cm^{-1}$. The band in the region 520-530 $cm^{-1}$ represents the C-S stretching vibrations. For DOS the C-N stretching vibration modes are observed in the region 728-1008 $cm^{-1}$. The nitrogen present in DOS is tertiary in form, the corresponding onium salt is commonly encountered and it displays strong broad N-H stretching vibrations in the region around 2500 $cm^{-1}$.

The degradation of DOS in the alkaline medium was evident from the comparison of FT-IR spectra of pure DOS with the that of post alkaline degradation drug. The missing of a prominent peak at 2428 $cm^{-1}$ corresponds to the N-H stretching vibrations of 'onium' salt form of tertiary amine group and bands in the region of 794-1033 $cm^{-1}$ due to C-N stretching vibrations indicates the degradation of DOS in alkaline medium. Further, the extension of study of DOS by stressing it to oxidation with peroxide revealed more than 50% degradation. The solid product left post-oxidation was found-insufficient. However, the resulted content was dissolved in 0.1 M AcOH and was recorded the UV spectrum. The absorbance at 300 nm indicated the recovery of 47.26% DOS and confirmed the degradation above 50%. Other than these, DOS was stable under acid, UV and thermal stress, as there was no significant difference between their FT-IR spectra and that of pure DOS. The FT-IR assignments were compared with the band regions calculated by Generalized Gradient Approximation methods developed by Perdew and Wang (GGA-PW91) and Becke-Lee-Yang-Parr (GGA-BLYP) and found to be robust.[40]

The UV spectra of DOS under different stressed conditions indicated that, DOS did not degrade under acidic, thermal and UV stressed conditions and the spectra is similar to that of spectrum of pure DOS in 0.1 M AcOH. The presence of wavelength shifted flat curve in the alkaline stressed DOS and the other with less intensity at 300 nm confirms that, almost complete degradation and partial degradation of DOS in 0.1 M NaOH and 3% $H_2O_2$, respectively.
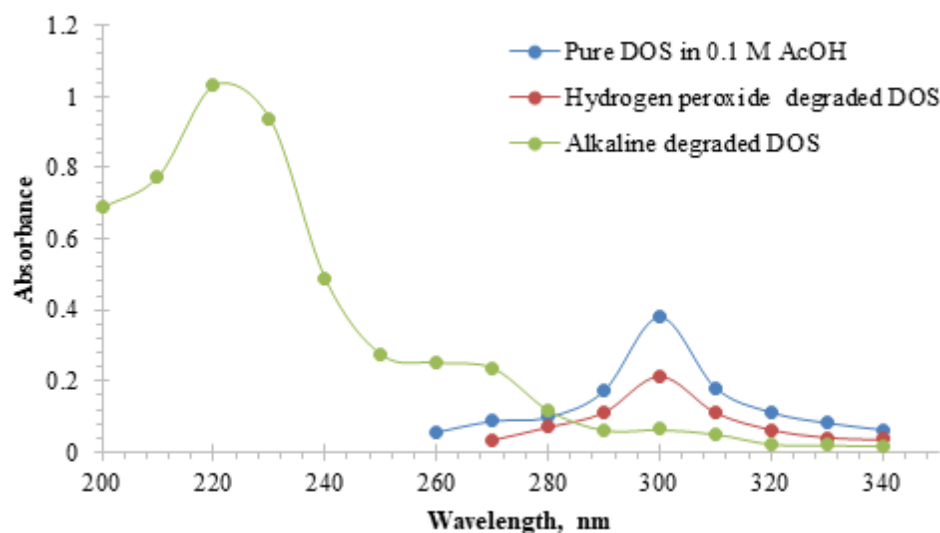


**Figure 4.** UV- spectra of Pure DOS in 0.1 M AcOH, $H_2O_2$ and alkaline degraded DOS.

**Table I.** Results of stability studies of DOS under various stressing conditions in Method A

| Stressing media/condition | %Recovery of DOS |
|---|---|
| HCl | 101.73 |
| NaOH | 11.42 |
| $H_2O_2$ | 47.26 |
| Exposed to UV rays for 24 h | 100.94 |
| Exposed to high temperature for 24 h | 101.08 |

## Method validation

### Linearity and sensitivity parameters

According to International Conference on Harmonisation (ICH) norms,[41] validation checks on the suggested methodologies were performed. The linear correlation between the absorbance at respective $\lambda_{max}$ and concentration of DOS were established in the range given in Table II. The regression Equation 1 was derived for each calibration line.

$$Y = a + bX \qquad \text{Equation 1}$$

where Y is the absorbance of a 1 cm layer of solution, *a* is the intercept, *b* is the slope and X is the concentration in µg mL$^{-1}$.

The obtained calibration curves (Figure 5) are experimental and calibration equations were derived using the Least Squares method. The non zero intercept values reported are for the best curve fitting line. For all the approaches, a, b, regression coefficient ($R^2$), Beer's law range, molar absorptivity, and Sandell sensitivity values were computed and provided in Table II. The limits of detection (LOD) and quantification (LOQ) were calculated following to ICH guidelines[41] using the formula LOD=3.3S/b and LOQ= 10S/b, where S is the standard deviation (SD) of blank absorbance values and b is the slope of the calibration plot.
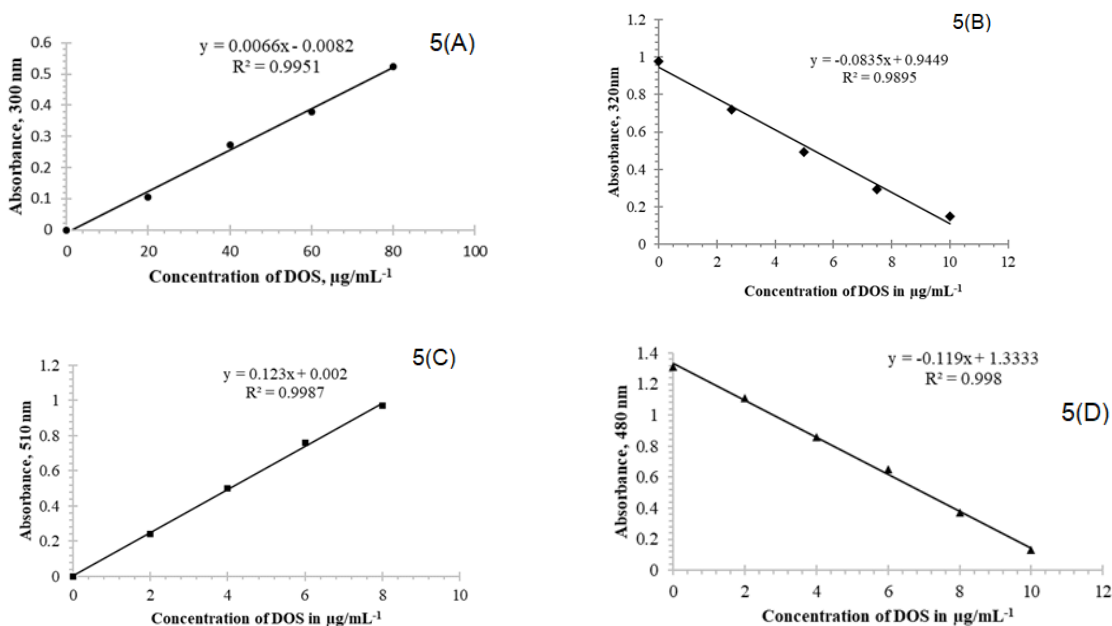


**Figure 5.** Calibration plots for: 5(A) – Method A; 5(B) – Method B; 5(C) – Method C; 5(D) – Method D.

**Table II.** Sensitivity and regression parameters for proposed methods

| Parameter | Method A | Method B | Method C | Method D |
|---|---|---|---|---|
| $\lambda_{max}$, nm | 300 | 320 | 510 | 480 |
| Linear range, $\mu g\ mL^{-1}$ | 1.0-80.0 | 0.25-10.0 | 0.5-8.0 | 0.5-10.0 |
| Molar absorptivity, $L\ mol^{-1}\ cm^{-1}$ | $2.067 \times 10^3$ | $3.1086 \times 10^4$ | $4.08 \times 10^4$ | $3.70 \times 10^4$ |
| Sandell sensitivity, $\mu g\ cm^{-2}$ | 0.1605 | 0.0106 | 0.0081 | 0.0089 |
| LOD, $\mu g\ mL^{-1}$ | 0.2347 | 0.0883 | 0.1204 | 0.7070 |
| LOQ, $\mu g\ mL^{-1}$ | 0.7113 | 0.2676 | 0.3650 | 2.1424 |
| Regression Data, $Y = a + bX$ | | | | |
| Intercept (a) | -0.0082 | 0.9449 | 0.0020 | 1.3333 |
| Slope (m) | 0.0066 | -0.0835 | 0.1230 | -0.1190 |
| Regression coefficient ($R^2$) | 0.9951 | 0.9895 | 0.9987 | 0.9980 |

*Accuracy and precision*

Triplicates of three different amounts of DOS were used to study the intra-day and inter-day variations to test the accuracy and precision of the suggested approaches. Intra-day measurements include the analysis of drug three times (forenoon, afternoon and at evening) within a day. Whereas, the inter-day analysis was performed on three consecutive days under optimal experimental conditions using developed procedures. The percentage relative error (%RE) and percentage relative standard deviation (%RSD) between the amounts obtained by measurement and the amounts subjected were evaluated, and used to assess the correctness and closeness of the proposed methods. The study findings presented in Table III imply a high degree of precision and accuracy between the computed and each individual values.

**Table III.** Intra-day and Inter-day Accuracy Precision

| Method | DOS taken $\mu g\ mL^{-1}$ | Inter-day accuracy and precision | | | Intra-day accuracy and precision | | |
|---|---|---|---|---|---|---|---|
| | | DOS found* $\mu g\ mL^{-1}$ | %RE | %RSD | DOS found* $\mu g\ mL^{-1}$ | %RE | %RSD |
| A | 10.00 | 10.05 | 0.51 | 1.45 | 10.10 | 1.00 | 2.21 |
| | 20.00 | 20.12 | 0.63 | 1.83 | 19.93 | 0.34 | 1.12 |
| | 30.00 | 28.93 | 3.56 | 3.05 | 29.07 | 3.07 | 0.77 |
| B | 2.50 | 2.53 | 0.01 | 1.54 | 2.53 | 1.46 | 1.24 |
| | 5.00 | 4.96 | 0.36 | 3.71 | 5.17 | 3.48 | 2.48 |
| | 7.50 | 7.63 | 0.16 | 1.67 | 7.56 | 0.86 | 0.48 |
| C | 2.00 | 1.94 | 2.72 | 2.42 | 1.91 | 4.08 | 4.25 |
| | 4.00 | 3.98 | 0.34 | 3.12 | 4.01 | 0.34 | 3.10 |
| | 6.00 | 5.91 | 1.36 | 1.37 | 6.05 | 0.90 | 2.05 |
| D | 2.00 | 2.04 | 2.20 | 4.10 | 1.96 | 1.96 | 4.28 |
| | 4.00 | 4.11 | 2.90 | 3.11 | 4.03 | 0.84 | 3.18 |
| | 6.00 | 5.93 | 1.02 | 2.16 | 5.99 | 0.09 | 2.80 |

*Mean values of three determinations

*Robustness and ruggedness*

The proposed procedures were shown to be reliable, despite purposefully varying the acid content, solvent, and other parameters, there was no appreciable change in RSD values above 5%.

Three analysts were performed the assays independently utilizing various lab instruments and spectrophotometers to test the robustness of the methods. It was found that the % RSD values were less than 5%, which amplifies the fact that the suggested approaches were reliable.

***Applications to tablet analysis and statistical evaluation of results***

Commercially available DOS tablets were evaluated using the suggested methodologies and the standard procedure of a reference method. As mentioned in the reference method, 0.1 M perchloric acid was the titrant for the potentiometric estimation of DOS in an anhydrous acetic acid and acetic anhydride medium.[5] The true titrating agent, however, was the acetyl perchlorate that generated during the course of titration.[42] The study findings were presented in Table IV. The results of proposed methods are not deviated with respect to accuracy as well as precision as it can be realised from calculated F and *t* values in the Table IV. Thus, the proposed methods are confirmed and as evolved at acceptable accuracy and precision.

**Table IV.** Results of analysis of prothiaden tablets by proposed methods and reference Method

| Nominal DOS amount (mg/tablet) | Found* (Percent label claim ± SD) | | | | |
|---|---|---|---|---|---|
| | Reference method | Method A | Method B | Method C | Method D |
| 50.00 | 100±0.57 | 99.92±0.64<br>F = 1.26<br>t = 0.21 | 100.06±0.59<br>F = 1.07<br>t = 0.16 | 99.93±0.87<br>F = 2.33<br>t = 0.15 | 100.17±0.81<br>F = 2.02<br>t = 0.39 |

*Mean value from three determinations
The tabulated F and *t* values at 95% confidence level for four degrees of freedom are 6.39 and 2.77, respectively.

***Recovery study***

To further evaluate and establish the reliability of the suggested procedures, the recovery tests were carried out using a standard addition procedure. Pre-analyzed tablet powder was spiked with pure DOS at three distinct concentration levels before being analyzed in triplicate. It was determined the total DOS present. The percentage recovery of DOS ranged from 97.77 to 103.34% in all cases (Table V), indicating that the co-formulated substances showed no effect on the test. This demonstrates that the assay methods were precise and the percentage recovery values were acceptable.

**Table V.** Recovery study of Prothiaden Tablets by the standard addition method

| Method | DOS in tablet µg mL$^{-1}$ | Pure DOS added µg mL$^{-1}$ | Total found* µg mL$^{-1}$ | %DOS recovered (Percent ± SD) |
|---|---|---|---|---|
| A | 20.00<br>20.00<br>20.00 | 10.00<br>20.00<br>30.00 | 29.33<br>41.33<br>49.33 | 97.77 ± 1.06<br>103.34 ± 1.02<br>98.66 ± 0.89 |
| B | 2.50<br>2.50<br>2.50 | 1.25<br>2.50<br>3.75 | 3.75<br>4.99<br>6.25 | 100.03 ± 0.78<br>99.95 ± 0.66<br>100.02 ± 0.71 |
| C | 2.00<br>2.00<br>2.00 | 2.00<br>4.00<br>6.00 | 3.95<br>6.09<br>7.95 | 98.83 ± 0.84<br>101.56 ± 1.09<br>99.41 ± 1.05 |

**Table V.** Recovery study of Prothiaden Tablets by the standard addition method (continuation)

| Method | DOS in tablet µg mL$^{-1}$ | Pure DOS added µg mL$^{-1}$ | Total found* µg mL$^{-1}$ | %DOS recovered (Percent ± SD) |
|---|---|---|---|---|
| D | 4.00 | 2.00 | 5.91 | 98.62 ± 0.53 |
|   | 4.00 | 4.00 | 8.16 | 102.06 ± 1.10 |
|   | 4.00 | 6.00 | 9.98 | 99.83 ± 1.18 |

*Mean value from three determinations

## CONCLUSION

For the purpose of determining DOS, four new spectrophotometric methods were designed and validated using 0.1 M AcOH as solvent in Method A. The oxidative ability of cerium (IV) was used in developing Methods B, C and D. Iron (II), o-phenanthroline and thiocyanate used as reagents in the oxidation and complexation steps post reaction between DOS and cerium (IV). It was possible to determine DOS concentrations as low as 0.71, 0.26 and 2.14 µg mL$^{-1}$ with confidence and a justifiable level of accuracy and precision. The procedures required no harsh experimental conditions and were straightforward, precise, rapid, cost-effective, and free from interference from common diluents and additives in the formulations. The reaction of cerium (IV) with DOS was used to design an assay procedure for the indirect quantification of DOS by reacting excess cerium (IV) with iron (II), followed by complexation of excess iron (II) with o-phenanthroline in Method C and stoichiometrically generated iron (III) with thiocyanate in Method D. The techniques for figuring out DOS in tablets worked well. Due to their straightforward operation and use of inexpensive instruments, these methods offer an advantage over currently used instrumental methods for DOS. Chemicals that were inexpensive and easily accessible were sufficient for the experiment, which increases the cost-effectiveness. It was advised that the techniques be applied in quality control labs.

### Conflicts of interest

The authors declare that there is no conflict of interest.

### Acknowledgements

## REFERENCES

(1)  Prasanthi, T.; Lakshman, R. A.; Nandini, M.; Hemanth, M.; Bhuvaneswari, M.; Chaitanya, M. Method development and validation for the estimation of dothiepin hydrochloride by using RP-HPLC in pure and tablet dosage form. *Indian J. Pharm. Educ. Res.* **2019**, *53 (2), 310-315.* https://doi.org/10.5530/ijper.53.2.39

(2)  Radhika, S.; Ragin, S. Stability indicating RP-HPLC method for simultaneous estimation of dosulepin hydrochloride and methylcobalamin in tablet dosage form. *Int. J. App. Pharm.* **2017**, *9* (4), 69-75. https://doi.org/10.22159/ijap.2017v9i4.19204

(3)  Sameer, A. M. A.; Basavaiah, K.; Cijo, M. X.; Vinay, K. B. Validation of UV spectrophotometric methods for the determination of dothiepin hydrochloride in pharmaceutical dosage form and stress degradation studies. *J. Appl. Spectrosc.* **2012,** *79* (5), 780-787. https://doi.org/10.1007/s10812-012-9670-7

(4)  Heba, S. E.; Fawzi, A. E.; Fatma, A. A. A.; Amina, M. B. Validated spectrophotometric and spectrofluorimetric methods for determination of dapoxetine hydrochloride and dosulepin hydrochloride in their dosage forms using mercurochrome. *Lumin.* **2018,** *33* (8), 1306-1313. https://doi.org/10.1002/bio.3566

(5)    The European Pharmacopoeia, 6th edition, 2007.

(6)    Shivakumar Reddy, L.; Prasad Reddy, S. L. N.; Srinivas Reddy, G. Validated stability indicating liquid chromatographic method for simultaneous estimation of dosulepin and methylcobalamin in combined pharmaceutical dosage form. *Orient. J. Chem.* **2014**, *30* (3), 1243-1251. http://dx.doi.org/10.13005/ojc/300340

(7)    Dhara, B. D.; Dimal, A. S.; Falgun, A. M.; Usmangani, K. C.; Kashyap, K. B. Liquid chromatographic estimation of dosulepin HCl and methylcobalamin in pharmaceutical formulation. *Res. Rev. J. Pharm. Nanotechnol*. **2014**, *2* (2), 29-35.

(8)    Xiang, C.; Ben, M. C.; Shao, G. L.; Fu-Liang, D.; Ping, Z. Determination of dothiepin in human plasma by LC–ESI–MS and its application to bioequivalence studies. *Chromatographia* **2008**, *68* (11), 941-947. http://dx.doi.org/10.1365/s10337-008-0835-8

(9)    David, R. B.; Barbara, K. H. Multi-residue determination of the sorption of illicit drugs and pharmaceuticals to wastewater suspended particulate matter using pressurised liquid extraction, solid phase extraction and liquid chromatography coupled with tandem mass spectrometry. *J. Chromatogr. A* **2011**, *1218* (44), 7901-7913. http://dx.doi.org/10.1016/j.chroma.2011.08.092

(10)   Richard, B.; Jason, M. W.; Cobus, G. Qualitative and quantitative temporal analysis of licit and illicit drugs in wastewater in Australia using liquid chromatography coupled to mass spectrometry. *Anal. Bioanal. Chem*. **2018,** *410* (2), 529-542. http://dx.doi.org/ 10.1007/s00216-017-0747-2

(11)   Jack, E. W.; Horace, E. H.; Rebecca, O.; Steven, C. H. Determination of doxepin by electron-capture gas chromatography. *J. Anal. Toxicol*. **1978**, *2* (2), 44-49. https://doi.org/10.1093/jat/2.2.44

(12)   Nicole, H. J.; Philippe, D. F.; Germain, M. B. Concurrent determination of second-generation antidepressants in plasma by using gas chromatography with nitrogen–phosphorus detection. *Clin. Chem*. **1997,** *43* (11), 2209-2210. https://doi.org/10.1093/clinchem/43.11.2209

(13)   Liliana, T.; Andre, L. C.; Sonia, T.; Pedro, C.; Goreti, F. S.; Helena, M. T. Antidepressants detection and quantification in whole blood samples by GC–MS/MS, for forensic purposes. *J. Pharm. Biomed. Anal*. **2016**, *128*, 496-503. https://doi.org/10.1016/j.jpba.2016.06.027

(14)   Brodie, R. R.; Chasseaud, L. F.; Crampton, E. L.; Hawkins, D. R.; Risdall, P. C. High performance liquid chromatographic determination of dothiepin and northiaden in human plasma and serum. *J. Int. Med. Res*. **1977**, *5* (6), 387-390. https://doi.org/10.1177/030006057300100201

(15)   Shibanoki, S.; Imamura, Y.; Arakawa, Y.; Ishikawa, K. Determination of dosulepin and its metabolite: Application of high-performance liquid chromatography with electrochemical detection. *J. Chromatogr. B Biomed. Appl*. **1987**, *415* (2), 365-371. https://doi.org/10.1016/s0378-4347(00)83228-4

(16)   Usharani, G.; Chendrashekar, B.; Devanna, N. Simultaneous estimation of dosulepin and methylcobalamin in bulk and pharmaceutical formulation by reverse phase high performance liquid chromatography (RP-HPLC). *IOSR J. Pharm. Biol. Sci*. **2014**, *9* (3), 55-59. https://doi.org/10.9790/3008-09365559

(17)   Aruna, P.; Ajitha, A.; Maheshwar, U. R. Analytical method development and validation of simultaneous estimation of dosulepin and methylcobalamin in tablet dosage form by RP-HPLC. *Int. J. Pharm*. **2014**, *4* (3), 267-274.

(18)   Anita, A.; Komal, G.; Mayuri, N.; Priya, M.; Paraag, G. Development and validation of RP-HPLC method for determination of dothiepin hydrochloride in bulk and pharmaceutical dosage form. *Int. J. Chem. Pharm. Anal*. **2013**, *1* (1), 9-13.

(19)   Mannfred, K.; Caroline, S. Simultaneous determination of seven tricyclic antidepressant drugs in human plasma by direct-injection HPLC-APCI-MS–MS with an ion trap detector. *Ther. Drug Monit*. **2002,** *24* (4), 537-544. https://doi.org/10.1097/00007691-200208000-00013

(20)   Li Wan, P. A.; Irwin, W. J. A high-performance liquid chromatographic assay of cis- and trans-isomers of tricyclic neuroleptic drugs. *J. Pharm. Pharmacol*. **1979**, *31* (8), 512-516. https://doi.org/10.1111/j.2042-7158.1979.tb13574.x

(21) Nour, T. A. G.; Rasha, M. E. N.; Abeer, A. B. Conductimetric determination of the antidepressants, amitriptyline and dothiepin hydrochlorides and tranylcypromine hemisulphate in their pharmaceutical formulations. *J. Pharm. Sci.* **2004**, *29,* 195-201.

(22) Abdel Ghani, N. T.; El-Nashar, R. M.; Bioumy, A. A. Flow injection potentiometric determination of dothiepin hydrochloride. *Anal. Lett.* **2004**, *37* (15), 3237-3254. https://doi.org/10.1081/AL-200040335

(23) Shimaa, A. A.; Ghada, A. S.; Fahima, A. M.; Doha, M. N.; Hala, E. Z. A novel sensor aluminum silicate modified carbon paste electrode for determination of anti-depressant dothiepin HCl in pharmaceutical formulation and biological fluids. *Microchem. J.* **2019**, *148*, 725-734. https://doi.org/10.1016/j.microc.2019.05.007

(24) Fatma, M. A. G.; Ahmed, G. H.; Eman, F. M. Potentiometric method for the determination of lamivudine and dothiepin hydrochloride in pharmaceutical preparations. *Anal. Bioanal. Electrochem*. **2013**, *5* (2), 222-235.

(25) Clark, B. J.; Barker, P.; Large, T. The determination of the geometric isomers and related impurities of dothiepin in a pharmaceutical preparation by capillary electrophoresis. *J. Pharm. Biomed. Anal.* **1992**, *10* (10-12), 723-726. https://doi.org/10.1016/0731-7085(91)80071-g

(26) Wafaa, E. S. H. Extractive colorimetric method for the determination of dothiepin hydrochloride and risperidone in pure and in dosage forms. *Chem. Pharm. Bull*. **2008**, *56,* 1092-1096. https://doi.org/10.1248/cpb.56.1092

(27) Hisham, E. A.; Magda, M. E. H.; Heba, M. E. S.; Magda, M. A. Spectrophotometric and spectrofluorimetric methods for analysis of tramadol, acebutolol and dothiepin in pharmaceutical preparations. *Mol. Biomol. Spectrosc*. **2006**, *65* (5),1087-1092. https://doi.org/10.1016/j.saa.2006.02.008

(28) Walash, M. I.; Belal, F.; El-Enany, N.; Elmansi, H. Spectrophotometric and spectrofluorimetric methods for the determination of dothiepin hydrochloride in its pure and dosage forms using eosin. *Int. J. Biomed. Sci.* **2010**, *6* (4), 327-334. PMID: 23675210.

(29) Sameer, A. M. A.; Basavaiah, K. Spectrophotometric determination of dothiepin hydrochloride in pharmaceuticals through ion-pair complexation reaction. *Chem. Ind. Chem. Eng.* **2012**, *18* (2), 339-347. https://doi.org/10.2298/CICEQ111009010A

(30) Umamaheshwar, K.; Naganjaneyulu, T.; Rambabu, C. Extractive spectrophotometric methods for the determination of dothiepin in pure and pharmaceutical formulations. *Glob. J. Pharmaceu. Sci.* **2017**, *2* (2), 25-29. https://doi.org/10.19080/GJPPS.2017.02.555582

(31) Sameer, A. M. A.; Basavaiah, K. Use of alizarin red S as a chromogenic agent for the colorimetric determination of dothiepin hydrochloride in pharmaceutical formulations. *J. Saudi Chem. Soc.* **2014**, *18*, 107-114. https://doi.org/10.1016/j.jscs.2011.05.018

(32) Elham, A. T. Kinetic spectrophotometric methods for the determination of dothiepin hydrochloride in bulk and in drug formulation. *Anal. Bioanal. Chem*. **2003**, *376* (7), 1131-1136. https://doi.org/10.1007/s00216-003-2040-9

(33) Sane, R. T.; Kothurkar, R. M.; Ladage, K. D.; Tendolkar, R. V.; Gangal, D. P. An extractive econometric method for the determination of dothiepin hydrochloride from pharmaceutical preparations. *Indian J. Pharm. Sci.* **1988**, *50*, 299.

(34) Sameer, A. M. A.; Basavaiah, K. Use of bromate-bromide mixture as a reagent for the determination of dothiepin hydrochloride in pharmaceuticals. *Thai. J. Pharm. Sci.* **2011,** *35,* 147-158.

(35) Elham, A. T.; Suzan, M. S.; Hisham, E. A.; Magda, M. A. Colorimetric methods for the determination of some tricyclic antidepressant drugs in their pure and dosage forms. *Microchim. Acta* **2002**, *140*, 175-182. https://doi.org/10.1007/s00604-002-0904-x

(36) Jeffery, G. H.; Bassett, J.; Mendham, J.; Denney, R. C. *Vogel's textbook of quantitative chemical analysis*, John Mendham, Pearson, **1989**, 5th edition, chapter 10, p. 381.

(37) Raghu, M. S.; Basavaiah, K. Simple, sensitive and eco-friendly methods for the determination of methdilazine in tablets and syrup using cerium (IV). *Chem. Sci. J.* **2012**, *3* (1), 1-14.

(38) Svehla, G. *Vogel's qualitative inorganic analysis*, 7th edition, Pearson education, **2002**, 112-116.

(39) Blessy, M.; Patel, R. D.; Prajapati, P. N.; Agrawal. Y. K. Development of forced degradation and stability indicating studies of drugs – A review. *J. Pharm. Anal*. **2014,** *4* (3), 159–165. https://doi.org/10.1016/j.jpha.2013.09.003

(40) Shojaie, F. Theoretical studies of the vibrational spectra and molecular structures of dosulepin and doxepin. *Phys. Chem. Res.* **2016**, *4* (2), 245-270. https://doi.org/10.22036/pcr.2016.13970

(41) International conference on harmonization of technical requirements for registration of pharmaceuticals for human use, ICH harmonized tripartite guideline, validation of analytical procedures: text and methodology, Q2(R1), complementary guideline on methodology dated 06 November **1996**, ICH, London, UK (2005).

(42) Volgyi, G.; Beni, S.; Takacs-Novak, K.; Gorog, S. Theoretical problems associated with the use of acetic anhydride as a co-solvent for the non-aqueous titration of hydrohalides of organic bases and quaternary ammonium salts. *J. Pharm. Biomed. Anal.* **2010**, *51* (1), 18–23. https://doi.org/10.1016/j.jpba.2009.07.022

**BrJAC**

# ARTICLE

# Ancient Rock Paintings at Region del Cabo-BCS, Mexico: An Analytical Study

Úrsula Méndez-Mejía[1,2] iD , Maria Dolores Tenorio*[2] iD ✉, Melania Jiménez-Reyes[2] iD , Rosa Elba Rodríguez-Tomp[1] iD

[1]Universidad Autónoma de Baja California Sur. Carretera al sur km 5.5. C.P. 23080. La Paz, Baja California Sur, México

[2]Departamento de Química. Instituto Nacional de Investigaciones Nucleares. Carretera México-Toluca La Marquesa s/n, C.P. 52750. Ocoyoacac, Estado de México, México

This study focused on the examination of six rock pictorial panels and a solitary figure from four archaeological sites in the Sierra de las Cacachilas (Sector A) in the Region del Cabo, Baja California Sur, Mexico. Scanning Electron Microscopy-energy dispersive X-ray spectroscopy was utilized to analyze tiny samples of the pictorial layers, patina, rocky supports, and natural pigments. The concentrations of C, Mg, Al, Si, P, S, K, Ca, Cr, Ti, Mn, and Fe were subjected to statistical methods and the samples were divided into various clusters. Iron and calcium compounds appear to be the primary constituents of the pictorial layers. The red pigment spectra obtained through Fourier-transform infrared spectroscopy revealed the presence of inorganic compounds and the likelihood of a flora-based composite as the binding agent. The minerals identified through X-ray diffraction in the rocky supports were determined to be intrusive igneous rocks. These findings are significant for the conservation and preservation of the artwork in the Sierra de las Cacachilas.

**Keywords:** Archaeometry, Rock-paintings, Baja California Sur México, Raw materials, SEM-EDS, XRD

## INTRODUCTION

Rock paintings are widespread and serve as a testament to the lives of prehistoric people, found in diverse places such as secluded caves and visible rock formations. The preservation of these paintings depends on various factors such as the microenvironment, the composition of the paint, and human-made events, among others. Recently, the study of rock paintings has gained increased attention and significance from various perspectives including discovery and location, documentation, and archaeometry.[1-5]

Research conducted in Europe (France, Italy, Spain), South America (Colombia, Chile, and Argentina), and Mexico (Baja California Sur) involved the utilization of diverse analytical techniques including XRD, PIXE, RBS, EDAX, FRXT, FT-IR, MS, and EDAX. These studies aimed to determine the composition of the pictorial layer in terms of various colors, minerals, rock substrates, and organic materials employed in paint manufacturing. The results provided valuable insights for interpreting certain connections within the extensive operational process.[1-9] Despite the variations in methodologies and objectives among these studies, the overall focus remained on comprehending the operational processes involved in creating pictorial panels.

The Region del Cabo, shown in (Figure 1), is located in the southern part of the Baja California peninsula in Mexico. It is a large, barren, and remote area inhabited by hunter-gatherer-fisher groups, the Guaycuras, and the Pericues.
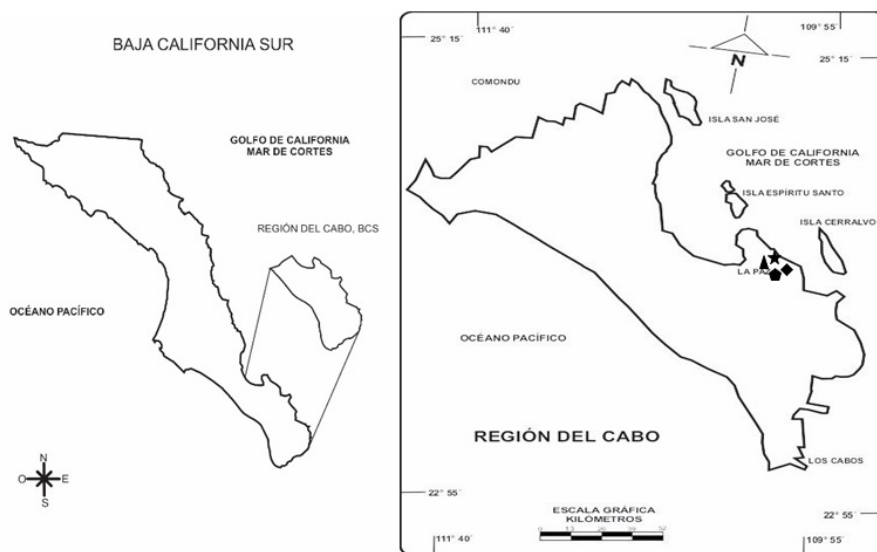


**Figure 1.** Map of localization of the Region del Cabo and the pictorial sites (in Sierra de las Cacachilas, Sector A): Cerro Pintada 1 (triangle) Cerro Pintada 2 (star) Castreña 2 (rhombus) Joyita de la Sierra de la Huerta (pentagon).

The pictorial rock art in this region was first recorded by Spanish missionaries in the 18th century and has since been studied by explorers and researchers, resulting in increased knowledge about the location, spatial distribution, quantity, designs, styles, and techniques used to create the art. However, no analytical studies have been conducted thus far. The main styles found in the Region del Cabo are the Cabo Representational and Cabo Abstract styles.[10,11] The ancient pictures in the Region del Cabo are a valuable contribution to Mexico's cultural heritage.

The Sierra de las Cacachilas, specifically Sector A, is part of the Region del Cabo. Among the numerous rock painting sites in this Sierra, the research selected four sites, Cerro Pintada 1, Cerro Pintada 2, Castreña 2, and Joyita de la Sierra de la Huerta (Figure 1), based on certain criteria. These criteria included the preservation status of the pictograms, the variety of styles and designs, minimal impact from the environment, ease of access to the site, and official recognition. Other factors considered were the absence of humidity, organic matter (such as fungi, bacteria, and insect nests), and contaminants (such as smoke from fires or spray paint) on the pictograms. As a result, six pictorial panels and a solitary figure were selected.

The goal of this research was to conduct a physicochemical characterization of the raw materials used in the creation of six pictorial panels, and one isolated figure found at the mentioned sites. This involved analyzing pictorial layers, patina, rocky supports, and natural pigments. The elemental composition was determined using scanning electron microscopy-energy dispersive X-ray spectroscopy (SEM-EDS). Fourier-transform infrared spectroscopy (FTIR) was used to identify the presence of organic and inorganic compounds, while X-ray diffraction (XRD) was used to determine the mineralogical composition. This groundbreaking study aims to provide new insights into the pictograms of the Sierra de Las Cacachilas, including the color palette used by prehistoric artists and the nature of the rocky supports.

## MATERIALS AND METHODS
### Materials
Figure 2 shows an example of one of the pictograms. Table I provides a brief overview of the characteristics of the pictorial panels at each site, including the style (Representative or Abstract), the predominant color (typically various shades of red), and the dimensions.
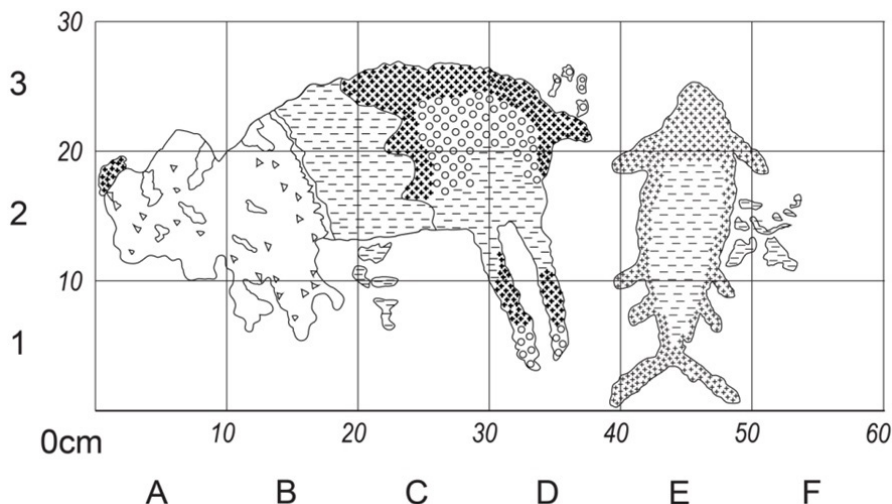


**Figure 2.** General view of Pictorial Panel 1: zoomorphic figures (deer and fish) and stains in Joyita de la Sierra de la Huerta. Cabo Representational style.

**Table I.** Description of the pictorial panels of Sierra de las Cacachilas (Sector A). (*) R: Representational; A: Abstract

| Site | Zone (Nr.) | Style (*) | Design | Color | Manufacture technique | Pictorial panels | Isolated figure | Dimensions (cm) | |
|------|-----------|-----------|--------|-------|----------------------|-----------------|----------------|-----------------|--|
| | | | | | | | | Height | Width |
| Cerro Pintada 1 | G12D8303001 (1801) | R | Zoomorphic and phytomorphic | Red (various tonalities) | Manual, hands and fingers | 1 | | 98 | 1.52 |
| | | | | | | | 1 | 14 | 24 |
| Cerro Pintada 2 | G12D8303002 (1803) | A | Crossed lines | Red (various tonalities) | Manual, hands and fingers | 1 | | 69 | 45 |
| Castreña 2 | G12D8303118 (46095) | R | Zoomorphic and phytomorphic | Red (various tonalities) | Manual, hands and fingers | 1 | | 59 | 78 |
| | | | | | | 2 | | 178 | 112 |
| Joyita de la Sierra de la Huerta | G12D8303108 (46085) | R & A | Zoomorphic and stains | Red-ocher and orange | Manual, hands and fingers | 1 | | 25 | 55 |
| | | | | | | 2 | | 68 | 2.00 |

*Methods*

Photographs and videos of each piece of pictorial art were taken using a Sony Alpha 6300 digital camera. Afterward, a portable optical microscope (Dino-Lite, model AM3011, VGA) was used to perform vertical and horizontal scans of the rocky surface, with a resolution ranging from 10X to 220X. At the same time, a grid (consisting of 10 cm² square marked by letters and numbers) was drawn for each pictogram using Adobe Illustrator CS5A software. The conservation status of the pictorial layer and the uniformity or variation of color on the surfaces were evaluated at the points where the quadrants intersected, which helped in determining the optimal area for sample extraction.

Small samples of the pictographs (as well as three from the patina) were collected by carefully attaching a 1 cm² carbon strip, which was then removed using a clamp and fixed to an aluminum sample holder. To prevent any harm to the design and size of the pictographs, between four and eight samples were taken from each. The samples collected on the carbon strips were properly labeled and stored for further analysis in the laboratory. Additionally, during the inspections of the pictorial sites, some granitic rocks with vivid red and orange veins were encountered, which were analyzed as well.

Photomicrographs and X-ray spectra of pictograph and patina samples were taken with a low vacuum scanning electron microscope (SEM) JSM-6610LV with a coupled Oxford probe, for elemental microanalysis EDS. Chemical compositions were determined by EDS analysis of several points chosen at random on the photomicrographs.

Fourier-transform infrared spectroscopy analyses of four red pigment samples of pictorial layers were carried out by a VARIAN® model 640-IR. The samples were crushed in an agate mortar and then the KBr pellets were prepared. Spectrum against that of the background from 4000 cm$^{-1}$ to 400 cm$^{-1}$, with 40 scans and a resolution of 4 cm$^{-1}$. The total number of data points was 1869.

A mineralogical analysis by XRD was performed for the rocky support samples at room temperature with a Siemens D-5000 diffractometer using Cu Kα radiation with a graphite monochromator; the diffraction pattern was collected from 2.5 to 70° 2θ with a step size of 0.02° 2θ to acquire X-ray patterns with sufficiently high intensities to identify the minerals present. For the qualitative identification of the mineralogical composition, the data file XRD JCPDS was used.

## RESULTS AND DISCUSSION

Table II lists the 73 samples that were analyzed using SEM-EDS for each site and figure, with 66 samples representing the pictorial layers, three for the patina, and four for the rocky supports.

**Table II.** Samples analyzed by site and figure (Sierra de las Cacachilas, Sector A). The number of cluster is according to the statistical analysis of chemical compositions.

| Site | Figure | Key | Cluster Nr. |
|---|---|---|---|
| Cerro la Pintada 1 | Biznaga | M 17 | C1 |
| | Biznaga | M 18 | C1 |
| | Biznaga | M 19 | C1 |
| | Biznaga | M 20 | C1 |
| | Biznaga | M 21 | C1 |
| | Coyote | M 22 | C4 |
| | Coyote | M 23 | C1 |
| | Coyote | M 24 | C3 |

**Table II.** Samples analyzed by site and figure (Sierra de las Cacachilas, Sector A). The number of cluster is according to the statistical analysis of chemical compositions. (continuation)

| Site | Figure | Key | Cluster Nr. |
|---|---|---|---|
| Cerro la Pintada 1 | Deer | M 11 | C1 |
| | Deer | M 12 | C1 |
| | Deer | M 13 | C1 |
| | Deer | M 14 | C1 |
| | Deer | M 15 | C1 |
| | Deer | M 16 | C1 |
| | Sea urchin | M 1 | C5 |
| | Sea urchin | M 2 | C4 |
| | Sea urchin | M 3 | C5 |
| | Sea urchin | M 4 | C1 |
| | Sea urchin | M 5 | C1 |
| | Whale | M 6 | C1 |
| | Whale | M 7 | C1 |
| | Whale | M 8 | C1 |
| | Whale | M 9 | C1 |
| | Whale | M 10 | C1 |
| | Patina | M 25 | C1 |
| | Patina | M 26 | C1 |
| | Patina | M 27 | C1 |
| | Rocky support | M177 | C6 |
| Cerro la Pintada 2 | Fingerprint lines | M 28 | C3 |
| | Fingerprint lines | M 29 | C1 |
| | Fingerprint lines | M 30 | C3 |
| | Fingerprint lines | M 31 | C1 |
| | Rocky support | M180 | C6 |
| La Castreña dos | Male deer | M 59 | C1 |
| | Male deer | M 60 | C1 |
| | Male deer | M 61 | C4 |

**Table II.** Samples analyzed by site and figure (Sierra de las Cacachilas, Sector A). The number of cluster is according to the statistical analysis of chemical compositions. (continuation)

| Site | Figure | Key | Cluster Nr. |
|---|---|---|---|
| La Castreña dos | Male deer | M 62 | C1 |
| | Male deer | M 63 | C1 |
| | Male deer | M 64 | C3 |
| | Female deer | M 65 | C2 |
| | Female deer | M 66 | C2 |
| | Female deer | M 67 | C1 |
| | Female deer | M 68 | C3 |
| | Female deer | M 69 | C3 |
| | Female deer | M 70 | C4 |
| | Female deer | M 71 | C3 |
| | Female deer | M 72 | C1 |
| | Pitahaya | M 53 | C1 |
| | Pitahaya | M 54 | C1 |
| | Pitahaya | M 55 | C1 |
| | Pitahaya | M 56 | C1 |
| | Pitahaya | M 57 | C1 |
| | Pitahaya | M 58 | C5 |
| | Rocky support | M183 | C6 |
| Joyita de la Sierra de la Huerta | Fish | M 32 | C3 |
| | Fish | M 33 | C3 |
| | Fish | M 34 | C3 |
| | Fish | M 35 | C3 |
| | Deer (incomplete) | M 36 | C3 |
| | Deer (incomplete) | M 37 | C1 |
| | Deer (incomplete) | M 38 | C1 |
| | Deer (incomplete) | M 39 | C1 |
| | Fingerprint lines 1 | M 49 | C1 |
| | Fingerprint lines 1 | M 44 | C2 |

**Table II.** Samples analyzed by site and figure (Sierra de las Cacachilas, Sector A). The number of cluster is according to the statistical analysis of chemical compositions. (continuation)

| Site | Figure | Key | Cluster Nr. |
|---|---|---|---|
| Joyita de la Sierra de la Huerta | Fingerprint lines 1 | M 46 | C2 |
| | Fingerprint lines 1 | M 47 | C2 |
| | Fingerprint lines 1 | M 45 | C4 |
| | Fingerprint lines 1 | M 43 | C5 |
| | Fingerprint lines 2 | M 48 | C2 |
| | Fingerprint lines 2 | M 50 | C2 |
| | Fingerprint lines 2 | M 51 | C2 |
| | Orange stain | M 52 | C2 |
| | Rocky support | M181 | C6 |

The X-ray spectra of EDS were used to identify and evaluate the following chemical elements C, Mg, Al, Si, P, S, K, Ca, Cr, and Fe, as demonstrated in a typical spectrum displayed in Figure 3 and Table III. Only a limited number of samples showed the presence of elements such as Ti and Mn, with Ti being found in 4 out of 73 samples (ranging from 0.3% to 4%) and Mn in 7 out of 73 samples (ranging from 0.3% to 9.3%). The average values of the element concentrations in each sample were calculated, and statistical treatments were performed by taking the log values of these average concentrations (excluding Ti and Mn).

The MURR (Missouri University Research Reactor) procedures refer to the use of a specific software, provided by that institution. This software, which is written in the GAUSS language,[12] has been used to conduct statistical analyses. The software calculates the probabilities of an individual sample belonging to various clusters, taking into consideration the Mahalanobis distance. For the analysis, the elemental concentrations are transformed into a logarithmic scale. The software also aids in visualizing these statistical outcomes. It helps in plotting principal component diagrams, which result in the artifacts being grouped into distinct clusters. Further, it enables drawing a diagram of vectors corresponding to those elemental concentrations that define the separation in clusters.
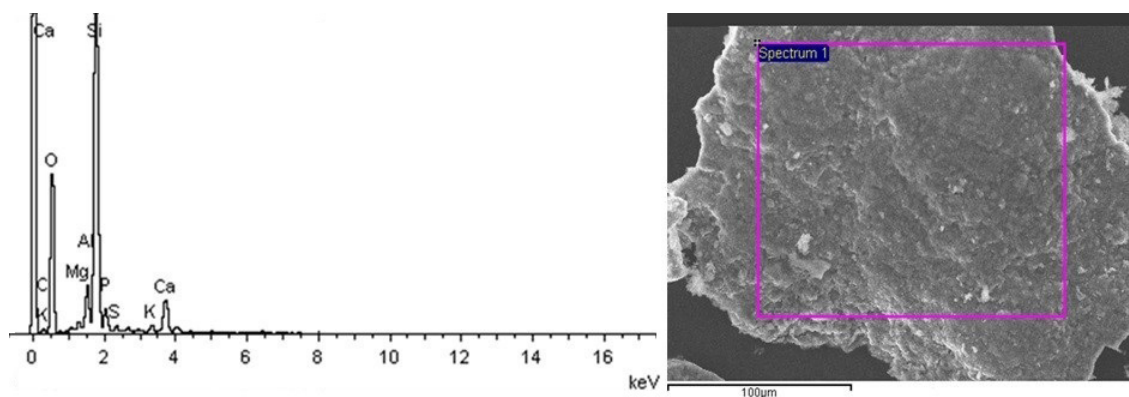


**Figure 3.** EDS spectrum and SEM micrograph typical of the samples of Cluster 1.

**Table III.** Elemental compositions of the statistical clusters formed. Data obtained by EDS, in %.

| | Cluster 1 (n=39) | | Cluster 2 (n=9) | | Cluster 3 (n=12) | | Cluster 4 (n=5) | | Cluster 5 (n=4) | | Cluster 6 (n=4) | |
|---------|------|---------|------|---------|------|---------|------|---------|------|---------|------|---------|
| Element | Mean | Min-Max | Mean | Min-Max | Mean | Min-Max | Mean | Min-Max | Mean | Min-Max | Mean | Min-Max |
| C | 13 | 5-24 | <0.1 | <0.1 | 21 | 8-58 | 17 | 8-25 | 9 | 6-12 | 16 | 10-24 |
| Mg | 0.7 | 0.1-2.7 | 1 | <0.1-4 | <0.1 | <0.1 | <0.1 | <0.1-1 | 3 | 2-4 | 3 | 2-5 |
| Al | 3.6 | 0.8-9 | 7 | 3-14 | 4 | <0.1-10 | 2 | 1-4 | 5 | 3-6 | 6 | 6 |
| Si | 21 | 4-31 | 25 | 15-37 | 12 | 2-21 | 15 | 9-22 | 21 | 16-26 | 22 | 15-33 |
| P | 1.7 | 0.1-5.3 | 3 | <0.1-9 | 1 | <0.1-2 | 1 | <0.1-2 | 1 | 1-2 | 1 | <0.1-2 |
| S | 0.4 | 0.1-2.8 | <0.1 | <0.1-1 | 1 | <0.1-9 | 2 | <0.1-8 | <0.1 | <0.1 | 2 | <0.1-7 |
| K | 0.8 | 0.1-1.3 | 2 | <0.1-5 | <0.1 | <0.1-1 | 1 | <0.1-1 | 3 | 2-6 | 4 | 2-7 |
| Ca | 4 | 1-16 | 3 | 1-11 | 8 | <0.1-20 | 2 | 1-7 | 2 | 1-4 | 1 | <0.1-2 |
| Cr | <0.1 | <0.1 | <0.1 | <0.1 | <0.1 | <0.1 | 6 | 1-9 | 2 | <0.1-6 | 1 | <0.1-6 |
| Fe | 1.5 | 0.4 – 4.8 | 1 | <0.1-8 | <0.1 | <0.1-1 | 28 | 4-43 | 10 | 8-13 | 12 | 6-21 |

Data of Table III show that trace elements were not detected and major elements (Si, Al) are similar for all samples; therefore, they are not significant for differentiation. Minor elements are the main ones for the separation of clusters. Figures 4A and 4B depict the diagrams of the principal components calculated. The first illustrates the grouping of the samples, while the second highlights the differentiation vectors. The main vectors of differentiation (Figure 4B) are based on the levels of C, Cr, and Fe, but Mg, K, P, and Ca played a role as well. Through this statistical analysis, we were able to identify six distinct clusters. Table I outlines the cluster number of each sample, and Table III presents the chemical composition data associated with each cluster. The results of the statistical analysis revealed six distinct clusters of samples.
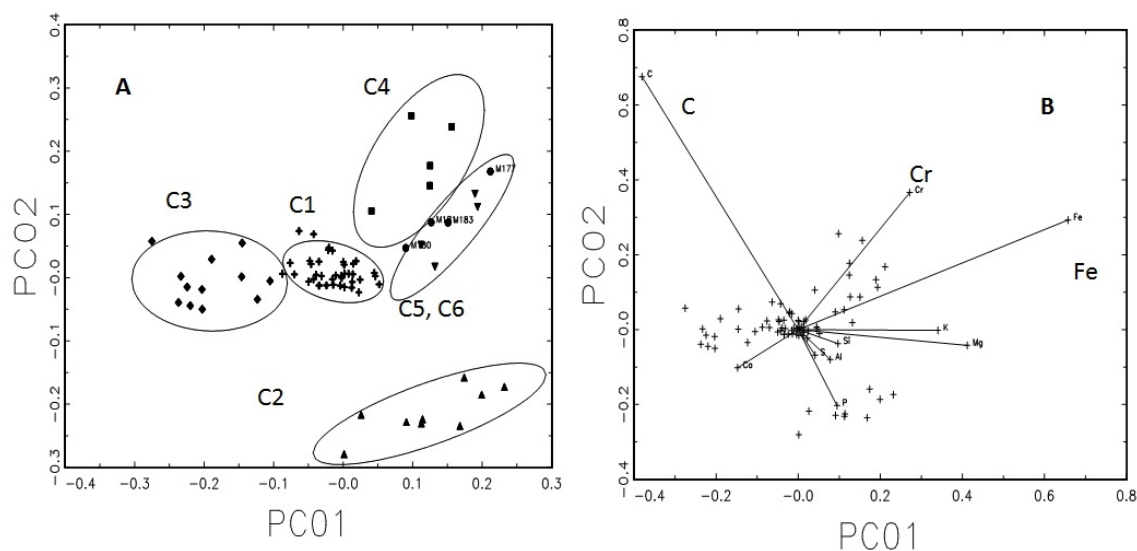


**Figure 4.** Principal component diagrams based on the concentration of ten chemical elements of 73 samples of pictorial layers. A) Clusters. B) Vectors.

Cluster 1 is the largest and its samples are present in all pictographs. Clusters 1, 2, and 3 do not show any significant presence of chromium, with values below the detection limit of the EDS technique. Cluster 2 has a virtually absence of carbon, while Cluster 3 has high levels of carbon and calcium, but no significant presence of iron.

The primary components of Cluster 3 could be either calcite ($CaCO_3$) or a combination of calcite and gypsum ($CaSO_4$) as sulfur was detected in some of its samples.

The highest concentration of iron can be found in the orange and red layers of C4, while the iron content in Clusters 1 and 2 is not as abundant but the samples possess a rich orange and red hue. The red and orange pigments might be composed of minerals such as hematite ($Fe_2O_3$), goethite ($\alpha$-$Fe^{3+}O(OH)$), and/or limonite ($FeO(OH) \cdot nH_2O$).[13] There is also evidence suggesting that the pigments could be derived from clays that contain hematite.[14-15]

Figure 5 presents the FTIR spectrum of a red pigment sample; the spectra obtained from the other four samples were virtually indistinguishable. Table IV lists the functional groups of both organic compounds (alcohols, ketones, benzene, and phenols, among others) and inorganic compounds that were identified.
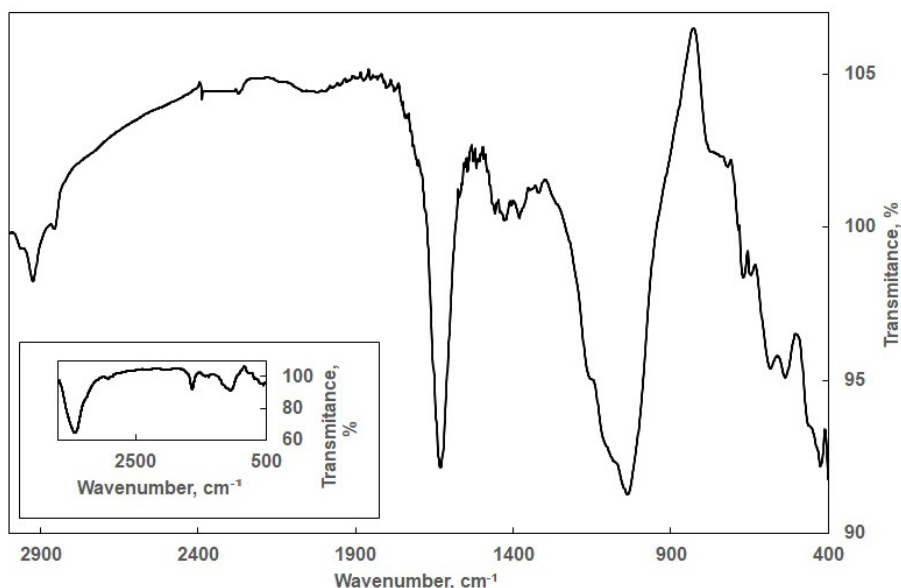


**Figure 5.** Typical FTIR spectrum of the analyzed pictorial layers.

**Table IV.** Data of the FTIR spectra of the pictorial layers

| Wavenumber, cm$^{-1}$ (*) | Functional groups (**) | Compounds |
|---|---|---|
| 3427 (s) | -OH Str. | Alcohol |
| 2920, 2854 (m) | -C–H$_n$ Str. | Alkyl, aliphatic aromatic |
| 1730 (w), 1517 (w) | -C=O Str. | Ketone and carbonyl |
| 1630 (s) | -C=C- | Benzene stretching ring |
| 1455 (w) | -O–CH$_3$ | Methoxyl |
| 1380 (w), 1317 (w) | -CH$_3$ | Methyl |
| 1232 (sh) | -C–O–C Str. | Aryl-alkyl ether linkage |

(continues on the next page)

**Table IV.** Data of the FTIR spectra of the pictorial layers (continuation)

| Wavenumber, cm$^{-1}$ (*) | Functional groups (**) | Compounds |
|---|---|---|
| 1211 (sh) | -C–O Str. | Phenol |
| 1087 (sh) | Ca-O | Calcium carbonate |
| 900 – 1100 (s) | Si-O Str. | Feldspar |
| 400-800 (s) | Si-O Flx | Feldspar |
| 400-1065 (s) | Fe-O | Hematite |

(*) s: strong, m: middle, w: weak, sh: shoulder. (**) Str.: stretching, Flx: Flexing.

The Fourier-transform infrared spectroscopy spectrum was compared to those obtained from the typical components of biomass, such as cellulose, hemicellulose, and lignin. The region between 1300 cm$^{-1}$ and 1700 cm$^{-1}$ is indicative of the presence of lignin,[16] and the main band in Figure 5 is situated at 1620 cm$^{-1}$ (C = C). The presence of lignin in the pictorial layer suggests the presence of plant matter. The absorption bands between 900-1000 cm$^{-1}$ and 400-800 cm$^{-1}$ are related to the Si-O bond of inorganic compounds such as feldspars, while the bands between 440 and 1065 cm$^{-1}$ are linked to hematite. In contrast, the bands of calcium carbonate (1408 cm$^{-1}$, 873 cm$^{-1}$, and 712 cm$^{-1}$)[2] are only faintly visible in the spectra.

The spectrum displayed in Figure 5 was also compared to those of the Nopal Cactus (Opuntia Ficus-Indica),[17] Nopal pectin,[18] and animal fat.[19] The spectra of these substances exhibit the bands related to carboxylic acids at 1712 cm$^{-1}$ and 1224 cm$^{-1}$, which are absent in the spectrum of Figure 5, indicating that these substances were not used as the binding agent in the pictorial layer.

The minerals identified in the samples of the rocky supports (La Castreña, Boca del Álamo and Cerro Pintada) through XRD analysis, as shown in Figure 6, include mainly: quartz, pholopita, albite, and anorthoclase. These mineral phases are consistent with the granitic structure typically found in igneous-plutonic rocks, as previously identified in the northern Baja California peninsula.[2] It's important to note that the Sierra de las Cacachilas, Sector A, is located on a surface made up of intrusive igneous rocks from the Cretaceous period, primarily granite and granodiorite.

The selection of the rocky support was important in the creation of the pictorial images. Some surfaces were smoothed with stone tools, but examination of the surfaces with a handheld optical microscope showed that this was not done in the case of the rocky supports of the specified area, as no signs of carving were found.

The natural pigments of red and orange colors sourced from the granitic rocks located in the pictorial sites were abundant in iron. The SEM-EDS results showed 11-20% of iron, likely due to hematite. The presence of silicon, aluminum, potassium (potentially from feldspars), and carbon was also identified. The elemental composition of these rocks was found to be similar to that of the pictorial layers, indicating that they were used as raw materials for the creation of rock art.
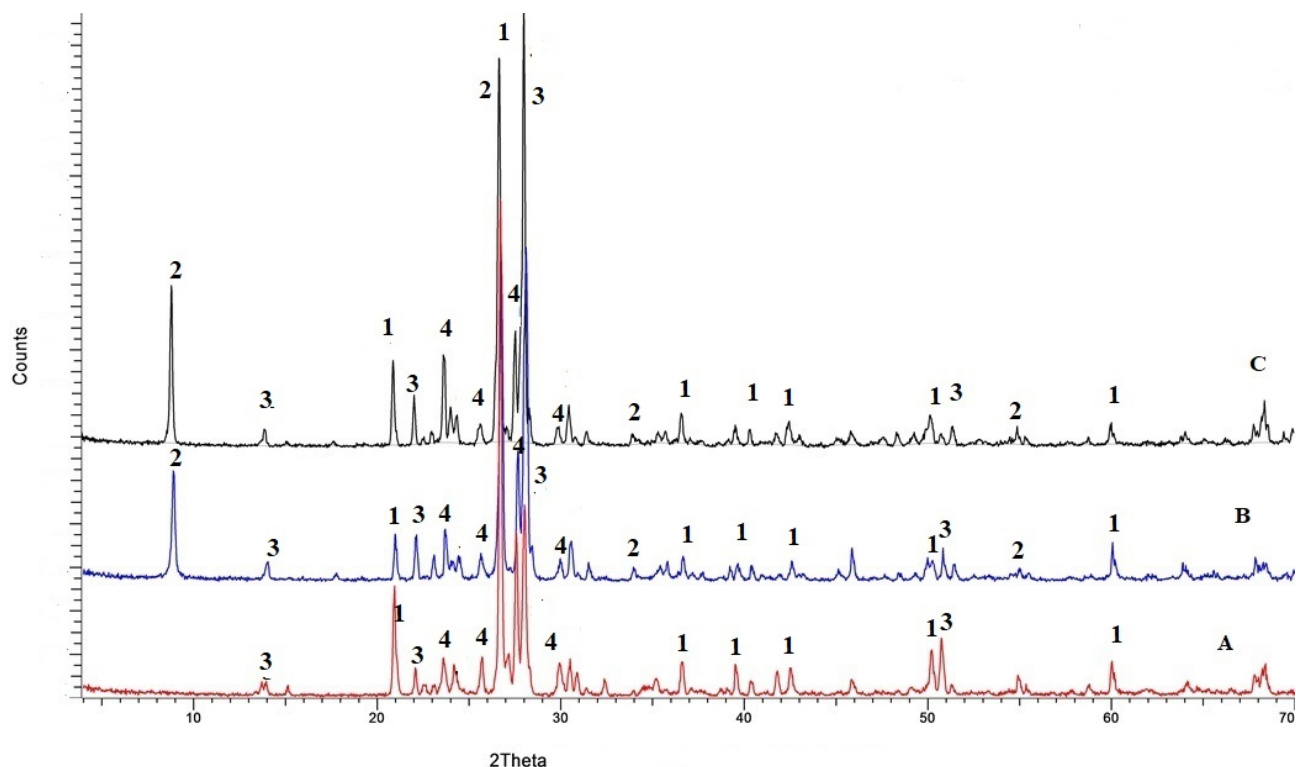
**Figure 6.** XRD spectra of the rocky supports from La Castreña (A), Boca del Álamo (B) and Cerro Pintada (C). The crystalline phases are: 1. Quartz, 2. Phlogopite, 3. Albite, 4. Anorthoclase.

## CONCLUSIONS

This is the initial examination of the pictograms of the Sierra de Las Cacachilas. A comprehensive study using multiple techniques on small samples gave us insights into the components used in the creation of the pictograms (pictorial layers, patina, rocky supports, and pigments). The combination of the various techniques used provided a comprehensive understanding of the samples and their context.

SEM/EDS can detect C, Mg, Al, Si, P, S, K, Ca, Cr, Ti, Mn, and Fe in pictorial layers, patina, and rocky supports. Statistical calculations identify differences in element concentrations, with data grouped accordingly. Most pictorial layers had a similar chemical composition (C1), while other groups differed mainly in C, Cr, and Fe. Rocky support (C6) composition differed from C1 to C4 and was richer in Fe while scarce in Ca and Cr. The composition of C5 was similar to C6, potentially indicating a measurement of the rocky support in those samples.

Orange and red are the predominant colors in most pictorial layers, possibly due to the presence of iron compounds like hematite. Alternatively, the presence of calcium, carbon, and sulfur may suggest the presence of loading materials like calcite and gypsum. The pigments' origin may be from granitic rocks containing iron oxides found in the region where the pictorial arts were created.

Fourier-transform infrared spectroscopy analysis of red pigment grains identified both inorganic and organic compounds. Inorganic compounds included feldspars from the rocky support and hematite, supporting the previous considerations of these compounds in the pictorial layers. Organic compounds were compared with typical biomass components reveling the presence of lignin. A composite of flora may have been used as a pigment binder, but its origin remains unclear.

Based on these results: a) Dark red colors (Red 2.5YR 4/4/6) correspond to a high concentration of iron oxides (red pigment), and sometimes Ti (dark red pigment), with little evidence of carbon (binder not identified), but a high gypsum content ($CaSO_4 \cdot 2H_2O$) as loading. b) Light red colors (Red 2.5YR 4/4/8) may be a mixture with low Fe content (red pigment), high carbon content (binder not identified), and a

low percentage of gypsum (loading). c) Dark colors (Greenish black 2.5/2.5/1 10G) are related to carbon content (pigment and binder) and gypsum content (loading).

Lastly, based on the mineral phases identified by XRD in the rocky supports (feldspars, quartz, and mica), it can be concluded that the structure is of granitic origin, specifically igneous-plutonic rock. The surfaces appear to be in their natural state, with no signs of previous polishing.

The findings obtained through the application of various analytical techniques provide significant knowledge for the conservation of ancient pictorial art in the Sierra de las Cacachilas region and in general they result useful for other archaeological studies.

## Conflicts of interest

The authors declare that they have no conflicts of interest.

## Acknowledgments

## REFERENCES

(1)  Zoppi, A.; Signorini, G. F.; Lucarelli, F.; Bachechi, L. Characterization of painting materials from Eritrea rock art sites with non-destructive spectroscopic techniques. *J. Cult. Herit.* **2002**, *3* (4), 299-308. https://doi.org/10.1016/S1296-2074(02)01234-7

(2)  Valdez, B.; Cobo, J.; Schorr, M.; Zlatev, R.; Cota, L. Characterisation of materials and techniques used in Mexican rock paintings. *J. Australian Rock Art Res. Assoc.* (AURA) **2008**, *25* (2), 131-135.

(3)  Yacobaccio, H. D.; Catá, M. P.; Solá, P.; Alonso, M. S. Estudio arqueológico y fisicoquímico de pinturas rupestres en Hornillos 2 (Puna de Jujuy). *Estudios Atacameños, Arqueol. y Antropol. Surandinas*, **2008**, No. 36.

(4)  Sepúlveda, M. A. Pinturas rupestres y tecnología del color en el extremo sur de Chile. *Magallania* **2011**, *39* (1), 193-210. http://www.magallania.cl/index.php/magallania/article/view/79

(5)  Mondragón, M. A.; Hernández-Padrón, G.; Solís, C. ; del Real, A.; Trespalacios-Quijano, R.; Jiménez-Mu, C.; Viramontes-Anzures, C. Multianalytical characterization of pigments from rock paintings in Guanajuato, Central México. *J. Archaeol. Sci. Rep*. **2019**, *26*, 101912. https://doi.org/10.1016/j.jasrep.2019.101912

(6)  Maier, M. S.; De Faria, D. L.; Boshin, M. T.; Parera, S. D.; Del Castillo, M. F. Combined use of vibrational spectroscopy and GC-MS methods in the characterization of archaeological pastes from Patagonia. *Vib. Spectrosc*. **2007**, *44* (11), 182-186. https://doi.org/10.1016/j.vibspec.2006.09.003

(7)  Ledesma, R. El Alisar y El Divisadero. Dos Sitios Arqueológicos con Pinturas Rupestres en Cafayate, Salta. *Cuadernos de Humanidades* N° 15, 2004. Facultad de Humanidades, Universidad Nacional de Salta. Salta, Argentina.

(8)  Sepúlveda, M. Aspectos tecnológicos en la pintura rupestre. Reflexiones elaboradas a partir de análisis físico-químicos aplicados al estudio de las pinturas de la localidad del río Salado (norte de Chile). In: Sepúlveda, M.; Briones, L.; Chacama, J. (Eds.) *Crónicas sobre la Piedra. Arte Rupestre de las Américas*. Publisher: Universidad de Tarapacá, Chile, 2006. Chapter 2, pp119-128.

(9)  Moreno, A. M.; Vargas, C. B. Técnica de elaboración de las pictografías ubicadas en el área de curso del río Farfacá, Tunja (Colombia). *Rupestreweb Arte rupestre en América Latina* **2001**. Available at: http://www.rupestreweb.info/farfaca.html [accessed on March 2023]

(10) Grant, C. *Rock art of Baja California, With Notes on the Pictographs of Baja California, by Leon Diguet (1895).* Publisher: Dawson´s book shop, Los Angeles, CA, 1974.

(11) Ritter, E. W. Baja California Rock Art: Problems, Progress, and Prospects. In: Hedges, K. (Ed.) *Rock Art Papers*, Volume 8, San Diego Museum Papers 27, 1991, pp 21-36. San Diego. U.S.A.

(12)  Neff, H. *Gauss Language Routines for Statistical Analyses of Multivariate Archaeometric Data*. Software accessed and used in 2018. No longer accessible via the internet.

(13)  Gutiérrez, M. L.; Hyland J. R. *Arqueología de la sierra de San Francisco: dos décadas de investigación del fenómeno Gran Mural*. Volume 433 de Colección Científica Serie arqueológica. Publisher: Instituto Nacional de Antropología e Historia (INAH), México, D.F. 2002.

(14)  Konta, J. Clay and man: Clay raw materials in the service of man. *Appl. Clay Sci.* **1995,** *10*, 275-335. https://doi.org/10.1016/0169-1317(95)00029-4

(15)  Hradil, D. T.; Grygar, J.; Hradilova Y.; Bezdicka. P. Clay and iron oxide pigments in the history of painting. *Appl. Clay Sci*. **2003,** *22*, 223-236. https://doi.org/10.1016/S0169-1317(03)00076-0

(16)  Yang, H.; Yan, R.; Chen, H.; Lee, D. H.; Zheng, C. Characteristics of hemicellulose, cellulose and lignin pyrolysis. *Fuel* **2007,** *86*, 1781-1788. https://doi.org/10.1016/j.fuel.2006.12.013

(17)  Olivares-Pérez, A.; Toxqui-López, S.; Padilla-Velasco, A. Nopal Cactus (*Opuntia ficus-indica*) as a Holographic Material. *Materials* **2012**, 5, 2383-2402. https://doi.org/10.3390/ma5112383

(18)  Ibarra-Rodríguez, D.; Lizardi-Mendoza, J.; López-Maldonado, E. A.; Oropeza-Guzmán, M. T. Capacity of 'nopal' pectin as a dual coagulant-flocculant agent for heavy metals removal. *Chem. Eng. J.* **2017,** *323*, 19-28. https://doi.org/10.1016/j.cej.2017.04.087

(19)  Man, Y. C.; Syahariza, Z. A.; Mirghani, M. E. S.; Jinap, S., Bakar, J. Analysis of potential lard adulteration in chocolate and chocolate products using Fourier transform infrared spectroscopy. *Food Chem*. **2005,** *90*, 815-819. https://doi.org/10.1016/j.foodchem.2004.05.029

**BrJAC**

# ARTICLE

# Use of Smartphone and Image Analysis in the Quantification of Vitamin C in Golden Berry (*Physalis peruviana* L.) Juice

**Wilber Vilcapoma Quispe*** (ID) (✉), **Julio Fernando Pérez Sáez** (ID)

*Universidad Nacional de San Cristóbal de Huamanga, Escuela Profesional de Ingeniería en Industrias Alimentarias. Portal Independencia N° 57, Ayacucho, Peru*
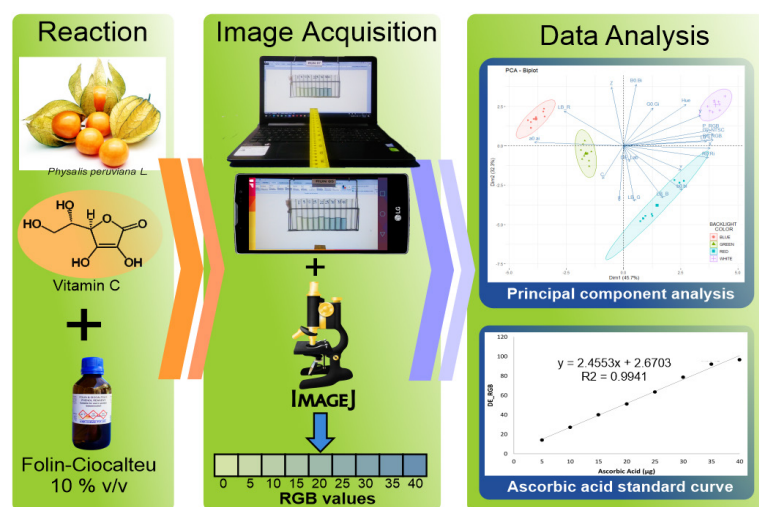
Conventional methods used to quantify vitamin C require expensive equipment; however, the image analysis method has proven to be effective in quantifying various bioactive compounds and could be useful for small industries due to its low cost. In this sense, the objective of the present work was to evaluate the use of a Smartphone and image analysis in the quantification of vitamin C in golden berries juice. Calibration curves were elaborated with ascorbic acid standards (2.5 – 20 mg $L^{-1}$) and the Folin-Ciocalteu chromophore reagent (10%). Fifteen color parameters (analytical responses) were obtained from images obtained with a smartphone and the ImageJ program of the colored samples using four backlight colors, to which a principal component analysis was applied using the integrated development environment for R, RStudio. Subsequently, one-way ANOVA and mean comparisons by Tukey's method ($\alpha$ = 0.05) were applied to the best-scoring analytical responses. Ultimately, the quantification of vitamin C in golden berry juice was performed using the image analysis method, which exhibited superior linearity and sensitivity ($R^2$ = 0.9941 and m = 4.91). A comparative assessment was conducted against a spectrophotometric method utilizing the *t*-Student test for independent samples ($\alpha$ = 0.05), demonstrating no statistically significant difference between the two methods ($p > 0.05$).

**Keywords:** Folin-Ciocalteu, ImageJ, RGB model, low-cost analysis, principal component analysis (PCA)

## INTRODUCTION

Vitamin C (VC) is an important antioxidant and should be consumed daily between 75-90 mg to maintain healthy blood vessels, skin, teeth, bones, and cartilage.[1] It is also essential in anti-allergic treatments, strengthens the immune system, and prevents flu and infections.[2] In this sense, the golden berries fruits

(*Physalis peruviana* L.) contain an important amount of VC ranging from 23.3 to 46.0 mg per 100 g of berries.[3–5] Additionally, there are exotic fruits that contain significant amounts of VC, which can be assessed by on-site investigations with portable and low-cost methods of analysis.[6]

On the other hand, one of the methods that are gaining momentum in the analysis and determination of biochemical compounds is the use of digital image analysis.[7] These methods proved to be effective and fast, efficient, and low-cost.[8] These methods have also demonstrated high sensitivity and good linearity based on the slope value and coefficient of determination ($R^2$) of the calibration curve in different studies.[7] Similarly, dos Santos et al.[6] demonstrated the possibility of using the method based on image analysis in the environment where it is required, being a portable method.

Nowadays, mobile devices have ceased to be a sumptuary object to become objects of common use with multiple utilities, one of them being the application in the capture of images of chromophore analytical samples.[2,6,7,9,10] Its availability in almost all types of social environments makes it possible to use it in the analysis of bioactive compounds *in situ*, mainly in communities with limited economic resources,[10] even in small companies that do not have sophisticated analysis equipment, where a quick analysis of VC is required.[6]

In this sense, the main objective of the present work was to evaluate the use of a smartphone and image analysis in the quantification of VC in golden berries juice (*Physalis peruviana* L.).

## MATERIALS AND METHODS

The golden berries fruits were purchased from the wholesale market "Nery García Zárate" in Ayacucho city, province of Huamanga, department of Ayacucho. Folin-Ciocalteu reagent (Loba Chemie PVT Ltd, India). Ascorbic acid (Sigma Aldrich, Germany). Tartaric acid (Insumos Químicos Perú. Peru). Trichloroacetic acid (Oxford, India).

### *Vitamin C standard preparation*

It was performed according to the methodology of Jagota & Dani[11] with some modifications. 0.05, 0.10, 0.15, 0.20, 0.25, 0.30, 0.35, and 0.40 mL of ascorbic acid stock solution (100 mg $L^{-1}$) were taken in test tubes. Subsequently, the samples were supplemented with a tartaric acid solution (200 mg $L^{-1}$) to a final volume of 2 mL, resulting in concentrations of 2.5, 5.0, 7.5, 10, 12.5, 15.0, 17.5, and 20 mg $L^{-1}$ of VC. In addition, the blank was made by placing 2 mL of tartaric acid solution (200 mg $L^{-1}$) in a test tube. Then, 0.2 mL of Folin-Ciocalteu's reagent diluted to 10% (v/v) was added to the nine prepared standards and allowed to react for 10 minutes. The calibration curve was elaborated by linear regression with the absorbance values ($\lambda$ = 760 nm) and using the colorimetric analytical responses.

### *Determination of VC in a sample*

The determination of VC used the technique described by Jagota & Dani[11] with some modifications. Five units of golden berries fruits were crushed in a mortar and pestle. 2 mL of the golden berries juice and 8 mL of 10% (w/v) trichloroacetic acid were added to a centrifuge tube and then centrifuged (P. Selecta, S240, Spain) at 3000 rpm for 15 min. Subsequently, VC determination was performed with 0.2 mL of the supernatant.

### *Acquisition and image processing conditions.*

The VC standards contained in test tubes were placed on a stand adapted to place the samples in front of a personal computer screen (HP, 250 G8, USA) that provided four backlight colors (BC); these are: white, red, green, and blue (Figure 1). In addition, 50% backlight brightness and 50 cm image acquisition distance were used.

**Figure 1.** Screens with backlight colors.

Images were acquired with a smartphone camera (LG, H440F, China), 8 MP (Megapixel), and an image acquisition resolution of 3264×2448 pixels. Furthermore, the numerical data of the images, corresponding to the values of the R, G, and B channels of the region of interest, were acquired using ImageJ 1.53k.

### Obtaining analytical responses (S)

Different analytical responses ($S_1$ to $S_{15}$) were explored by mathematical combinations of the RGB color space and CIE Lab parameters (Table I). Equations (1) to (15) were used for this purpose. The color parameters lightness (L*), redness (a*), and yellowness (b*) were obtained using the worksheet (Microsoft Excel®) developed by Boronkay[12] called Colour Conversion Centre (4.0a), using the RGB channel values.

**Table I.** Mathematical combinations of the RGB color space and CIE Lab parameters

| Analytical responses (S) | Equation | Reference |
|---|---|---|
| $S_1 = \dfrac{R_i + G_i + B_i}{3}$ | (1) | Osorio et al.[13] |
| $S_2 = 0.299R_i + 0.587G_i + 0.114B_i$ | (2) | Zhao et al.[14] |
| $S_3 = -log\left(\dfrac{R_i}{R_0}\right)$ | (3) | Zhao et al.[14] |
| $S_4 = -log\left(\dfrac{G_i}{G_0}\right)$ | (4) | Zhao et al.[14] |
| $S_5 = -log\left(\dfrac{B_i}{B_0}\right)$ | (5) | Zhao et al.[14] |
| $S_6 = R_0 - R_i$ | (6) | Porto et al.[2] |
| $S_7 = G_0 - G_i$ | (7) | Porto et al.[2] |
| $S_8 = B_0 - B_i$ | (8) | Porto et al.[2] |

(continues on the next page)

**Table I.** Mathematical combinations of the RGB color space and CIE Lab parameters (continuation)

| Analytical responses (S) | Equation | Reference |
|---|---|---|
| $S_9 = \sqrt{(R_0 - R_i)^2 + (G_0 - G_i)^2 + (B_0 - B_i)^2}$ | (9) | Abderrahim et al.[15] |
| $S_{10} = L_0^* - L_i^*$ | (10) | Wongthanyakram et al.[16] |
| $S_{11} = a_0^* - a_i^*$ | (11) | Wongthanyakram et al.[16] |
| $S_{12} = b_0^* - b_i^*$ | (12) | Wongthanyakram et al.[16] |
| $S_{13} = \sqrt{\left(L_0^* - L_i^*\right)^2 + \left(a_0^* - a_i^*\right)^2 + \left(b_0^* - b_i^*\right)^2}$ | (13) | Wongthanyakram et al.[16] |
| $S_{14} = \sqrt{a^{*2} + b^{*2}}$ | (14) | Otálora et al.[17] |
| $S_{15} = \dfrac{180}{\pi} arctan\left(\dfrac{b^*}{a^*}\right)$ | (15) | Otálora et al.[17] |

Red (R), green (G), and blue (B) are color parameters from the RGB color space. The color parameters lightness (L*), redness (a*), and yellowness (b*) from the CIE Lab color space. The subscripts "i" and "0" correspond to the values of the color parameters at different concentrations of vitamin C and without vitamin C, respectively.

### Statistical analysis

The statistical software RStudio (version 2022.12.0, Build 353) was employed as the integrated development environment for R (version 4.2.2). The 'stats' library was utilized for the analysis of variance, while the 'EnvStats' library was utilized for obtaining the lack of fit analysis. Multivariate analysis, specifically Principal Component Analysis (PCA), was conducted using the 'missForest', 'FactoMineR', 'ggplot2', and 'factoextra' libraries. Mean comparisons were performed using Tukey's method at a 95% confidence level, with the 'agricolae' library employed for this purpose. The $t$-Student test for independent samples ($\alpha = 0.05$) was applied using the 'stats' library.

## RESULTS AND DISCUSSION

### Vitamin C calibration curves (VCCC)

In the realm of analytical chemistry, linear regression has conventionally been employed, although it may not always be the optimal approach. To ascertain the model's suitability and evaluate linearity, it is crucial to assess both the ANOVA and the "lack of fit" value.[18,19] In our study, the models displayed high significance ($p < 0.001$), indicating their linearity and effective utilization as calibration curves. Additionally, the lack of fit value was determined to be non-significant ($p > 0.05$), implying that the experimental data align well with the mathematical model in all three examined cases (Table II).

**Table II.** $p$-value for the model and lack of fit for different linear models

| Source of variation | Red | Green | Blue |
|---|---|---|---|
| Model | < 0.001 | < 0.001 | < 0.001 |
| Lack of fit | 0.9646 | 0.9700 | 0.9121 |

Figure 2 illustrates the concentrations of vitamin C (CVC) and their corresponding analytical responses based on color channels (R, G, and B). Notably, the red channel exhibits more pronounced changes

in the analytical response as the CVC varies, whereas the blue channel demonstrates a comparatively lower response. In both cases, the analytical response shows an inverse relationship with the CVC. This finding aligns with the work of Fan et al.,[7] who emphasized that the color of a sample can be related to its concentration within a specific range, often exhibiting linearity. Consequently, establishing a standard curve enables sample analysis.
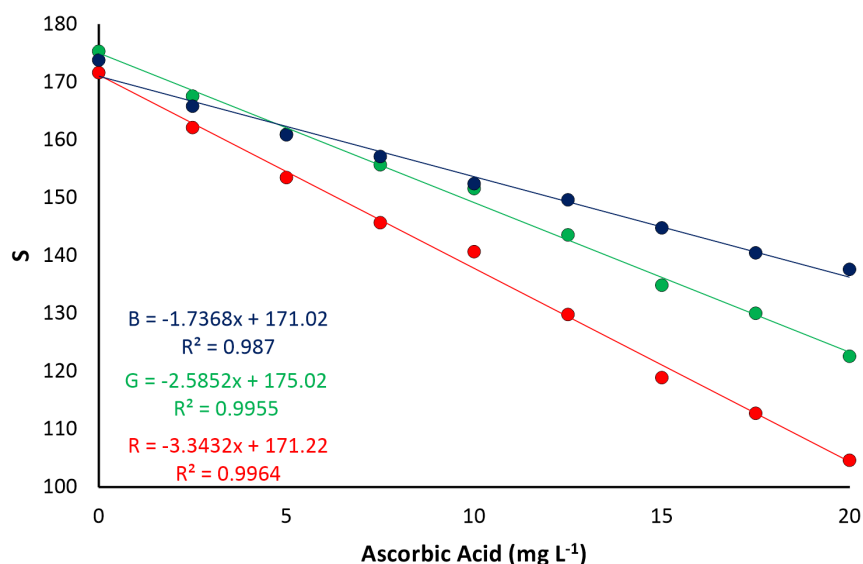


**Figure 2.** Vitamin C concentration with respect to analytical response (R, G, and B).

*Principal component analysis (PCA)*

To the fifteen analytical responses ($S_1$ to $S_{15}$) shown in Table I, a PCA analysis was applied with respect to the applied background color (BC). The purpose of this analysis was to explore this relationship and its effect on the slope values and the coefficient of determination ($R^2$) of the VCCC. In this regard, it was observed that certain background colors were associated with certain analytical responses.

The slope values of the VCCC were represented in the PCA-Biplot graph shown in Figure 3-a, and it was observed that BC were grouped in different areas of the graph. In addition, the slope values that had the lowest dispersion were those that worked with white BC. Also, this is located in the first quadrant, which indicated that it contributes significantly to dimension 1 (Dim1), which had a higher contribution value (47.7%). By reducing the variables (Figure 3-b), it was possible to better observe the analytical responses that provided the greatest contribution to increasing slope values. The analytical response's: $S_1$, $S_2$, and $S_9$, had a high positive correlation with respect to Dim1. This is due to the angles formed, these were closer to zero. On the contrary, the $S_{11}$, had a negative correlation with respect to Dim1, and probably the slope values obtained with this analytical response are lower in relation to the analytical response's found in quadrant 1 of the PCA-Biplot. However, the highest values obtained with this analytical response were with the blue BC. On the other hand, analytical response $S_8$ did not show a correlation in Dim1, but it did show a correlation in dimension 2 (Dim2). The PCA analysis accounted for 77.9% of the variability in the model, specifically in relation to the slope values of the calibration curve. On the other hand, Attar et al.[20] mentioned that the opposite directions of the arrows indicate inverse correlations between groups of factors. Therefore, the analytical response's that are in the first quadrant provide higher slope values for the white BC and lower values for the blue BC, the inverse happened for the $S_{11}$. On the other hand, Ballesteros et al.[9] suggested that a higher slope value in a calibration curve would be indicative of a higher sensitivity of the method, which is why the analytical response's "$S_1$", "$S_2$", and "$S_9$" was chosen, in addition to the white BC.
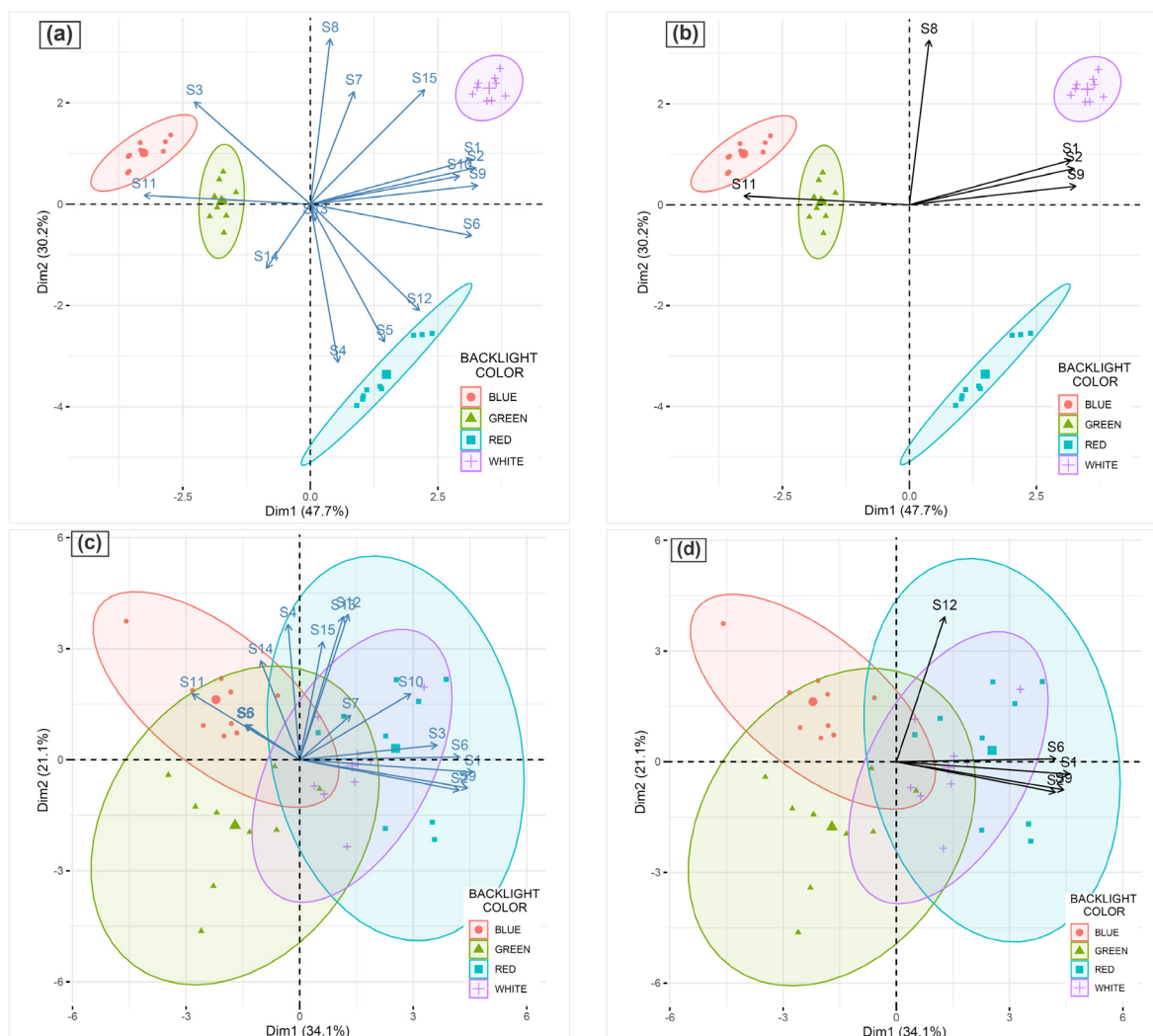
**Figure 3.** PCA-Biplot in the analysis of the VCCC slope. (a) Complete variables and (b) with variable reduction. PCA-Biplot in the analysis of the $R^2$ of the VCCC. (c) Complete variables and (d) with variable reduction.

There was no defined group in the analysis of the coefficient of determination with respect to the BC because they appear to form a single group (Figure 3-c). However, the red BC dominates the entire graph, and its center point is on the right, and higher $R^2$ values can be obtained with this BC. On the other hand, the white BC is in the first quadrant, and its values were not as dispersed as those of the red BC. The analytical response's that contributed the most were $S_9$, $S_1$, and $S_2$ (Figure 3-d). In this second evaluation, the PCA analysis for the $R^2$ variable explained 55.2% of the model variability. It should be noted that a higher $R^2$ value would provide greater linearity of method.[21] In addition, Fan et al.[7] analyzed several studies where an $R^2$ greater than 0.9577 showed good linearity.

After the multivariate analysis, an analysis of mean comparisons was performed using Tukey's method, and evaluated at 95% confidence. Table III shows that the slope value using the analytical response "$S_9$" was higher and was significantly different ($p < 0.05$) with respect to the analytical response's "$S_2$" and "$S_1$". However, when the $R^2$ was evaluated, none of the analytical response's had significant differences ($p > 0.05$) and their values were above 0.99.

**Table III.** Comparisons of means between the chosen color parameters

| Analytical response's | Slope | $R^2$ |
|---|---|---|
| $S_9$ | $4.56 \pm 0.0772^a$ | $0.9960 \pm 0.0014^a$ |
| $S_2$ | $2.72 \pm 0.0411^b$ | $0.9957 \pm 0.0012^a$ |
| $S_1$ | $2.56 \pm 0.0473^c$ | $0.9960 \pm 0.0016^a$ |

Different lowercase letters (a,b and c) indicate significant differences ($p < 0.05$) in the same column. Values were expressed as mean ± standard deviation ($n = 9$).
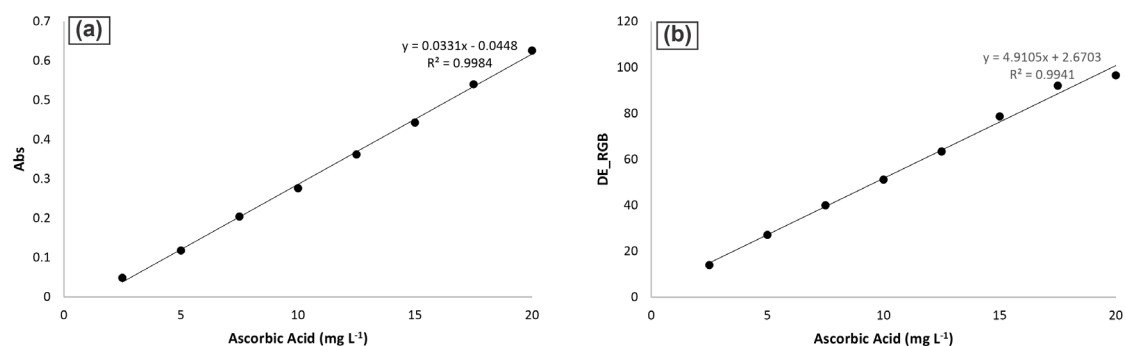


**Figure 4.** VCCC by spectrophotometric UV-Vis method (a) and image analysis (b).

### Analysis of VC in golden berries juice using a smartphone

The VCCC shown in Figure 4 showed high coefficients of determination ($R^2 > 0.99$). According to Fan et al.,[7] this result means that the linearity of the method is very good. On the other hand, the VCCC obtained with the analytical response $S_9$ and the white BC gave a slope value of 4.91 (Figure 4-b). The LOD and LOQ values of the new method were 1.28 and 3.87 mg L$^{-1}$ VC, respectively. In this regard, Porto et al.[2] found a LOQ of 5.4 mg L$^{-1}$ VC. In our study, the obtained value was slightly lower. However, based on this result, we can still conclude that the new method could be suitable for the analysis of VC in golden berries juice.

Table IV displays the VC values obtained using both the spectrophotometric and image analysis methods utilizing a smartphone. The analysis of VC using these two methods did not yield any significant differences ($p > 0.05$) when evaluated through the t-Student method for independent samples with a 95% confidence level. As a result, it can be concluded that there is insufficient evidence to support the claim that the VCC values obtained differ significantly between the two analysis methods.

**Table IV.** Vitamin C according to method of analysis

| Methods | mg of vitamin C $100^{-1}$ mL$^{-1}$ |
|---|---|
| Spectrophotometric* | $34.9 \pm 0.682^a$ |
| Image analysis | $36.4 \pm 1.842^a$ |

*UV-Vis method ($\lambda = 760$ nm). Values expressed as mean ± standard deviation for $n = 3$. Values with equal letters indicate non-significance between treatments according to the Student's $t$-test for independent samples ($\alpha = 0.05$).

## CONCLUSIONS

The utilization of a smartphone and image analysis for quantifying vitamin C (VC) in golden berries juice (*Physalis peruviana* L.) was successfully evaluated, resulting in a value of 36.4 mg VC 100$^{-1}$ mL$^{-1}$ of juice. The Euclidean distance of RGB ($S_9$) and white backlight color proved to be the optimal analytical response and backlight color, respectively.

Different backlight colors exhibited variations in method sensitivity. However, linearity remained consistent, with high coefficients of determination observed across all backlight colors. Moreover, when employing various color parameters as analytical responses, the method's sensitivity showed significant variability, with slope values ranging from 2.86 × 10$^{-3}$ to 4.69.

The quantification of VC via smartphone image analysis demonstrated itself as a fast, simple, and cost-effective tool. It exhibited high accuracy comparable to traditional methods. Moreover, this method holds potential for implementation in higher education institutions located in remote areas, where it can be utilized for teaching a low-cost colorimetric analysis method. Furthermore, it opens avenues for the analysis of VC in other sample types.

### Conflicts of interest

The authors declare that there is no conflict of interest/competing interest (financial or not) for this study.

## REFERENCES

(1)  Choy, C. K.; Benzie, I. F. Vitamin C – Health Professional Fact Sheet. *National Institutes of Health, Office of Dietary Supplements.* 2018. https://ods.od.nih.gov/FACTSHEETS/VITAMINC-HEALTHPROFESSIONAL/ (accessed 2021-08-10).

(2)  Porto, I. S. A.; Santos Neto, J. H.; dos Santos, L. O.; Gomes, A. A.; Ferreira, S. L. C. Determination of Ascorbic Acid in Natural Fruit Juices Using Digital Image Colorimetry. *Microchem. J.* **2019**, *149*. https://doi.org/10.1016/j.microc.2019.104031

(3)  Silva, M. H. B.; Pinheiro, K.; Pereira, M.; Almeida, N. E.; Graciliano, J.; da Silva, F. J.; da Silva, A. Characterization of Physiological Maturity of *Physalis Peruviana* L. Fruits. *Semin. Agrar.* **2021**, *42* (3), 929–947. https://doi.org/10.5433/1679-0359.2021v42n3p929

(4)  Arenas, T. Y.; Díaz, I. S. Capacidad Antioxidante del Aguaymanto (*Physalis Peruviana* L.) en tres presentaciones para el Consumo Humano, Universidad Femenina del Sagrado Corazón, Lima-Perú, 2020. http://hdl.handle.net/20.500.11955/725 (accessed 2021-07-07).

(5)  Briones-Labarca, V.; Giovagnoli-Vicuña, C.; Figueroa-Alvarez, P.; Quispe-Fuentes, I.; Pérez-Won, M. Extraction of *β*-Carotene, Vitamin C and Antioxidant Compounds from *Physalis Peruviana* (Cape Gooseberry) assisted by High Hydrostatic Pressure. *Food Nutr. Sci.* **2013**, *04* (08), 109–118. https://doi.org/10.4236/fns.2013.48a014

(6)  dos Santos, V. B.; da Silva, E. K. N.; de Oliveira, L. M. A.; Suarez, W. T. Low Cost in Situ Digital Image Method, Based on Spot Testing and Smartphone Images, for Determination of Ascorbic Acid in Brazilian Amazon Native and Exotic Fruits. *Food Chemistry* **2019**, *285*, 340–346. https://doi.org/10.1016/j.foodchem.2019.01.167

(7)  Fan, Y.; Li, J.; Guo, Y.; Xie, L.; Zhang, G. Digital Image Colorimetry on Smartphone for Chemical Analysis: A Review. *Meas. J. Int. Meas. Confed.* **2021**, *171*, 108829. https://doi.org/10.1016/j.measurement.2020.108829

(8)  Berlín, M. P.; López, A. *Imágenes Digitales En Las Determinaciones Analíticas: Estudio Del Iluminante.* Zaguan Universidad de Zaragoza Repository, 2015. https://zaguan.unizar.es/record/32301 (accessed 2020-12-14).

(9)  Ballesteros, J. I.; Caleja-Ballesteros, H. J. R.; Villena, M. C. Digital Image-Based Method for Iron Detection Using Green Tea (*Camellia sinensis*) Extract as Natural Colorimetric Reagent. *Microchem. J.* **2021**, *160* (Part A), 105652. https://doi.org/10.1016/j.microc.2020.105652

(10)  Mohamed, A. A.; Shalaby, A. A. Digital Imaging Devices as Sensors for Iron Determination. *Chem. Food* **2019**, *274*, 360–367. https://doi.org/10.1016/j.foodchem.2018.09.014

(11) Jagota, S. K.; Dani, H. M. A New Colorimetric Technique for the Estimation of Vitamin C Using Folin Phenol Reagent. *Anal. Biochem.* **1982**, *127* (1), 178–182. https://doi.org/10.1016/0003-2697(82)90162-2

(12) Boronkay, G. *Colour Conversion Centre*. http://ccc.orgfree.com/ (accessed 2021-08-08).

(13) Osorio, J. A. C.; Urueña, W. A.; Vargas, J. A. M. Técnicas alternativas para la conversión de imágenes a color a escala de grises en el tratamiento digital de imágenes. *Scientia et Technica* **2011**, *1* (47), 207–212.

(14) Zhao, W.; Cao, P.; Zhu, Y.; Liu, S.; Gao, H.-W.; Huang, C. Rapid detection of Vitamin C content in fruits and vegetables using a digital camera and color reaction. *Quim. Nova* **2020**, *43* (10), 1421–1430. http://dx.doi.org/10.21577/0100-4042.20170642

(15) Abderrahim, M.; Arribas, S. M.; Condezo-Hoyos, L. A. A Novel High-Throughput Image Based Rapid Folin-Ciocalteau Assay for Assessment of Reducing Capacity in Foods. *Talanta* **2016**, *152*, 82–89. https://doi.org/10.1016/j.talanta.2016.01.051

(16) Wongthanyakram, J.; Harfield, A.; Masawat, P. A Smart Device-Based Digital Image Colorimetry for Immediate and Simultaneous Determination of Curcumin in Turmeric. *Comput. Electron. Agric.* **2019**, *166*. https://doi.org/10.1016/j.compag.2019.104981

(17) Otálora, M. C.; Wilches-Torres, A.; Gómez Castaño, J. A. Mucilage from yellow pitahaya (*Selenicereus megalanthus*) fruit peel: Extraction, Proximal Analysis, and Molecular Characterization. *Molecules* **2023**, *28* (2), 786. https://doi.org/10.3390/molecules28020786

(18) de Oliveira, E. C. Critical Metrological Evaluation of Fuel Analyses by Measurement Uncertainty. *Metrol. Meas. Syst.* **2011**, *18* (2), 6. https://doi.org/10.2478/v10178-011-0006-4

(19) Chui, Q. S. H. Uncertainties Related to Linear Calibration Curves: A Case Study for Flame Atomic Absorption Spectrometry. *J. Braz. Chem. Soc.* **2007**, *18* (2), 424–430. https://doi.org/10.1590/S0103-50532007000200027

(20) Attar, Ş. H.; Gündeşli, M. A.; Urün, I.; Kafkas, S.; Kafkas, N. E.; Ercisli, S.; Ge, C.; Mlcek, J.; Adamkova, A. Nutritional Analysis of Red-Purple and White-Fleshed Pitaya (*Hylocereus*) Species. *Molecules* **2022**, *27* (3). https://doi.org/10.3390/MOLECULES27030808

(21) Zumbado, H. *Análisis Químico de Los Alimentos: Métodos Clásicos*. International Union of Pure and Applied Chemistry (IUPAC): Cuba, 2004. https://doi.org/10.1351/goldbook

**BrJAC**

# ARTICLE

# Systematic Study for Determining As, Pb, Cd, and Se in Steel and Nickel Alloy Samples by GF AAS:

## *Circumventing Matrix Interference with Extraction Based on Micellar Separation*

**Natália Tostes Canevari Viola**[iD]**, Brian Cardoso Ferreira**[iD]**, Lilian Rodrigues Rosa Souza**[iD]**,
Márcia Andreia Mesquita Silva da Veiga** [iD][✉]

*Departamento de Química, FFCLRP, Universidade de São Paulo, 14040-901, Ribeirão Preto, SP, Brazil*
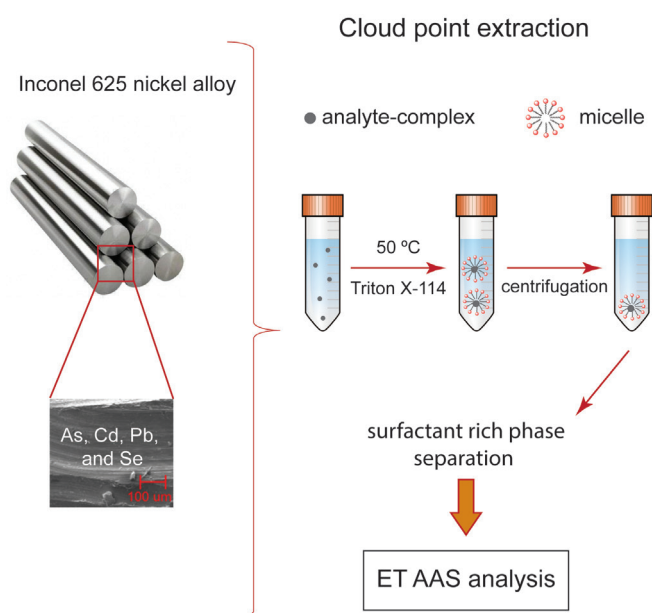
This study proposes a matrix separation procedure based on micellar-mediated extraction (cloud point extraction - CPE) for determining As, Cd, Pb, and Se (potential contaminants) in nickel alloy and steel samples. Structural characterization and qualitative analysis of Ni alloy were conducted on the nickel alloy using scanning electron microscopy-energy-dispersive X-ray spectroscopy (SEM-EDS). After sample decomposition, ammonium o,o-diethyl dithiophosphate (DDTP) was used to complex the analytes and Triton X-114 as a non-ionic surfactant in CPE for matrix separation and extraction. Methanol acidified with 0.1 mol L$^{-1}$ HNO$_3$ was added to the surfactant-rich phase before the analytes determination by graphite furnace atomic absorption spectrometry (GF AAS). Parameters such as pH, complexing agent and surfactant concentrations, acid medium, complexation time, and type of diluent were evaluated. The obtained results indicated that the ratio DDTP:As was 3:1, DDTP:Cd and DDTP:Pb was 2:1, and DDTP:Se was 1:1. The enrichment factors were 6, 8, 14, and 13, and limits of detection were 1.5, 0.06, 0.31 and 0.27 µg g$^{-1}$ for As, Cd, Pb, and Se, respectively. The method was applied for As, Cd, Pb, and Se determination in Inconel 625 nickel alloy and standard reference materials (AISI 4340 Steel - SRM® 361, AISI 94B17 Steel - SRM® 362, Chromium-Vanadium Steel - SRM® 363, and Nickel Alloy UNS - SRM® 864). Analyte recoveries lay above 88%, and relative standard deviations were lower than 5%. Application of cloud point extraction for matrix separation allowed the determination of low concentrations of As, Cd, Pb, and Se, constituting an environmentally friendly method.

**Keywords:** steel; nickel alloy; cloud point extraction; As, CD, Pb, and Se; GF AAS

## INTRODUCTION

The production and global trade of metals and alloys are critical to modern industrial infrastructure. Continuous improvement of metallurgical processes and manufacturing technologies have paved the way for developing nickel alloys,[1] commonly employed under circumstances requiring strength and corrosion resistance at high temperatures, e.g., for application in nuclear, chemical, and petrochemical plants as aerospace and navigation industry.[2] Several factors influence the properties of nickel alloys, including the major constituent elements, the production process, and the thermal treatment of the intermediate product.[3] Moreover, the presence of trace contaminants such as Ag, As, Bi, Cd, Pb, Sb, Se, Sn, Te, Tl, and Zn at concentrations above a certain limit may impacts the mechanical and magnetic properties of these materials negatively. Remarkably, As, Cd, Pb, and Se can affect the properties related to the mechanical and thermal resistance of steel and nickel alloys by lowering the melting point, which leads to severe disruption and a disastrous failure of the final product.[4-6]

Quality control with respect to elements concentration is crucial to ensure the development and application of nickel alloys. However, trace elements determination is a challenging task, considering that the alloy matrix is quite complex.[4] To prevent interferences, matrix separation has been employed in trace element determination.[7] Cloud point extraction (CPE) has also been employed for purpose; it complies with green chemistry principles[8] has some advantages: it is safe to operate (the reagents are not volatile or toxic); it generates a lower amount of laboratory residues (small volumes of reagents are used); and it allows pre-concentration of many species with good enrichment factors.[9,10]

CPE is based on micelles formation by surfactants in aqueous solutions. They promote phase separation upon a change in temperature or the addition of a salting-out agent. The surfactants, above the critical micelle concentration (CMC), can self-assemble in water into supra-molecular aggregates and, when heated at a given temperature (cloud point), result in a biphasic system with a surfactant-rich phase of a small volume containing the hydrophobic compounds initially present in the solution and a surfactant-poor phase that can be separated from the surfactant rich phase. Inorganic species, which are hydrophilic, are is extracted in the surfactant-rich phase by using a complexing agent that produces hydrophobic compounds under suitable conditions.[11,12] Different complexing agents have been used in CPE, e.g., ammonium pyrrolidine dithiocarbamate (APDC),[13] 1,2-tiazolylazo-2-naphthol (TAN),[14] 8-hydroxyquinoline (8-HQ),[15] and ammonium O,O-diethyl dithiophosphate (DDTP). DDTP has a sulfur atom as the electron donor. They behave like a soft base and can complex elements that are mildly acidic and does not form a stable complex with alkaline metals. This selectivity is desirable since it avoids the potential matrix effects as in the case of metal alloys analysis.[16,17]

Ammonium O,O-diethyl dithiophosphate has been employed for As preconcentration and subsequent determination in corn and rice samples by hydride generation coupled to atomic fluorescence spectrometry,[18] Cd and Pb in urine[19] and Cd, Pb, and Pd in blood, with subsequent determination using graphite furnace atomic absorption spectrometry (GF AAS).[20] DDTP has also been used for As, Bi, Cd, and Pb preconcentration in river water, wine, fertilizer, and urine prior the analytes determination by inductively coupled plasma optical emission spectrometry (ICP OES).[21]

Cloud point extraction has already been employed in the analysis of alloy samples as reported by Kassem and Amin, who determined rhodium in a metallic alloy using 5-(4′-nitro-2′,6′-dichlorophenylazo)-6-hydroxypyrimidine-2,4-dione (NDPHPD) as a complexing agent and Triton X-114 as a surfactant[22] and Bahchevanska et al. determined vanadium in aluminum alloy using 1-(2-thiazolylazo)-2-naphthol (TAN) and complexing agent and Triton X-114 as a surfactant.[23] However, this approach has yet to be explored for other elements and metal alloys.

In the present work, CPE is proposed for As, Cd, Pb and Se separation from Ni alloy and steel digestates of cloud point extraction, followed by the determination of analytes by GF AAS. The proposed CPE procedure involves analyte extraction with the complexing agent DDTP in the presence of the non-ionic surfactant Triton X-114.

## MATERIALS AND METHODS

### Samples

Carbon steel saw was employed to cut the nickel alloy sample (Inconel 625) into the most diminutive possible dimensions. After this procedure, pieces with a rectangular shape, measuring 1x1 cm and weighing approximately 2.5 g, were obtained. For accuracy evaluation, samples of the following standard reference materials (CRMs) were analysed: AISI 4340 Steel (SRM® 361), AISI 94B17 Steel (SRM® 362), Chromium-Vanadium Steel (SRM® 363), and Nickel Alloy UNS N06600 (SRM® 864), produced at the National Institute of Standards and Technology (NIST).

### Reagents and solutions

Experiments were performed with reagents of analytical grade. Ultrapure water (resistivity of 18.2 $M\Omega$ cm$^{-1}$), obtained from a Milli-Q® water purification system (Millipore, Billerica, MA, USA), was used to prepare the reagents and solutions. All the glassware was decontaminated in 30% (v v$^{-1}$) $HNO_3$ for 48 h and rinsed in ultrapure water for a few minutes.

To decompose the Inconel 625 nickel alloy sample and CRMs, 37% m m$^{-1}$ HCl (JT Baker) and 65% m m$^{-1}$ $HNO_3$ (JT Baker) were employed.

Concerning CPE, the Cd and Pb solutions were prepared by diluting stock standard solutions containing 1000 mg L$^{-1}$ of the respective analytes (Titrisol® standards from Merck). A standard stock solution of 4000 mg L$^{-1}$ As was prepared by dissolving 0.1 g of $As_2O_3$ (Acros) in 25 mL of previously heated water containing 3 mL of 37% m m$^{-1}$ HCl (JT Baker). A 7.5 mg L$^{-1}$ Se(IV) solution was obtained from a 1000 mg L$^{-1}$ standard solution of Se(VI) (Fluka) by heating this solution in 6 mol L$^{-1}$ HCl for 30 min at 100 °C. A 5% (m v$^{-1}$) ammonium o,o-diethyl dithiophosphate solution was prepared daily using the DDTP ammonium salt (Aldrich) dissolved in deionized water. 37% m m$^{-1}$ HCl (JT Baker) was employed to adjust pH of solutions. A 5% (m v$^{-1}$) octylphenoxypolyethoxyethanol (Triton X-114) solution was prepared by weighing 2.5 g of the reagent (Sigma-Aldrich) in a graduated tube followed by the addition of 50 mL of water. To reduce the viscosity of the surfactant-rich phase, methanol (Panreac) acidified with 0.1 mol L$^{-1}$ $HNO_3$ was used. Ascorbic acid (Sigma-Aldrich) and citric acid (Carlo Erba) were used for Fe and Ni interference studies, respectively. The chemical modifier $Pd(NO_3)_2$ + $Mg(NO_3)_2$ employed in Cd and Pb determination was prepared by mixing 1 mL of $Pd(NO_3)_2$ 10 g L$^{-1}$ (Fluka) and 100 µL of $Mg(NO_3)_2$ 10 g L$^{-1}$ (Merck) in a graduated flask, followed by addition of 10 mL of deionized water. For As, $Pd(NO_3)_2$ was employed as chemical modifier, which was prepared by diluting 1 mL of 10 g L$^{-1}$ $Mg(NO_3)_2$ in 10 mL of water in a graduated flask. For Se, Ni + $Mg(NO_3)_2$ was used as chemical modifier, which was prepared by mixing 801 µL of 1000 mg L$^{-1}$ Ni standard solution (Fluka) and 79 µL of 10 g L$^{-1}$ $Mg(NO_3)_2$, followed by the addition of 1 mL of water.

### Instrumentation

The nickel alloy sample and CRMs were decomposed in a metallic block (TE-040/25, Tecnal, Piracicaba, São Paulo, Brazil). For the CPE experiments, a water bath with controlled temperature (MA127, Marconi, Piracicaba, São Paulo, Brazil) and a centrifuge (Z 326K, Hermle Labortechnik, Wehingen, Germany) were employed.

Arsenic, Cd and Se were determined using an atomic absorption spectrometer (AAnalyst 800, PerkinElmer, Norwalk, CT, USA) whereas Pb was by using with a high-resolution continuum source atomic absorption spectrometer (ContrAA 700, Analytik Jena AG, Jena, Germany). Both instruments were equipped with an autosampler for sample introduction and a transversely heated pyrolitic graphite tube. Twenty microliters of sample or reference solutions, 5 µL of the chemical modifiers $Pd(NO_3)_2$ + $Mg(NO_3)_2$ for Cd and Pb and $Pd(NO_3)_2$ for As, or 10 µL of Ni + $Mg(NO_3)_2$ for Se were pipetted into the graphite tube. Argon with 99.998% purity (White Martins, Sertãozinho, São Paulo, Brazil) was used as the purge gas. Tables SI and SII (Suplementary information) summarize the instrumental parameters.

The graphite furnace temperature programs given in Tables SIII and SIV were run during As, Cd, Se, and Pb determination.

### Structural characterization of the nickel alloy sample

The structural characterization and qualitative analysis of the Inconel 625 nickel alloy sample were carried out using a scanning electron microscope (EVO 50, ZEISS - Carl Zeiss, Cambridge, England) equipped with an EDS system (IXRF Systems 500 Digital Processing Si(Li) diode, Liechtenstein). The detector was employed in the secondary electron mode, the chamber pressure was 1.8 x 10$^{-5}$ Torr, and the accelerating voltage was 20 kV.

To avoid possible contamination during the cut of the Inconel 625 sample. It was placed in a glass beaker containing 50 mL of 2-propanone (Merck) and sonicated in an ultrasonic bath (USC-1400, Unique, Indaiatuba, São Paulo, Brazil) for 15 min.

### Sample preparation

Regarding the decomposition of the nickel alloy sample before As, Cd, and Se determination, each fragment was weighed (2.5 g of a fragment of 1x1 cm), placed in a glass flask, to which with 24 mL of an acid mixture containing 37% HCl (m m$^{-1}$) and 65% HNO$_3$ (m m$^{-1}$) (3:1 ratio) were added. Experiments were conducted in triplicate. The flasks were placed in a digestor block, and the mixture was heated from 50 to 85 °C. Between 2 and 4 h was required for complete sample digestion. After cooling, the solutions were transferred to graduated tubes, and the volume was adjusted to 30 mL with water. This procedure was also applied to check the analytes recovery, where sample aliquots were spiked to obtain 20 µg L$^{-1}$ As, 0.45 µg L$^{-1}$ Cd, 10 µg L$^{-1}$ Pb, and 8 µg L$^{-1}$ Se to assay analyte recoveries. The sample solutions were then submitted to CPE. The same methodology was employed to decompose the standard reference materials; however, in this case, the sample mass was 0.250 g, and the volume of the acid mixture was 8 mL.

For Pb, 25 mL of 65% (m m$^{-1}$) HNO$_3$ were added to the sample. The mixture was heated at 50 to 120 °C for 24 h in this case, a more extended period was necessary for complete sample decomposition. Analyte recovery was assessed for samples aliquots spiked to contain 10 µg L$^{-1}$ Pb. The same procedure was followed to decompose the CRMs; however, the sample mass was 0.250 g, and the 65% HNO$_3$ (m m$^{-1}$) volume was 5 mL.

### Cloud point extraction

Initially, aliquots of digestate (100 µL), ascorbic acid (0.1 g) (for the elimination of Fe interference), and 37% HCl (m m$^{-1}$) (for pH adjustment, ensuring the best absorbance for each analyte) were transferred to graduated flask. The volume was adjusted to 9 mL with water, and the mixture left to rest during 15 min for the complete dissolution of the ascorbic acid. Subsequently, different amounts of DDTP solution were added (according to the optimization of CPE parameters) and the solution left resting for 20 min. Then, Triton X-114 was added, and the volume was adjusted to 15 mL with water. The solutions were heated in a water bath at 50 °C for 20 min, followed by centrifugation at 1233 G for 20 min. Next, the flasks were immersed in an ice bath for 15 min and then the sobrenatant aqueous phase was removed with a micropipette. 500 µL of methanol containing 0.1 mol L$^{-1}$ HNO$_3$ was added to the extracts to reduce the viscosity of the surfactant-rich phase before the determination of analytes by GF AAS. Calibration solutions and analytical blanks were also submitted to CPE in the same conditions as the samples. The concentrations of DDTP, Triton X-114, and HCl, the acid medium for complexation, the type of diluent for the surfactant-rich phase, and the complexation time were evaluated.

### Optimization of CPE

Analyte preconcentration using CPE requires careful optimization of experimental parameters because it affects the extraction efficiency, phases separation and enrichment factor. As such the HCl, complexant, and surfactant concentrations, acid medium, complexation time, and type of diluent of the surfactant-rich phase were considered.

The complexation time was for 20 min, and 0.1 mol L$^{-1}$ HNO$_3$ in methanol was used to dilute the surfactant-rich phase unless stated otherwise.

## RESULTS AND DISCUSSION
### *Structural characterization of the nickel alloy sample*

The structural characterization and qualitative analysis were carried out using scanning electron microscopy-energy-dispersive X-ray spectroscopy (SEM-EDS). In Figures 1 and 2 shows the SEM-EDS images obtained from the nickel alloy sample.
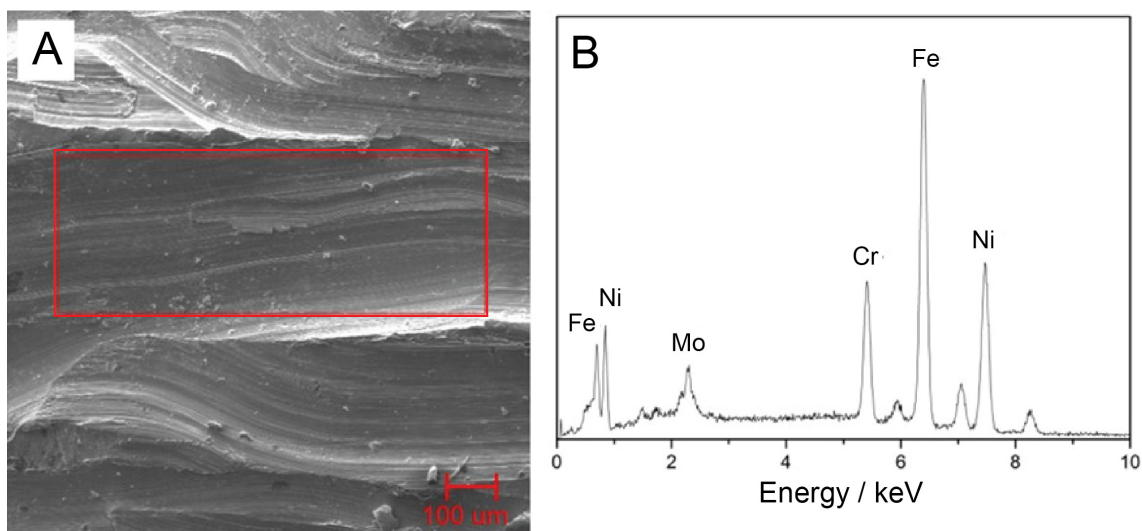


**Figure 1.** Image obtained of the nickel alloy sample by SEM-EDS in the secondary electron mode (a) and respective EDS spectrum (b).
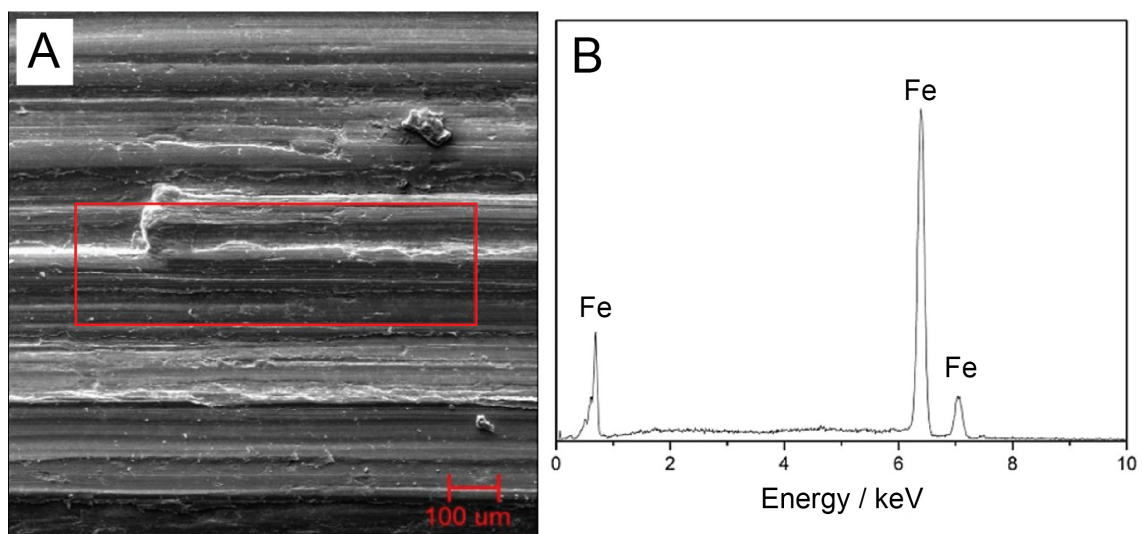


**Figure 2.** Image obtained of the internal structure of the nickel alloy sample by SEM-EDS (a) and respective EDS spectrum (b).

All the SEM imaging was carried out using the secondary electron mode, which can provide helpful information about the material surface and topography. Considering the analyzed region, represented in red color in Figure 1 (a), the surface portion of the nickel alloy sample demonstrates that Cr, Fe, and Ni were present in this material, constituting respectively, 11, 44 and 33% of the analyzed portion. Besides, Nb (2%) and Mo (4%) were also present in this portion. The presence of these elements was expected, as they are constituents of the Inconel 625 nickel alloy.[24,25]

With respect to the images of Ni internal portion, Figure 2 (a) and (b), elements present were Fe (94%) oxygen (5%), and carbon (1%). Unlike the surface portion, Ni and Cr were not observed. This is y due to the differences of the material, as the surface has a coating of Inconel 625, and the internal part is carbon steel.

Identifying the major chemical elements is possible using SEM-EDS; however, the elements evaluated in this study (As, Cd, Pb, and Se) were not detected. The SEM-EDS technique does not have sufficient sensitivity to detect elements present as impurities in the alloy, reinforcing the need to employ other techniques to ensure the quality control of the alloy. These elements (as impurities) are commonly present in Ni alloys in concentration bellow 100 mg $kg^{-1}$ and therefore, not detected using SEM-EDS.

### Concentration of DDTP

The complexing agent concentration must be enough to compensate for any reagent consumption by other elements that can compete with the analytes. Furthermore, complexing agents with lower partition coefficients must be present is large excess for efficient analytes complexation and subsequent separation.[26]

In this study, the DDTP concentrations evaluated, ranged from 0 to 2% (m $v^{-1}$) for As and Pb, 0 to 3% (m $v^{-1}$) for Cd, and from 0 to 0.3% (m $v^{-1}$) for Se. Figure 3 shows how the As, Cd, Pb, and Se absorbances changed as a function of the logarithm of the DDTP concentration. The As signal increased with the DDTP concentration increase up to 0.5% (m $v^{-1}$) of DDTP. After that, the As signal decreased gradually because charged complexes were produced at higher DDTP concentrations. This phenomenon can reduce the extraction efficiency because uncharged complexes are preferentially extracted in the hydrophobic core of the micelles.[16,26] Furthermore, according to Fiorentini et al., the excess of DDTP reduces the As absorbance, which can be attributed to the increase in the organic content injected in the atomizer.[27] For 0.5% (m $v^{-1}$) DDTP the highest absorbance of As was observed.

The Cd absorbance increased up to 1% (m $v^{-1}$) of DDTP. It stabilized around 0.3% (m $v^{-1}$) of DDTP, increased slightly up to 1% (m $v^{-1}$) of DDTP, and then decreased. The Pb absorbance also increased with the DDTP concentration increase up to 1% (m $v^{-1}$) DDTP. Regarding to Se, its absorbance was slightly affected by the DDTP concentration whereas the highest absorbance was observed for 0.06% (m $v^{-1}$) DDTP. Thus, considering the highest absorbance observed, the DDTP concentration in the later experiments was 0.5% (m $v^{-1}$) for As, 1% (m $v^{-1}$) for Cd and Pb, and 0.06% for Se.
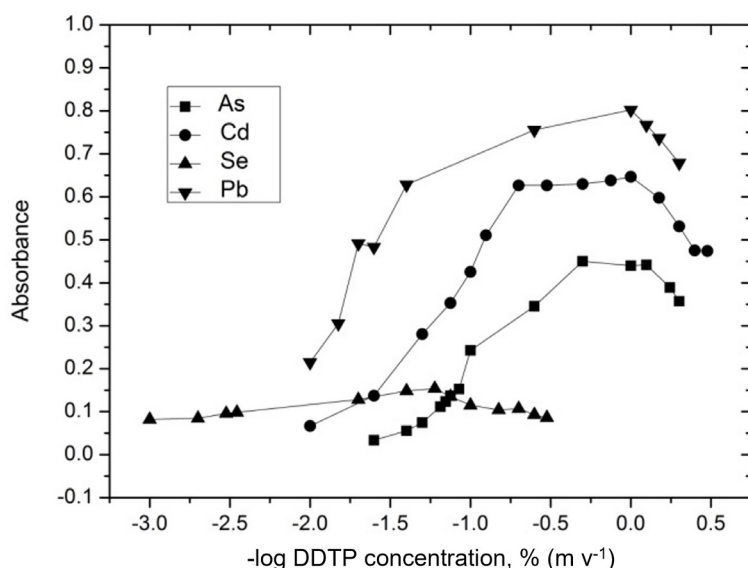


**Figure 3.** Effect of DDTP concentration on 50 µg $L^{-1}$ As(III), 1 µg $L^{-1}$ Cd(II), 20 µg $L^{-1}$ Pb(II), and 10 µg $L^{-1}$ Se(IV) in the following conditions: As - 0.96 mol $L^{-1}$ HCl, 0.5% (m $v^{-1}$) Triton X-114; Cd - 0.3 mol $L^{-1}$ HCl, 1% (m $v^{-1}$) Triton X-114; Pb - 0.32 mol $L^{-1}$ HCl, 1% (m $v^{-1}$) Triton X-114; Se - 0.1 mol $L^{-1}$ HCl, 0.2% (m $v^{-1}$) Triton X-114. (n = 3).

The differences observed in Figure 3 are due to the affinity of the elements with the DDTP affinities, according to Pearson's theory, which will be discussed further in section "Determination of the ratio DDTP: analysis in the complex".

### Concentration of HCl

Optimizing the pH is also crucial for CPE, especially for ionizable species such as metals. An appropriate pH range is mandatory in which uncharged analyte species exist and can be incorporated into micelles, allowing a quantitative extraction of the analyte.[28]

The cloud point increases with the solution pH decrease because the attractive forces between the surfactants and the water molecules increase. Consequently, surfactant molecules become more repulsive, leading to lower extraction efficiency and a smaller volume of the surfactant-rich phase. In addition, high acid concentration and temperature can accelerate DDTP decomposition,[29] mainly if $HNO_3$ is used, as it is a strong oxidant.

In the present study HCl concentrations ranging from 0 to 1 mol $L^{-1}$ HCl for As, Cd, and Se and from 0 to 0.75 mol $L^{-1}$ HCl for Pb were evaluated to find the best conditions for CPE. Figure 4 illustrates how the HCl concentration affected the As, Cd, Pb, and Se absorbances. The As absorbance increased when the HCl concentration was up 0.32 mol $L^{-1}$ HCl, but remained constant for HCl concentrations above 0.32 mol $L^{-1}$ (pH = 0.49). The Cd absorbance remained constant for 0.1 to 0.2 mol $L^{-1}$ HCl, increased slightly for 0.32 mol $L^{-1}$ HCl and stabilized afterward. Hence, 0.32 mol $L^{-1}$ HCl was used in subsequent experiments for Cd and As. The more appropriate HCl concentration for the Pb CPE was 0.1 mol $L^{-1}$ (pH = 1), considering that it corresponded to the highest absorbance for of Pb. The maximum Se absorbance was observed using 0.1 mol $L^{-1}$ HCl. Therefore, 0.1 mol $L^{-1}$ HCl was used for Cd and Ob in further experiments.
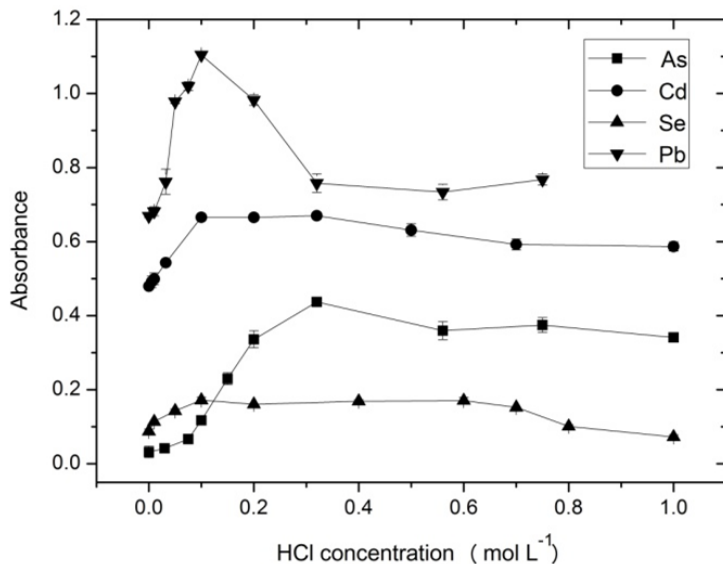


**Figure 4.** Effect of HCl concentration on 50 µg $L^{-1}$ As(III), 1 µg $L^{-1}$ Cd(II), 20 µg $L^{-1}$ Pb(II), and 10 µg $L^{-1}$ Se(IV) in the following conditions: As - 0.5% (m v$^{-1}$) DDTP, 0.5% (m v$^{-1}$) Triton X-114; Cd and Pb - 1% (m v$^{-1}$) DDTP, 1% (m v$^{-1}$) Triton X-114; Se - 0.06% (m v$^{-1}$) DDTP; 0.2% (m v$^{-1}$) Triton X-114. (n = 3).

### Triton X-114 concentration

An effective CPE also depends on the surfactant concentration. The, surfactants molecules can aggregate above the CMC and form micelles where the complexed analyte is retained. The analyte extraction from solution increases with the increasing surfactant concentration up to a maximum value,

providing quantitative analyte recovery. If the surfactant concentration is too high both the extraction and preconcentration factor are worsened; excess of surfactant increases the volume of the surfactant rich phase that became too diluted.[30]

On the other hand, if the surfactant concentration is lower than the necessary it results in inefficient extraction analyte, probably because the micelles cannot capture the hydrophobic complexes quantitatively.[20] In this study, the surfactant Triton X-114 was employed because it has a relatively low CPE temperature (between 22 and 25 °C), is low cost and is not volatile or toxic.[9]

The Triton X-114 concentration influence on the analytes absorbances is depicted in Figure 5. Triton X-114 at 1% (m v$^{-1}$) yield the highest As absorbance As, and this concentration was selected for As. For Triton X-114 concentrations below 0.05% (m v$^{-1}$), a surfactant-rich phase was not obtained; i.e., the critical micelle concentration (CMC) and/or cloud point were not attained under the experiment conditions. Concerning Cd, the volume of the surfactant-rich phase obtained at higher Triton X-114 concentrations was visible. The absorbance increased until the surfactant concentration was 0.5% (m v$^{-1}$) decreasing thereafter, and the same condition was observed for Pb. Therefore, 0.5% (m v$^{-1}$) Triton X-114 was further employed for Cd and Pb experiments. The same concentration of Triton X-114 (0.6%) was also used in the determination of Cd in food, by to Anzum et al.[31] On the other hand, Rihana-Abdallah employed a lower Triton X-114 concentration (0.2%) in Pb and Cd determination in water samples using CPE.[32] Regarding to Se, the highest absorbance was observed when the Triton X-114 concentration was 0.1% (m v$^{-1}$). For surfactant concentrations lower than 0.025% (m v$^{-1}$) solution turbidity and phase separation were not observed. As such, 0.1% (m v$^{-1}$) Triton X-114 was adopted for Se.
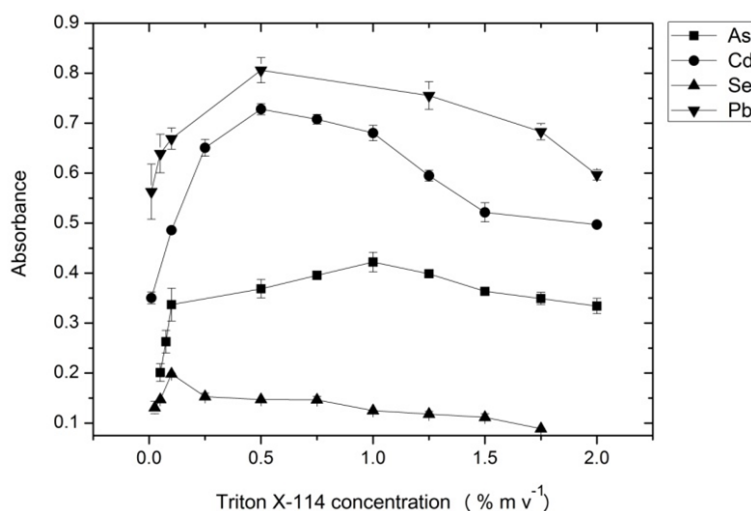


**Figure 5.** Effect of Triton X-114 concentration on 50 µg L$^{-1}$ As$^{3+}$, 1 µg L$^{-1}$ Cd$^{2+}$, 20 µg L$^{-1}$ Pb$^{2+}$ and 10 µg L$^{-1}$ Se$^{4+}$ in the following conditions: As - 0.5% (m v$^{-1}$) DDTP, 0.32 mol L$^{-1}$ HCl; Cd - 1% (m v$^{-1}$) DDTP, 0.32 mol L$^{-1}$ HCl; Pb - 1% (m v$^{-1}$) DDTP, 0.1 mol L$^{-1}$ HCl; Se - 0.06% (m v$^{-1}$) DDTP, 0.1 mol L$^{-1}$ HCl.

Considering the stability of DDTP in strong acid medium,[16] a study was conducted to determine the appropriate medium for the analyte complexation and subsequent CPE; 0.96 mol L$^{-1}$ HCl or HNO$_3$ (pH = 0.018), 0.3 mol L$^{-1}$ HCl or HNO$_3$ (pH = 0.5) and 0.32 mol L$^{-1}$ HCl or HNO$_3$ (pH = 0.49) were used for As, Cd, and Pb, respectively. It was observed that the absorbances of the analytes were not affected by the type and acid concentration. However, considering the oxidant property of HNO$_3$, which can react with the DDTP and degrade it,[33] HCl (0.1 mol L$^{-1}$ for Pb and Se, and 0.32 mol L$^{-1}$ for As and Cd) was the acid adopted for CPE of As, Cd and Pb. For Se, the effect of HCl concentration was not evaluated, since Se (VI) must be reduced to Se (IV) because DDTP complex only with Se (IV). To this end, before the CPE

procedure the Se(VI) solution in 6 mol L$^{-1}$ HCl was heated at 100 °C[34] for 30 min. This step is crucial to guarantee that all Se is present as Se(IV) since only this Se species complexes with DDTP.[17]

To verify whether the type of diluent for the surfactant-rich phase could influence the analyte signal, methanol, ethanol, and methanol or ethanol acidified with 0.1 mol L$^{-1}$ HNO$_3$ were evaluated. Differences for As, Cd, Pb, and Se absorbances were not observed for the diluents evaluated. However, considering that methanol is volatile and adding HNO$_3$ favors its stabilization via hydrogen bonding, methanol with 0.1 mol L$^{-1}$ HNO$_3$ was chosen as diluent of the surfactant-rich phase for the four analytes.

The complex formation rate is worth considering in the case of species separation by CPE. Complexation time is a critical parameter for on-line procedures as it requires the reaction to be as complete as possible in a short time for efficient extraction. The complexation time between the analytes and DDTP was evaluated and there were no significant differences for time periods up to 60 min. Hence, the previously adopted time of 20 min was maintained. The optimized conditions of CPE are summarized in Table I.

**Table I.** Optimized conditions for CPE

| Parameter | As | Cd | Pb | Se |
|---|---|---|---|---|
| DDTP (% m v$^{-1}$) | 0.5 | 1 | 1 | 0.06 |
| HCl (mol L$^{-1}$) | 0.32 | 0.32 | 0.1 | 0.1 |
| Triton X-114 (% m v$^{-1}$) | 1 | 0.5 | 0.5 | 0.1 |
| Time (min) | 20 | 20 | 20 | 20 |
| Diluent | Methanol in HNO$_3$ | Methanol in HNO$_3$ | Methanol in HNO$_3$ | Methanol in HNO$_3$ |

### *Determination of the ratio DDTP: analysis in the complex*

Da Silva et al.[29] have developed a mathematical approach based on the absorbance values in the graph constructed for the optimized DDTP concentration, to determine the ratio between the ligand and the analyte in the complex formed in a study dealing with CPE.

The distribution ratio (D) is the ratio between the complex analyte concentration in the surfactant-rich phase and the analyte concentration in the aqueous phase. This parameter is essential for CPE because the more hydrophobic the surfactant, the greater the D value. In this study, D values were calculated from normalized absorbance values obtained from the DDTP concentration optimization graph for As, Cd, Pb, and Se (Figure 3), according to Equation 1:

$$D = \frac{(A_C - A_0)}{(A_\infty - A_C)} \qquad \text{Equation 1}$$

A$_C$ is the analyte absorbance for a given DDTP concentration, A$_0$ is the absorbance when no ligand is used, and A$_\infty$ is the absorbance for the maximum extraction. Under the conditions used in this study, the free ligand concentration was assumed to be approximately equal to the total ligand concentration.

Values of D calculated with Equation 1 were employed to obtain Equation 2, where n is the charge of the analyte ion in the complex, Kp', βn', and [HL] are the conditional distribution constant, total formation constant, and the free ligand concentration, respectively.

$$\log D = \log\left(K'_p \beta'_n\right) + n\log[HL] \qquad \text{Equation 2}$$

Considering that the pH is constant, the charge (n) of the analyte ion in the complex can be found using Equation 3.

$$n = \left( \frac{\partial \log D}{\partial \log[HL]} \right)_{pH} \qquad\qquad \text{Equation 3}$$

The value of n also can be found by plotting of the logarithm of D (log D) versus the logarithm of free ligand concentration (log [DDTP]) for As, Cd, Pb, and Se gives straight lines, and the angular coefficient provides information on the ligand/analyte proportion in the complex formed (which is the value of n), according to Figure 6. The absorbance values taken from linear regions of the graphs shown in Figure 3; 0 to 0.1, 0 to 0.125, 0 to 0.04 and 0 to 0.0035% (m $v^{-1}$) for As, Cd, Pb, and Se, respectively.
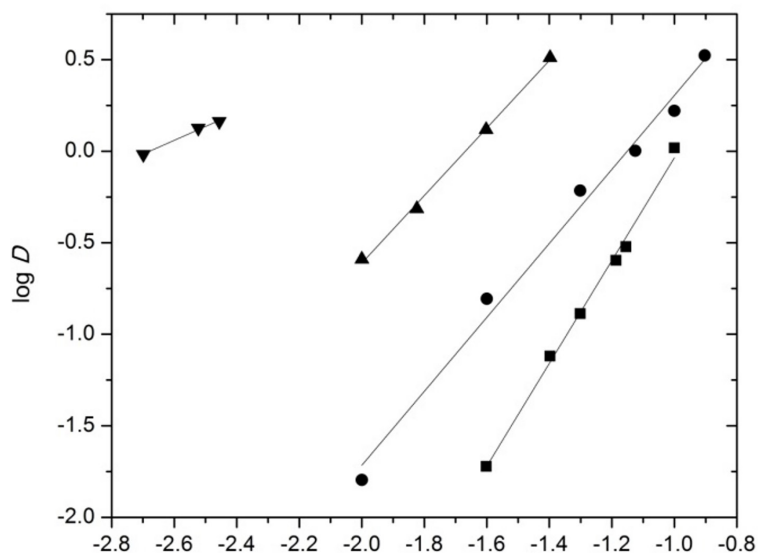


**Figure 6.** Determination of the proportion between DDTP and As ( ■ ), Cd ( ● ), Pb ( ▲ ), and Se ( ▼ ).

For As, the angular coefficient of the line shown in Figure 6 was 2.81, which indicates a 3:1 ratio DDTP:analyte. This ratio value had not yet been reported for As complexed with DDTP. The logarithm of the product of conditional constants $K_p$ (distribution constant) and $\beta_n$ (total formation constant) $\left( \log K_p'\beta_n' \right)$ obtained from equation 2 was 2.77.

The angular coefficient values of the lines (Figure 6) for Cd and Pb were 2.02 and 1.84, respectively, corresponding to a 2:1 ratio DDTP:analyte. This is consistent with the value reported by Borges et al.[20] The logarithm values of the product of conditional constants $\left( \log K_p'\beta_n' \right)$ for Cd and Pb were 2.35 and 3.08, respectively. Regarding Se, the angular coefficient of the line in from the graph of Figure 6 was 0.8, which indicates a 1:1 ratio DDTP:analyte. The pH of the medium was 1.0 where the predominant species of Se are monovalent dimers.[35] Moreover, the logarithm of the product of conditional constants $\left( \log K_p'\beta_n' \right)$ was equal to 2.02.

According to the Pearson acid base concept, DDTP is a soft base and forms complexes preferentially with soft ($Cd^{2+}$) and borderline acids ($Pb^{2+}$). $Se^{4+}$ and $As^{3+}$ are defined as hard acids[30] and also complex with DDTP, however, as calculated, the conditional constants are lower than for Pb. Considering that the product of the conditional constants $\left( \log K_p'\beta_n' \right)$ indicates the extent of the reaction between the analytes and DDTP is:

2.02 (Se) < 2.35 (Cd) < 2.77 (As) < 3.08 (Pb)

It demonstrates that the distribution of the species between the aqueous and the surfactant-rich phases is influenced not only by the complexation with DDTP but also by the oxyethylene units in the Triton X-114 molecule.

## Pyrolysis and atomization curves

The pyrolysis and atomization temperatures were optimized by constructing pyrolysis and atomization curves for As, Cd, Pb, and Se (Figure 7). Experiments were conducted using reference solutions of the respective analytes and solutions of acid digested Inconel 624 sample to evaluate matrix effect. All solutions were submitted to CPE at the optimized conditions.
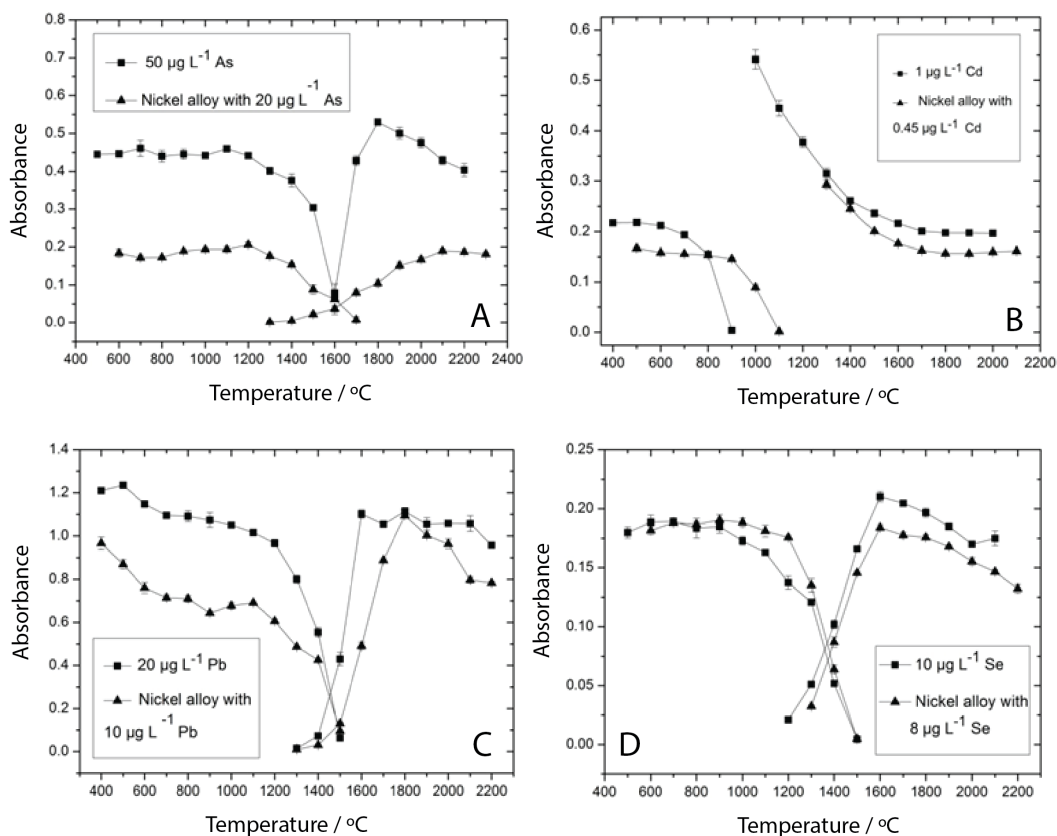


**Figure 7.** Pyrolysis and atomization temperature curves for (A) 50 µg L$^{-1}$ As and nickel alloy sample solution spiked with 20 µg L$^{-1}$ As. Conditions: 0.5% (m v$^{-1}$) DDTP, 0.32 mol L$^{-1}$ HCl, 1% (m v$^{-1}$) Triton X-114; (B) 1 µg L$^{-1}$ Cd and nickel alloy sample spiked with 0.45 µg L$^{-1}$ Cd. Conditions: 1% (m v$^{-1}$) DDTP, 0.32 mol L$^{-1}$ HCl, 0.5% (m v$^{-1}$) Triton X-114; (C) 20 µg L$^{-1}$ Pb and nickel alloy sample spiked with 10 µg L$^{-1}$ Pb. Conditions: 1% (m v$^{-1}$) DDTP, 0.1 mol L$^{-1}$ HCl, 0.5% (m v$^{-1}$) Triton X-114; and (D) 10 µg L$^{-1}$ Se and nickel alloy sample spiked with 8 µg L$^{-1}$ Se. Conditions: 0.06% (m v$^{-1}$) DDTP, 0.1 mol L$^{-1}$ HCl, 0.1% (m v$^{-1}$) Triton X-114. All solutions were submitted to CPE.

Figure 7A depicts the pyrolysis and atomization curves obtained, in both solutions the element absorbance was almost stable up to 1200 ºC and then decreased. Therefore, this pyrolysis temperature was adopted in As determination in the samples. Regarding the atomization temperature, more symmetrical and stable peak arose at 2000 °C for As in reference solution, and although the absorbance increased at temperature higher than 2200 ºC for spiked sample, to avoid compromising accuracy, the temperature adopted for As determination in the samples was 2000 ºC.

As shown in Figure 7B, the Cd absorbance for reference solution remains almost stable for temperature in the range of 400 to 700 ºC while the absorbance for spiked sample solution remains stable up to 900 ºC. On the other hand, a similar behavior on the Cd absorbance is observed for both solutions in respect to the atomization temperature. Thus, the pyrolysis and atomization temperatures used for Cd determination in the samples were 700 and 1300 ºC, respectively.

The pyrolysis and atomization temperatures curves for Pb in Figure 7C demonstrate similar absorbance behavior for both solutions. The pyrolysis and atomization temperatures chosen for Pb were 900 and 1900 °C. They were chosen in view of the better shape of transient signals observed.

Concerning Se, whose pyrolysis and atomization temperature curves are shown in Figure 7D, similar absorbance is observed for both solutions. Thus, taking into account the highest observed absorbance and signal stability, the pyrolysis and atomization temperatures chosen for Se in the analysis of the samples were 900 and 1600 °C, respectively.

### Figures of merit of the method

Table II lists the figures of merit of the developed method for As, Cd, Pb, and Se determination in Ni alloy and parameters of calibration curves.

**Table II.** Figures of merit and parameters of calibration curves

| Analytical parameter | Analyte | | | |
|---|---|---|---|---|
| | As | Cd | Pb | Se |
| Limit of detection ($\mu g\ L^{-1}$; $\mu g\ g^{-1}$) | 0.8; 1.5 | 0.01; 0.06 | 0.2; 0.3 | 0.1; 0.3 |
| Limit of quantification ($\mu g\ L^{-1}$; $\mu g\ g^{-1}$) | 2.8; 5.0 | 0.04; 0.2 | 0.6; 1.0 | 0.5; 0.9 |
| Linear correlation coefficient | 0.996 | 0.998 | 0.999 | 0.997 |
| Relative standard deviation[a] (%) | 4 | 3 | 2.5 | 3.4 |
| Enrichment factor | 6 | 8 | 14 | 13 |
| Concentration range of calibration curve ($\mu g\ L^{-1}$) | 10-50 | 0.15-1.2 | 5-20 | 2-15 |

a: n = 5 (50 $\mu g\ L^{-1}$ $As^{3+}$; 1 $\mu g\ L^{-1}$ $Cd^{2+}$; 20 $\mu g\ L^{-1}$ $Pb^{2+}$; 8 $\mu g\ L^{-1}$ $Se^{4+}$)

The limits of detection and quantification were calculated according to IUPAC recommendations by means of Equations 4 and 5.[36]

$$\text{Limit of detection (LOD)} = \frac{3s}{m} \qquad \text{Equation 4}$$

$$\text{Limit of quantification (LOQ)} = \frac{10s}{m} \qquad \text{Equation 5}$$

in which $s$ is the standard deviation of ten consecutive measurements of the analytical blank and $m$ is the slope of the calibration curve.

The LOD and LOQ values in $\mu g\ L^{-1}$ and $\mu g\ g^{-1}$ in Table I correspond to instrumental limits (in $\mu g\ L^{-1}$) LODs and LOQs, method limits (in $\mu g\ L^{-1}$) considering the Inconel 625 sample mass (2.5 g), the digestate diluted to 30 mL, dilution of 200 times for CPE, and respective enrichment factor. Low limits of detection and quantification were achieved, particularly for Cd, demonstrating appropriate sensitivity concerning As, Cd, Pb, and Se determination in Ni alloy.

The maximum specification limits for the analytes in nickel alloys are 50 $\mu g\ L^{-1}$ (As and 495 Cd), 2 $\mu g\ L^{-1}$ (Pb), and 1 $\mu g\ L^{-1}$ (Se) according to AMS 2280. Thus, the LOQs obtained (Table I) comply with the legislation. The obtained linear correlation coefficients values were higher than 0.995, which is highly acceptable for the CPE method. The relative standard deviation, which express the method precision, was below 5% which is acceptable.

The enrichment factor values were considered satisfactory. They were obtained from the ratio of the slopes of the calibration curves constructed with calibration solutions submitted or not to CPE for the respective analytes. When CPE was not used the calibration solutions were matched to the final surfactant-rich phase (matrix-matched calibration curve); containing Triton X-114, and methanol mixed with 0.1 mol L$^{-1}$ HNO$_3$.

### Sample analysis

The As, Cd, Pb, and Se concentrations found in the Inconel 625 nickel alloy sample and standard reference materials analyzed by following the developed method are given in Table III.

**Table III.** Arsenic, Cd, Pb, and Se determination in the nickel alloy sample (Inconel 625) and standard reference materials (CRMs) (n = 3)

| Analyte | | Sample | | | | |
|---|---|---|---|---|---|---|
| | | Inconel 625 | SRM® 361 (AISI 4340 Steel) | SRM® 362 (AISI 94B17 Steel) | SRM® 363 (Chromium-Vanadium Steel) | SRM® 864 (Nickel alloy UNS N06600) |
| **As** | Certified (µg g$^{-1}$) | - | 170 ± 10 | 920 ± 5 | 100 ± 10 | - |
| | Found (µg g$^{-1}$) | < LD | 173 ± 9 | 904 ± 11 | 94 ± 5 | < LD |
| | Added (µg L$^{-1}$) | 20 | - | - | - | 20 |
| | Obtained (µg L$^{-1}$) | 18.6 ± (0.5) | - | - | - | 19.9 ± (0.3) |
| **Cd** | Certified (µg g$^{-1}$) | - | - | - | - | - |
| | Found (µg g$^{-1}$) | < LD | < LD | < LD | < LD | < LD |
| | Added (µg L$^{-1}$) | 0.45 | 0.45 | 0.45 | 0.45 | 0.45 |
| | Obtained (µg L$^{-1}$) | 0.45 ± (0.01) | 0.46 ± (0.01) | 0.42 ± (0.03) | 0.47 ± (0.01) | 0.44 ± (0.02) |
| **Pb** | Certified (µg g$^{-1}$) | - | - | - | - | - |
| | Found (µg g$^{-1}$) | < LD | < LD | < LD | < LD | < LD |
| | Added (µg L$^{-1}$) | 10 | 10 | 10 | 10 | 10 |
| | Obtained (µg L$^{-1}$) | 9.1 ± (0.6) | 9.5 ± (0.3) | 9.4 ± (0.3) | 9.8 ± (0.4) | 9.7 ± (0.3) |
| **Se** | Certified (µg g$^{-1}$) | - | - | - | - | - |
| | Found (µg g$^{-1}$) | < LD | < LD | < LD | < LD | < LD |
| | Added (µg L$^{-1}$) | 8 | 8 | 8 | 8 | 8 |
| | Obtained (µg L$^{-1}$) | 8.1 ± (0.6) | 8.2 ± (0.3) | 7.6 ± (0.07) | 7.0 ± (0.2) | 7.7 ± (0.3) |

Considering that Inconel 625 contains Ni (65.5%) and Fe (1.1%) capable of forming complexes with DDTP, the interference of these elements on As, Cd, Pb, and Se extraction was investigated. According to Pearson's theory, DDTP is a soft base and tends to interact preferentially with soft acids or intermediated acids such as Cd$^{2+}$, Ni$^{2+}$, or Ag$^+$; and besides this, Ni also interferes in CPE due to the high ionic strength.[17] Citric acid helped to eliminate the interference of Ni because it has a masking effect on this element.[37] Ascorbic acid aided the elimination of Fe because Fe$^{3+}$ reacts with DDTP, consuming the complexing agent and forming a black precipitate. Upon reaction with ascorbic acid, Fe$^{3+}$ was reduced to Fe$^{2+}$, which does

not form a complex with DDTP.[29] Moreover, because both reagents have an acid character, experiments were conducted with and without pH adjustment with HCl.

Arsenic, Cd, Pb, and Se were not detected in the analytical samples, with the exception of As in three CRMs. For this reason, analyte spiking was carried out to assess the method's accuracy. Better analyte recovery was obtained by adding ascorbic acid and HCl to the sample solutions whereas non reproducible results were obtained using citric acid only. The analytes recovery in Inconel samples ranged from 91 to 101% when acid ascorbic and citric acid were used.

For the CRMs SRM® 361, SRM® 362, and SRM® 363, an unpaired t-test of As results showed thar they agreed with certified values, and no differences were found for a 95% confidence level and recovery ranged from 88 to 104%.

## CONCLUSIONS

This study demonstrated the efficiency of CPE for matrix separation/analyte extraction of As, Cd, Pb, and Se in nickel alloy samples. Among the variables investigated for CPE optimization, DDTP, HCl, and Triton X-114 concentrations were the most meaningful.

The SEM-EDS characterization of the samples identified Fe, Ni and Cr as the major elements and due to the possible interference of $Fe^{3+}$ in CPE, ascorbic acid was added to reduce $Fe^{3+}$ species to $Fe^{2+}$ which does not complex with DDTP. Due to the low concentration of As, Cd, Pb, and Se in Inconel samples (lower than limit of detection), their determination was not possible.

Therefore, the Inconel samples and standard reference materials were spiked with known concentrations of analytes to assesses their recovery which presented satisfactory results (88 – 104%) demonstrating that the method is adequate for As, Cd, Pb, and Se determination.

### Conflicts of interest

There are no conflicts to declare.

### Acknowledgements

### REFERENCES

(1) Shao, X.; Liu, Y.; Li, F.; Wu, J. Progress in analytical methods of composition in nickel-base alloy pipes, ICPTT 2011: Sustainable solutions for water, sewer, gas, and oil pipelines - Proceedings of the International Conference on Pipelines and Trenchless Technology **2011**. https://doi.org/10.1061/41202(423)113

(2) Ashino, T.; Takada, K. Determination of trace amounts of selenium and tellurium in nickel-based heat-resisting superalloys, steels and several metals by electrothermal atomic absorption spectrometry after reductive coprecipitation with palladium using ascorbic acid. *Anal. Chim. Acta*. **1995**, *312*, 157-163. https://doi.org/10.1016/0003-2670(95)00215-L

(3) Wiltsche, H.; Prattes, K.; Knapp, G. A novel approach for an automated liquid/liquid extraction system - principle and application for the determination of several trace contaminants in highly alloyed steels and base alloys. *Anal. Bioanal. Chem*. **2011**, *400*, 2329-2338. https://doi.org/10.1007/s00216-011-4666-3

(4) Shekhar, R.; Arunachalam, J.; Das, N.; Murthy, A. M. S. Determination of Cu, Zn, As, Cd, In, Sn, Pb, and Bi in nickel-based superalloys after multi-matrix separation. *At. Spectrosc*. **2005**, *26*, 191-196. https://doi.org/10.46770/AS.2005.05.005

(5) Weipeng, L.; Zhishan, M.; Sixiao, Q.; Lei, G.; Jianying, H.; Liqiu, G.; Lijie, Q. CS-AFM study on Pb-induced degradation of passive film on nickel-based alloy in high temperature and high pressure water. *Corros. Sci*. **2018**, *144*, 249-257. https://doi.org/10.1016/j.corsci.2018.08.054

(6) SAE Aerospace Material Specification AMS-2280D. *Trace Element Control - Nickel Alloy Castings*, **1992**. Available at: https://www.sae.org/standards/content/ams2280d/ (Accessed: 07/2023).

(7) Wiltsche, H.; Günther, D. Capabilities of femtosecond laser ablation ICP-MS for the major, minor, and trace element analysis of high alloyed steels and super alloys. *Anal. Bioanal. Chem*. **2011**, *399*, 2167-2174. https://doi.org/10.1007/s00216-010-4605-8

(8) Sahin, Ç. A.; Efeçinar, M.; Satiroglu, N. Combination of cloud point extraction and flame atomic absorption spectrometry for preconcentration and determination of nickel and manganese ions in water and food samples. *J. Hazard. Mater*. **2010**, *176*, 672-677. https://doi.org/10.1016/j.jhazmat.2009.11.084

(9) Bader, N. R.; Edbey, K.; Telgheder, U. Cloud point extraction as a sample preparation technique for trace element analysis: an overview. *J. Chem. Pharm. Res*. **2014**, *6*, 496-501.

(10) Ojeda, C. B.; Rojas, F. S. Separation and preconcentration by cloud point extraction procedures for determination of ions: recent trends and applications. *Microchim. Acta*. **2012**, *177*, 1-21. https://doi.org/10.1007/s00604-011-0717-x

(11) Di Giacomo, M.; Bertoni, F. A.; Rocha, M. V.; Nerli, B. B.; Rodríguez, F. Cloud point extraction based on non-ionic surfactants: An ecofriendly tool for recovering papain from papaya latex. *J. Environ. Chem. Eng*. **2022**, *10*, 108762. https://doi.org/10.1016/j.jece.2022.108762

(12) Temel, N. K.; Çöpür, M. Determination of Trace Cobalt (II) in Spices Samples by Ultrasonic Assisted Cloud Point Extraction with Spectrophotometry. *J. Mol. Struct*. **2023**, *1284*, 135433. https://doi.org/10.1016/j.molstruc.2023.135433

(13) Llaver, M.; Wuilloud, R. G. Studying the effect of an ionic liquid on cloud point extraction technique for highly efficient preconcentration and speciation analysis of tellurium in water, soil and sediment samples. *Talanta* **2020,** *212*, 120802. https://doi.org/10.1016/j.talanta.2020.120802

(14) Silva, S. G.; Oliveira, P. V.; Rocha, F. R. P. A green analytical procedure for determination of copper and iron in plant materials after cloud point extraction. *J. Braz. Chem. Soc*. **2010**, *21*, 234-239. https://doi.org/10.1590/S0103-50532010000200007

(15) Sorouraddin, S. M.; Farajzadeh, A. M.; Okhravi, T. A green solventless temperature-assisted homogeneous liquid–liquid microextraction method based on 8-hydroxyquinoline simultaneously as complexing agent and extractant for preconcentration of cobalt and nickel from water and fruit juice samples. *Int. J. Environ. Anal. Chem*. **2019**, *99*, 124-138. https://doi.org/10.1080/03067319.2019.1578351

(16) Pytlakowska, K.; Kozik, V.; Dabioch, M. Complex-forming organic ligands in cloud-point extraction of metal ions: A review. *Talanta* **2013**, *110*, 202-228. https://doi.org/10.1016/j.talanta.2013.02.037

(17) Ramos, J. C.; Curtius, A. J.; Borges, D. L. G. Diethyldithiophosphate (DDTP): A review on properties, general applications, and use in analytical spectrometry. *Appl. Spectrosc. Rev*. **2012**, *47*, 583-619. https://doi.org/10.1080/05704928.2012.682286

(18) Castor, J. M. R.; Portugal, L.; Ferrer, L.; Hinojosa-Reyes, L.; Guzmán-Mar J. L.; Hernández-Ramírez, A.; Cerdà, V. An evaluation of the bioaccessibility of arsenic in corn and rice samples based on cloud point extraction and hydride generation coupled to atomic fluorescence spectrometry. *Food Chem*. **2016**, *204*, 475-482. https://doi.org/10.1016/j.foodchem.2016.02.149

(19) Maranhão, T. A.; Martendal, E.; Borges, D. L. G.; Carasek, E.; Welz, B.; Curtius, A. J. Cloud point extraction for the determination of lead and cadmium in urine by graphite furnace atomic absorption spectrometry with multivariate optimization using Box-Behnken design. *Spectrochim. Acta, Part B* **2007**, *62*, 1019-1027. https://doi.org/10.1016/j.sab.2007.05.008

(20) Borges, D. L. G.; Veiga, M. A. M. S.; Frescura, V. L. A.; Welz, B.; Curtius, A. J. Cloud-point extraction for the determination of Cd, Pb and Pd in blood by electrothermal atomic absorption spectrometry, using Ir or Ru as permanent modifiers. *J. Anal. At. Spectrom*. **2003**, *18*, 501-507. https://doi.org/10.1039/B209680C

(21) Depoi, F. S.; Oliveira, T. C.; Moraes, D. P.; Pozebon, D. Preconcentration and determination of As, Cd, Pb and Bi using different sample introduction systems, cloud point extraction and inductively coupled plasma optical emission spectrometry. *Anal. Methods* **2012**, *4*, 89-95. https://doi.org/10.1039/C1AY05246B

(22) Kassem, M. A.; Amin, A. S. Determination of rhodium in metallic alloy and water samples using cloud point extraction coupled with spectrophotometric technique. *Spectrochim. Acta Part A* **2015**, *136*, 1955-1961. https://doi.org/10.1016/j.saa.2014.10.116

(23) Stefanova-Bahchevanska, T.; Milcheva, N.; Zaruba, S.; Andruch, V.; Delchev, V.; Simitchiev, K.; Gavazov, K. A green cloud-point extraction-chromogenic system for vanadium determination. *J. Mol. Liq.* **2017**, *248*, 135-142. https://doi.org/10.1016/j.molliq.2017.10.046

(24) Bakkar, A.; Ahmed, M. M. Z.; Alsaleh, N. A.; Seleman, M. M. E.; Ataya, S. Microstructure, wear, and corrosion characterization of high TiC content Inconel 625 matrix composites. *Mater. Res. Technol*. **2019**, *8*, 1102-1110. https://doi.org/10.1016/j.jmrt.2018.09.001

(25) Borowski, T.; Brojanowska, A.; Kost, M.; Garbacz, H.; Wierzchoń, T. Modifying the properties of the Inconel 625 nickel alloy by glow discharge assisted nitriding, *Vacuum* **2009**, *83*, 1489-1493. https://doi.org/10.1016/j.vacuum.2009.06.056

(26) Stalikas, C. D. Micelle-mediated extraction as a tool for separation and preconcentration in metal analysis. *Trends Anal. Chem*. **2002**, *21*, 343-355. https://doi.org/10.1016/S0165-9936(02)00502-2

(27) Fiorentini, E. F.; Canizo, B. V.; Wuilloud, R. G. Determination of As in honey samples by magnetic ionic liquid-based dispersive liquid-liquid microextraction and electrothermal atomic absorption spectrometry. *Talanta* **2019**, *198*, 146-153. https://doi.org/10.1016/j.talanta.2019.01.091

(28) Mortada, W. I. Recent developments and applications of cloud point extraction: A critical review. *Microchem. J.* **2020**, *157*, 105055 https://doi.org/10.1016/j.microc.2020.105055

(29) Silva, M. A. M.; Frescura, V. L. A.; Aguilera, F. J. N.; Curtius, A. J. Determination of Ag and Au in geological samples by flame atomic absorption spectrometry after cloud point extraction. *J. Anal. At. Spectrom*. **1998**, *13*, 1369-1373. https://doi.org/10.1039/A806309E

(30) Mandal, S.; Lahiri, S. A review on extraction, preconcentration and speciation of metal ions by sustainable cloud point extraction. *Microchem. J.* **2022**, *175*, 107150. https://doi.org/10.1016/j.microc.2021.107150

(31) Anzum, R.; Alawamleh, H. S. K.; Bokov, D. O.; Jalil, A. T.; Hoi, H. T.; Abdelbasset W. K.; Thoi, N. T.; Widjaja, G.; Kurochkina, A. A review on separation and detection of copper, cadmium, and chromium in food based on cloud point extraction technology. *Food Sci. Technol*. **2022**, *42*, 1-7. https://doi.org/10.1590/fst.80721

(32) Rihana-Abdallah, A.; Li, Z.; Lanigan, K. C. Using Cloud Point Extraction for Preconcentration and Determination of Iron, Lead, and Cadmium in Drinking Water by Flame Atomic Absorption Spectrometry. *Anal. Lett*. **2022**, *55*, 1296–1305. https://doi.org/10.1080/00032719.2021.2002349

(33) Silva, M. A. M.; Frescura, V. L. A.; Curtius, A. J. Determination of trace elements in water samples by ultrasonic nebulization inductively coupled plasma mass spectrometry after cloud point extraction. *Spectrochim. Acta B* **2000**, *55*, 803-813.

(34) Smrkolj, P.; Stibilj, V. Determination of selenium in vegetables by hydride generation atomic fluorescence spectrometry. *Anal. Chim. Acta* **2004**, *512*, 11-17. https://doi.org/10.1016/j.aca.2004.02.033

(35) Kretzschmar, J.; Jordan, N.; Brendler, E.; Tsushima, S.; Franzen, C.; Foerstendorf, H.; Stockmann, M.; Heim, K.; Brendler, V. Spectroscopic evidence for selenium(IV) dimerization in aqueous solution, *Dalton Trans*. **2015**, 44, 10508-10515. https://doi.org/10.1039/C5DT00730E

(36)  Harris, D. C. *Quantitative Chemical Analysis*, 7th Edition, 2007, W. H. Freeman and Company New York.

(37)  Danadurai, K. S. K.; Hsu, Y.; Jiang, S. Determination of selenium in nickel-based alloys by flow injection hydride generation reaction cell inductively coupled plasma mass spectrometry. *J. Anal. At. Spectrom*. **2002**, *17*, 552-555. https://doi.org/10.1039/B202878F

# Supplementary Material

**Table SI.** Instrumental parameters for As, Cd, and Se determination after cloud point extraction using AAnalyst 800 (PerkinElmer)

| Parameter | Condition |
|---|---|
| Wavelength (nm) | 193.7[a], 228.8[b], 196.0[c] |
| Radiation source | Hollow cathode lamps of As, Cd, and Se |
| Electrical current (mA) | 18[a], 8[b], 25[c] |
| Slit (nm) | 0.7[a,b], 2[c] |
| Argon flow (mL min$^{-1}$) | 250 |
| Background correction | Longitudinal Zeeman Effect |

a = As; b = Cd; c = Se.

**Table SII.** Instrumental parameters for Pb determination after cloud point extraction using ContrAA 700 (Analytik Jena)

| Parameter | Condition |
|---|---|
| Wavelength (nm) | 283.3060 |
| Radiation source | Short-arc lamp of Xenon |
| Electrical current (A) | 13 |
| Argon flow (L min$^{-1}$) | 2 |
| Background correction | Simultaneous background correction |

**Table SIII.** Graphite furnace temperature program for As, Cd, and Se determination after cloud point extraction using AAnalyst 800 (PerkinElmer)

| Step | Temperature (°C) | Ramp (s) | Hold (s) | Ar flow rate (mL min$^{-1}$) |
|---|---|---|---|---|
| Drying | 110 | 1 | 30 | 250 |
| Drying | 130 | 15 | 30 | 250 |
| Pyrolysis | (800[a], 1200[b])[1]; (600[a], 500[b])[2]; (900[a,b])[3] | 10 | 20 | 250 |
| Atomization | (2000[a,b])[1]; (1700[a], 1300[b])[2]; (1900[a],1800[b])[3] | 0 | 5 | 0 |
| Cleaning | 2450 | 1 | 3 | 250 |

1 = As; 2 = Cd; 3 = Se; a = optimization of the CPE experimental parameters; b = after obtainment of the pyrolysis and atomization curves.

**Table SIV.** Graphite furnace temperature program for Pb determination after cloud point extraction using ContrAA 700 (Analytik Jena)

| Step | Temperature (°C) | Ramp (°C s$^{-1}$) | Hold (s) | Air flow rate (L min$^{-1}$) |
|---|---|---|---|---|
| Drying | 90 | 3 | 20 | 2 |
| Drying | 110 | 5 | 10 | 2 |
| Pyrolysis | 900[a], 1000[b] | 300 | 10 | 2 |
| Atomization | 1900[a,b] | 3000 | 3 | 0 |
| Cleaning | 2450 | 500 | 4 | 2 |

a = optimization of the CPE experimental parameters; b = after obtainment of the pyrolysis and atomization curves.

# TECHNICAL NOTE

# Validation and Uncertainty Calculation of Rodenticide Analysis Methods in a Simulated Gastric Content Matrix – *Uncertainty of Rodenticide Analysis Methods*

**Flávio Augusto Ferreira Martins Bezerra** (ID), **Youssef Bacila Sade** (ID), **Jailton Carreteiro Damasceno** (ID), **Renata Carvalho Silva\*** (ID) ✉

*Instituto Nacional de Metrologia, Qualidade e Tecnologia (Inmetro), Avenida Nossa Senhora das Graças, 50, Duque de Caxias-Xerém, Postal code 20250-020, RJ, Brazil*
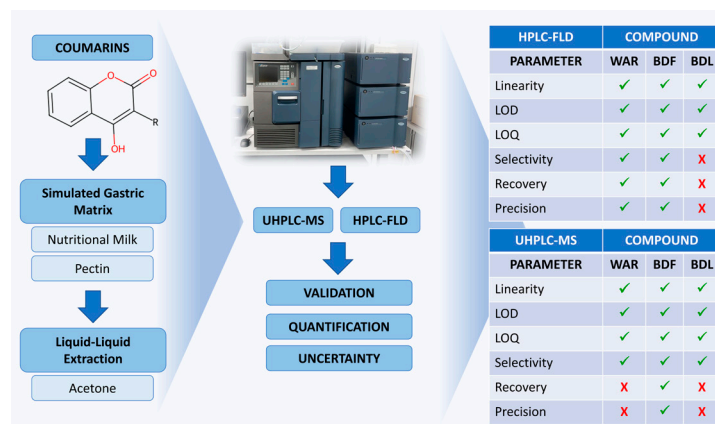
Warfarin (WAR), brodifacoum (BDF) and bromadiolone (BDL) are compounds present in rodenticides, highly toxic to rats, humans and other animals. These compounds can be detected in complex matrices, such as stomach contents, by liquid chromatography techniques (HPLC) with mass spectrometry (MS) or fluorescence detection (FLD). However, no validated method showed determination of uncertainty in the quantification of these compounds. In this study, we compare the validation parameters of two analytical methods, HPLC-FLD and ultra high performance liquid chromatography (UHPLC-MS), with uncertainty estimation for the three cited compounds. The results showed that UHPLC-MS outperformed HPLC-FLD, however both methods were considered adequate for detection of WAR, BDF or BDL in samples of simulated human stomach contents, especially in cases of suspected contamination.

**Keywords:** chromatography, complex matrix, coumarin, measurement uncertainty, quantification

## INTRODUCTION

Rodenticide poisoning is a common global health problem. The groups most affected by rodenticide poisoning in Brazil are children (accidental exposure) and adults (homicide and suicide attempts). Rodenticide poisoning typically occurs via ingestion of coumarin-derived anticoagulant rodenticides, such as warfarin (WAR - Structure A), brodifacoum (BDF - Structure B), bromadiolone (BDL - Structure C) (Figure 1), and indandione.[1] Coumarins are metabolic derivatives of phenylalanine comprising a benzene

ring attached to a pyran ring. They can be isolated from plants, fungi, and bacteria and have potent anticoagulant properties.[2]
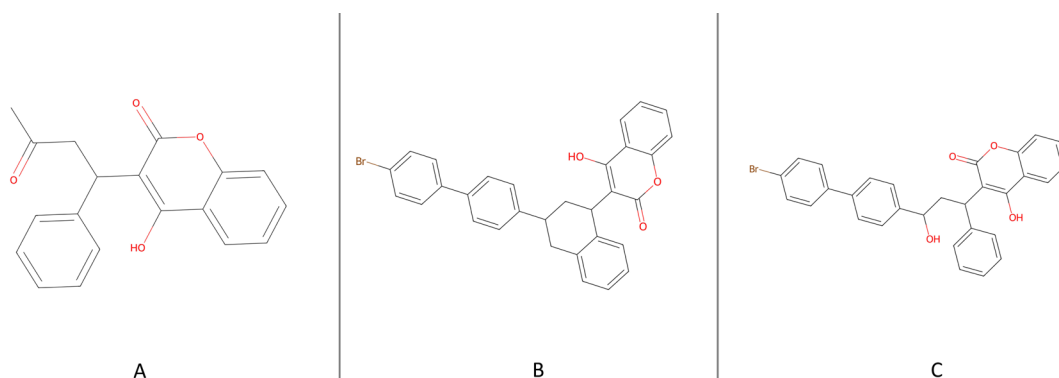


**Figure 1**. The structures of the coumarin compounds.

In Brazil, 25,892 cases of rodenticide poisoning were reported between 2017 and 2021, including 19,267 cases of attempted suicide, 4742 accidents, and 362 cases of attempted murder.[3] Biological samples can be collected and sent to forensic toxicology laboratories for analysis in cases of suspected rodenticide poisoning due to accidental ingestion or criminal intoxication.[4]

Rodenticides inhibit vitamin K epoxide reductase, causing active vitamin K deficiency, such that vitamin-K-dependent clotting factors are not activated and remain non-functional, causing massive bleeding. Coumarin rodenticides can be distributed in different tissues, and blood and liver are the primary matrices used in forensic analysis. Owing to the long half-life of coumarin rodenticides, blood and liver tissue samples are preferred for *ante-* and *post-mortem* analyses, because they contain the highest concentrations of active compounds.[1] However, in Brazil, stomach content samples have frequently been collected for the forensic analysis of coumarin compounds, and a validated method for the identification of coumarin compounds in animal stomach contents has recently been published.[5–7] However, the only validated methods for the analysis of coumarin rodenticides involve the use of other matrices such as blood and liver samples.[5–17]

The stomach content is a complex matrix; therefore, several researchers have used artificial media to mimic it. Simulated gastric fluids containing pepsin, small amounts of bile salts, lecithin, and synthetic surfactants have been widely used in in vitro drug dissolution studies. However, simulated gastric fluids cause numerous interferences during analysis and lead to overestimating the physiologically important conditions of the actual stomach content. Therefore, simulated gastric fluids have recently been replaced with media containing Ensure® Plus nutrition shake, which have been more efficient in simulating "fed stomachs" and have facilitated the analysis of different compounds.[18]

Liquid chromatography (LC) methods, such as high-performance liquid chromatography (HPLC) and ultra-high-performance liquid chromatography (UHPLC), and gas chromatography (GC) in conjunction with mass spectrometry (MS), ultraviolet (UV), and fluorescence detection (FLD), have been used for compound analysis. Although CG-MS and LC-UV are commonly used to analyse rodenticides in biological samples, the types of samples that can be analysed using these methods are limited. This is attributed to the detection limit of GC-MS being approximately 10 times higher than that of LC-MS. Conversely, methods based on UV detection have low sensitivity for rodenticide quantification, especially in the concentration range of 10–100 ng mL$^{-1}$.[1] Therefore, HPLC-FLD,[8–10] HPLC-MS,[11] and UHPLC-MS [7,12–17] are the most commonly used methods for analysing rodenticides in biological samples.[1] A crucial step prior to chromatographic analysis is sample preparation using methods such as liquid–liquid extraction or solid-phase extraction (SPE), which can be used to isolate, purify, and concentrate analytes.[1,5–17] Once the extraction and chromatography methods have been selected, they must be validated, if necessary.[19] Furthermore, it is critical to evaluate the measurement uncertainty of quantitative methods.

According to the International Vocabulary of Metrology, measurement uncertainty is a non-negative parameter that characterises the dispersion of values assigned to a measurement.[20] The ISO/IEC 17025 standard states that testing laboratories should evaluate the uncertainty of measurements. If the measurement uncertainty of a method cannot be accurately estimated, an estimate should be made based on a theoretical understanding of the method or practical experience of the method performance. Furthermore, uncertainty evaluation should consider the contributions that are significant to the measurement results.[21]

Validation and evaluation of the uncertainty of a method are critical for forensic toxicology laboratories that quantify rodenticides in gastric content matrices. Established procedures are inadequate for yielding reliable results because they do not have measurement uncertainty. Materials should be collected and extracted prior to analysis, and these steps should be reproducible and allow for satisfactory analyte recovery. Therefore, in this study, we optimised and compared the performance of HPLC-FLD and UHPLC-MS as methods for identifying rodenticidal coumarin compounds in simulated human stomach content samples. Furthermore, we determined the factors that contributed to measurement uncertainty.

## MATERIALS AND METHODS
### Chemicals and reagents
The WAR, BDF, and BDL standards were purchased from LGC-GmbH (Germany). Ultra-high-temperature–processed Ensure® Plus nutrition shakes were obtained from Abbott (Brazil). Acetone, acetonitrile, and methanol were acquired both from Sigma-Aldrich (Brazil) and SK Chemicals (South Korea). Apple pectin, acetic acid, ammonium acetate, triethylamine, and ammonium hydroxide were purchased from Sigma-Aldrich (Brazil).

### Preparation of the stock solutions
Stock solutions of WAR, BDF, and BDL in acetonitrile were prepared in triplicate, and their concentrations were determined gravimetrically. The working solutions were stored at 2–8 °C according to Chalermchaikit et al.[22] The concentrations of the WAR, BDF, and BDL stock solutions were 597.4, 617.6, and 590.9 µg g$^{-1}$; 661.2, 546.5, and 646.8 µg g$^{-1}$; and 636.9, 589.2, and 625.2 µg g$^{-1}$, respectively.

### Preparation of the working solutions
To construct the calibration curves of the WAR, BDF, and BDL solutions, working solutions with nominal concentrations of 300, 500, 700, 900, and 1100 ng g$^{-1}$ were prepared in triplicate by diluting the stock solutions with a methanol–water mixed solvent (1:1 (v/v)).[23] The dilutions were performed in vials by adding predetermined volumes of the working solutions to the mixed solvent. The volumes of the working solutions were measured gravimetrically using an analytical balance, and the actual concentrations of the diluted solutions were calculated using the experimental data.

### Sample preparation
#### Preparation of the simulated stomach content matrix and enriched matrices
A simulated stomach content matrix was used because of the complex and diverse chemical composition of the real stomach content matrix. The experimental medium simulated the initial composition of the postprandial stomach ('fed state'). Furthermore, it contained numerous interferents and mimicked the physiological conditions of a real stomach matrix, which could interfere with rodenticide analysis (e.g. pH, osmolarity, and analyte adsorption on the surfaces of the solid matrix components).[24]

Simulated stomach content samples were prepared as follows. The nutrient composition of the Ensure® Plus nutrition shake used in this study was comparable to that of the standard North American breakfast, according to the Food and Drug Administration. The viscosity of Ensure® Plus nutrition shake was increased using 0.45% pectin to obtain a medium simulating the initial composition of the postprandial stomach.[25]

WAR, BDF, and BDL stock solutions were added to simulated stomach content matrices to obtain enriched matrices with five analyte concentrations (in triplicate) at nominal concentrations of 300, 500,

700, 900, and 1100 ng g$^{-1}$. The concentrations of WAR, BDF, and BDL in the enriched matrices were determined gravimetrically, and the volumetric masses of the stock solutions and enriched matrices were measured in 50 mL conical tubes using an analytical balance to a final mass of 5 g.

### Extraction of the enriched matrices

Both the preparation of the fortified matrix and the extraction process were carried out on the same day in the ambient temperature range of the test laboratory (20-25 °C).

Approximately 5 g of acetone was added to each enriched matrix under shaking. The mixtures were then centrifuged at 17,000 g at 4 °C for 15 min to obtain two-phase systems. The supernatants were collected, filtered into 5 mL borosilicate glass flasks using 0.22 μm polyvinylidene fluoride membranes (Analítica, Brazil), and allowed to rest overnight in a refrigerator (2-8 °C) to decant any suspended particles that could interfere with the analysis. Thereafter, 1 mL of each supernatant sample was collected and transferred to a 2 mL HPLC glass vial (Waters, USA).

### Instrumentation

Chromatographic separation was performed using an Alliance HPLC system (Waters, USA) equipped with a separation module (e2695) and an analytical column (Symmetry C-18, 4.6 mm × 75 mm, 3.5 μm particle size; Waters, USA). The temperature of the column was maintained at 50 °C during separation, and the sample injection volume was 10 μL. Gradient elution was performed using a mobile phase comprising 40 mM ammonium acetate, 0.2% acetic acid, and 0.2% triethylamine in ultrapure water (mobile phase A) or methanol (mobile phase B) at a flow rate of 0.5 mL min$^{-1}$. The gradient used for BDF and BDL was as follows: 0–2 min, 52% B; 2–13 min, linear gradient to 82% B; 13–16 min, linear gradient to 87% B; and 16–30 min, linear gradient to 52% B. The gradient used for WAR was as follows: 0–2 min, 20% B; 2–10 min, linear gradient to 52% B; 10–16min, linear gradient to 70% B; 16–23 min, linear gradient to 82% B; 23–27 min, linear gradient to 52% B; and 27–30 min, linear gradient to 20% B. The analytes were detected using a Waters 2475 multiwavelength fluorescence detector (FLD) with emission and excitation wavelengths of 390 and 318 nm, respectively.[22] The Empower software (Waters, USA) was used to process and analyse the chromatograms.

UHPLC analysis was performed using an Acquity H-Class system (Waters, USA) equipped with an Acquity UPLC® BEH C-18 column (2.1 mm × 50 mm, 1.7 μm particle size; Waters, USA). The column temperature during separation was maintained at 50 °C, and the injection volume was 1 μL. Gradient elution was performed using a mobile phase comprising water (mobile phase A) and acetonitrile (mobile phase B) at a flow rate of 0.3 mL min$^{-1}$. The gradient used was as follows: 0–2 min, 5% B; 2–6 min, linear gradient to 90% B; 6–8 min, 90% B; and 8–10 min, linear gradient to 5% B. The analytes were detected using a Xevo® TQ-S triple quadrupole mass spectrometer (Waters, USA) equipped with an electrospray ionisation (ESI) source. Data were collected under the following experimental conditions: nebulisation pressure of 69 kPa; source temperature of 150 °C; and collision flux, desolvation, and gas cone of 0.15 mL min$^{-1}$, 1000 L h$^{-1}$, and 150 L h$^{-1}$, respectively. The capillary voltage was optimised to 2.35 kV in the negative ESI mode. Dwell times ranging between 10 and 110 ms per transition were selected for each analyte. The multiple reaction monitoring (MRM) mode was used to monitor ion transitions. For each compound, the most and second-most intense product ions were selected for quantitative and qualitative analyses, respectively. The monitored transitions were as follows: 307.1 → 161.0 and 307.1 → 250.1 for the identification and quantification of WAR, respectively, 523.1 → 143.0 and 523.1 → 80.0 for the quantification and identification of BDF, respectively, and 527.0 → 181.0 and 527.1 → 275.0 for the quantification and identification of BDL, respectively.[17] The MassLynx software with the TargetLynx add-on (Waters) was used to process and analyse the experimental data.

### Validation
*Calibration curves of WAR, BDF, and BDL in solutions and enriched matrices*

Linearity was investigated by analysing the calibration curves of WAR, BDF, and BDL in solutions and enriched matrices in the concentration range of 300–1100 ng g$^{-1}$. Five points were selected in this concentration range, and experiments were performed in triplicate for a total sample space of 15. Calibration curves were constructed by plotting the instrument response signal (peak area) against the analyte concentration, which was determined gravimetrically. Linearity was evaluated by analysing the results of the linear regression curves.[23] Prior to performing linear regression, the raw data were analysed using the Grubbs and Cochran tests to identify outlier values and determine the homoscedasticity of the data. A linear regression model was then applied to the experimental data using the Excel Data Analysis tool to evaluate the statistical significance of the regressions (at a confidence level of 95%), obtain the standardised residual plots, and determine the correlation coefficients ($r^2$). The acceptance criteria for the linearity parameter were $r^2 \geq 0.98$ (7), a *p*-value of the F-test for regression of < 0.05, and a residual plot with a random distribution around the Y-axis (no trends), confirming linearity.[19] The limits of detection and quantification (*LOD* and *LOQ*, respectively) were defined as the lowest concentrations with signal-to-noise ratios of 3 and 10, respectively, and were calculated according to Equations 1 and 2:[19]

$$LOD = 3.3\,\frac{s}{b} \qquad\qquad \text{Equation 1}$$

$$LOQ = 10.0\,\frac{s}{b} \qquad\qquad \text{Equation 2}$$

where *s* and *b* are the standard deviation of the blank solution and slope of the calibration curve of the matrix, respectively.

Considering previously reported data on coumarin rodenticides in the stomach contents of animals, we established that the *LOQ* acceptance criterion was *LOQ* ≤ 1 µg g$^{-1}$.[6] As *LOD* was three times smaller than *LOQ*, the *LOD* acceptance criterion was defined as *LOD* ≤ 0.33 µg g$^{-1}$.

### Selectivity

To determine the selectivity of the quantitative analysis methods, a *t*-test was performed to compare the slopes of the curves of the WAR, BDF, and BDL solutions and matrices enriched with these compounds. Before performing the *t*-test, an F-test was conducted to check the variance homogeneity between the curves for the solutions and matrices. Subsequently, a *t*-test was performed with a confidence level of 95% to compare the values of slopes (from the straight lines of the compounds in solutions and matrices) within the minimum and maximum slope values of the linear regressions.[19] To assess the selectivity of the qualitative analysis methods, the response (peak area) of the blank (rodenticide-free matrix) was compared with those of the first points of the matrix curves, and the results were used to evaluate the degree of interference of the matrix with the analyte signal.[26] The acceptance criterion for quantitative methods was a *p*-value of the *t*-test > 0.05.[19] For qualitative analysis methods, the signal of the blank matrix should not exceed 20% of the response at a concentration of 300 ng g$^{-1}$.[26]

### Recovery

Recovery was determined by selecting two concentrations from the curves of the WAR, BDF, and BDL solutions and enriched matrices (300 and 700 ng g$^{-1}$). Using the matrix peak areas and equations describing the curves of the WAR, BDF, and BDL solutions, we determined the actual concentrations of WAR, BDF, and BDL in the enriched matrices at preselected concentrations. Recovery was determined by calculating the recovery rate (*EP* (%)) according to Equation 3:

$$EP\,(\%) = R \times 100 = \frac{Xmr}{Xmt} \times 100 \qquad \text{Equation 3}$$

where $R$ is the ratio between the mean real concentration of the enriched matrix ($Xmr$) and mean gravimetric concentration of the enriched matrix ($Xmt$).[19]

The acceptance criterion for the EP was determined to be EP ≥ 62% using a method for analysing coumarin rodenticides in matrices extracted with acetone.[1]

*Precision*
The precision of the analytical methods was determined by preparing enriched matrices with concentrations of 300 and 700 ng g$^{-1}$ in septuplicate. After the samples were extracted and analysed using LC, we determined the actual concentrations of WAR, BDF, and BDL in the enriched matrices at preselected concentrations using matrix signal data and the equations describing the curves of the WAR, BDF, and BDL solutions. The precision of each method was determined by calculating the coefficient of variation ($CV$), according to Equation 4:[19]

$$CV\,(\%) = \frac{s}{Xv} \times 100 \qquad \text{Equation 4}$$

where $Xv$ is the actual concentration of the enriched matrix.

To determine the intra-day precision of the analytical methods, chromatographic analyses were performed on the day that the enriched matrices were prepared and extracted with acetone (day 1). To determine the inter-day precision of the analytical methods, chromatographic analyses were performed using the same samples, equipment, and analysts as those used for the intra-day precision experiments, and measurements were performed on two consecutive days (days 2 and 3). The $CV$ value of the inter-day precision was calculated as the mean of the $CV$ values of the data collected during the three days.[19] The acceptance criterion for precision was CV < 12.2%, which was established based on a method used to analyse coumarin rodenticides in matrices extracted with acetone.[1]

*Uncertainty of concentration measurements*
The concentrations of WAR, BDF, and BDL ($x_R$) were predicted using the calibration curves of the corresponding solutions and by the dilution factor ($F_d$), according to Equation 5:

$$x_R = \frac{y_d - a}{b} \frac{1}{F_d} \qquad \text{Equation 5}$$

where $y_R$ is the average signal value (peak area) of the sample and $a$ and $b$ are the coefficients of the fitted line.[27]

The dilution factor was calculated by the ratio between the matrix mass and the total mass after addition of acetone and its uncertainty ($u_{Fd}$) was determined considering the repeatability of matrix masses and the calibration uncertainty of the analytical balance as sources. In addition, the uncertainty of the average $x_R$ values was determined using the law of propagation of the uncertainty to the prediction equation, according to Equation 6:

$$u_{x_R}^2 = \left(\frac{\partial x_R}{\partial F_d}\right)^2 u_{F_d}^2 + \left(\frac{\partial x_R}{\partial y_R}\right)^2 u_{y_d}^2 + \left(\frac{\partial x_R}{\partial a}\right)^2 u_a^2 + \left(\frac{\partial x_R}{\partial b}\right)^2 u_b^2 + 2\left(\frac{\partial x_R}{\partial a}\right)\left(\frac{\partial x_R}{\partial b}\right)u_a u_b r_{a,b} \qquad \text{Equation 6}$$

where $u_{yd}$ is the standard uncertainty of the reproducibility of the measurements of the sample signal, $u_a$ is the standard uncertainty of $a$, $u_b$ is the standard uncertainty of $b$, and $r_{a,b}$ is the correlation coefficient between the coefficients of the fitted line.[27]

These data allowed us to build a cause-effect diagram for the established mathematical model (Figure 2). The inputs of the uncertainty model were the repeatability of the responses or signals ($Y_R$), the coefficients of the fitted line ($a$ and $b$) as well as the dilution factor ($F_d$), and the output was $X_R$.
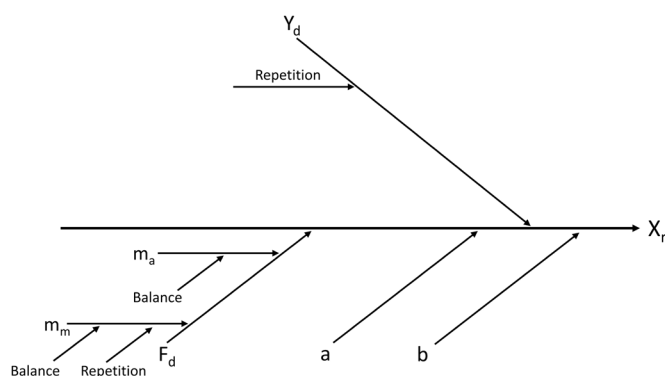


**Figure 2**. Sources of uncertainty considered in the Ishikawa diagram.

## RESULTS AND DISCUSSION
### *Optimization*

Acetonitrile[6,16] was used to prepare the working solutions, and acetone was used as the extraction solvent[5,6,15] because of the high solubilities of WAR, BDF, and BDL in these solvents. Acetonitrile, which is commonly used for rodenticide extraction,[14,16] was also tested; however, the average recoveries of WAR, BDF, and BDL in acetonitrile were lower than the acceptance criteria. Once the optimal solvents were selected for the preparation of the stock, working, and extraction solutions, we determined the method best suited for LC.

We used a gradient chromatography method because it yielded better separation of analytes from matrices than the isocratic method, as described in several recent papers on the analysis of rodenticides.[16,17] An HPLC-FLD gradient method (the chromatographic run method most indicated in articles for analysis in complex matrices)[22] was used, and it yielded satisfactory results for the analysis of WAR, BDF, and BDL in the gastric content matrix, as the analyte peaks were separate from the matrix interference peaks. The gradient UHPLC-MS method was based on a previously described protocol.[17] For these methods, the signals of the compounds were detected only at concentrations higher than 200 ng g$^{-1}$; therefore, a working concentration range of 300–1100 ng g$^{-1}$ was selected to compare the validation parameters of the HPLC-FLD and UHPLC-MS methods. This concentration range was similar to that used for the analysis of raticides in animal gastric matrices (100–1000 ng g$^{-1}$).[7]

The acquisition mode of the MS instrument was set to MRM after selecting the gradient UHPLC method and working concentration range. These settings have been widely used in recent studies, as they allow the monitoring of different reactions and selection of fragments with good signal-to-noise ratios.[14–16] In contrast, the selected reaction monitoring (SRM) mode is used in rodenticide analysis only when bulk analyte data are available.[16] SRM is often used when researchers have already collected analyte data and would like to monitor the product ions produced by specific reactions of the *m/z* precursor ions selected during a previous MS stage instead of acquiring the entire mass spectra of the product ions.[28] However, the MRM mode yields lower *LOD* values; hence, the MRM mode is the most suitable mass acquisition mode for the analysis of coumarins, as it enables monitoring several transitions and selection of high signal-to-noise responses.[14] After optimising the methods and generating the calibration curves, the methods were evaluated by comparing the results considering the validation parameters and previously established acceptance criteria.

### *Validation parameters used to evaluate method performance*

Table I summarises the results of the chromatographic validation methods for the analysis of rodenticides in the simulated stomach content matrices. The compounds that yielded unsatisfactory results were not used for subsequent parameter evaluation. The linearity values were analysed first.

**Table I.** Performance parameters for high-performance liquid chromatography-fluorescence detection (HPLC-FLD) and ultra-high-performance liquid chromatography-mass spectrometry (UPLC-MS). Here, WAR, BDF, BDL, *LOD, LOQ, EP*, and *CV* denote warfarin, brodifacoum, bromadiolone, limit of detection, limit of quantification, recovery rate, and coefficient of variation, respectively.

| Parameter | Acceptance criteria | Results for HPLC-FLD | Satisfactory? | Results for UHPLC-MS | Satisfactory? |
|---|---|---|---|---|---|
| Linearity (matrix) | $r^2 \geq 0.98$, *p*-value < 0.05, and residual plot with random distribution | WAR: $r^2 = 0.99$ and *p*-value < 0.0001<br>BDF: $r^2 = 0.98$ and *p*-value < 0.0001<br>BDL: $r^2 = 0.98$ and *p*-value < 0.0001 | Yes, for all coumarins | WAR: $r^2 = 0.98$ and *p*-value < 0.0001<br>BDF: $r^2 = 0.99$ and *p*-value < 0.0001<br>BDL: $r^2 = 0.99$ and *p*-value < 0.0001 | Yes, for all coumarins |
| *LOD* (matrix) | $LOD \leq 330$ ng g$^{-1}$ | *LOD* of WAR = 24.4 ng g$^{-1}$<br>*LOD* of BDF = 77.8 ng g$^{-1}$ and<br>*LOD* of BDL = 138.2 ng g$^{-1}$ | Yes, for all coumarins | *LOD* of WAR = 0.1 ng g$^{-1}$<br>*LOD* of BDF = 3.2 ng g$^{-1}$ and<br>*LOD* of BDL= 11.2 ng g$^{-1}$ | Yes, for all coumarins |
| *LOQ* (matrix) | $LOQ \leq 1000$ ng g$^{-1}$ | *LOQ* of WAR = 74.1 ng g$^{-1}$<br>*LOQ* of BDF = 235.7 ng g$^{-1}$ and<br>*LOQ* of BDL = 418.6 ng g$^{-1}$ | Yes, for all coumarins | *LOQ* of WAR = 0.3 ng g$^{-1}$<br>*LOQ* of BDF = 9.8 ng g$^{-1}$ and<br>*LOQ* of BDL = 33.9 ng g$^{-1}$ | Yes, for all coumarins |
| Selectivity | response should be lower than 20% of the response for a concentration of 300 ng g$^{-1}$ | WAR: white sign = 0 u.a. and smallest point sign = 2 245 254 u.a.<br><br>BDF: white sign = 0 u.a. and smallest point sign = 15 782 643 u.a.<br><br>BDL white sign = 3 286 426 u.a. and smallest point sign = 8930648 u.a. | Only for WAR and BDF | WAR: white sign = 39 u.a. and smallest point sign = 695 413 u.a.<br><br>BDF: white sign = 743 u.a. and smallest point sign = 60 945 u.a.<br><br>BDL white sign = 98 u.a. and smallest point sign = 3560 u.a. | Yes, for all coumarins |
| Recovery | $EP \geq 62\%$ | *EP* of WAR = 67.2% | Yes | *EP* of WAR = 49.5% and<br>*EP* of BDF = 64.5% | BDF only |
| Precision | $CV \leq 12\%$ | *CV* of WAR: intra-day precision = 1.0% and inter-day precision = 1.2% | Yes | *CV* of BDF: intra-day precision = 2.1% and inter-day precision = 2.0% | Yes |
| Relative uncertainty | N.A.[a] | u WAR = 6.4% | N.A.[a] | u BDF = 11.5% | N.A.[a] |

[a] N.A. = Not Applicable

*Linearity, LOD, and LOQ values of the chromatography methods*

The linearity of the curves for the WAR, BDF, and BDL solutions and enriched matrices was evaluated in the working concentration range of 300–1100 ng g$^{-1}$. In recent studies on the validation of analytical methods for rat poison, only $r^2$ values were used to evaluate linearity, with $r^2 > 0.99$.[14,16,17] The $r^2$ values in this study were lower than those previously reported. However, the $r^2$ values of the curves were close to the $r^2$ value considered satisfactory in the linearity acceptance criterion in a recent study on rodenticides in an animal gastric content matrix.[7] In addition, the results met the criteria for evaluating linearity in terms of the *p*-values of the F-test and inspection of the residual plots.[19]

According to the acceptance criteria, the curves of the WAR, BDF, and BDL solutions and enriched matrices were linear. However, the curves of BDF and BDL obtained using HPLC-FLD exhibited wider residue scattering at higher concentrations. This was ascribed to the low solubilities of BDF and BDL in methanol and water, which were the solvents used to prepare the working solutions and mobile phases. The residue plots of the HPLC curves of WAR, BDF, and BDL in the enriched matrices did not show the same patterns of residue scattering (WAR, BDF, and BDL were present in the acetone-containing supernatant). For the UHPLC-MS data, we encountered no problems during the visual evaluation of the residue graphs for all samples, except for the BDL solutions. This further emphasised the usefulness of UHPLC-MS for the quantitative analysis of rodenticides and justified its use in recent studies.[16,17]

The *LOD* and *LOQ* values were determined using the curves of WAR, BDF, and BDL in the enriched matrices. The results were considered satisfactory, as they were comparable to those reported recently by researchers who analysed WAR, BDF, and BDL in stomach content matrices of animals[7] and other matrices using acetone extraction followed by LC-FLD[8,9] and LC-MS.[11,13] The *LOD* values obtained in this study were lower than the critical *LOD* (260 ng g$^{-1}$). Therefore, our methods are suitable for the detection of coumarin compounds at concentrations below the critical *LOD*. The critical *LOD* was calculated considering the theoretical poisoning of a two-year-old child (the age group with the highest number of poisoning cases in Brazil,[29] the gastric volume after 1 h of fasting[30] and the toxic rodenticide dose for children of 0.014 mg kg$^{-1}$.[31] After confirming the linearity of the curves in solutions and the enriched matrices, the curves were compared to determine the selectivities of the methods and confirm whether the methods were quantitative.

*Comparison of method selectivity and evaluation of intended use*

Considering the acceptance criteria for qualitative methods, our results indicated that HPLC-FLD and UHPLC-MS were selective for all the coumarins evaluated, except for HPLC-FLD for BDL. This was attributed to the presence of a diastereomeric pair at different retention times in the chromatograms of all solutions and matrices using different mobile phases and isocratic and gradient methods, except for the BDF chromatograms, which presented only one peak, although BDF consisted of a diastereomeric pair. Therefore, the selectivity of the HPLC-FLD method for BDL was unsatisfactory because two well-separated analyte peaks were present in the chromatograms of BDL. The integration method used for the enriched matrices was the same as that used for the blank matrices. Therefore, the two peaks corresponding to the diastereoisomer pair were integrated and processed together. The mean signal obtained from the blanks was 20% stronger than the mean signal for the lowest concentration point on the curve, an unsatisfactory result for selectivity. We hypothesised that the physical and chemical properties of the cis and trans diastereoisomers of BDL were different,[17] causing their different distributions in organic solvents and different retention times.

The diastereomers of BDL can be separated using achiral columns. Some researchers have reported the presence of two peaks in the chromatograms of BDL using C-8 and C-18 reversed-phase columns under acidic conditions and acetate or ammonium formate ions in the mobile phase and used the first and primary peaks to quantify BDL.[15] The use of only the primary peak of BDL for integration was not considered because the two peaks were not completely separated and commercial raticides typically contain two diastereoisomers.[17] Therefore, in this study, chromatographic analysis of BDL was performed by integrating the peaks of both diastereoisomers.

Selectivity analysis was performed to determine whether the matrix components interfered with the signals of the rodenticide isomers, and the methods were determined to be selective for detecting coumarins.

*Comparison of method recovery and matrix complexity*

The recovery values of HPLC-FLD and UHPLC-MS were satisfactory according to the acceptance criteria. The recovery values obtained herein were similar to those reported in recent publications on the analysis of WAR, BDF, and BDL in animal gastric content matrices[7] and other matrices using acetone extraction followed by LC-FLD analysis;[8,9] In contrast, the recovery values obtained herein were lower than those reported in publications on the use of LC-MS in other matrices[13,15] and the values recommended by the Association of Official Analytical Chemists (AOAC).[19] The matrix used in this study was complex, as the Ensure® Plus nutrition shake contains many macromolecules, such as carbohydrates, lipids, proteins, and vitamin K,[32] which can interact with rodenticides and hinder their recovery. Therefore, the composition of the extraction solvent can be changed to increase its affinity for the analytes. Nevertheless, the HPLC FLD and UHPLC–MS methods were classified as qualitative, such that recovery values were not required for validation. The recovery values of HPLC-FLD for BDF and BDL and those of UHPLC-MS for BDL were not calculated because of the challenges encountered in constructing the curves of the compounds in solution. This is one of the reasons why rat toxin analysis via LC-MS has been used more frequently because it is considered more reliable and selective according to the reported validation parameters.[1]

*Comparison of method precision values*

The precision values of the HPLC-FLD and UHPLC-MS methods were considered satisfactory based on the acceptance criteria. The intra- and inter-day precision values were consistent with those recently reported in papers on the analysis of WAR and BDF in an animal gastric content matrix[7] and other matrices using acetone extraction followed by LC-FLD[8,9] and LC-MS analyses.[11,13,15] Moreover, the values were within the range recommended by the AOAC.[19] The performances of the HPLC-FLD and UHPLC-MS methods were comparable, demonstrating the accuracy of the methods. The precision of the UHPLC-MS method for WAR was not calculated because the recovery of the method was unsatisfactory. The recovery values of UHPLC-MS for WAR, BDF, and BDL were lower than those of HPLC-FLD, probably because of ionic suppression, a common shortcoming of methods using MS detectors.[10]

Ionic suppression is defined as the loss of signal from the analyte of interest owing to the co-elution and ionisation of an interfering compound in the matrix. To avoid false recovery values, the degree of ion suppression must be determined by analysing the degree of matrix interference in the analyte signal, which is evaluated using the selectivity parameter. If the blank matrix signal is too high, it is likely to be noise and should be corrected accordingly. To diminish the effect of ion suppression, the signal processing method (noise reduction) or extraction technique (e.g. using SPE) can be refined to diminish matrix interference.[33] The uncertainty of each method was calculated after all validation steps were performed.

*Comparison of the uncertainty values of the HPLC–FLD and UHPLC–MS methods*

Uncertainty (%) was calculated as the ratio between the uncertainties and averages of the measured values. The uncertainty of UHPLC-MS was lower than that of HPLC-FLD (Table II). The expanded uncertainty was calculated using the contributions of the solution curve uncertainty at the concentration midpoint and repeatability uncertainty. Although the ABNT NBR 17025:2017 standard can be used to estimate the uncertainty of testing methods, measurement uncertainty in rodenticide analysis studies using LC has not yet been reported. Although not mandatory for qualitative methods, uncertainty is critical for guaranteeing result validity and ensuring accurate and reliable rodenticide concentration measurements. The uncertainties of the concentration values determined using rodenticide quantification assays can significantly help forensic experts identify the cause of poisoning, providing a method for conducting conformity assessment analyses with specified confidence levels. A well-executed analysis can help resolve many cases of rodenticide poisoning that have not yet been elucidated.

**Table II.** Concentrations of warfarin (WAR) and brodifacoum (BDF) solutions determined using high-performance liquid chromatography-fluorescence detection (HPLC-FLD) and ultra-high-performance liquid chromatography-mass spectrometry (UHPLC-MS) and relative measurement uncertainties.

| Compound | Chromatographic method | Concentration (ng g$^{-1}$) | Relative uncertainty (%) |
|----------|------------------------|-----------------------------|--------------------------|
| WAR | HPLC-FLD | 802 ± 51 | 6.4 |
| BDF | UHPLC-MS | 842 ± 97 | 11.5 |

## CONCLUSION

According to the validation parameters, the HPLC-FLD and UHPLC-MS methods were satisfactory for the detection of rodenticides in human gastric content matrices and forensic toxicology applications. For analyses that require quantitative tests, the UHPLC-MS method should be used, and the extraction step should be optimised to obtain adequate selectivity and recovery values.

Although in this study we did not use a real matrix, the performance of the artificial medium during the validation steps was similar to that reported for animal gastric content samples.[7] Therefore, HPLC-FLD and UHPLC-MS can be used as references for the validation of real human gastric content matrices.

## Conflicts of interest

The authors declare that they have no conflict of interest.

## REFERENCES

(1) Imram, M.; Shafi, H.; Wattoo, S. A.; Chaudhary, M. T.; Usman, H. F. Analytical methods for determination of anticoagulant rodenticides in biological samples. *Forensic Sci. Int.* **2015**, *253*, 94–102. https://doi.org/10.1016/j.forsciint.2015.06.008

(2) Guerra, F. Q. S. *Avaliação da atividade antifúngica dos compostos cumarínicos frente às cepas do gênero Aspergillus*. Doctoral thesis, 2016, Universidade Federal da Paraíba, João Pessoa, PB, Brazil. https://repositorio.ufpb.br/jspui/handle/tede/9517

(3) Departamento de informática do Sistema Único de Saúde (DATASUS) do Ministério da Saúde, Governo Federal, Brasil. http://tabnet.datasus.gov.br/cgi/tabcgi.exe?sinannet/cnv/Intoxbr.def (accessed 2021-05-03).

(4) Ferreira, A. G. Química forense e técnicas utilizadas em resoluções de crimes. *Revista Acta de Ciência & Saúde* **2016**, *2*, 32–44. https://doi.org/10.17921/1890-1793.2021v16n16p16-23

(5) Hernandez-Moreno, D.; de la Casa-Resino, I.; Lopez-Beceiro, A.; Fidalgo, L. E.; Soler, F.; Perez-Lopez, M. Secondary poisoning of non-target animals in an Ornithological Zoo in Galicia (NW Spain) with anticoagulant rodenticides: a case report. *Veterinarni Medicina* **2013**, *58*, 553–559. https://doi.org/10.17221/7087-VETMED

(6) Gallocchio, F.; Basilicata, L.; Benetti, C.; Angeletti, R.; Binato, G. Multi-residue determination of eleven anticoagulant rodenticides by high-performance liquid chromatography with diode array/fluorimetric detection: investigation of suspected animal poisoning in the period 2012-2013 in north-eastern Italy. *Forensic Sci. Int.* **2014**, *244*, 63–69. https://doi.org/10.1016/j.forsciint.2014.08.012

(7)   Gallocchio, F.; Moressa, A.; Stella, R.; Rosin, R.; Basilicata, L.; Bille, L.; Toson, M.; Biancotto, G.; Lega, F.; Angeletti, R.; Binato, G. Fast and simultaneous analysis of carbamate pesticides and anticoagulant rodenticides used in suspected cases of animal poisoning. *Forensic Sci. Int.* **2021**, *323*, 110810. https://doi.org/10.1016/j.forsciint.2021.110810

(8)   Meiser, H. Detection of anticoagulant residues by a new HPLC method in specimens of poisoned animals and a poison control case study. *J. Anal. Toxicol.* **2005**, *29*, 556–563. https://doi.org/10.1093/jat/29.6.556

(9)   Armentano, A.; Iammarino, M.; Lo Magro, S.; Muscarella, M. Validation and application of multi-residue analysis of eight anticoagulant rodenticides by high-performance liquid chromatography with fluorimetric detection. *J. Vet. Diagn. Invest.* **2012**, *24*, 307–311. https://doi.org/10.1177/1040638711433354

(10)  Hernández, A. M.; Bernal, J.; Bernal, J. L.; Martín, M. T.; Caminero, C.; Nozal, M. T. Analysis of anticoagulant rodenticide residues in *Microtus arvalis* tissues by liquid chromatography with diode array, fluorescence and mass spectrometry detection. *J. Chromatogr. B* **2013**, *925*, 76–85. https://doi.org/10.1016/j.jchromb.2013.02.032

(11)  Vandenbrouckev, V.; Desmet, N.; De Backer, P.; Croubels, S. Multi-residue analysis of eight anticoagulant rodenticides in animal plasma and liver using liquid chromatography combined with heated electrospray ionization tandem mass spectrometry. *J. Chromatogr. B* **2008**, *869*, 101–110. https://doi.org/10.1016/j.jchromb.2008.05.011

(12)  Fourel, I.; Hugnet, C.; Goy-Thollot, I.; Berny, P. Validation of a new liquid chromatography–tandem mass spectrometry ion-trap technique for the simultaneous determination of thirteen anticoagulant rodenticides, drugs, or natural products. *J. Anal. Toxicol.* **2010**, *34*, 95–102. https://doi.org/10.1093/jat/34.2.95

(13)  Dong, X.; Lianga, S.; Sun, S. Determination of seven anticoagulant rodenticides in human serum by ultra-performance liquid chromatography-mass spectrometry. *Anal. Methods* **2015**, *7*, 1884–1889. https://doi.org/10.1039/C4AY02536A

(14)  Cao, X.; Yang, X.; Liu, Z.; Jiao, H.; Liu, S.; Liu, L.; Meng, Q. Rapid simultaneous screening and detection of 12 anticoagulant rodenticides in food by ultra-performance liquid chromatography-triple quadrupole/linear ion trap tandem mass spectrometry. *Food Analytical Methods* **2017**, *10*, 3538–3547. https://doi.org/10.1007/s12161-017-0922-2

(15)  Fourel, I.; Damin-Pernik, M.; Benoit, E.; Lattard, V. Core-shell LC-MS/MS method for quantification of second generation anticoagulant rodenticides diastereoisomers in rat liver in relationship with exposure of wild rats. *J. Chromatogr. B* **2017**, *1041–1042*, 120–132. https://doi.org/10.1016/j.jchromb.2016.12.028

(16)  Seljetun, K. O.; Eliassen, E.; Karinen, R.; Moe, L.; Vindenes, V. Quantitative method for analysis of six anticoagulant rodenticides in faeces, applied in a case with repeated samples from a dog. *Acta Vet. Scand.* **2018**, *60*. https://doi.org/10.1186/s13028-018-0357-9

(17)  Nosal, D.; Feinstein, D. L.; Chen, L.; van Breemen, R. B. Separation and quantification of superwarfarin rodenticide diastereomers—bromadiolone, difenacoum, flocoumafen, brodifacoum, and difethialone—in human plasma. *Journal of AOAC International* **2020**, *103*, 770–778. https://doi.org/10.1093/jaoacint/qsaa007

(18)  Jantratid, E.; Janssen, N.; Reppas, C.; Dressman, J. B. Dissolution media simulating conditions in the proximal human gastrointestinal tract: An update. *Pharm. Res.* **2008**, *25*, 1663–1676. https://doi.org/10.1007/s11095-008-9569-4.

(19)  Instituto Nacional de Metrologia, Normalização e Qualidade Industrial – Inmetro, Brasil. http://www.inmetro.gov.br/Sidoq/Arquivos/Cgcre/DOQ/DOQ-Cgcre-8_08.pdf (accessed 2021-05-03).

(20)  Organisation Internationale De Métrologie Légale. https://www.oiml.org/en/files/pdf_v/v002-200-e07.pdf (accessed 2021-05-03).

(21)  International Organization for Standardization. *General requirements for the competence of testing and calibration laboratories*. ISO/IEC 17025:2017. Geneva, 2017.

(22) Chalermchaikit, T.; Felice, L. J.; Murphy, M. J. Simultaneous determination of eight anticoagulant rodenticides in blood serum and liver. *J. Anal. Toxicol.* **1993**, *17*, 56–61. https://doi.org/10.1093/jat/17.1.56

(23) Bertoldi, F. C.; Deschamps, F. C.; Silva Junior, A. A.; Correa, A. F.; Franco, M. F.; Eberlin, M. N. Validação de um método analítico rápido por CLAE-UV para determinação de cumarina em guaco (*Mikania glomerata* Sprengel) confirmado com espectrometria de massas. *Revista Brasileira de Plantas Medicinais* **2016**, *18*, 316–325. https://doi.org/10.1590/1983-084X/15_160

(24) Marques, M. R. C.; Loebenberg, R.; Almukainzi, M. Simulated biological fluids with possible application in dissolution testing. *Dissolution Technol.* **2011**, *18*, 15–28. https://doi.org/10.14227/DT180311P15

(25) Klein, S.; Butler, J.; Hempenstall, J. M.; Reppas, C.; Dressman, J. B. Media to simulate the postprandial stomach I. Matching the physicochemical characteristics of standard breakfast. *J. Pharm. Pharmacol.* **2004**, *56*, 605–610. https://doi.org/10.1211/0022357023367

(26) Verbic, T.; Dorkó, Z.; Horvai, G. Selectivity in analytical chemistry. *Revue Roumaine de Chimie* **2013**, *58*, 569–575. https://www.researchgate.net/publication/285481211

(27) Ramsey, M. H.; Ellison, S. L. R.; Rostron, P. (Eds.) *Measurement uncertainty arising from sampling – A guide to methods and approaches*. Eurachem / CITAC Guide, 2nd edition, 2019. https://www.eurachem.org/images/stories/Guides/pdf/UfS_2019_EN_P2.pdf (accessed 2021-05-03).

(28) Vessecchi, R.; Lopes, N. P.; Gozzo, F. C.; Dörr, F. A.; Murgu, M.; Lebre, D. T.; Abreu, R.; Bustillos, O. V.; Riveros, J. M. Nomenclaturas de espectrometria de massas em língua portuguesa. *Quím. Nova* **2011**, *34*, 1875–1887. https://doi.org/10.1590/S0100-40422011001000025

(29) Vilaça, L.; Volpea, F. M.; Ladeira, R. M. Intoxicações exógenas em crianças e adolescentes atendidos em um serviço de toxicologia de referência de um hospital de emergência brasileiro. *Revista Paulista de Pediatria* **2020**, *38*, e2018096. https://doi.org/10.1590/1984-0462/2020/38/2018096

(30) Carmona, B. M.; Almeida, C. C. A.; Vieira, W. B.; Fascio, M. N. C.; de Carvalho, L. R.; Vane, L. A.; Barbosa, F. T.; Nascimento Junior, P.; Módolo, N. S. P. Dinâmica ultrassonográfica dos volumes do conteúdo gástrico após a ingestão de água de coco ou sanduíche de carne. Um estudo cruzado controlado e randômico com voluntários saudáveis. *Revista Brasileira de Anestesiologia* **2018**, *68*, 584–590. https://doi.org/10.1016/j.bjan.2018.06.008

(31) Roberts, J. R.; Reigart, J. R. Environmental Protection Agency (EPA). *Recognition and Management of Pesticide Poisonings*. https://www.epa.gov/pesticide-worker-safety/recognition-and-management-pesticide-poisonings (accessed 2021-05-03).

(32) Abbott. https://www.ensure.abbott/br/nossos-produtos/ensure-plus-advance.html (accessed 2021-03-18).

(33) Lanetwork. https://www.labnetwork.com.br/noticias/decodificando-a-espectrometria-de-massas-supressao-ionica/ (accessed 2021-05-03).

**BrJAC**

## FEATURE

# 9th Analitica Congress and National Meeting of Analytical Chemistry (ENQA) Addressed Medicinal Cannabis for the First Time

The 9th Analitica Congress and the National Meeting of Analytical Chemistry (ENQA) were held on September 26–27, 2023, at the São Paulo Expo Exhibition & Convention Center, São Paulo, SP, Brazil. The event broke attendance records with approximately 135 attendees, about 35% more than the previous edition. With about 10 hours of exclusive content, important topics such as "3D Printing in Analytical Chemistry" and "New Strategies for Food Analysis" were discussed. Two topics attracted a lot of attention: "Forensic Analysis", which focused on a new method in Brazil for testing drugs with sublingual absorption, and "Cannabis Characterization and Analytical Methods". This was the first time that the topic of medicinal cannabis was addressed at the Analitica Congress.
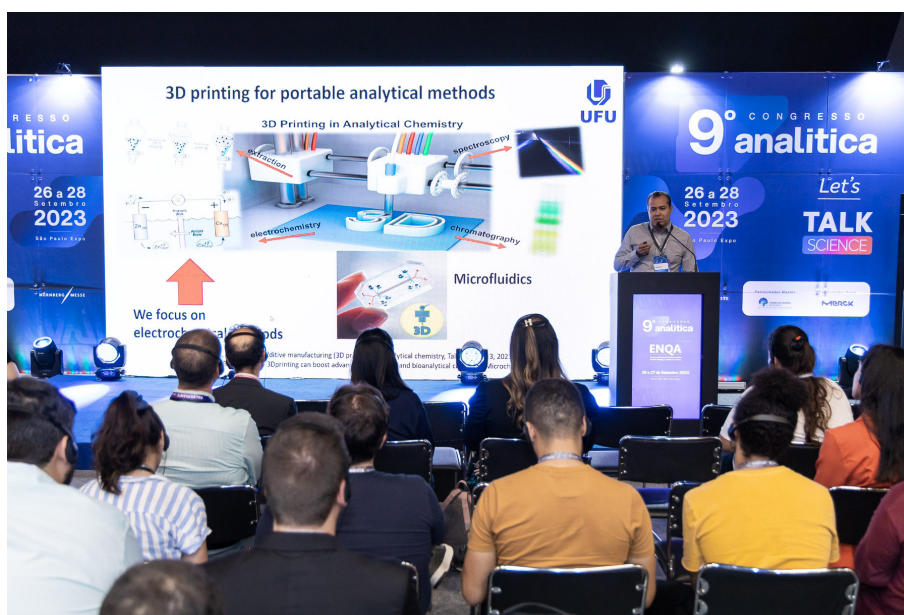


*Participants attending a presentation at the Analitica Congress. Photo: Analitica Latin America (ALA) Press Office.*

The event also featured awards for scientific studies in the field of analytical chemistry. Out of 25 finalists, three were selected as the best works and each received a voucher to be used at NMB Travel, the travel agency of NürnbergMesse Brasil. All the finalist works were displayed as posters during the three-day event. According to Nadja Bento, Director of the Life Science Portfolio at NürnbergMesse Brasil, "Initiatives such as these awards help to promote scientific development. Analytical chemistry is present in many areas of our lives, from the development of new medicine to the quality control of the food we eat. That's why we must not only generate business but also generate knowledge, and value our scientists.".

At this event, the first Analitica Road Show was announced, which will take place in Santiago, Chile, on April 10, 2024. The creation of the Analitica Road Show aims to disseminate the knowledge generated at the Analitica Congress to other Latin American countries. "It will be a unique opportunity for us to continue promoting the development of analytical chemistry and the link between academia and the market in Latin America," concluded Nadja Bento.

### Commemorative Panel

*The Brazilian Journal of Analytical Chemistry (BrJAC) held a panel session to celebrate the achievement of the Journal Impact Factor$_{2022}$ of 0.7*

During this panel session, the Young Talent in Analytical Chemistry Award, created by BrJAC to recognize outstanding young researchers in (bio)analytical chemistry, was presented. The winner of the 2023 award was Prof. Dr. Boniek Gontijo Vaz, who holds a degree in chemistry from the Federal University of São Carlos (2007), a master's degree in chemistry from the State University of Campinas - Unicamp (2009), and a Ph.D. in science from Unicamp (2011). Dr. Vaz is currently an Associate Professor at the Institute of Chemistry of the Federal University of Goiás (IQ-UFG), General Secretary of the Latin American Association of Organic Geochemistry (ALAGO) since 2018, and Associate Editor of the journal *Quimica Nova*. He also coordinates the Chromatography and Mass Spectrometry Laboratory (LaCEM) at IQ-UFG.

Additional information on the BrJAC Commemorative Panel is presented in BrJAC 2024, Vol 11, No. 42, pp 131-132.



*Dr. Boniek G. Vaz, Luciene Campos (BrJAC Publisher) and Dr. Arruda (BrJAC Editor-in-chief) at the Young Talent in Analytical Chemistry award ceremony. Photo: Luciene Campos.*

### A short interview with Prof. Dr. Boniek Gontijo Vaz

**BrJAC:** How did it feel to receive the Young Talent in Analytical Chemistry Award?
**Dr. Vaz:** Receiving this recognition from BrJAC was a milestone for me. BrJAC is not just a symbol, but a living testimony to the resilience and incredible success of our scientific community, which serves as an inexhaustible source of inspiration. For me, this award is not just a trophy, but a boost, a spark that rekindles and fuels the flame of my passion for scientific research. It strengthens my mission to continue investing in analytical chemistry in Brazil and to train qualified professionals who will drive the scientific and technological growth of our country.

**BrJAC:** How did you begin your career?

**Dr. Vaz:** My journey into the world of science took shape during my master's and Ph.D. studies when I immersed myself in the fascinating world of mass spectrometry. I remember that time like it was yesterday, especially because of the installation of the pioneering FT-ICR MS instrument at Unicamp. Together with Petrobras, the national oil and gas company of Brazil, I was able to develop productive partnerships, always looking for methodological innovations and analytical solutions that made a significant contribution to the field of analytical chemistry. Then, in 2012, as a result of the recognition of my expertise, I was approved for a professorship at UFG, which opened doors and allowed me to build a solid research group in the field of mass spectrometry. This path not only shaped my career, but also solidified my passion for research and innovation.



*Prof. Dr. Boniek Gontijo Vaz, winner of the Young Talent in Analytical Chemistry award. Photo: Boniek G. Vaz.*

**BrJAC:** What advice can you give to someone starting a career in analytical chemistry?

**Dr. Vaz:** I would say that passion is your compass. If you put your heart into it and love what you do, success will follow naturally. First, young researchers need to make sure that the field they have chosen matches their interests and aspirations. Once they have this clarity, they must dedicate themselves deeply to their chosen purpose. As in any field, patience is essential. Standing firm and persevering in the face of challenges is the way to quickly see the fruits of their work appear.

**BrJAC:** What are your plans for the future?

**Dr. Vaz:** In the future, I intend to deepen my research into the universe of complex mixtures and try to extract even more detailed data. I'm about to start a new phase of research that focuses on the isotopic composition of molecules commonly found in these mixtures. Isotopic data bring complementary layers of information, giving us tools to trace the history of a given sample. This has the potential to answer many questions in the geosciences, environmental studies, and medicine. My goal is to lead the development of innovative isotopic analysis methods that take advantage of the capabilities of high-resolution mass spectrometry.

**BrJAC:** What are you currently working on?

**Dr. Vaz:** I am currently immersed in the fascinating world of mass spectrometry and organic geochemistry, with a focus on complex mixture analysis and petroleomics. In short, I'm dedicated to understanding the chemical composition, origin, migration, and transformation of organic compounds over time on Earth. Mass spectrometry has become an invaluable tool in this process, helping us identify molecules that tell us stories from millions of years ago. It's like being a molecular detective, unraveling mysteries hidden deep within the Earth. In addition to technical research, I am deeply committed to education. Teaching at the postgraduate level is a passion, as it allows me to mentor and shape the next generation of scientists. And, of course, I remain heavily involved with the Latin American Association of Organic Geochemistry (ALAGO), an organization that fosters an environment for discussion and interaction in the field of organic geochemistry, and with the journal *Quimica Nova*, where I am an associate editor, giving me a unique perspective on advances in the field of chemistry in Brazil and Latin America.

*Chromatography and Mass Spectrometry Laboratory (LaCEM) Research Group at the Institute of Chemistry of the Federal University of Goiás. Photo: Boniek G. Vaz.*

### *Analitica Latin America Expo welcomed nearly 10,000 visitors*

Analitica Latin America Expo, the most important trade show for the chemical industry in Latin America, was held on September 26–28, 2023, at the São Paulo Expo Exhibition & Convention Center, São Paulo, SP, Brazil, and set a new record for attendance: 9,708 attendees. This figure represents a 77% increase over the previous edition of the event.

With more than 300 exhibitors, Analitica Latin America Expo is back to being a biennial event and the next one has already been scheduled. It will take place between September 23 and 25, 2025, at the São Paulo Expo Exhibition & Convention Center.

Companies have noticed an increase in the number of visitors to their stands. The creation of new contacts and the generation of business is a common point cited by most exhibitors and visitors alike.

The interest in signing new contracts was also reflected in the Business Roundtable session organized by NürnbergMesse Brasil, the show's organizer. The Business Roundtable brought together 67 companies, 20 sellers, and 47 buyers, and generated an audited value of R$ 14.4 million in just two hours of meetings. "This is what makes our event different. By bringing together a qualified audience and focusing on sectors that involve the entire analytical chemical industry chain, we can generate relevant connections that move the market." explained Nadja Bento.
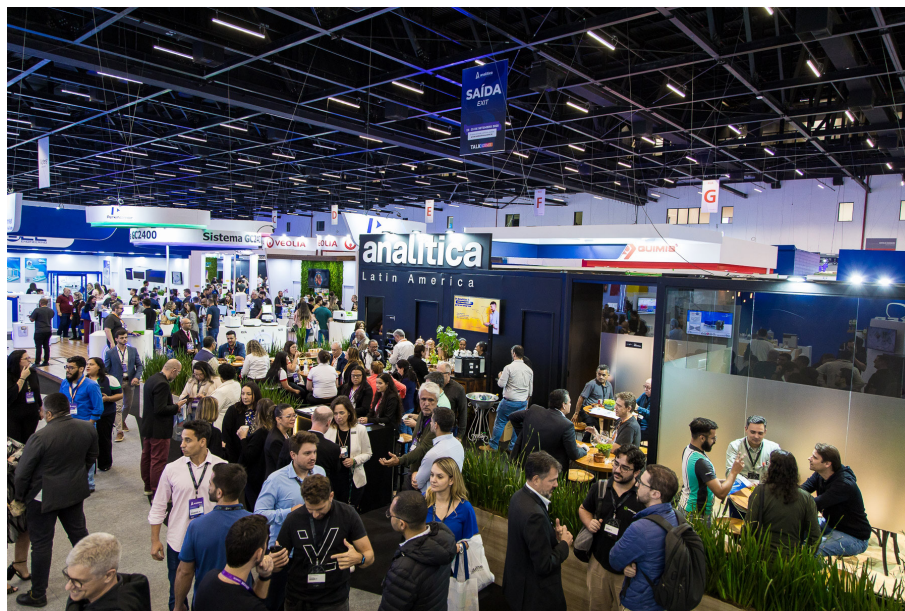
*Visitors walking around the Analitica Latin America Exposition. Photo: ALA Press Office.*

During the event, suppliers, distributors, and manufacturers from the laboratory technology, biotechnology, and quality control sectors presented the latest news and trends in the analytical chemistry industry to visitors.

**Nova Analítica,** founded in 1992, was present at the exhibition and presented its products. Nova Analítica's objective is to promote and guarantee customer satisfaction, meeting, or exceeding expectations with the quality of its products and services. To achieve this, Nova Analítica is committed to supplying the best equipment and accessories for laboratories, manufactured by internationally renowned companies, and to providing technical and commercial support to meet the needs of each customer, however specific or complex they may be. Read more.

**Thermo Fisher Scientific,** a world leader in scientific products and solutions, was also present at the exhibition. In Brazil, more than 500 employees, from operations to customer service, reinforce the company's scientific focus. Thermo Fisher Scientific's mission is to enable customers to make the world healthier, cleaner, and safer by accelerating life science research, solving complex analytical challenges, improving patient diagnosis, and increasing laboratory productivity. Read more.

**Milestone,** founded in 1988 as the first specialized laboratory instrument manufacturer to focus on advanced microwave technology for sample preparation, with over 50 patents and 20,000 users worldwide, was also present at the exhibition. Read more.

**Corning Incorporated,** a global leading innovator in materials science, developing products for optical communications, mobile consumer electronics, display technologies, automotive, and life sciences, presented Videodrop at the Analitica Latin America Expo. "Videodrop is a device that revolutionizes real-time nanoparticle detection and analysis. It can analyze a sample in less than 60 seconds, requiring only a single drop of 5 to 10 microliters of material for testing. Videodrop is designed to accelerate the research, development, and production of drugs, vaccines, and cell and gene therapies. The new product is easy to use, fast and reliable, and should arrive in Brazil very soon, promising to optimize the process in several laboratories." said Ricardo Artur Vian, Corning's Quality and Technical Support Coordinator in Latin America. Read more.

**Waters Corporation,** a world leader in specialty measurement focused on improving the health and well-being of people through the application of advanced analytical technologies and industry-leading scientific expertise, has introduced the Aliance iS HPLC system. This product is based on robust technology but applied in a much more modern, intuitive way that eliminates up to 40% of common errors in a research center. Read more.

### *SENAI Mobile Schools*

One of the novelties presented at this year's Analitica Latin America Expo was the unprecedented partnership with the National Industrial Learning Service – SENAI. An absolute hit with the public, nearly 700 visitors visited the trucks that housed the Mobile Schools of Nanotechnology and Industry 4.0. With this initiative, visitors and exhibitors were able to see how these mobile classrooms work and explore the equipment that students have access to.

SENAI's mobile schools offer short, customized courses for companies throughout the state of São Paulo. "The courses offered by SENAI are in areas of the future, both for the young people who come to us and for industry that needs skilled workers. Managers are already aware of the need to add digital transformation to industrial parks.", said Vinicius Ferreira, professor of Industry 4.0 at SENAI.



*Nearly 700 visitors passed by the trucks with the Mobile Schools of Nanotechnology and Industry 4.0. Photo: ALA Press Office.*

### **"Cromatografando"**

Another new attraction to the 2023 edition of Analitica Latin America Expo was the presence of Miller Pulito Rufino, a chemist and specialist in liquid chromatography and founding partner of "Cromatografando". Rufino has more than 15,000 followers on Instagram and almost 6,000 subscribers on his YouTube channel, and he was very much in demand at the Expo. The content that Rufino posts on his social networks aims to make chromatography easier to understand. "About 600 people stopped by the booth to talk to me. I didn't expect that, it was amazing." said Rufino. In addition to interacting with visitors and answering their questions, Rufino also highlighted the main chromatography solutions on display at the Expo. This was a unique opportunity for those interested to observe the operation of many instruments.

Source: Analitica Latin America Press Office

**BrJAC**

## FEATURE

# BrJAC promoted a Panel Session to Celebrate the achievement of Journal Impact Factor$_{2022}$ of 0.7

On September 27, 2023, the *Brazilian Journal of Analytical Chemistry* held a panel session during the Analitica Latin America Expo and Conference, at the São Paulo Expo, São Paulo, SP, Brazil. The panel session began at 9 a.m. with an opening conference presentation by Prof. Dr. Marco Aurélio Zezzi Arruda, BrJAC's editor-in-chief, who highlighted important steps in BrJAC's trajectory, from its beginnings in 2010 to the present. "The achievement of Impact Factor 0.7 results from the journal's ethics and seriousness. It makes the articles published in the journal even more valuable, which contributes to the development of the (Bio)Analytical Chemistry segment.", said Dr. Arruda. Afterwards, the journal's first editor-in-chief Prof. Dr. Lauro Kubota contextualized the time in which BrJAC was created and explained the journal's goal and the initial composition of its editorial board.
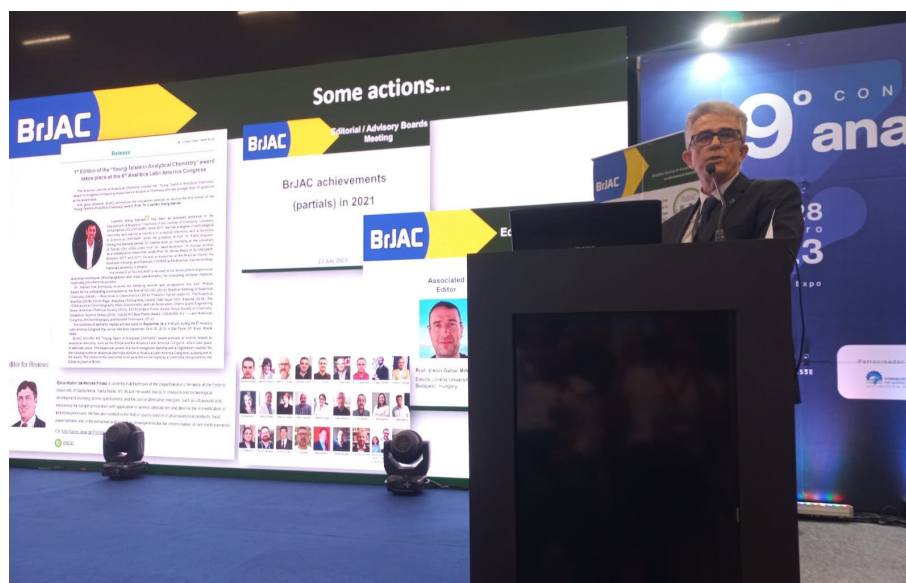


*Prof. Dr. Marco Aurélio Zezzi Arruda, BrJAC's editor-in-chief, presenting the opening conference.*

The "Young Talent in Analytical Chemistry" award, created by BrJAC to recognize outstanding young researchers in (Bio)Analytical Chemistry, was then presented. The winner of the 2023 award was **Prof. Dr. Boniek Gontijo Vaz**, who has a degree in Chemistry from the Federal University of São Carlos (2007), a master's degree in chemistry from the State University of Campinas (2009) and a PhD in science from the State University of Campinas (2011). Dr. Vaz is currently an Associate Professor at the Institute of Chemistry of the Federal University of Goiás (IQ-UFG), General Secretary of the Latin American Association of Organic Geochemistry (ALAGO) since 2018, and Associate Editor of the journal *Quimica Nova*. He also coordinates the Chromatography and Mass Spectrometry Laboratory (LaCEM) at IQ-UFG. After receiving the award, Dr. Vaz presented a lecture entitled, "The Art of Molecular Characterization: Advances and Applications of High-Resolution Mass Spectrometry".

Afterwards, Déborah Maria Assis Dias, Regional Solutions Consultant, Web of Science Group, Clarivate Analytics, presented a talk entitled, "Getting to Know Journal Citation Reports". Déborah Dias has more than 30 years of experience in training and support and has participated in symposia and conferences in the area of bibliometrics and analysis of scientific production, as well as analysis of journal visibility.

*Déborah M. A. Dias (Clarivate Analytics) presenting a talk entitled "Getting to Know Journal Citation Reports".*



To close the panel session, which was attended by around 50 people, there was a round table to discuss the topic "Open Access Scientific Journals". The round table mediator was Dr. Arruda, and the discussion was held by professors Dr. Emanuel Carrilho (São Carlos Institute of Chemistry, University of São Paulo), Dr. Leandro Hantao (Institute of Chemistry, University of Campinas) and Dr. Lauro Kubota (Institute of Chemistry, University of Campinas).

*Dr. Lauro Kubota, Dr. Emanuel Carrilho, Dr. Leandro Hantao and Dr. Arruda. Round table discussion on "Open Access Scientific Journals".*

"The Impact Factor is an achievement not only for the journal itself but mainly for national and international (Bio)Analytical Chemistry. This is just the beginning of a new journey and a new reality for BrJAC, and the perspective is one of the best. Now is the time to celebrate and then continue working even harder to make BrJAC grow in all its fullness.", said Dr. Arruda.

Writing by: Lilian Freitas, BrJAC Publisher
Photos: BrJAC

BrJAC

PDF

# Simultaneous Digestion of Food Samples for Trace Element Analysis

*Mixed-batch digestion of large sample amounts for high productivity and improved detection limits*

This report was extracted from a Milestone Industry Report on ultraWAVE / FOOD

## INTRODUCTION

Growing awareness and concern regarding food safety is reflected in the tightening of regulations governing toxic elements and compounds in food. Many toxic elements such as As, Hg, Cd, Pb etc. are routinely monitored, while minerals that are beneficial/essential to human health such as Se, Na, Mg, K, Ca, etc., are also measured. Traditional sample preparation techniques for food include hot block and closed-vessel microwave digestion.

Hot block digestions are time consuming, suffer from airborne contamination, poor digestion quality, and poor recovery of volatile compounds.

Closed-vessel microwave digestion has proven to be an effective technique with fast, complete digestions, a clean environment, and superior recovery of volatile compounds.

Milestone's innovative ultraWAVE with Single Reaction Chamber (SRC) technology further improves upon closed-vessel microwave digestion, by simplifying the sample preparation step, and providing fast, easy, effective, and the highest quality digestions of any food matrix with a single digestion method.

## EXPERIMENTAL

In this industry report, a recovery study was performed on certified reference materials and pharmaceutical samples spiked with a multielement standard (impurities according to ICH Q3D) to demonstrate the efficacy of the ultraWAVE in the preparation of mixed samples from 0.5 g to 2 g in a single digestion program.

### Instrumentation

The ultraWAVE is designed with a 1 Liter reactor, capable of operating at very high temperature and pressure (300 °C and 199 bar respectively). This capability ensures complete digestion of even the largest sample sizes (up to 3-5 g) as well as highly reactive and difficult-to-digest samples.

For the first time, a microwave digestion system ensures equal temperature and pressure conditions in all positions, even when different samples and/or chemistries are used. This results in superior digestion capabilities, higher productivity and better workflow for the lab.

The ultraWAVE's base load and positive pressure load prior to heating generates an equilibrium of temperature and pressure in each position, thus avoiding sample/elemental loss and cross contamination.

Samples can be weighed directly into disposable glass vials, eliminating the cleaning step. The easy handling of the vials and racks greatly reduces the operator time and associated labor costs.

**Figure 1.** Milestone's ultraWAVE.
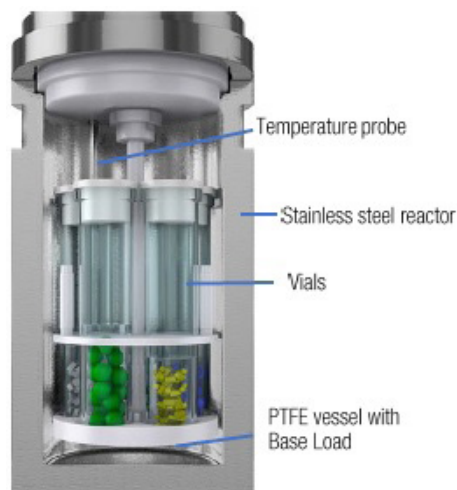


**Figure 2.** Schematic of the ultraWAVE's single reaction chamber (SRC).

## *Samples*

**Table 1.** Acid used: 5 mL of $HNO_3$ 67% and 0.5 mL of HCl 37%

| Reference Material Code | Sample name |
|---|---|
| NIST 1567b | Wheat flour |
| NIST1568b | Rice Flour |
| NIST 1515 | Apple Leaves |
| NIST 1573a | Tomato Leaves |

## *Procedure and method*

Sample weights up to 1.0 g for each of the flour CRMs (NIST 1567b, NIST 1568b) and up to 0.5 g for each of the other sample types (NIST 1515, NIST 1573a) were accurately weighed into PTFE vials (quartz and disposable glass vials are also available). Five mL of $HNO_3$ 67% and 0.5 mL of HCl 37% (electronics (EL) grade acids, Kanto Chemicals) were added to the PTFE vials. A base load of 130 mL DI $H_2O$ and 5 mL $HNO_3$ 67% was added into the 1 Liter PTFE vessel. The analysis was performed with a Triple Quadrupole ICP-MS.

**Table 2.** UltraWAVE digestion heating programs for simultaneous digestion of four CRM food samples

| Step | Time | Power (W) | Temp T1 (°C) | Temp T2 (°C) | Pressure (bar) |
|---|---|---|---|---|---|
| 1 | 00:10:00 | 800 | 110 | 70 | 90 |
| 2 | 00:10:00 | 1200 | 180 | 70 | 90 |

**Table 2.** UltraWAVE digestion heating programs for simultaneous digestion of four CRM food samples (continuation)

| Step | Time | Power (W) | Temp T1 (°C) | Temp T2 (°C) | Pressure (bar) |
|------|------|-----------|--------------|--------------|----------------|
| 3 | 00:10:00 | 1500 | 220 | 70 | 120 |
| 4 | 00:10:00 | 1500 | 220 | 70 | 120 |



**Figure 2.** Internal temperature (red), external temperature (orange), pressure (blue) and power (black) graphs.

**Table 3.** Triple Quadrupole ICP-MS operating conditions

| Parameter | Setting | |
|-----------|---------|---|
| Cell mode | He mode | O$_2$ mode |
| Scan type | Single Quad | MS/MS |
| Plasma conditions | UHM-4 | |
| RF power (W) | 1600 | |
| Sampling depth (mm) | 10 | |
| Carrier gas flow rate (L/min) | 0.77 | |
| Dilution gas flow rate (L/min) | 0.15 | |
| Extract 1 (V) | 0 | |
| Extract 2 (V) | -250 | |
| Omega bias (V) | -140 | |
| Omega lens (V) | 8.8 | |
| Cell gas flow (mL/min) | 5.5 | 0.3 (20% of full scale) |
| KED (V) | 5 | -7 |

## RESULTS AND DISCUSSION

The ultraWAVE system performed simultaneous digestion of four different reference materials with different sample amounts. The total time from weighing to analysis was less than one hour.

As shown in Figure 2, the system automatically adjusts the microwave power to follow the temperature profile.

Digestion of reactive samples such as oil, butter and other high fat content samples require precise, accurate and direct temperature control, which is especially important to control exothermic reactions and to ensure complete digestion.

The data shows excellent recoveries for all elements including volatiles, which is reflected in Tables 4 to 7.

**Table 4.** Results for NIST 1567b, Wheat flour, n=24

| Element | Measured Solution Concentration (µg/L) | RSD (%) | Calculated Sample Concentration (mg/kg) | Certified Concentration (mg/kg) | Recovery (%) |
|---|---|---|---|---|---|
| 23 Na | 65.2 | 2.3 | 6.50±0.15 | 6.71±0.21 | 97 |
| 24 Mg | 3842 | 1.6 | 383±6 | 398±12 | 96 |
| 27 Al | 39 | 2.8 | 3.9±0.1 | 4.4±1.2 | 88 |
| 31->47 P | 12936 | 2.0 | 1291±26 | 1333±36 | 97 |
| 32->48 S | 15496 | 2.2 | 1546±34 | 1645±25 | 94 |
| 39 K | 12700 | 2.3 | 1267±29 | 1325±20 | 96 |
| 44 Ca | 1871 | 1.8 | 186.7±3.4 | 191.4±3.3 | 98 |
| 51 V | 0.10 | 8.1 | 0.010±0.001 | 0.01* | 100 |
| 55 Mn | 86 | 1.7 | 8.54±0.14 | 9.00±0.78 | 95 |
| 56 Fe | 142 | 1.6 | 14.20±0.22 | 14.11±0.33 | 101 |
| 63 Cu | 19 | 1.6 | 1.94±0.03 | 2.03±0.14 | 96 |
| 66 Zn | 112 | 1.9 | 11.17±0.21 | 11.61±0.26 | 96 |
| 75 As | 0.047 | 16.5 | 0.0046±0.001 | 0.0048±0.0003 | 97 |
| 75->91 As | 0.049 | 19.4 | 0.0049±0.001 | 0.0048±0.0003 | 101 |
| 78 Se | 11.5 | 4.2 | 1.15±0.05 | 1.14±0.10 | 101 |
| 78->94 Se | 11.8 | 1.9 | 1.17±0.02 | 1.14±0.10 | 103 |
| 85 Rb | 6.54 | 1.8 | 0.652±0.012 | 0.671±0.012 | 97 |
| 95 Mo | 4.60 | 2.1 | 0.459±0.009 | 0.464±0.034 | 99 |
| 111 Cd | 0.239 | 5.7 | 0.0238±0.0014 | 0.0254±0.0009 | 94 |
| 118 Sn | 0.0355 | 12.8 | 0.0035±0.0005 | 0.003* | 118 |
| 202 Hg | 0.0066 | 11.3 | 0.0007±0.0001 | 0.0005* | 131 |
| 208 Pb | 0.0937 | 4.4 | 0.0094±0.0004 | 0.0104±0.0024 | 90 |

*Reference value.

**Table 5.** Results for NIST 1568b Rice Flour, n = 24

| Element | Measured Solution Concentration (µg/L) | RSD (%) | Calculated Sample Concentration(mg/kg) | Certified Concentration (mg/kg) | Recovery (%) |
|---|---|---|---|---|---|
| 23 Na | 65.6 | 3.2 | 6.54±0.28 | 6.74±0.19 | 97 |
| 24 Mg | 5454 | 1.5 | 543±8 | 559±10 | 97 |
| 27 Al | 40.3 | 3.3 | 4.01±0.13 | 4.21±0.34 | 95 |
| 31->47 P | 15162 | 2.8 | 1510±43 | 1530±40 | 99 |
| 32->48 S | 11369 | 2.5 | 1133±28 | 1200±10 | 94 |
| 39 K | 12371 | 2.0 | 1233±24 | 1282±11 | 96 |
| 44 Ca | 1158 | 2.1 | 115.3±2.5 | 118.4±3.1 | 97 |
| 51 V | 182.3 | 1.0 | 18.2±0.2 | 19.2±1.8 | 95 |
| 55 Mn | 75.4 | 1.0 | 7.51±0.08 | 7.42±0.44 | 101 |
| 56 Fe | 0.173 | 1.7 | 0.0173±0.0003 | 0.0177±0.0005* | 98 |
| 63 Cu | 22.7 | 1.0 | 2.26±0.02 | 2.35±0.16 | 96 |
| 66 Zn | 191.7 | 1.4 | 19.10±0.26 | 19.42±0.26 | 98 |
| 75 As | 2.97 | 1.4 | 0.296±0.004 | 0.285±0.014 | 104 |
| 75->91 As | 3.01 | 1.7 | 0.300±0.005 | 0.285±0.014 | 105 |
| 78 Se | 3.4 | 8.9 | 0.341±0.030 | 0.365±0.029 | 93 |
| 78->94 Se | 3.5 | 3.8 | 0.352±0.013 | 0.365±0.029 | 96 |
| 85 Rb | 61.1 | 1.1 | 6.088±0.069 | 6.198±0.026 | 98 |
| 95 Mo | 13.96 | 1.2 | 1.391±0.017 | 1.451±0.048 | 96 |
| 111 Cd | 0.201 | 4.9 | 0.0201±0.0010 | 0.0224±0.0013 | 90 |
| 118 Sn | 0.060 | 7.4 | 0.0060±0.0004 | 0.005±0.001* | 121 |
| 202 Hg | 0.0529 | 2.1 | 0.0053±0.0001 | 0.0059±0.0004 | 89 |
| 208 Pb | 0.068 | 3.0 | 0.0068±0.0002 | 0.008±0.003* | 85 |

*Reference value.

**Table 6.** Results for NIST 1515 Apple leaves, n=24

| Element | Measured Solution Concentration (μg/L) | RSD (%) | Calculated Sample Concentration (mg/kg) | Certified Concentration (mg/kg) | Recovery (%) |
|---|---|---|---|---|---|
| 11 B | 141 | 2.9 | 28±0.8 | 27±2 | 104 |
| 23 Na | 196 | 1.6 | 39.1±0.6 | 24.4±1.2 | 160*[1] |
| 24 Mg | 14083 | 1.3 | 2812±36 | 2710±80 | 104 |
| 27 Al | 1458 | 1.6 | 291±5 | 286±9 | 102 |
| 31->47 P | 8088 | 2.2 | 1615±35 | 1590* | 102 |
| 32->48 S | 9211 | 1.4 | 1839±26 | 1800* | 102 |
| 39 K | 80429 | 2.2 | 16057±361 | 16100±200 | 100 |
| 44 Ca | 74060 | 1.2 | 14786±172 | 15260±1500 | 97 |
| 51 V | 1.20 | 2.8 | 0.24±0.01 | 0.26±0.03 | 92 |
| 52 Cr | 1.3 | 1.4 | 0.25±0.00 | 0.3* | 85 |
| 55 Mn | 265 | 1.0 | 53±1 | 54±3 | 98 |
| 56 Fe | 379 | 0.8 | 76±1 | 80* | 95 |
| 59 Co | 0.44 | 1.5 | 0.088±0.001 | 0.09* | 98 |
| 60 Ni | 4.4 | 1.7 | 0.88±0.02 | 0.91±0.12 | 97 |
| 63 Cu | 28.2 | 1.0 | 5.62±0.06 | 5.64±0.24 | 100 |
| 66 Zn | 60.3 | 0.9 | 12.0±0.1 | 12.5±0.3 | 96 |
| 75->91 As | 0.2 | 3.7 | 0.036±0.001 | 0.038±0.007 | 94 |
| 78-> 94 Se | 0.271 | 13.8 | 0.054±0.008 | 0.050±0.009 | 108 |
| 85 Rb | 46.3 | 0.9 | 9.2±0.1 | 9* | 103 |
| 88 Sr | 123.0 | 1.0 | 25±0 | 25±2 | 98 |
| 95 Mo | 0.44 | 5.3 | 0.088±0.005 | 0.094±0.013 | 94 |
| 111 Cd | 0.06 | 7.0 | 0.013±0.001 | 0.014* | 91 |
| 121 Sb | 0.06 | 4.6 | 0.011±0.001 | 0.013* | 85 |
| 138 Ba | 245 | 1.9 | 49±1 | 49±2 | 100 |
| 202 Hg | 0.21 | 2.0 | 0.041±0.001 | 0.044±0.004 | 93 |
| 208 Pb | 2.3 | 1.3 | 0.452±0.006 | 0.470±0.024 | 96 |
| 232 Th | 0.14 | 2.2 | 0.028±0.001 | 0.03* | 93 |
| 238 U | 0.034 | 3.7 | 0.0068±0.0003 | 0.006* | 113 |

*Reference value.

*[1]The measured Na result was high compared to the reference value; the same result was obtained from a repeated analysis of the same solution, so a spike recovery test was performed for confirmation. The spike recovery result was good (recovery: 99%), suggesting that the original sample had suffered Na contamination.

**Table 7.** Results for NIST 1573a Tomato Leaves, n = 24

| Element | Measured Solution Concentration (µg/L) | RSD (%) | Calculated Sample Concentration (mg/kg) | Certified Concentration (mg/kg) | Recovery (%) |
|---|---|---|---|---|---|
| 11 B | 167 | 1.9 | 33.3±0.6 | 33.3±0.7 | 100 |
| 23 Na | 613 | 2.5 | 122±3 | 136±4 | 90 |
| 24 Mg | 57311 | 2.0 | 11412±225 | 12000* | 95 |
| 27 Al | 2573 | 2.4 | 512±12 | 598±12 | 86 |
| 31->47 P | 10928 | 2.7 | 2176±59 | 2160±40 | 101 |
| 32-< 48 S | 48387 | 1.4 | 9635±131 | 9600* | 100 |
| 39 K | 134250 | 2.2 | 26732±591 | 27000±500 | 99 |
| 44 Ca | 243939 | 1.4 | 48574±671 | 50500±900 | 96 |
| 51 V | 4.0 | 2.2 | 0.792±0.017 | 0.835±0.010 | 95 |
| 52 Cr | 9.3 | 1.6 | 1.85±0.03 | 1.99±0.06 | 93 |
| 55 Mn | 1236.5 | 1.5 | 246±4 | 246±8 | 100 |
| 56 Fe | 1843.3 | 1.7 | 367±6 | 368±7 | 100 |
| 59 Co | 2.8 | 1.4 | 0.55±0.01 | 0.57±0.02 | 96 |
| 60 Ni | 7.9 | 1.9 | 1.56±0.03 | 1.59±0.07 | 98 |
| 63 Cu | 23.7 | 1.5 | 4.71±0.07 | 4.70±0.14 | 100 |
| 66 Zn | 149.4 | 1.5 | 29.8±0.5 | 30.9±0.7 | 96 |
| 75 As | 0.7 | 2.3 | 0.141±0.003 | 0.112±0.004 | 126 |
| 75->91 As | 0.6 | 1.7 | 0.112±0.002 | 0.112±0.004 | 100 |
| 78-> 94 Se | 0.31 | 11.2 | 0.061±0.007 | 0.054±0.003 | 113 |
| 85 Rb | 69.7 | 1.2 | 13.88±0.16 | 14.89±0.27 | 93 |
| 88 Sr | 421.0 | 1.3 | 84±1 | 85* | 99 |
| 95 Mo | 2.1 | 2.8 | 0.42±0.01 | 0.46* | 91 |
| 107 Ag | 0.09 | 9.1 | 0.018±0.002 | 0.017* | 104 |
| 111 Cd | 7.4 | 1.4 | 1.47±0.02 | 1.52±0.04 | 97 |
| 121 Sb | 0.28 | 3.4 | 0.055±0.002 | 0.063±0.006 | 88 |
| 138 Ba | 302.8 | 2.1 | 60.3±1.3 | 63* | 96 |
| 202Hg | 0.15 | 2.4 | 0.030±0.001 | 0.034±0.004 | 88 |
| 232 Th | 0.52 | 2.1 | 0.104±0.002 | 0.12* | 87 |
| 238 U | 0.14 | 2.3 | 0.029±0.001 | 0.035* | 81 |

*Reference value.

## CONCLUSION

The data illustrated in this industry report demonstrates the ultraWAVE's ability to provide full recovery of all elements, while avoiding cross contamination even when different samples and sample weights are digested in the same run. The ultraWAVE's ability to simultaneously digest different sample types, easy sample handling and superior throughput surpass the capabilities of hot blocks and traditional rotor-based microwave digestion systems. Its superior capabilities in terms of processing mixed samples, large sample amounts and ease of use provide unmatched productivity. The superior digestion quality achieved at high temperature and pressure maximizes the performance of the ICP-MS by reducing interferences, blanks and overall maintenance.

***About Milestone***

    At Milestone we help chemists by providing the most innovative technology for metals analysis, direct mercury analysis and the application of microwave technology to extraction, ashing and synthesis. Since 1988 Milestone has helped chemists in their work to enhance food, pharmaceutical and consumer product safety, and to improve our world by controlling pollutants in the environment.

*This Sponsor Report is the responsibility of Milestone.*

**BrJAC**

## *SPONSOR REPORT*

This section is dedicated for sponsor responsibility articles.

# Improving Targeted Peptide Quantification

*Combining a TSQ Altis with a FAIMS Pro interface for peptides in complex matrices*

**Michael Volný, Cornelia L. Boeser, Michael W. Belford, Claudia P. B. Martins, Mary L. Blackburn**

*Thermo Fisher Scientific, San Jose, CA*

This report was extracted from the Thermo Scientific Application Note 65902

## GOAL

When quantifying peptides using LC-MS/MS, background interferences often negatively impact limit of quantification (LOQ). Here we show that by using the Thermo Scientific™ FAIMS Pro™ interface in combination with nanoflow chromatography and triple-stage quadrupole (TSQ) technology, the background can be reduced significantly, which leads to increased signal-to-noise (S/N) and improved dynamic range and LOQ.

## INTRODUCTION

Characterization and accurate quantification of proteins in complex matrices is becoming increasingly important for a variety of applications in the pharma/biopharma sector. Targeted quantitative assays are used in PKPD, discovery, regulated bioanalysis, and therapeutic drug research. LC-MS/MS can provide quantitative information about proteins that is complementary to traditional techniques, such as ligand-binding assays (LBA). In some cases, proteins and native peptides, such as insulin, renin, and IGF-1, are analyzed directly; for instance, large therapeutic peptides are often quantified by LC-MS/MS without enzymatic digestion. But more often, protein quantification by LC-MS/MS is based on identification of signature peptides specific for the given protein of interest. After enzymatic digestion of the protein, the quantitative analysis of resulting peptides is performed, usually in the presence of spiked isotopically labeled peptides as internal standards. This approach, common for protein quantification by LC-MS/MS, is complicated by the fact that analyte peptides can be present across a wide concentration range and in complex matrices that contain many other coeluting peptides as well as other chemical background.



**Figure 1.** EASY-Spray ion source and FAIMS Pro interface mounted to TSQ Altis triple quadrupole mass spectrometer.

Triple quadrupole mass spectrometers operated in selected reaction monitoring (SRM) mode typically offer the most competitive LOQs for a large spectrum of analytes in a variety of matrices. The Thermo Scientific™ TSQ Altis™ triple quadrupole mass spectrometer (Figure 1) offers excellent sensitivity, speed, and dynamic range and is the platform of choice for the analysis of low abundant peptides. In a typical peptide quantification experiment by LC-MS/MS, the resolving power of reversed-phase chromatography is combined with selectivity and sensitivity of the mass spectrometer to extend the quantitative dynamic range. However, the LOQ is often negatively impacted by background chemical noise. These background interferences cannot be removed by LC separation alone and often overlap with the target analyte on multiple SRM transitions. This can limit the utility of an assay.

The FAIMS Pro interface is a differential ion mobility device, which can be used to selectively transmit ions of interest while suppressing transmission of interfering compounds. Selectivity is achieved by alternating between high and low electric field strengths applied to a set of cylindrical electrodes. Depending on the structural orientation of an ion and loosely on its mass and charge, ions experience different mobilities through the electrode gap while the electric field of alternating strength is applied. By applying an additional compensation voltage (CV), ions of specific mobility can be transmitted through the high field asymmetric waveform ion mobility spectrometry (FAIMS) device, while interfering ions are prevented from passing through. The respective CV value that allows transmission of a specific analyte of interest can be optimized for each analyte and becomes an additional parameter in the SRM table for each precursor ion. The additional separation provided by the FAIMS Pro interface is orthogonal to LC and MS, and results in improved S/N for analytes of interest and therefore better quantitative performance.

## EXPERIMENTAL

A PRTC peptide standard (Thermo Scientific™ Pierce™ Peptide Retention Time Calibration Mixture, P/N 88321) was spiked into Thermo Scientific™ Pierce™ HeLa protein digest (Pierce catalog number 1862824) at concentrations ranging from 0.001 to 100 fmol/µL. The Thermo Scientific™ Pierce™ LC-MS/MS System Suitability Standard (7 x 5 Mix, P/N 88320) was prepared according to the manufacturer protocol to yield concentrations of 0.13–200 fmol/µL in 0.3 µg/µL digested plasma matrix. Angiotensin I standard (Sigma-Aldrich, St. Louis, MO) was prepared in 0.5 µg/µL digested plasma in concentrations ranging from 0.07 to 700 fmol/µL. For all analyses, 1 µL of each sample was injected onto a Thermo Scientific™ EASY-Spray™ column with integrated emitter (P/N ES800A) using a Thermo Scientific™ EASY-nLC™ 1200 system. A 40 min gradient was used at a flow rate of 200 nL/min. The column heater was set to 45 °C. The TSQ Altis instrument global settings are shown in Table 1. The peptides were detected as doubly charged ions and fragmented using optimized SRM transitions (4–5 per peptide). The FAIMS Pro interface was operated in normal resolution mode with no additional user gas. Data were analyzed using Thermo Scientific™ TraceFinder™ software.

**Table 1.** TSQ Altis triple quadrupole MS instrument settings

| Parameter | Value |
|---|---|
| Resolution | 0.7 (Q1 and Q3) |
| Cycle time | 1 s |
| RF lens | Calibrated |
| CID gas pressure | 1.5 mTorr |
| Ion transfer tube temperature | 325 °C |
| Spray voltage | 2,100 V |

### *FAIMS Pro compensation voltage optimization*

FAIMS Pro compensation voltage (CV) values for each peptide were optimized by infusing the neat standard peptide solution and using the CV scan tool in the Tune interface (available in Tune 3.1 and above). Optimum CV values were transferred into the method file and each peptide was analyzed at its respective optimum CV value to yield maximum transmission. If standards are not available, FAIMS CV values can be optimized by injection using either one of two strategies:

1. For assays involving only a small number of peptides, CV optimization can be done within 1–2 injections (depending on the number of precursors in the method). To achieve this, each precursor is entered into

the SRM table multiple times, depending on how many different CV values the user wants to compare. In each row, the precursor is entered with a slightly different precursor *m/z* value (for example, *m/z* 433.34, 433.33, 433.32, etc.) For each of these "pseudo-precursors", one CV value is assigned. It is sufficient to monitor only one product ion for CV optimization because the FAIMS Pro interface mounts between the ion source and the mass spectrometer inlet; hence, the additional selectivity is applied at the precursor level. For coarse optimization, the CV values should be distributed in 10 V steps, usually between -80 and -20 V. After execution of the optimization run, the optimum CV value range for each precursor is determined by comparing peak areas for each CV value. The number of necessary coarse optimization injections depends on the LC peak width, size of the peptide panel and the elution overlaps, and thus on the available cycle time. Once the approximate optimal value range has been determined, the exact optimal value can be found by probing values in a narrower range around the coarse CV optimum, for example in steps of 2–3 V. An example of optimization by injection is shown in Table 2 and Figure 2.

**Table 2.** Example of compensation voltage (CV) optimization by injection in 10 V steps. Peak areas indicate that the optimum CV is around -65 V. In the next injection the value can be optimized in more narrow steps around -65 V.

| Precursor *m/z* | Adjusted precursor for CV optimization | CV value | Peak area |
|---|---|---|---|
| 433.3 | 433.34 | -45 | 973 |
| | 433.33 | -55 | 9,765 |
| | 433.32 | -65 | 47,470 |
| | 433.31 | -75 | 386 |
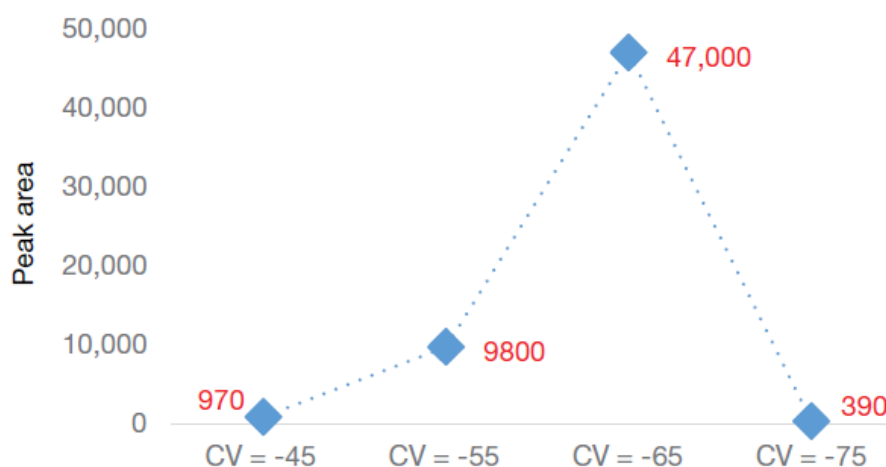


**Figure 2.** Integrated peak areas at different compensation voltage (CV) values.

2.  When assays involve a large number of precursors, not every precursor can be analyzed at multiple CV values within a few injections. In this case, multiple injections need to be performed, and each injection will be at one dedicated CV value global for all peptides. For example, injection 1 will be at a CV of -10 V, injection 2 will be at a CV of -15 V, etc. The CV optimum for each peptide will be determined based on peak area at each CV value.

## RESULTS AND DISCUSSION

### PRTC peptides

Figure 3a–d shows a comparison of peptide HVLTSIGEK at a level of 50 attomol on column in HeLa digest analyzed by the TSQ Altis mass spectrometer with and without the FAIMS Pro interface. Although the retention time can be determined by looking at the internal standard signal, at this concentration level the peak of the analyte cannot be properly integrated without use of the FAIMS Pro device. The additional level of selectivity that the FAIMS Pro interface provides removes the chemical background, which enables the detection and integration of the HVLTSIGEK peptide for quantitative determination. Without the FAIMS Pro device, HVLTSIGEK cannot be clearly distinguished from the background at levels below 100 attomol, while with the FAIMS Pro device, the peptide can be detected at 25 attomol.
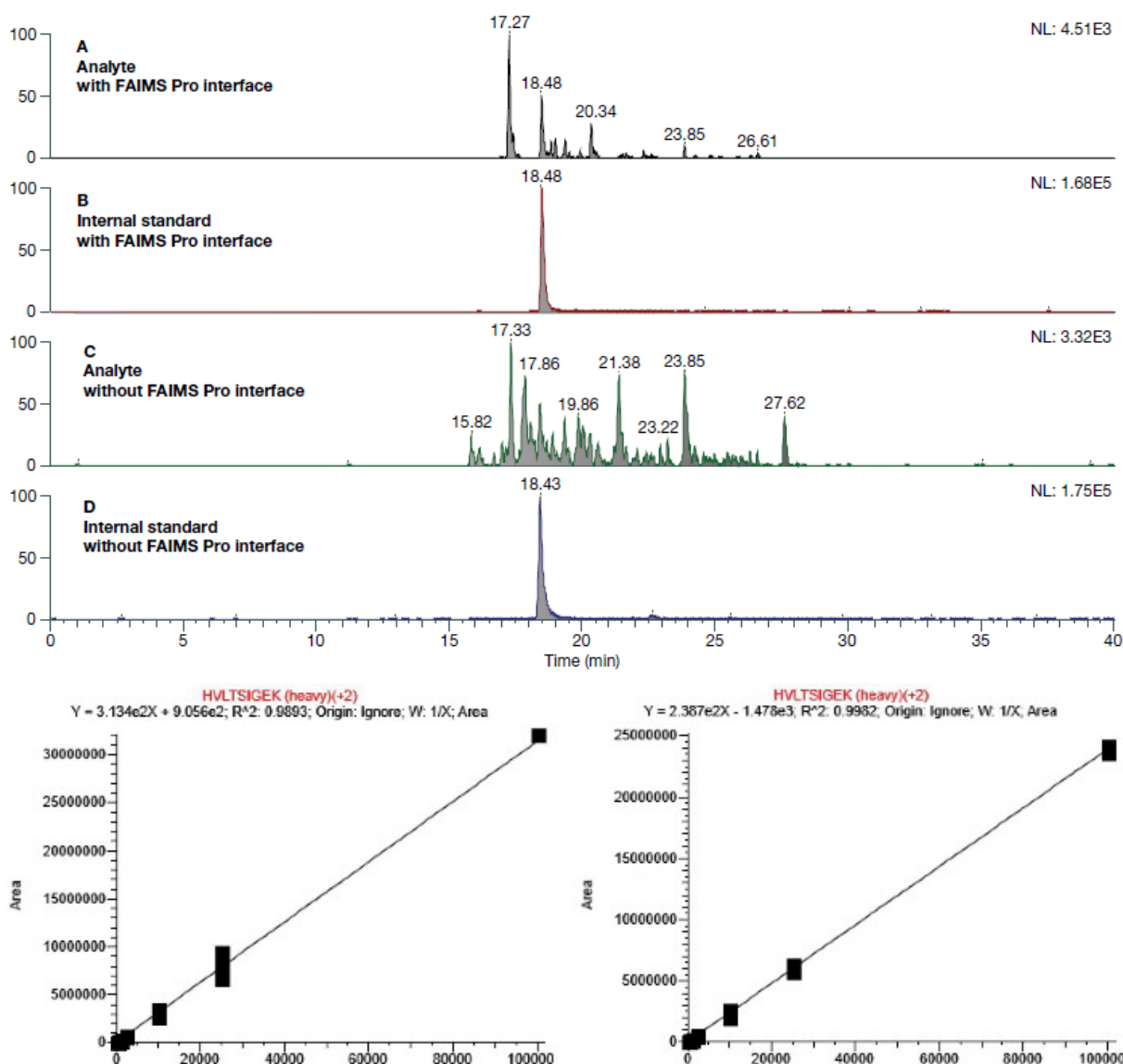


**Figure 3. Suppression of background noise by FAIMS Pro interface improves S/N.** Panel A shows a detectable peak of peptide HVLTSIGEK analyzed by TSQ Altis triple quadrupole mass spectrometer with the FAIMS Pro interface at 50 attomol on column. The retention time was confirmed by internal standard (Panel B). The same sample at the same concentration was analyzed without the FAIMS Pro interface. Strong background noise (Panel C) at the retention time determined by internal standard (Panel D) limits the S/N. Calibration curves are shown for the peptide HVLTSIGEK measured both with (Panel E), and without (Panel F), the FAIMS Pro interface.

*Angiotensin I (non-tryptic peptide)*

Peptide hormone angiotensin I (proangiotensin) was monitored by SRM assay in digested plasma as a doubly charged precursor ion at *m/z* 649.0 with five SRM transitions (*m/z* 583.5; 591.3; 784.4; 1000.6, and 1028.5). For the experiment with the FAIMS Pro interface, the device was optimized for maximum signal of the precursor ion by direct infusion. The optimum CV value for doubly charged angiotensin I was determined to be -56 V. Figure 4 shows angiotensin I chromatograms at various concentrations in plasma both with and without the FAIMS interface. At high on-column amounts (700 femtomol), there is no difference in the results obtained with and without the FAIMS Pro interface. This is because the absolute analyte signal is high enough to make noise practically irrelevant for peak integration and S/N value. However, as the analyte on-column amount decreases, the background noise becomes an important factor for data quality. Eventually, at 70 attomol of angiotensin I on-column, the signal is indistinguishable from the background without the FAIMS Pro interface. Utilization of the FAIMS Pro device removes background noise sufficiently enough that the peak can be detected and integrated at a level as low as 70 attomol.

To demonstrate system robustness, the 700 femtomol on column sample in 0.5 µg/µL digested plasma was injected 40 times over a period of two full days. Figure 5 shows excellent reproducibility of the 40 injections with an RSD of 9.9%. Despite the concentrated matrix, area counts were consistent throughout the experiment. No cleaning of the FAIMS electrodes or of the TSQ Altis inlet was performed during the experiment. Solvent blank injections were run after every 10 plasma injections to keep the column and emitter in good condition.
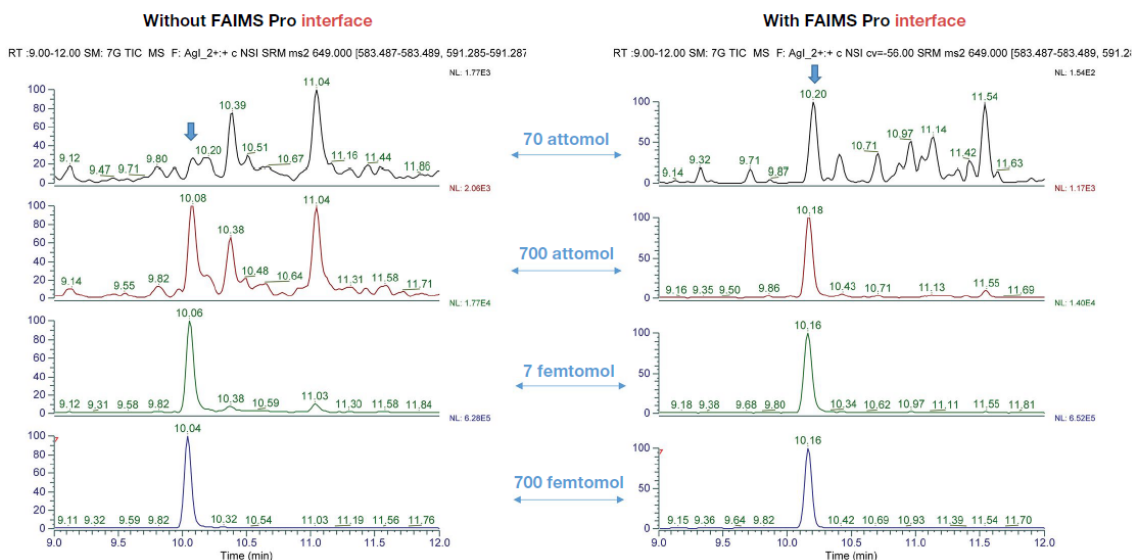


**Figure 4. Quantification of angiotensin I in digested plasma.** Combining the FAIMS Pro interface with an optimized CV value as part of the SRM table provides selective noise reduction, which results in a quantifiable signal (right panels) even at concentration levels where analyte signal is impacted by noise interference without FAIMS Pro interface (left panels).
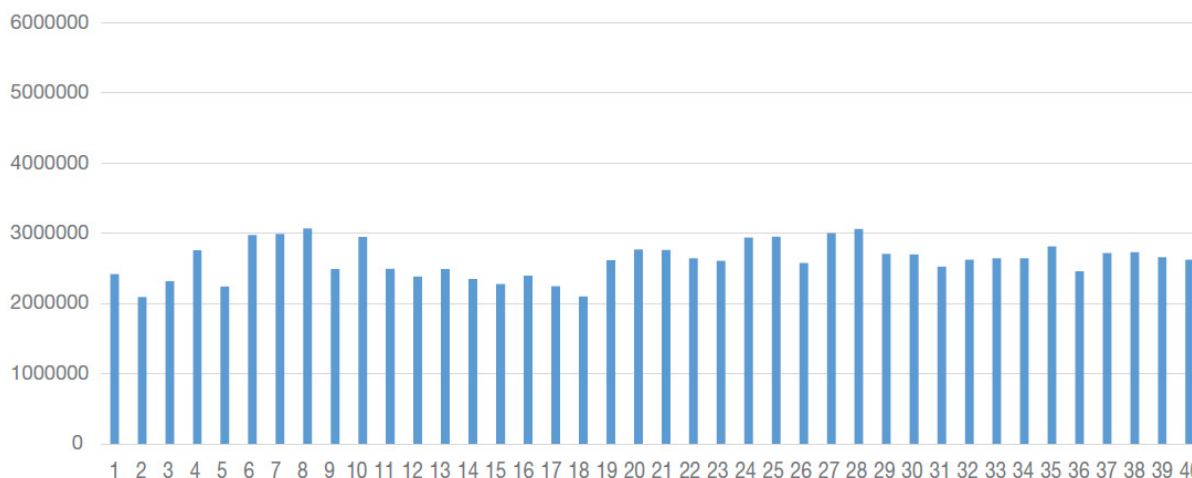
**Figure 5. 40 consecutive injections of angiotensin I in 0.5 µg/µL digested plasma were performed with the FAIMS Pro device on the TSQ Altis triple quadrupole mass spectrometer.** The overall % RSD was <10% across a 2-day experiment. (Thermo Fisher™ ChromaCare™ solution was injected every 10 analytical injections for column clean-up.)

*Pierce System Suitability Standard (7 x 5 peptide mix)*

The Pierce LC-MS/MS System Suitability Standard (7 x 5 mixture) contains seven peptides provided at five dilution levels, distinguished by differential isotopic labelling. Each concentration level has different labelling for each of the seven peptides (no heavy, 1 heavy, 2 heavy, 3 heavy, and 4 heavy labelled amino acids). Data from only one injection allows construction of five-point calibration curves for all seven analytes at once. The 7 x 5 mixture is intended to be used for testing LC-MS/MS systems for sensitivity, reproducibility, and response linearity. The 7 x 5 mixture prepared in 0.3 µg/µL digested plasma was analyzed on the TSQ Altis mass spectrometer with the FAIMS Pro interface using an optimized SRM method and optimized CV values for each of the seven peptides. Figure 6 shows linearity across the entire concentration range of the assay. Five repeated injections of the 7 x 5 standard were performed to assess robustness. The calculated % RSD of absolute peak areas showed very good reproducibility for all peptides (Table 3). This demonstrates that when using the FAIMS Pro interface, data is consistent and reproducible.

**Table 3.** % RSDs (absolute peak areas) for five replicate injections of seven peptides at five concentration levels (isotopologues included in the Pierce System Suitability Test)

| Peptide | 0.13 fmol [%RSD] | 0.5 fmol [%RSD] | 2 fmol [%RSD] | 20 fmol [%RSD] | 200 fmol [%RSD] |
|---------|------------------|-----------------|---------------|----------------|-----------------|
| ELASGLSFPVGFK | 6.1 | 8.9 | 10.6 | 10.8 | 7.4 |
| ELGQSGVDTYLQTK | 6.6 | 4.1 | 8.9 | 6.1 | 5.9 |
| GISNEGQNASIK | 6.1 | 8.1 | 8.7 | 5.6 | 5.9 |
| IGDYAGIK | 2.9 | 2.1 | 2.9 | 3.1 | 1.9 |
| LTILEER | 8.2 | 8.8 | 12.6 | 4.3 | 11.7 |
| SFANQPLEVVYS | 9.6 | 8.4 | 11.8 | 15.1 | 15.1 |
| TASEFDSAIAQDK | 4.8 | 3.8 | 3.8 | 2.9 | 3.5 |
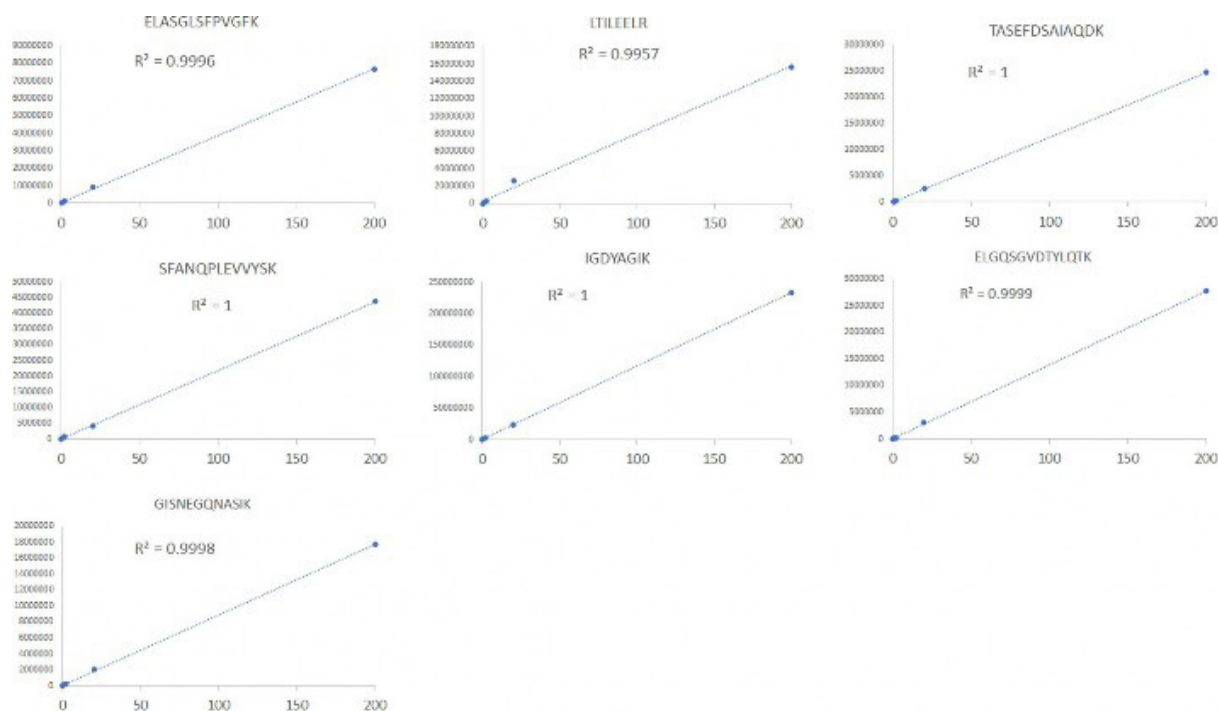
**Figure 6. The Pierce 7 x 5 System Suitability Test was used to evaluate the performance of the FAIMS Pro interface with the TSQ Altis triple quadrupole mass spectrometer.** The mixture was prepared according to manufacturer's protocol and 0.3 µg/µL digested plasma was used as a matrix.

*Isomeric interference*

The FAIMS Pro interface is a differential ion mobility device that utilizes separation principles orthogonal to both LC and MS. The main benefit of using the FAIMS Pro interface for targeted assays is the removal of background interferences and therefore an increase in S/N and improvement of LOQ. However, depending on the assay, isomeric species can exhibit different behavior inside the FAIMS electrodes. Differences in CV values can then be used to remove isobaric interference. An example is shown in Figure 7. Two isomeric peptides, one analyte and one unknown interference from the sample matrix, co-elute at very close retention times and have identical SRM transitions. For demonstration purposes, the analyte peptide was replaced by its labelled internal standard. In the standard assay without the FAIMS Pro interface, the unknown interfering peptide makes quantification impossible because its signal fully overlaps with the analyte peak. The FAIMS Pro device separates the isobaric peptides based on different CV values. At a CV value of -45 V, the analyte is transmitted with the same efficiency as without the FAIMS Pro interface. The background isobaric interference, however, is significantly suppressed (roughly by 20x, from 7000 to 300 intensity counts (Figure 7). This enables accurate quantification of the analyte of interest.
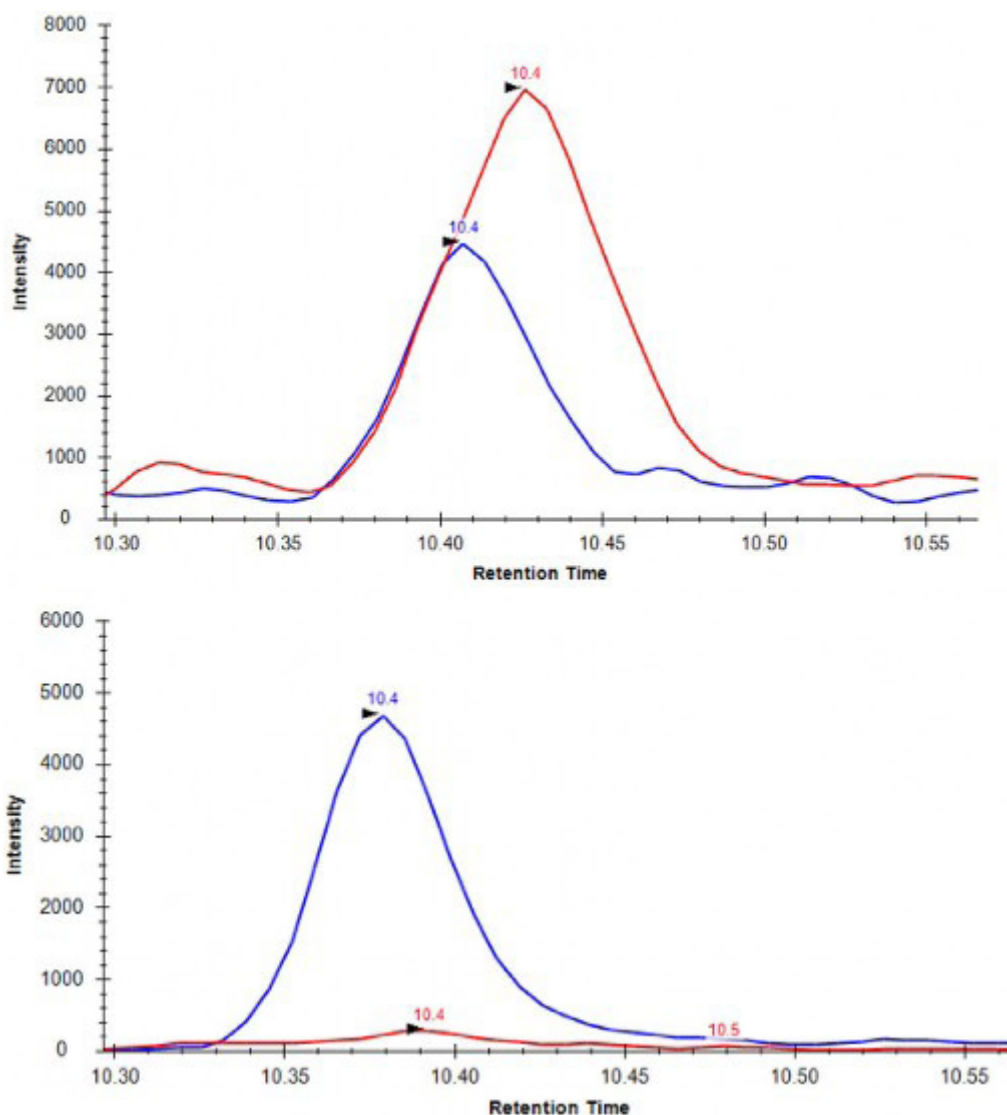
**Figure 7. FAIMS Pro interface suppresses interfering isomeric peptide species.** Two isomeric peptides, one analyte and one unknown interference from the sample matrix, co-elute at very close retention times and have identical SRM transitions. For demonstration purposes, the analyte peptide was replaced by its labelled internal standard to be distinguishable. Top: Standard assay without the FAIMS Pro interface. The interfering peptide (red) makes quantification impossible because its signal overlaps with the analyte peak (blue). Bottom: Using the FAIMS Pro interface at the optimized CV value of the analyte (blue), the interference (red) is sufficiently suppressed to enable quantification. Data processed in Skyline (University of Washington).

## CONCLUSION

The FAIMS Pro interface offers orthogonal precursor ion selectivity based on differential gas phase mobility. The compensation voltage (CV) setting determines which groups of ions pass the FAIMS Pro interface to the mass spectrometer. In targeted workflows on triple quadrupole mass spectrometers, the CV value is used as an additional parameter in the SRM table to selectively transmit precursor ions, while suppressing background interferences. The FAIMS Pro interface coupled to the TSQ Altis triple quadrupole mass spectrometer improves peptide quantification due to reduced noise and removal of co-eluting interferences. Utilization of the FAIMS Pro interface is robust and analyte signals are reproducible. FAIMS technology can significantly improve LOQs for assays where noise is the limiting factor. Because

of its capabilities to remove background ions and reduce the level of interferences, combining the FAIMS Pro interface with the TSQ Altis triple quadrupole mass spectrometer increases the dynamic range and enables accurate quantification of peptides at low levels even from complex matrices.

## Acknowledgements

## REFERENCES

(1) Kolakowski, B.M. et al. Review of applications of high-field asymmetric waveform ion mobility spectrometry (FAIMS) and differential mobility spectrometry (DMS). Analyst 2007 Sep, 132(9), 842–864.
(2) Bonneil, E. et al. Enhancement of mass spectrometry performance for proteomic analyses using high-field asymmetric waveform ion mobility spectrometry (FAIMS). J. Mass Spectrom. 2015 Nov, 50(11), 1181–95.
(3) Swearingen, K.E. et al. High-field asymmetric waveform ion mobility spectrometry for mass spectrometry-based proteomics. Expert Rev. Proteomics 2012 Oct, 9(5), 505–17.

**Speak to a Specialist**

**Find out more at thermofisher.com/FAIMSPro**

This Sponsor Report is the responsibility of Thermo Fisher Scientific.

**BrJAC**

## SPONSOR REPORT

This section is dedicated for sponsor responsibility articles.

# Analysis of the Elemental Composition of Fine Particulate Matter (PM$_{2.5}$) emitted as Air Pollution using Triple Quadrupole ICP-MS

**Tomoko Vincent[1], Naoki Iwayama[2], Tokutaka Ikemoto[3] and Daniel Kutscher[1]**

*[1]Thermo Fisher Scientific, Germany. [2]Seikan Kensa Center, Japan. [3]Thermo Fisher Scientific, Japan*

This report was extracted from the Thermo Scientific Application Note 001169

## GOAL

To demonstrate the suitability of the Thermo Scientific™ iCAP™ TQ ICP-MS equipped with the PLUS torch for monitoring the elemental composition of fine particulate matter such as the PM$_{2.5}$ fraction.

## INTRODUCTION

Particulate matter (PM) is a significant contributor to environmental pollution globally. In particular, fine particulate matter with an aerodynamic diameter of 2.5 μm or smaller, commonly classified as PM$_{2.5}$, is of great concern on a global level. In contrast to exposure to bigger particles such as PM$_{10}$, which can be easily recognized and potentially avoided through protective equipment, exposure to PM$_{2.5}$ is more dangerous as the small diameter makes it effectively invisible to the human eye, and it has the potential to penetrate deep into the respiratory system when inhaled. The chemical composition of these fine particles may comprise both organic and inorganic components, and, depending on the geographical location, PM$_{2.5}$ can possibly be contaminated with toxic elements such as arsenic, cadmium, or lead. Due to its high mobility, the presence of PM$_{2.5}$ can be influenced by local environmental conditions such as location, season, weather, and other factors.

Inhalation of fine dust containing silicon particles poses serious health risks after both short- and long-term exposure; for example, the development of lung cancer.[1] In response to this particle pollution, a maximum allowable concentration of PM$_{2.5}$ of up to 12 μg m$^{-3}$ was set by the United States Environmental Protection Agency (EPA) in 2012,[2] and similar regulated levels have been set by the WHO and the Japanese Ministry of the Environment (Table 1).

**Table 1.** Maximum allowable concentration for PM$_{2.5}$

| Organization | Maximum allowance (μg m$^{-3}$) |
| --- | --- |
| U.S. Environmental Protection Agency (EPA) | <12 |
| World Health Organization (WHO) | 5–10 |
| Ministry of the Environment (MOE), Japan | <15 |

The composition of $PM_{2.5}$ is commonly measured using X-ray diffraction (XRD) or X-ray fluorescence (XRF), allowing direct and non-destructive analysis without prior sample preparation. However, for some lighter elements, including silicon, measuring low concentrations in the samples can be a challenge. Inductively coupled plasma mass spectrometry (ICP-MS) is the most widely employed technique for the analysis of trace elements in environmental samples, as it allows rapid multi-element analysis and enables unmatched detection limits to be achieved. Its high detection power provides a way to overcome the above stated limitations of other analytical techniques.

In this study, ambient air samples were collected using a high-volume air collector system at two different locations. The $PM_{2.5}$ fraction was collected on PTFE filters and then analyzed using a Thermo Scientific™ iCAP™ TQ ICP-MS following microwave digestion. The resulting concentrations in the measured solutions were typically below 1 µg·$L^{-1}$, so the high detection power of ICP-MS was needed for accurate quantitation of the elemental composition.

## EXPERIMENTAL
### Experimental optimization of instrument parameters
An iCAP TQ ICP-MS was used for all measurements. The instrument used in this study was equipped with the hydrofluoric acid resistant sample introduction kit (i.e., PFA cyclonic spray chamber, PFA nebulizer, sapphire injector, platinum interface cone) and a PLUS torch.[3] The PLUS torch, together with superior interference removal based on the use of triple quadrupole technology, enabled the detection of silicon at concentration levels well below the regulatory requirement. To remove all potentially occurring interferences, the ICP-MS was operated in He KED,[4] $TQ-H_2$ and $TQ-O_2$ modes. Table 2 gives an overview of the full configuration of the system.

**Table 2.** Instrument configuration and operating parameters

| Parameter | Value | | |
|---|---|---|---|
| Nebulizer | ESI™ PFA ST nebulizer, 100 µL $min^{-1}$, pumped at 40 rpm | | |
| Pump tubing | Orange–green, 0.38 mm i.d. | | |
| Spray chamber | PFA cyclonic, cooled at 2.7 °C | | |
| Torch | PLUS torch | | |
| Injector | 2.0 mm i.d., sapphire | | |
| Interface | Platinum sampler and platinum skimmer cone with high sensitivity skimmer cone insert | | |
| Plasma power | 1,550 W | | |
| Nebulizer gas | 0.98 L $min^{-1}$ | | |
| **QCell setting** | **$TQ-O_2$** | **$TQ-H_2$** | **He KED** |
| Gas flow | 100% $O_2$, 0.36 mL $min^{-1}$ | 100% $H_2$, 9.7 mL $min^{-1}$ | 100% He, 4.8 mL $min^{-1}$ |
| CR bias | -6.3 V | -6.3 V | -21 V |
| Q3 bias | -12 V | -12 V | -18 V |
| Scan settings | 0.1 s dwell time, 10 sweeps, 3 main runs | | |

### Data acquisition and data processing

The Thermo Scientific™ Qtegra™ Intelligent Scientific Data Solution™ (ISDS) Software was used to create LabBooks for sample analysis, data acquisition, processing, and reporting. The Reaction Finder Method Development Assistant was used to set up the method, with settings for specific analytes (i.e., using H$_2$) being manually modified.

### Sample collection and preparation

Each air sample was collected from two different locations in Kanagawa prefecture in Japan over 24 hours onto a 47 mm diameter PFTE filter (PALL Corporation) with 2 μm pore size, using a Thermo Scientific™ Partisol™ sequential ambient particulate sampler (Figure 1) at 16.7 L min$^{-1}$ (or 1 m$^{-3}$ hr$^{-1}$). One sampling location was within a municipal area, whereas the second location chosen was close to a motorway.



**Figure 1.** Sample collection at Kanagawa prefecture (location 1) using the Partisol 2025i system.

To monitor and potentially quantify changes over time in the elemental composition of PM$_{2.5}$, air samples were collected over a period of 14 days at one of the sampling sites. In a second study, the influence from climate effects, such as the wind conditions, were evaluated at the second sampling location. For example, Asian dust is a seasonal metrological phenomenon, where large amounts of yellow sand are transported from the deserts of Western Asia (Kazakhstan, Mongolia, and northern China) eastward towards China, the Korean Peninsula, and Japan. Due to industrial pollution in the dust, this phenomenon has become an increasing concern. A summary of the sampling details is shown in Table 3.

**Table 3.** Details on the sampling locations and conditions, including sampling duration

| Location | Season | Weather conditions | Remark | # of testing days |
|----------|--------|--------------------|--------|-------------------|
| 1 | Winter | N/A | Municipal area (near to an airport) | 14 |
| 2 | Winter | Normal weather conditions | Sampling location was close to a motorway | 1 |
|   | Winter | Strong wind from northwest | Sampling occurred during a day with a strong wind from northwest of Japan | 1 |

The filters with collected air were digested using a mixture of 5 mL $HNO_3$ (68% Optima™ grade, Fisher Chemical), 2 mL HF (48% Optima™ grade, Fisher Chemical) and 1 mL $H_2O_2$ (31% Optima™ grade, Fisher Chemical) in a microwave digestion system (Milestone ETHOS™ 1). After digestion, the samples were made up to a volume of 50 mL using ultrapure water. In all digestions, an unused filter was digested using the same procedure as a control to assess potential contamination in the process of sample preparation. All blanks and calibration standards were prepared from 2% (v/v) $HNO_3$ with multi-element standards (XSTC-1667 and XSTC-1668, SPEX™ CertiPrep™, Metuchen, NJ, USA). An internal standard solution containing 5 µg·L$^{-1}$ lithium, yttrium, indium, and thallium was added to all samples. Table 4 shows the details of the final calibration standard concentration ranges for each element.

**Table 4.** Concentrations of calibration solutions

| Element | Calibration standard concentration range (µg L$^{-1}$) |
| --- | --- |
| Na, Al, K, Ca | 1, 5, 10, 25, 50, and 100 |
| Si | 5,10, 25, 50, and 100 |
| Sc, Cr, Mn, Co, Ni, Sb, Cs, Ba, La, Ce, Sm, Hf, Ta, W, Pb, Th | 0.01, 0.05, 0.1, 0.25, 0.5, 1, 5, and 10 |
| Fe | 0.5, 1, 5, 10, 25, and 50 |
| Ti, Cu | 0.1, 0.25, 0.5, 1, 5, 10, and 25 |
| Zn | 0.25, 0.5, 1, 5, 10, 25, 50, and 100 |
| V, As, Se, Rb, Mo, Cd | 0.05, 0.1, 0.25, 0.5, 1, 5, and 10 |

## RESULTS AND DISCUSSION
### Improved detection of silicon

Silicon is an analyte of special importance for the evaluation of the elemental composition of fine dust due to its potential to cause severe respiratory diseases (such as silicosis) when able to penetrate deeply into the human body. Silicon is often one of the main components of PM$_{2.5}$ and current legislation set by the Ministry of the Environment in Japan sets a minimum required detection limit (MRDL) of 10 ng m$^{-3}$ for this element. It is therefore necessary to detect this element with high sensitivity and low background. The regulatory limit corresponds to a final concentration of less than 5 µg L$^{-1}$ in a sample collected over 24 hours and following the above stated sample preparation. Often, the filter sample may be split in half to allow additional measurements to be performed, further reducing the concentration in the analyzed solution for this critical contaminant.

In addition, silicon is known as a challenging analyte in ICP-MS, mostly due to polyatomic interferences arising from nitrogen in the ambient atmosphere (creating $^{14}N_2^+$ on the most abundant isotope $^{28}Si$), but also contamination from the ubiquitous presence of the element in the laboratory and the glassware used in the ICP-MS source. The excellent calibration curve achieved for silicon (Figure 2) in this work was obtained using a mass shift reaction with oxygen (Figure 3) to eliminate the polyatomic interferences using TQ-O$_2$ mode. Thanks to the PLUS torch, minimization of the Si background from the ICP-MS sample introduction parts was achieved, resulting in an instrumental detection limit (IDL) of 0.081 µg·L$^{-1}$, blank equivalent concentration (BEC) of 1.9 µg·L$^{-1}$, and coefficient of determination (R$^2$) of 0.9991. The IDL was calculated using three times the standard deviation of ten replicate measurements of the calibration blank.

### Sensitivity and linearity

Table 5 summarizes the obtained analytical figures of merit (IDL, BEC, and R$^2$) for all 31 elements analyzed in this study. The typically achieved instrumental detection limits were well below 0.1 µg L$^{-1}$, even for often challenging analytes such as arsenic, selenium, and cadmium.
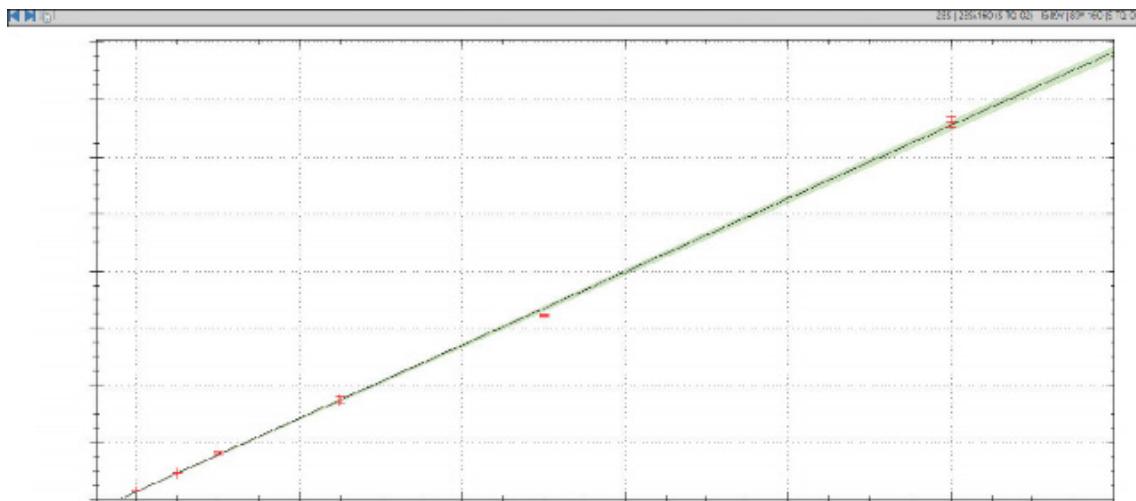


**Figure 2.** Calibration curve for silicon from 5 to 100 µg L$^{-1}$.
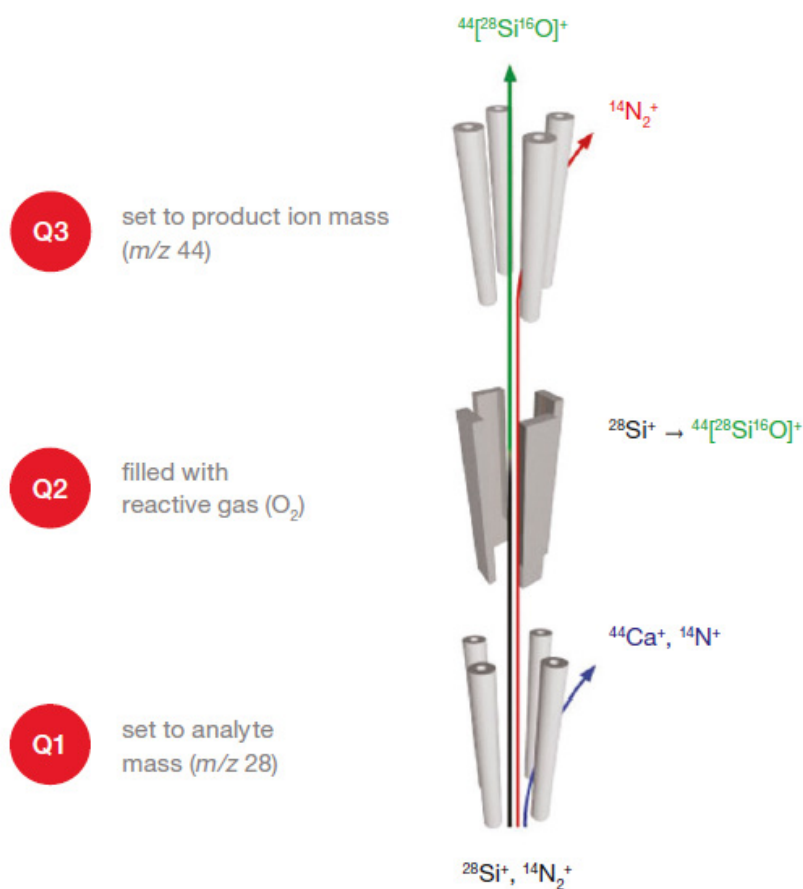


**Figure 3.** Schematic diagram showing the use of TQ-O$_2$ mode to selectively analyze silicon as $^{28}$Si$^{16}$O.

**Table 5.** Summary of analysis modes, internal standards, and calibration results (LODs, BECs) for all target analytes

| Analyte | Internal standard | Mode | LOD (µg L$^{-1}$) | BEC (µg L$^{-1}$) | R$^2$ |
|---|---|---|---|---|---|
| $^{23}$Na | $^7$Li | TQ-H$_2$ | 0.091 | 0.900 | >0.9999 |
| $^{27}$Al | $^7$Li | TQ-H$_2$ | 0.009 | 0.079 | >0.9999 |
| $^{28}$Si as $^{28}$Si.$^{16}$O $m/z$ 44 | 89$_Y$ | TQ-O$_2$ | 0.081 | 1969 | 0.9991 |
| $^{39}$K | $^7$Li | TQ-H$_2$ | 0.030 | 0.714 | >0.9999 |
| $^{40}$Ca | $^7$Li | TQ-H$_2$ | 0.012 | 0.12 | >0.9999 |
| $^{45}$Sc as $^{45}$Sc.$^{16}$O at $m/z$ 61 | 89$_Y$ | TQ-O$_2$ | 0.001 | 0.001 | >0.9999 |
| $^{48}$Ti as $^{48}$Ti.$^{16}$O at $m/z$ 64 | 89$_Y$ | TQ-O$_2$ | 0.0004 | 0.004 | >0.9999 |
| $^{51}$V as $^{51}$V.$^{16}$O at $m/z$ 66 | 89$_Y$ | TQ-O$_2$ | 0.003 | 0.003 | >0.9999 |
| $^{52}$Cr | 89$_Y$ | SQ-KED | 0.009 | 0.060 | >0.9999 |
| $^{55}$Mn | 89$_Y$ | SQ-KED | 0.006 | 0.012 | >0.9999 |
| $^{56}$Fe | 89$_Y$ | SQ-KED | 0.006 | 0.195 | 0.9999 |
| $^{59}$Co | 89$_Y$ | SQ-KED | 0.002 | 0.010 | >0.9999 |
| $^{60}$Ni | 89$_Y$ | SQ-KED | 0.0002 | 0.014 | >0.9999 |
| $^{63}$Cu | 89$_Y$ | SQ-KED | 0.004 | 0.020 | 0.9999 |
| $^{66}$Zn | 89$_Y$ | SQ-KED | 0.023 | 0.030 | >0.9999 |
| $^{75}$As as $^{75}$As.$^{16}$O at $m/z$ 91 | 89$_Y$ | TQ-O$_2$ | 0.002 | 0.010 | 0.9999 |
| $^{78}$Se as $^{78}$Se.$^{16}$O at $m/z$ 94 | 89$_Y$ | TQ-O$_2$ | 0.008 | 0.025 | >0.9999 |
| $^{85}$Rb | 89$_Y$ | SQ-KED | 0.006 | 0.060 | >0.9999 |
| $^{95}$Mo | 89$_Y$ | SQ-KED | 0.011 | 0.014 | >0.9999 |
| $^{111}$Cd | 89$_Y$ | SQ-KED | 0.007 | 0.007 | >0.9999 |
| $^{121}$Sb | 115$_{In}$ | SQ-KED | 0.0003 | 0.001 | >0.9999 |
| $^{133}$Cs | 115$_{In}$ | SQ-KED | 0.007 | 0.016 | >0.9999 |
| $^{137}$Ba | 115$_{In}$ | SQ-KED | 0.006 | 0.007 | >0.9999 |
| $^{139}$La | 115$_{In}$ | SQ-KED | 0.006 | 0.006 | >0.9999 |
| $^{140}$Ce | 205$_{Tl}$ | SQ-KED | 0.006 | 0.006 | >0.9999 |
| $^{149}$Sm | 205$_{Tl}$ | SQ-KED | 0.006 | 0.006 | >0.9999 |
| $^{178}$Hf | 205$_{Tl}$ | SQ-KED | <0.0001 | <0.0001 | >0.9999 |
| $^{181}$Ta | 205$_{Tl}$ | SQ-KED | 0.0001 | 0.0002 | >0.9999 |
| $^{182}$W | 205$_{Tl}$ | SQ-KED | 0.0002 | 0.0003 | >0.9999 |
| $^{208}$Pb | 205$_{Tl}$ | SQ-KED | 0.006 | 0.009 | >0.9999 |
| $^{232}$Th | 205$_{Tl}$ | SQ-KED | 0.005 | 0.006 | >0.9999 |

## PM$_{2.5}$ analysis results

To comply with applicable legislation, all analysis results (obtained as µg L$^{-1}$) were converted into mass per volume in the PM$_{2.5}$ fraction (in ng m$^{-3}$) using the following equation:

$$C = \frac{(M_s - M_b)E\,S}{s\,V}$$

Where:

C    Mass of analyte in fine particulate matter PM$_{2.5}$ in 1 m$^3$ of sampled air (ng m$^{-3}$)

Ms    Result of the analysis of the sample (ng mL$^{-1}$)

Mb    Result of the analysis of the preparation blank (ng mL$^{-1}$)

E    volume of test solution (mL)

S    PM$_{2.5}$ filter area where the sample was collected (cm$^2$)

s    Filter area used for analysis (¼ of S, (cm$^2$))

V    Collected volume of ambient air (m$^3$)

Table 6 shows the results for all elements under study across both sampling locations. The results obtained for the analysis of the elemental composition of the PM$_{2.5}$ fraction clearly provide meaningful data to evaluate the pollution level due to the ability of ICP-MS to measure a wide range of elements in a single analysis.

**Table 6. Summary of ambient air analysis results, maximum allowable concentration in Japan, and method detection limits (MDLs).** All results are in ng m$^{-3}$. The high RSDs observed for the measurements over 14 days can be explained by the significant influence of weather conditions (such as rain) on the formation and transportation of PM$_{2.5}$.

|  | MDL | Required MDL* | Maximum allowable concentration | Location 1 — Average concentration of 14 days in winter | Location 2 — Normal weather conditions | Location 2 — With strong wind |
|---|---|---|---|---|---|---|
| Na | 0.76 | 10 | – | 66.1 ± 39.5 | <MDL | <MDL |
| Al | 0.08 | 6 | – | 29.8 ± 19.9 | <MDL | 42.38 |
| Si | 1.4 | 10 | – | 45.1 ± 40.4 | <MDL | 125.48 |
| K | 0.25 | 10 | – | 65.6 ± 45.6 | 62.72 | 197.74 |
| Ca | 0.1 | 10 | – | 23.7 ± 15.9 | 24.69 | 99.65 |
| Sc | 0.01 | 0.04 | – | 0.005 ± 0.004 | <MDL | 0.01 |
| Ti | 0.004 | 0.7 | – | 3.44 ± 1.99 | 2.34 | 7.59 |
| V | 0.02 | 0.2 | – | 0.61 ± 0.85 | 0.24 | 0.64 |
| Cr | 0.07 | 0.4 | – | 0.88 ± 0.70 | 1.8 | <MDL |
| Mn | 0.05 | 0.5 | 140 | 5.55 ± 3.20 | 15.99 | 27.36 |
| Fe | 0.05 | 10 | – | 92.8 ± 55.0 | 188.24 | 368.87 |
| Co | 0.02 | 0.04 | – | 0.04 ± 0.02 | 0.03 | 0.07 |
| Ni | 0.002 | 0.2 | 25 | 0.46 ± 0.53 | 1.18 | 1.4 |
| Cu | 0.03 | 0.4 | – | 2.50 ± 1.38 | 9.01 | 14.65 |

**Table 6. Summary of ambient air analysis results, maximum allowable concentration in Japan, and method detection limits (MDLs).** All results are in ng m$^{-3}$. The high RSDs observed for the measurements over 14 days can be explained by the significant influence of weather conditions (such as rain) on the formation and transportation of PM$_{2.5}$. (continued)

| | MDL | Required MDL* | Maximum allowable concentration | Location 1 | Location 2 | |
|---|---|---|---|---|---|---|
| | | | | Average concentration of 14 days in winter | Normal weather conditions | With strong wind |
| Zn | 0.19 | 3 | – | 16.6 ± 12.4 | 60.41 | 84.45 |
| As | 0.02 | 0.09 | 6 | 0.41 ± 0.24 | <MDL | <MDL |
| Se | 0.06 | 0.2 | – | 1.56 ± 2.93 | 0.85 | 0.94 |
| Rb | 0.005 | 0.03 | – | 0.18 ± 0.11 | 0.1 | 0.41 |
| Mo | 0.009 | 0.07 | – | 0.84 ± 1.07 | 1.23 | 1.54 |
| Cd | 0.006 | 0.02 | – | 0.09 ± 0.06 | 0.16 | 0.29 |
| Sb | 0.001 | 0.09 | – | 0.72 ± 0.45 | 1.81 | 2.97 |
| Cs | 0.006 | 0.02 | – | 0.02 ± 0.01 | <MDL | 0.02 |
| Ba | 0.005 | 0.3 | – | 2.07 ± 1.20 | 5.44 | 11.4 |
| La | 0.005 | 0.02 | – | 0.04 ± 0.03 | 0.09 | 0.17 |
| Ce | 0.005 | 0.02 | – | 0.08 ± 0.05 | 0.22 | 0.32 |
| Sm | 0.005 | 0.03 | – | 0.001 ± 0.001 | <MDL | <MDL |
| Hf | 0.0002 | 0.03 | – | 0.02 ± 0.03 | 0.02 | 0.03 |
| Ta | 0.0005 | 0.02 | – | 0.001 ± 0.001 | <MDL | 0.01 |
| W | 0.002 | 0.05 | – | 0.14 ± 0.13 | 0.29 | 0.28 |
| Pb | 0.005 | 0.6 | – | 3.43 ± 1.67 | 6.1 | 11.76 |
| Th | 0.004 | 0.02 | – | 0.004 ± 0.003 | <MDL | <MDL |

*Required MDLs are from the guidelines of the Ministry of Environment (MOE) in Japan.

The composition of PM$_{2.5}$ at sample location 2 (under normal weather conditions) shows a higher presence of typical wear metals such as iron, nickel, copper, or zinc compared to location 1. Other metals, such as molybdenum, antimony, and lead were also significantly increased in samples from this location. This is very likely related to the higher urbanization and the specific sampling location near a motorway.

The composition of the PM$_{2.5}$ fraction obtained under the influence of the strong wind clearly differs from the composition under normal weather conditions. Considering the climate (wind direction) information and the PM$_{2.5}$ simulation results in Japan on the same day as the measurements, a possible impact of Asian dust on the results can be assumed.

The iCAP-TQ ICP-MS analysis results also show that typical soil components, such as Si, Al, Ti, and Fe, which are thought to be derived from Asian dust, are clearly found in higher concentrations under the likely influence of Asian dust (in location 2) as compared to normal weather conditions.

This technique can be used to improve the accuracy of analysis of potential sources of anthropogenic pollution, transported by meteorological phenomena such as Asian dust.

However, whether this is due to transportation from other locations or contamination within the area around the sampling location could not be confirmed without additional research data, which were not in the scope of this work.

Also, to presume Asian dust effects, it is important to obtain data from multiple sampling locations and include data for other species, for example the water soluble ionic components (e.g., $NH_4^+$, $Cl^-$, $NO_3^-$, $SO_4^{2-}$) and the weather conditions.

## CONCLUSION

A highly sensitive method for the analysis of the elemental composition of PM$_{2.5}$ was developed and applied to the analysis of samples collected from two sampling locations in Japan using the iCAP TQ ICP-MS equipped with the PLUS torch:

- Using a combination of TQ-O$_2$, TQ-H$_2$, and He KED mode, common interferences on important contaminants were eliminated and excellent signal-to-noise (S/N) ratios were obtained for all the elements studied, with detection capability well below global PM$_{2.5}$ analysis requirements.

- As an analyte of concern, silicon could be detected at levels well below the minimum required detection limit, because of the superior interference removal obtained with the iCAP TQ ICP-MS and the reduced backgrounds achieved using the PLUS torch.

- The method allowed the simultaneous assessment of 31 elements in one analysis, helping to get a better understanding of the natural and anthropogenic processing contributing to the composition of PM$_{2.5}$.

- In summary, the combination of sample collection using the Partisol 2025i and analysis with the iCAP TQ ICP-MS has been successfully demonstrated for the characterization of the inorganic components in the composition of PM$_{2.5}$.

### Acknowledgments

### REFERENCES

(1) Sato, T.; Shimosato, T. Silicosis and lung cancer: current perspectives, Lung Cancer: Targets and Therapy 2018, 9, 91–101.
(2) National Ambient Air Quality Standards for Particulate Matter, Final Rule, United States Environmental Protection Agency, 2013.
(3) Thermo Scientific Product Spotlight 44485: Thermo Scientific iCAP Qnova Series ICP-MS PLUS Torch for improved ICP-MS analysis of challenging samples.
(4) Thermo Scientific Smart Note 44415: iCAP RQ ICP-MS. https://assets.thermofisher.com/TFS-Assets/CMD/brochures/sn-44415-icp-ms-single-quadrupole-sn44415-en.pdf
(5) Ministry of the Environment Air Pollutant Wide Area Monitoring System, Japan Homepage: https://soramame.env.go.jp/

Learn more at **thermofisher.com/iCAPTQ**

This Sponsor Report is the responsibility of Thermo Fisher Scientific.

**BrJAC**

## *RELEASE*

# ultraWAVE 3
*Taking Productivity and Performance to New Heights*
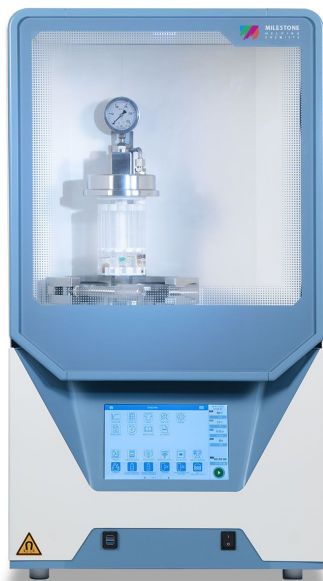
The new ultraWAVE 3 is the latest generation of SRC technology that further elevates the value of this technology for elemental analysis in terms of performance, time, workflow, and cost of ownership.

### *Single Reaction Chamber Technology*

Updated construction that includes several technology advances further enhances the well-proven benefits of the SRC technology.

The new features of ultraWAVE 3 merge with those already intrinsic in the technology, so that labs will experience higher performance, greater productivity, and more streamlined workflow, providing them with improved competitiveness and a lower cost of ownership.

Thanks to its **superior digestion capabilities** that result from its **higher temperature and pressure features**, ultraWAVE's unique SRC technology provides greater digestion efficiency.

Several aspects of the system, such as **reduced handling and cleaning** and the ability **to process any samples simultaneously, reduce turnaround time** and increase lab efficiency.

## BENEFITS

### *Rugged construction*
Designed with all wetted components made of PTFE-TFM, fully compatible with any acid mixture and ensuring minimal maintenance to lower the cost of ownership.

### *High-pressure lines*
Made of acid-resistant stainless steel, the two pressure lines, one for inlet and one for outlet, ensure high safety and lower blanks.

### *Racks*
Available with racks of 7, 20, 27 and 40 vials to provide even higher throughput than previous generations.

### *easyTEMP Temperature control*
True contactless temperature sensor to directly control the digestion of the samples from the inside out, without reading delays.

### *Advanced heating technology*
The noiseless water-cooled magnetron ensures higher heating efficiency along with superior working conditions.

### *User interface*
Equipped with the most up-to-date features to bring all digestion information within easy reach of the operator.

**Find out more at milestonesrl.com**

# ultraWAVE 3

# Single Reaction Chamber Technology

Updated construction that includes several technology advances further enhances the well-proven benefits of the SRC technology.

The new features of **ultraWAVE 3** merge with those already intrinsic in the technology, so that labs will experience higher performance, greater productivity, and more streamlined workflow, providing them with improved competitiveness and a lower cost of ownership.

Thanks to its superior digestion capabilities that result from its higher temperature and pressure features, ultraWAVE's unique SRC technology provides greater digestion efficiency.

Several aspects of the system, such as reduced handling and cleaning and the ability to process any samples simultaneously, reduce turnaround time and increase lab efficiency.

**VIDEO**  **WEBSITE**

*RELEASE*

# TSQ Altis Plus Triple Quadrupole Mass Spectrometer
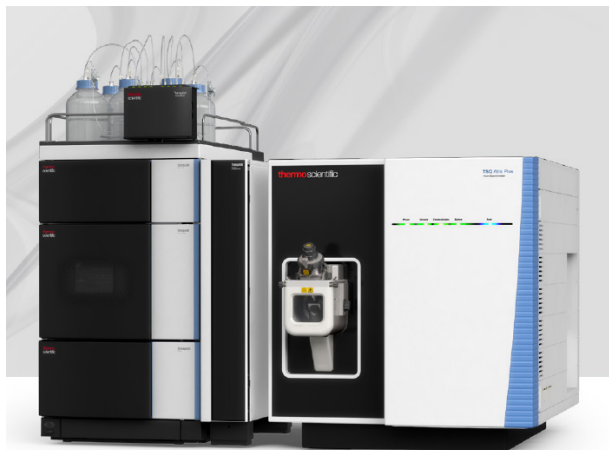
**Ultimate quantitative performance made possible**

Overcome the most demanding quantitative workflow challenges. With superior acquisition speeds, enhanced sensitivity, prototypical selectivity, and exceptional robustness, the TSQ Altis Plus mass spectrometer delivers unprecedented accuracy and precision for low-level compound detection and quantitation in complex matrices that redefines ultimate instrument performance.

**Achieve the highest confidence in targeted compound detection and quantitation**

Greater than 6 orders of linear dynamic range with high selectivity. Enhanced acquisition speeds empower large-scale studies for translational workflow development or method optimization with effective dwell time settings as low as 0.3 – 5 millisecond polarity switching maximizes productivity in fewer experiments.

**High-throughput screening and quantitation**

Innovations in the ion source, mass analyzer, active Q2 collision cell, and RF electronics offer high sensitivity, selectivity, and superior acquisition speeds/polarity switching times that are ideal with UHPLC separations.

**Expanded experimental capabilities**

Integrated workflow solutions centered on the TSQ Altis Plus mass spectrometer address regulated requirements targeting a growing list of diverse compounds. New UHPLC and ion chromatography (IC) systems maximize sample delivery and separation capabilities, maintaining the sensitivity to meet minimum residue limits without costly sample preparation or derivatization steps.

**Operational simplicity**

Simplified calibration approach consolidates steps needed by the operator, combining an intelligent instrument check and calibration routine. Experimental determination of dwell times assigned to each transition has been automated based on user-defined chromatographic peak width and the option of fixed cycle time or optimal number of data points per chromatographic peak.

**Database integration**

Utilization of experimental libraries created from discovery experiments can by-pass the need for purified standards and lengthy optimization routines. The output from processed data in Thermo Scientific TraceFinder software can be directly imported into the instrument method editor, streamlining large-scale study creation.

Discovery experiments, however, may not contain all compounds targeted in a study. Integration with Thermo Scientific mzCloud databases enables selection of additional compounds from the most advanced mass spectral database to be added into existing experimental methods.

Read more

*RELEASE*

# Redefining ICP-MS Triple Quadrupole Technology with Unique Ease of Use



Thermo Scientific iCAP TQ ICP-MS

Empowering you with technology to achieve more today and be ready to master future challenges tomorrow, the Thermo Scientific iCAP™ TQ ICP-MS helps futureproof your laboratory against evolving legislation requirements, enables you to explore developing markets, and pushes the boundaries of your research.

Harness the power of Triple Quadrupole (TQ) ICP-MS with incredible accuracy and detection limits for the most challenging applications. Improved interference removal allows laboratories to tackle complex samples with ease and deliver data with the confidence of 'right first time' results.

Ease of use is the core concept behind the Thermo Scientific™ iCAP™ TQ ICP-MS, which has been designed for laboratories working in both routine and research applications. The system is based on a platform with an intuitive hardware design that simplifies the user experience. The operator-focused software streamlines workflows and integrates control of peripherals to automate sample handling.

## Key features of the iCAP TQ ICP-MS
### *Unique ease-of-use*
Combining user-inspired hardware with intelligent software, the iCAP TQ ICP-MS and the iCAP TQs ICP-MS both enable laboratories to effortlessly develop and maintain methods that ensure confidence in data quality. Reaction Finder, which is the systems' unique method development assistant, enables you to tackle challenging matrices without wasting time on complex method development.

### *Right-first-time results*
Employ the power of triple quadrupole technology for uncomplicated analyses with superior accuracy during both research and routine applications. Thanks to the advanced interference removal capabilities of the iCAP TQ ICP-MS, analysis of samples with complex matrices can be performed with superior limits of detection for more accurate data.

### *Boundless capabilities*
Fully integrated plugins for Thermo Scientific Qtegra Intelligent Scientific Data Solution (ISDS) Software enable the easy implementation of advanced applications, including automated sample handling, autodilution, speciation, nanoparticle analysis and laser ablation.

**Find out more at** https://www.thermofisher.com

# Thermo Scientific iCAP TQ ICP-MS

Delivering research level trace elemental analysis, combined with routine ease-of-use, the Thermo Scientific™ iCAP™ TQ ICP-MS is a high-performance, future-proof ICP-MS solution. Harness the power of Triple Quadropole (TQ) technology, in combination with a wide variety of reactive gases and experience, for uncomplicated analysis with incredible accuracy. Expand your applications and enhance your laboratory efficiency with breakthrough triple quadrupole technology that is so easy to use, any analyst can operate it.

Performance | Versatility | Operational Simplicity

**VIDEO**   **WEBSITE**

# Pittcon Conference & Expo

Pittcon is a catalyst for the exchange of information, a showcase for the latest advances in laboratory science, and a venue for international connectivity.



Pittcon is a dynamic, transnational conference and exposition on laboratory science, a venue for presenting the latest advances in analytical research and scientific instrumentation, and a platform for continuing education and science-enhancing opportunity. Pittcon is for anyone who develops, buys, or sells laboratory equipment, performs physical or chemical analyses, develops analysis methods, or manages these scientists.

### *Pittcon Awards*
*Honoring scientists who have made outstanding contributions to Analytical Chemistry*



Each year, Pittcon provides a venue where scientists who have made outstanding contributions to laboratory science, analytical chemistry, and applied spectroscopy are honored.

Among these awards is the **Pittcon Heritage Award** which honors those visionaries whose entrepreneurial careers shaped the instrumentation and laboratory supplies community and by doing so have transformed the scientific community at large.

The award has been presented jointly with Pittcon since 2002 and is given out each year at a special ceremony during the Pittcon Conference and Expo. The recipient's name and achievements are added to the Pittcon Hall of Fame, which conference attendees can visit at the show each year.

**Pittcon 2024 – Conference on Analytical Chemistry and Applied Spectroscopy**
February 24-28, 2024
San Diego, California, USA

**Celebrating 75 Years
February 24-28, 2024
San Diego, California, USA**

Pittcon®
Conference and Exposition

Perfect weather, the wind in your hair, the tranquil tones of some far-off soft rock, and a gold rush of cool, quality science.

**LEARN MORE**

## You asked... we listened.

Pittcon – the event made for scientific breakthroughs – will be collaborating on the US West Coast for the first time in our nearly 75-year history.

### ATTEND

Create connections on the California coast.

Enter to win free dinner with the Pittcon Marketing Team if you attend Pittcon in 2024.

### EXHIBIT

Take part in a Gold Rush of quality leads.

Enter to win a free floor plan logo advertisement for your company's registered 2024 booth.

Pittcon®
Conference and Exposition

*RELEASE*

# SelectScience® Pioneers online Communication and Promotes Scientific Success



SelectScience® promotes scientists and their work, accelerating the communication of successful science. Through trusted lab product reviews, virtual events, thought-leading webinars, features on hot scientific topics, eBooks and more, independent online publisher SelectScience® provides scientists across the world with vital information about the best products and techniques to use in their work.

## Some recent contributions from SelecScience® to the scientific community

### Editorial Articles

*Marine research sails into the future with UV-Vis spectroscopy*

Dr. Sarah Kingston, Assistant Professor of Oceanography and Chief Scientist for Marine Biodiversity and Conservation at Sea Education Association, discusses the use of UV-Vis spectroscopy in her research and the future of molecular marine research. In the hands of researchers like Dr. Sarah Kingston, the applications of UV-Vis spectroscopy in oceanography and marine science is making waves – both literally and figuratively. This article describes how she is employing UV-Vis spectroscopy to explore and understand the mysteries of our planet's oceans. Access **here**

*How to achieve the Lab of the Future with expert insights from industry, academia, and manufacturing*

JIn this article, three experts across biopharma, academia, and manufacturing provide a comprehensive overview of the LoF concept, exploring its potential impact on various sectors, the challenges involved, and the critical steps that labs must take to align themselves with this transformative vision. Access **here**

### Webinar

*An industry perspective of the current regulatory landscape for nitrosamines*

In this webinar, Lance Smallshaw, Head of Compendial Affairs at UCB Pharma S.A. (Belgium), provides an overview of the regulatory landscape today including recent significant updates related to nitrosamines in human medicines. This webinar also offers a perspective on the differences that exist between the health authorities, and explains how there is a continued need from the industry, to do more in order to harmonize these regional differences. Access **here**

# SelectScience® is the leading independent online publisher connecting scientists to the best laboratory products and applications.
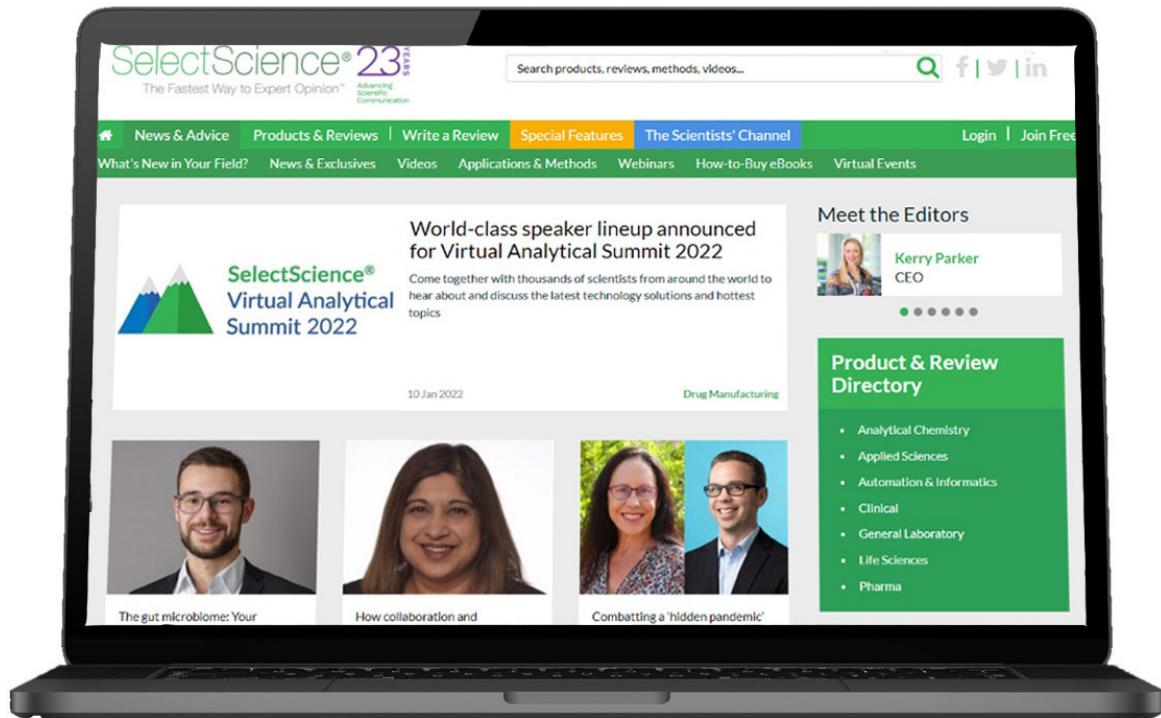


- Working with Scientists to Make the Future Healthier.

- Informing scientists about the best products and applications.

- Connecting manufacturers with their customers to develop, promote and sell technologies.

SelectScience®
The Fastest Way to Expert Opinion

*RELEASE*

# CHROMacademy is the leading provider of eLearning for analytical science
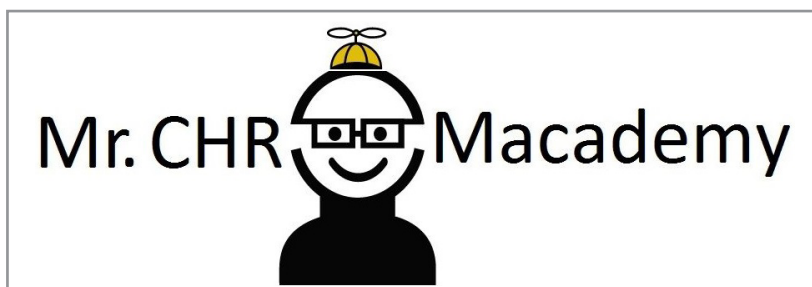


CHROMacademy *helps scientific organizations acquire and maintain excellence in their laboratories*.

For over 10 years, CHROMacademy has increased knowledge, efficiency and productivity across all applications of chromatography. With a comprehensive library of learning resources, members can improve their skills and knowledge at a pace that suits them.

CHROMacademy covers all chromatographic applications – HPLC, GC, mass spec, sample preparation, basic lab skills, and bio chromatography. Each paradigm contains dozens of modules across theory, application, method development, troubleshooting, and more. Invest in analytical eLearning and supercharge your lab.



**For more information, please visit www.chromacademy.com/**

# *NOTICES OF BOOKS*

### Applications of Analytical Chemistry in Industry

Silvio Vaz Junior, Author

September 2023, Springer Cham

This book deals with analytical techniques and methods applied in several sectors of technology and industry and serves as a concise and up-to-date reference for the practical application of analytical chemistry. Readers will find valuable insights, including real-life examples, of how classical and instrumental techniques can be used by industry, to help professionals in the quality control of raw materials, products and processes, in the assessment of the formulation contamination, environmental pollution and in the evaluation of sustainability, among others.
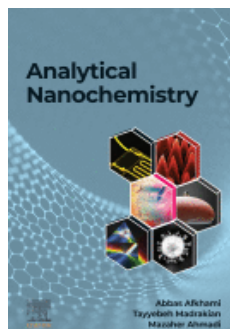
### Analytical Nanochemistry

Abbas Afkhami, Tayyebeh Madrakian and Mazaher Ahmadi, Authors

2023 Elsevier

This book provides readers with a comprehensive review of the application of nanomaterial in analytical chemistry. It explains the fundamental concepts involved in utilizing nanomaterials including their classification, synthesis, functionalization, characterization methods, separation, and isolation techniques, as well as toxicity. It also covers fundamental information on different aspects of analytical procedures and method development. Furthermore, it emphasizes micro- and nano-enabled analytical devices and instruments as well as nanotools for nanoanalysis.
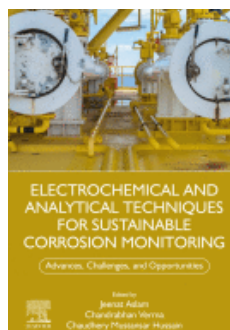
### Electrochemical and Analytical Techniques for Sustainable Corrosion Monitoring – Advances, Challenges and Opportunities

Jeenat Aslam, Chandrabhan Verma and Chaudhery Mustansar Hussain, Editors
2023 Elsevier

This is the first book that collectively describes corrosion inhibition measurements using chemical, electrochemical, and analytical methods. The book presents state-of-the art techniques for corrosion monitoring by providing detailed studies and testing methods. It also covers the most advanced, industry-oriented challenges for sustainable corrosion monitoring and measurements. The book is a valuable resource for scholars in academia, materials science and applied engineering and chemistry students, and corrosion engineers.
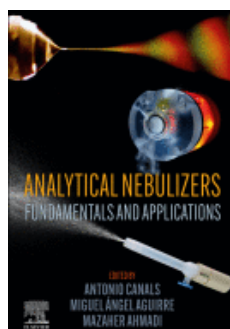
### Analytical Nebulizers: Fundamentals and Applications

Antonio Canals, Miguel Ángel Aguirre and Mazaher Ahmadi, Editors
2023 Elsevier

Although the book mainly focuses on the application of analytical nebulizers in analytical sciences, specifically in sample preparation, it is also useful to those in other disciplines (e.g., organic chemistry, catalysis, sensors, nanotechnology, biomedicine and nanomedicine, and environmental chemistry) where these nebulizers have great potential. Non-conventional applications of nebulizers such as aerosol-assisted synthesis nanoparticles and ultrasonic nebulization extraction are also presented.

## *PERIODICALS & WEBSITES*

### American Laboratory

American Laboratory® is a platform that addresses basic research, clinical diagnostics, drug discovery, environmental, food and beverage, forensics and other markets, and combines in-depth articles, news, and video to deliver the latest advances in their fields.
**Featured Article:** *Novel Biosensor Method to Predict Adverse Drug Reactions* Researchers at Karolinska Institutet have developed a novel method that can predict adverse reaction potential before the drugs are administered to patients. **Read more**

### LCGC

Chromatographyonline delivers practical, nuts-and-bolts information to help scientists and lab managers become more proficient in the use of chromatographic techniques and instrumentation. *Green, Greener, Greenest—Sustainability at All Points of the Analytical Process.* Mary Ellen McNally and Doug Raynie covered green chemistry and sustainable separations, from sample preparation through analysis with chromatographic techniques, at the Eastern Analytical Symposium 2023. **Read more**
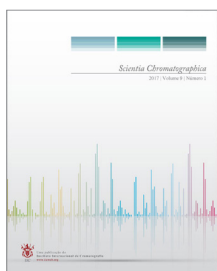
### Scientia Chromatographica

*Scientia Chromatographica* is the first and to date the only Latin American scientific journal dedicated exclusively to Chromatographic and Related Techniques. With a highly qualified and internationally recognized Editorial Board, it covers all chromatography topics in all their formats, in addition to discussing related topics such as "The Pillars of Chromatography", Quality Management, Troubleshooting, Hyphenation (GC-MS, LC-MS, SPE-LC-MS/MS) and others. It also provides columns containing general information, such as: calendar, meeting report, bookstore, etc. **Read more**

### Select Science

SelectScience® has transformed global scientific communications and digital marketing over the last 23 years. Informing scientists about the best products and applications. Connecting manufacturers with their customers to develop, promote and sell technologies promotes scientists and their work, accelerating the communication of successful science. Scientists can make better decisions using independent, expert information and gain easy access to manufacturers. SelectScience® informs the global community through Editorial, Features, Video and Webinar programs. **Read more**

### Spectroscopy

With the *Spectroscopy* journal, scientists, technicians, and lab managers gain proficiency through unbiased, peer-reviewed technical articles, trusted troubleshooting advice, and best-practice application solutions.
**Feature article:** *Key Steps in the Workflow to Analyze Raman Spectra.* By Shuxia Guo, Jürgen Popp, Thomas Bocklitz. A more successful blueprint for analyzing Raman spectral data is outlined by following the 11 important steps, which are outlined here.

# *EVENTS in 2024*

**February 24 – 28**
**PITTCON Conference & Expo**
San Diego, California, USA
https://pittcon.org/pittcon-2024/


**March 18 – 21**
**XV Latin American Symposium on Environmental Analytical Chemistry (LASEAC) & X Encontro Nacional de Química Ambiental (ENQAmb)**
Ouro Preto, Minas Gerais, Brazil
https://www.xvlaseac-xenqamb2024.com/


**May 22 – 25**
**47th Annual Meeting of the Brazilian Chemical Society (RASBQ)**
Águas de Lindóia, SP, Brazil
https://www.sbq.org.br/reunioes-anuais


**October 6 – 10**
**34th International Symposium on Chromatography – ISC 2024**
Liverpool, UK
https://isc2024.org/


**October 20 – 25**
**SciX Conference 2024**
Raleigh, NC, United States
https://www.scixconference.org/scix-future-conferences


**September 15 – 18**
**21st National Meeting on Analytical Chemistry (ENQA) & 9th Ibero-American Congress on Analytical Chemistry (CIAQA)**
Hangar Centro de Convenções & Feiras da Amazônia, Belém, PA, Brasil
https://www.enqa2024.com.br//

**BrJAC**

## *Acknowledgments*

## *Acknowledgments (Continuation)*

## *Acknowledgments (Continuation)*

## *Acknowledgments (Continuation)*

# AUTHOR GUIDELINES

## Aims & Scope

*Brazilian Journal of Analytical Chemistry* is a double-blind peer-reviewed research journal dedicated to the diffusion of significant and original knowledge in all branches of Analytical and Bioanalytical Chemistry. It is addressed to professionals involved in science, technology, and innovation projects at universities, research centers and in industry. **BrJAC welcomes** the submission of research papers reporting studies devoted to new and significant analytical methodologies, putting in evidence the scientific novelty, the impact of the research and demonstrating the analytical or bioanalytical applicability. BrJAC **strongly discourages** those simple applications of routine analytical methodologies, or the extension of these methods to new sample matrices, unless the proposal contains substantial novelty and unpublished data, clearly demonstrating advantages over existing ones.

Additionally, there are other submission categories to BrJAC such as:

**Reviews:** They should be sufficiently broad in scope, but specific enough to permit an appropriate depth discussion, including critical analyses of the bibliographic references and conclusions. Manuscripts submitted for publication as Reviews must be original and unpublished. Reviews undergo double-blind full peer review and are handled by the Editor of Reviews.

**Technical Notes:** Concise descriptions of developments in analytical methods, new techniques, procedures, or equipment falling within the scope of the BrJAC. Technical notes also undergo double-blind full peer review.

**Letters:** Discussions, comments, and suggestions on issues related to Analytical Chemistry or Bioanalytical Chemistry. Letters are welcome and will be published at the discretion of the BrJAC Editor-in-Chief.

**Point of View:** This category is exclusively invited by the Editor-in-Chief.

See the next items for more information on the journal, the documents preparation, manuscript types, and how to prepare the submission.

## Professional Ethics

**Originality:** manuscripts submitted for publication in BrJAC cannot have been previously published or be currently submitted for publication in another journal.

**Preprint:** BrJAC does not accept manuscripts that have been posted on preprint servers prior to the submission.

**Integrity:** the submitted manuscripts are the full responsibility of the authors. Manipulation/invention/ omission of data, duplication of publications, the publication of papers under contract and confidentiality agreements, company data, material obtained from non-ethical experiments, publications without consent, the omission of authors, plagiarism, the publication of confidential data and undeclared conflicts of interests are considered serious ethical faults.
BrJAC discourages and restricts the practice of excessive self-citation by the authors.
BrJAC does not practice coercive citation, that is, it does not require authors to include references from BrJAC as a condition for achieving acceptance, purely to increase the number of citations to articles from BrJAC without any scientific justification.

**Conflicts of interest:** when submitting their manuscript for publication, the authors must include all potential sources of bias such as affiliations, funding sources and financial, management or personal relationships which may affect the work.

**Copyright:** will become the property of the Brazilian Journal of Analytical Chemistry, if and when a manuscript is accepted for publication. The copyright comprises exclusive rights of reproduction and distribution of the articles, including reprints, photographic reproductions, microfilms or any other reproductions similar in nature, including translations.

**Request for permission to reuse figures and tables published in the BrJAC:** researchers who want to reuse any document or part of a document published in the BrJAC should request reuse permission from the BrJAC Editor-in-Chief, even if they are the authors of such document. A template for requesting reuse permission can be downloaded **here**.

**Misconduct will be treated according to** the COPE's recommendations (https://publicationethics.org/) and the Council of Science Editors White Paper on Promoting Integrity in Scientific Journal Publications (https://www.councilscienceeditors.org/).

## Manuscript submission

**The BrJAC does not charge authors an article processing fee.**

Manuscripts must be prepared according to the BrJAC manuscript template. Manuscripts in disagreement with the BrJAC guidelines are not accepted for revision.

The BrJAC uses an online manuscript manager system for the submission of manuscripts. This system guides authors stepwise through the entire submission process.

After the submitting author logs in to the system and enters his/her personal and affiliation details, the submission can be started.

All co-authors must be added to the Authors section.

Four documents are mandatorily uploaded by the submitting author: Cover letter, Title Page, Novelty Statement and the Manuscript. Templates for these documents are available for download **here**.

The four documents mentioned above must be uploaded as Word files. The manuscript Word file will be converted by the system to a PDF file which will be used in the double-blind peer review process.

All correspondence, including notification of the Editor's decision and requests for revision, is sent by e-mail to the submitting author through the manuscript manager system.

## Documents Preparation

**It is highly recommended that authors download and use the templates to create their four mandatory documents to avoid the suspension of a submission that does not meet the BrJAC guidelines.**

**Cover Letter**
The cover letter template should be downloaded and filled out carefully.
Any financial conflict of interest or lack thereof and agreement with BrJAC's copyright policy must be declared.
It is the duty of the submitting author to inform his/her collaborators about the submission of the manuscript and its eventual publication.
The Cover Letter must be signed by the corresponding author.

**Title Page**
The Title Page must contain information for each author: full name, affiliation and full international postal address, and information on the contribution of each author to the work. Acknowledgments must be entered on the Title Page. The submitting author must sign the Title Page.

**Novelty Statement**
The Novelty Statement must contain clear and succinct information about what is new and innovative in the study in relation to previously related works, including the works of the authors themselves.

**Manuscript (all submission categories)**

It is highly recommended that authors download the Manuscript template and create their manuscript in this template, keeping the layout of this file.

- **Language**: **English** is the language adopted by BrJAC. The correct use of English is of utmost importance. In case the Editors and Reviewers consider the manuscript to require an English revision, the authors will be required to send an English proofreading certificate before the final approval of the manuscript by BrJAC.

- **Required items**: the manuscript must include a title, abstract, keywords, and the following sections: Introduction, Materials and Methods, Results and Discussion, Conclusion, and References.

- **Identification of authors**: as the BrJAC adopts a double-blind review, the manuscript file must **NOT** contain the authors' names, affiliations nor acknowledgments. Full details of the authors and their acknowledgements should be on the Title Page.

- **Layout**: the lines in the manuscript must be numbered consecutively and double-spaced.

- **Graphics and Tables**: must appear close to the discussion about them in the manuscript. For **figures** use **Arabic** numbers, and for **tables** use **Roman** numbers.

- **Figure files:** when a manuscript is approved for publication, the BrJAC production team will contact the corresponding author to request separate files of each figure and a graphical abstract. These files must have **good resolution** and the extension **PNG or JPG**. The graphical abstract should preferably be created in landscape format. In the article diagrammed in the journal, the graphical abstract will occupy a space of 8 to 9 cm in length and 6 cm in height. Chemical structures must have always the same dimensions.

- **Permission to use content already published**: to use figures, graphs, diagrams, tables, etc. identical to others previously published in the literature, even if these materials have been published by the same submitting authors, a publication permission from the publisher or scientific society holding the copyrights must be requested by the submitting authors and included among the documents uploaded in the manuscript management system at the time of manuscript submission.

- **Chemical nomenclature, units and symbols**: should conform to the rules of the International Union of Pure and Applied Chemistry (IUPAC) and Chemical Abstracts Service. It is recommended that, whenever possible, the authors follow the International System of Units, the International Vocabulary of Metrology (VIM) and the NIST General Table of Units of Measurement. Abbreviations are not recommended except for those recognized by the International Bureau of Weights and Measures or those recorded and established in scientific publications. Use L for liters. Always use superscripts rather than /. For instance: use mg mL$^{-1}$ and NOT mg/mL. Leave a space between numeric values and their units.

- **References throughout the manuscript:** the references must be cited as superscript numbers. It is recommended that references older than 5 (five) years be avoided, except in relevant cases. Include references that are accessible to readers.

- **References item:** This item must be thoroughly checked for errors by the authors before submission. From 2022, BrJAC is adopting the American Chemical Society's Style in the Reference item. Mendeley Reference Manager users will find the Journal of American Chemical Society citation style in the Mendeley View menu. Non-users of the Mendeley Reference Manager may refer to the ACS Reference Style Quick Guide DOI: https://doi.org/10.1021/acsguide.40303

## *Review process*

Manuscripts submitted to the BrJAC undergo an initial check for compliance with all of the journal's guidelines. Submissions that do not meet the journal's guidelines will be suspended and an alert sent to the corresponding author. The authors will be able to resend the submission within 30 days. If the submission

according to the journal's guidelines is not made within 30 days, the submission will be withdrawn on the first subsequent day and an alert will be sent to the corresponding author.

Manuscripts that are in accordance with the journal's guidelines are submitted for the analysis of similarities by the iThenticate software.

The manuscript is then forwarded to the Editor-in-Chief who will check whether the manuscript is in accordance with the journal's scope and will analyze the similarity report issued by iThenticate.

If the manuscript passes the screening described above, it will be forwarded to an Associate Editor who will also analyze the iThenticate similarity report and invite reviewers.

Manuscripts are reviewed in double-blind mode by at least 2 reviewers. A larger number of reviewers may be used at the discretion of the Editor. As evaluation criteria, the reviewers employ originality, scientific quality, contribution to knowledge in the field of Analytical Chemistry, the theoretical foundation and bibliography, the presentation of relevant and consistent results, compliance with the BrJAC's guidelines, clarity of writing and presentation, and the use of grammatically correct English.

**Note:** In case the Editors and Reviewers consider the manuscript to require an English revision, the authors will be required to send an English proofreading certificate, by the ProofReading Service or equivalent service, before the final approval of the manuscript by the BrJAC.

The 1st-round review process usually takes around 5-6 weeks. If the manuscript is not rejected but requires corrections, the authors will have one month to submit a corrected version of the manuscript. In another 3-4 weeks, a new decision on the manuscript may be presented to the corresponding author.

The manuscripts accepted for publication are forwarded to the BrJAC production department. Minor changes to the manuscripts may be made, when necessary, to adapt them to BrJAC guidelines or to make them clearer in style, respecting the original content. The articles are sent to the authors for approval before publication. Once published online, a DOI number is assigned to the article.

## *Final Considerations*

Whatever the nature of the submitted manuscript, it must be original in terms of methodology, information, interpretation or criticism.

With regard to the contents of published articles and advertisements, the sole responsibility belongs to the respective authors and advertisers; the BrJAC, its editors, editorial board, editorial office and collaborators are fully exempt from any responsibility for the data, opinions or unfounded statements.

**Submit manuscripts at www.brjac.com.br**